

Occupant-centered control strategies for decentralized residential ventilation

Zur Erlangung des akademischen Grades eines Doktors der
Ingenieurwissenschaften (Dr.-Ing.) von der KIT-Fakultät für
Architektur des Karlsruher Instituts für Technologie (KIT)
genehmigte Dissertation von

Nicolas Carbonare
aus Buenos Aires, Argentinien

Tag der mündlichen Prüfung:	11.03.2021
Vorsitzende:	Prof. Dr. Barbara Engel
Referent:	Prof. Dipl.-Ing. Andreas Wagner
Korreferent:	Prof. Dr. Marcel Schweiker
Weiteres Mitglied:	Prof. Dipl. Arch. Dirk Hebel

Acknowledgements

I would like to thank Prof. Andreas Wagner for accepting me as his PhD student and for his guidance and support during the whole process, both professional and personal. I thank also Prof. Dr. Marcel Schweiker for his valuable contribution to the quality of this work. I am also grateful to Prof. Dr. Barbara Engel and Prof. Dirk Hebel for integrating the commission in my thesis defense.

I would also like to express my gratitude to the whole team at the Fraunhofer Institute of Solar Energy Systems in Freiburg. Firstly, Fabien Coydon and Arnulf Dinkel, who accepted me in their team and believed in me since the first day. Secondly, I would like to thank my supervisor Constanze Bongs, who supported and guided me during these years. A very heartfelt thanks to Thibault Pflug, without whom it would not have been possible to complete the work. Only he knows the true dimension of this thesis. Last but not least, I thank Sebastian Herkel and Peter Engelmann for their valuable scientific contributions.

I want to thank to all the students that contributed to this thesis: Ugur Halden, Fanlin Cheng, Abdella Alzade, Diana Maier, Krishna Devineni and Sebastian Rohrer. I would like to thank all my office colleagues for the friendly and productive atmosphere we created together: Sven Auerswald, Felix Ohr, Martin Kleinstück, Konstantin Klein and Mehmet Elci. Their scientific and human contribution to this thesis meant a lot to me. A special thanks to Paula Alfonso and Bruno Bueno for the countless advice and support in Spanish. A special thanks to the whole team at the Karlsruhe Institute of Technology (fbta, IEH and IIP), especially during the campaign at the Energy Smart Home Lab.

To my family and friends: quiero agradecer a mis padres Miguel y Claudia. Todo lo que soy se los debo a ellos. A mis hermanos, por estar siempre. A mis abuelos, por todo el amor recibido. A mis amigos en Argentina, por haberme apoyado siempre desde el otro lado del océano Atlántico. Y también a mis amigos en Alemania, por haberme acompañado y escuchado siempre. El más profundo agradecimiento es para mi compañera de vida, Romi, quién estuvo a mi lado cada día desde que empecé este trabajo, y sin quién esta tesis ni siquiera habría comenzado.

Abstract

This thesis addresses ventilation control strategies from the perspective of the occupant. The use of decentralized mechanical ventilation systems has grown sustainably in the past ten years in Germany as a cost-effective solution to guarantee air exchange in highly airtight renovated residential buildings. Even though occupant-centered control strategies for residential ventilation are often neglected, they could potentially improve the trade-off between energy efficiency, hygrothermal comfort, and indoor air quality.

Window operation remains the primary occupant action to obtain fresh air. Existing window opening models are reviewed and compared to real building measurements. A real-time logistic regression analysis with a window opening detection algorithm is investigated to learn about user preferences without deploying extra sensors. This proposed method fails to grasp the occupant behavior properly when information about user preferences is not available in advance. Therefore, feedback is required to achieve the targeted individualization.

Market and scientific research has identified the lack of multivariable solutions and occupant-centered approaches as the main gap in residential ventilation controllers. Therefore, three main solutions are proposed: a comfort-oriented cost function, a fuzzy demand-based controller and a self-learning controller based on a classification algorithm.

These controllers target the indoor relative humidity and CO_2 concentration. A co-simulation approach can evaluate the performance of these solutions and their impact on energy, comfort, and air quality. Full-automatic multivariable controllers can provide around 13% primary energy savings compared to state-of-the-art strategies without compromising comfort or air quality. The self-learning solution offers a suitable individualization of the occupants' preferences using their feedback.

The self-learning controller was implemented in a real building with decentralized ventilation systems using a smart ventilation concept (Internet of Things-based). The controller identified different occupant preferences in every room. Further analysis of user preferences indicates that fan noise and high relative humidities are key triggers for the operation of ventilation systems in residential buildings. Smart solutions were mentioned as one of the key aspects to increase the acceptance of the system. In conclusion, occupant-centered control strategies achieve sufficient levels of energy performance, hygrothermal comfort, and indoor air quality.

Kurzfassung

Diese Arbeit befasst sich mit Lüftungsregelungsstrategien aus der Perspektive des Bewohners. Der Einsatz dezentraler Lüftungssysteme ist in den letzten zehn Jahren in Deutschland nachhaltig gewachsen, als kostengünstige Lösung zur Gewährleistung des Luftaustausches in luftdicht sanierten Wohngebäuden. Auch wenn nutzerorientierte Regelungen oft vernachlässigt werden, könnten diese den Zielkonflikt zwischen den betrachteten Aspekten Energieeffizienz, hygrothermischem Komfort und Raumluftqualität verbessern.

Die Fensteröffnung bleibt den Bewohnern als primäre Maßnahme zur Frischluftzufuhr erhalten. Bestehende Fensteröffnungsmodelle werden überprüft und mit realen Gebäudemessungen verglichen. Eine logistische Regressionsanalyse in Echtzeit mit einem Algorithmus zur Erkennung der Fensteröffnung wird untersucht, um Nutzerpräferenzen ohne den Einsatz zusätzlicher Sensoren zu erlernen. Diese vorgeschlagene Methode kann das Verhalten der Bewohner nicht richtig erfassen, wenn Informationen über Nutzerpräferenzen nicht im Voraus verfügbar sind. Daher ist eine Rückmeldung erforderlich, um die angestrebte Individualisierung zu erreichen.

Eine Markt- und wissenschaftliche Recherche identifizierte den Mangel an multivariablen Lösungen und nutzerorientierten Ansätzen als das vordringliche Defizit bei den Wohnungslüftungsregelungen. Daher werden die drei Lösungen Komfort-orientierte Kostenfunktion, ein Regler basierend auf einer Fuzzy-Logik und eine selbstlernende Regelung auf Basis von einem Klassifizierungsalgorithmus untersucht.

Diese Regler zielen auf die relative Raumluftfeuchtigkeit und die Kohlendioxidkonzentration ab. Ein Co-Simulationsansatz kann die Leistung dieser Lösungen bewerten. Vollautomatische, multivariable Regler können im Vergleich zu modernsten Strategien rund 13% Primärenergieeinsparungen erzielen, ohne den Komfort oder die Luftqualität zu beeinträchtigen. Die selbstlernende Lösung bietet eine geeignete Individualisierung der Nutzerpräferenzen anhand ihrer Rückmeldung.

Der selbstlernende Regler wurde in einem realen Gebäude mit dezentralen Lüftungsanlagen unter Verwendung eines intelligenten Lüftungskonzepts implementiert. Der Regler identifizierte unterschiedliche raumindividuelle Präferenzen. Analysen der Nutzerpräferenzen zeigen, dass Ventilatorgeräusche und hohe relative Luftfeuchten wichtige Einflüsse für die Betriebsweise von Lüftungsanlagen sind. Intelligente Lösungen wurden als einer der Schlüsselaspekte genannt, um die Akzeptanz des Systems zu erhöhen. Zusammenfassend lässt sich sagen, dass nutzerorientierte Regelungen ein gutes Niveau in Bezug auf die drei Zielaspekte erreichen können.

Contents

1	Introduction	1
1.1	Background	1
1.2	Problem statement	2
1.3	Research questions	6
1.4	Structure and methodology	7
2	Requirements and evaluation of residential decentralized ventilation	9
2.1	General aspects	9
2.2	Energy consumption	11
2.2.1	Heat recovery	11
2.2.2	Fan energy consumption	13
2.2.3	Primary energy consumption	13
2.2.4	Energy label	14
2.3	Indoor air quality	15
2.3.1	Mold growth protection	15
2.3.2	Health effects	16
2.3.3	Indicators	18
2.4	Hygrothermal comfort	22
2.4.1	Influence of ventilation	22
2.4.2	Indicators	24
2.5	Noise	26
2.6	User-friendliness	27
2.7	Costs	28
2.8	Summary	29
3	Window opening behavior and residential ventilation	31
3.1	Modeling window opening behavior	32
3.2	Representativeness of available models	37
3.2.1	Data collection	38
3.2.2	Clustering method development	39
3.2.3	Clustering the measured window opening profiles	43
3.2.4	Comparison of measurements and available models	48
3.3	Window opening behavior as user feedback for mechanical ventilation	52
3.3.1	Learning preferences using logistic regression	53
3.3.2	A real-time window opening detection algorithm	56

3.3.3	A combination of detection and preference learning	60
3.4	Summary	62
4	Innovative control strategies for decentralized ventilation	64
4.1	State-of-the-art	64
4.1.1	Market research	64
4.1.2	Scientific research	66
4.1.3	Reference control strategies	68
4.2	Modeling and simulation	69
4.2.1	Co-simulation	69
4.2.2	Building model	71
4.2.3	Decentralized ventilation system	74
4.2.4	Occupant behavior	76
4.2.5	User interaction with mechanical ventilation	79
4.2.5.1	Model assumptions and limitations	80
4.2.5.2	Artificial comfort profiles	80
4.2.5.3	User interaction algorithm	81
4.3	User-centered control strategies	85
4.3.1	Cost function DCV	85
4.3.2	Fuzzy logic control	87
4.3.3	Self-learning DCV	91
4.3.3.1	Default comfort profile	92
4.3.3.2	Algorithm selection	93
4.3.3.3	Learning DCV process	96
4.4	Simulation case studies	99
4.4.1	Multivariable fully automated control strategies	100
4.4.1.1	Methodology	100
4.4.1.2	Results for an average week	101
4.4.1.3	Sensitivity analysis	105
4.4.1.4	Discussion	109
4.4.2	Learning DCV using different user profiles	111
4.4.2.1	Methodology	111
4.4.2.2	Control results for a single user type	112
4.4.2.3	Learning results for different comfort profiles	115
4.4.2.4	Influence of interaction frequency	121
4.4.2.5	Learning results for a mixed comfort profile	124
4.4.2.6	Discussion	126

4.5	Summary	128
5	Real building case study: Energy Smart Home Lab	130
5.1	General aspects	130
5.2	Implementation and design	131
5.2.1	Ventilation concept	131
5.2.2	Electronic set up and monitoring	135
5.2.3	User interface	137
5.3	Results	138
5.3.1	Performance indicators	138
5.3.2	Performance of the learning controller	143
5.3.3	Practical lessons learned from the field	148
5.4	Occupant behavior analysis	149
5.4.1	Analysis of user behavior and mechanical ventilation	149
5.4.2	User satisfaction	153
5.5	Summary	154
6	Conclusions and outlook	156
A	Appendix	163
A.1	Real-time logistic regression for window opening	163
A.2	Multifamily building model	166
A.3	Decentralized ventilation system model	173
A.4	Market research	180
A.5	Support vector machines	184
A.6	Learned user artificial comfort profiles	188
A.7	Room-individual results in the ESHL	192
	Nomenclature	198
	List of Figures	203
	List of Tables	209
	References	211

1 Introduction

1.1 Background

Residential building energy retrofit is necessary to accomplish the proposed energy targets in the European Union. Between 2012 and 2016, yearly primary energy savings of 1% were achieved and should increase towards 3% [72]. Ventilation heat losses were always low in comparison to transmission heat losses through the envelope, but became relevant in low-energy and passive houses where the projected ventilation and envelope heat losses are in a similar range [102]. Figure 1.1 illustrates this evolution.

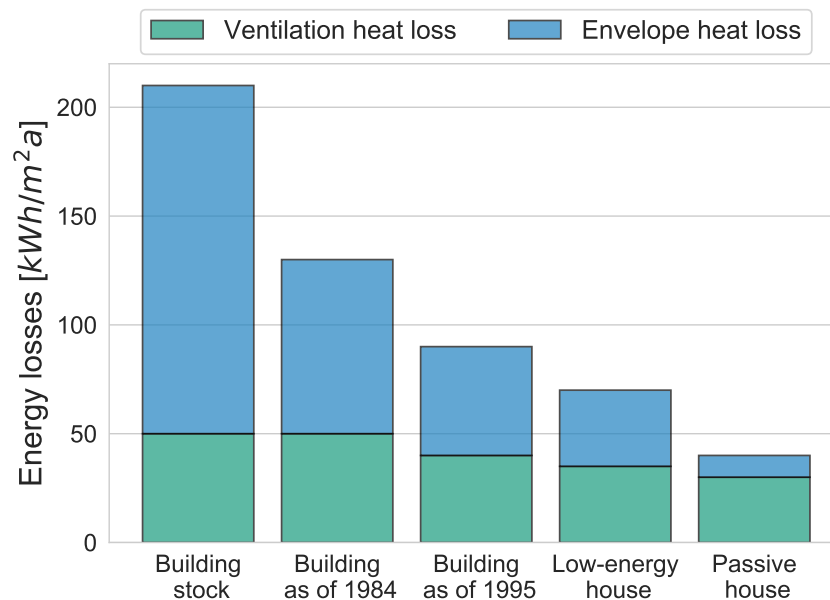


Figure 1.1: Evolution of energy losses in residential buildings [102].

Airtightness is increased in retrofitted buildings, which affects the indoor environmental conditions. In renovated multifamily buildings without ventilation in Slovakia, increased levels of indoor contaminants were observed [82]. The occupants perceived the indoor air quality as better before the renovation. This resulted also in a higher prevalence of sick building syndrome (SBS) symptoms. Francisco et al. [83] concluded that indoor air quality (IAQ) and health improved drastically when building retrofits comply with appropriate residential ventilation standards. This increasing attention to healthy indoor environments requires a response from building and ventilation system commissioners [88]. Higher ventilation rates in residences can reduce negative health outcomes generally, and there are even minimum

ventilation rates at which some health-related issues can be avoided [40]. In the case of energy renovation, designing and installing mechanical ventilation systems with heat recovery are required for ensuring the indoor environment quality and maximizing energy savings [212]. In Germany, the standard DIN 1946-6 [58] covers the design of ventilation measures, according to the building requirements. This standard applies to every new residential building and to every renovated building where ventilation-related changes were carried out. The ventilation concept assesses both natural ventilation (window opening) and mechanical ventilation systems. The main objectives of the ventilation concept are building protection as well as occupant comfort and indoor air quality. In Europe, there is no standard that covers the design of residential ventilation systems. However, there are comfort and air quality-related european standards that suggest minimum ventilation rates per room and per person to ensure indoor air quality, such as the DIN EN 15251 [59] and DIN EN ISO 7730 [61]. The DIN EN 15251 has been updated in Germany to the DIN EN 16798-1 [60] (from the British standard BS EN 16798-1) but this has not been yet extended to the rest of Europe.

1.2 Problem statement

The market for residential ventilation systems has grown in the last ten years at an average pace of 4.2 % [110]. Specifically in Germany, decentralized ventilation systems (DVS) gained relevance in both the market and scientific community. The sales trend of ventilation systems in Germany is depicted in Figure 1.2 [110]. DVS represented 17% of the total sales in 2012, and climbed to 36% in 2018, becoming the market leader in sales in that year. In 2019, the latest version of the German ventilation standard DIN 1946-6 included individual room ventilation for the first time [58].

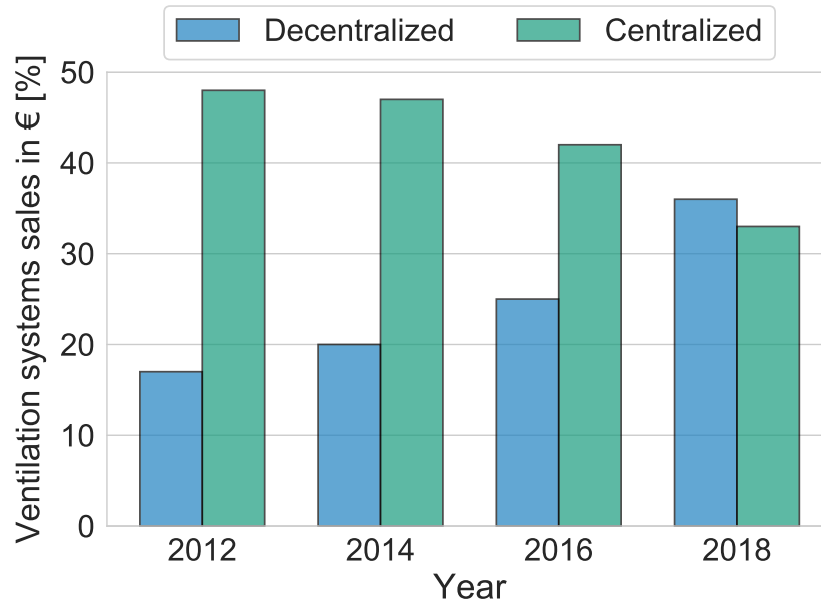


Figure 1.2: Evolution of residential ventilation market (2012-2018) in Germany [110].

Decentralized ventilation aims at providing room-individual airflow rates, which can be controlled separately. Supply and exhaust airflow is present in every room where these devices are installed, in contrast to centralized systems, where there are fixed supply rooms (living room and bedrooms) and exhaust rooms (kitchen and bathroom). An exemplary façade-integrated decentralized ventilation system (DVS) is illustrated in Figure 1.3. These units are usually equipped with a reversible fan and a heat storage. A filter is included on the room side of the device. This device operates alternating periodically in supply and exhaust mode (60 seconds respectively). These devices are often referred to as "push-pull" devices.



Figure 1.3: Exploded axonometric of a DVS [216]. 1 - Indoor panel. 2 - Reversible fan. 3 - Heat storage system. 4 - Outdoor panel.

Decentralized ventilation systems offer a cost-effective solution to guarantee air exchange in residential buildings. Maier et al. [143] report lower installation costs by about 40–55% in comparison to centralized ventilation systems and air handling units, respectively. As façade-integrated systems provide fresh air directly from the outdoor environment, the installation process is relatively simple since there is no need for ducts. However, maintenance, limited filter options, and noise pollution are known unresolved issues of these systems. Angsten et al. [16] summarizes the advantages and drawbacks of decentralized ventilation. Merzkirch et al. [151] measured different performance indicators regarding centralized and decentralized ventilation systems. Decentralized ventilation systems have typically lower fan power consumption, with heat recovery efficiencies around 70%. Short-circuit problems when two devices are placed too close to each other were also recognized.

Furthermore, Gruner [91] concluded that when embodied energy is considered, decentralized systems show a trend to be more sustainable than centralized systems. In addition, he showed that individual room control enables the improvement of indoor air quality and user satisfaction. Smith [198] studied the impact of room-individual control of ventilation systems on building moisture protection, concluding that the removal of excess humidity in kitchens and bathroom was successful. Coydon [49] conceptualized and developed an innovative dwelling-centralized ventilation solution with individualized fans, highlighting the potential of a room-individual solution to optimize energy consumption, hygrothermal comfort and IAQ. Angsten et al. [16] identified the use of advanced control strategies with indoor environmental sensors as one of the future trends for decentralized ventilation.

Despite the increasing interest in control strategies for ventilation systems in the last years, there is still a need for research, especially regarding the relationship between comfortable and healthy indoor environments [43]. The most popular control strategy in decentralized ventilation is called demand-controlled ventilation (DCV), which is an open-loop controller where the fan speed is determined by a certain sensor measurement [80]. This has already been identified as a solution to minimize energy losses and ensuring mold growth protection [184], as well as guaranteeing improvement of the IAQ [112]. Different versions of the same controller have been published in recent years, although a lack of innovation can be identified [218]. Recently, the Air, Infiltration and Ventilation Centre (AIVC) published their definition of "smart ventilation" [66]:

Smart ventilation: *”Smart ventilation is a process to continually adjust the ventilation system in time, and optionally by location, to provide the desired indoor air quality benefits while minimizing energy consumption, utility bills and other non-IAQ costs (such as thermal discomfort or noise).”*

Moreover, a smart ventilation system should adjust the ventilation rates to be responsive to one or more of the following: occupancy, indoor and outdoor thermal and air quality conditions, or electricity grid needs, among others. The occupant behavior regarding the manual operation of residential ventilation systems has been largely ignored by the scientific community until recently. A review about occupant-centric building and control design [168] showed plenty of available user-oriented solutions in several fields, except for residential ventilation. According to another review [160], controllers are being lately developed mostly reactive or predictive to presence or comfort. The implementation of demand-based solutions based on the Internet of Things (IoT) could enable adaptive control strategies to maximize IAQ in dwellings [132]. This opens the door for potential user-centered solutions for decentralized ventilation.

According to Wirth [224], balanced ventilation systems enable primary energy savings, but these can be undermined by the occupant behavior (OB). Users tend to adjust the airflow levels to their individual needs, resulting in higher airflow levels than designed. The impact of the occupant behavior concerning control of the indoor environment and operation of ventilation systems has been stated as the top research priority in this area [221]. As investigated by Gaetani et al. [86], a fit-for-purpose modeling strategy can lead to successful design in buildings. Therefore, the representation of the OB towards residential ventilation is key to the realization of occupant-centered controllers for decentralized ventilation systems.

Nevertheless, there is a lack of research connecting user behavior and residential ventilation. The AIVC published a report over ten years ago describing the occupant attitudes towards ventilation [208]. Occupants generally reported a dissatisfaction with their ventilation facilities, meaning there is a need for better solutions. Hasseelaar [103] measured the ventilation running time in about 350 dwellings. He observed that 14% of the apartments had the system turned off permanently, and in the rest, the lowest ventilation level was set for an average of 17 hours. He concluded that the industry focuses merely on meeting the minimum requirements and that the user preferences are not considered. In another study, Park et al. [166] recognized the high costs and difficulty of operation as the main reasons for not ventilating. This indicates once again that the needs of the occupant should be involved in the design

process, especially considering user interfaces.

1.3 Research questions

This work focuses exclusively on the following points:

- Residential renovated multifamily buildings
- Decentralized ventilation systems with decoupled heating systems
- Central European zone focusing on Germany, as a requirement for the definition of occupant behavior models
- Temperate climate without a dry season, as a representation of central european climate, focusing on the winter season

This thesis tackles the lack of knowledge about the relationship between occupants and residential mechanical ventilation. Understanding the needs of the users without neglecting the sight of the manufacturer is the first step to develop the mentioned occupant-centered solutions. The analysis of the occupant behavior towards ventilation (natural and mechanical) will help to gain some insight into the targets of a user-oriented system. Moreover, novel ventilation control strategies for residential buildings are proposed that are flexible enough to grasp the nature of the occupant, while still meeting the minimum requirements of the regulations. The implementation of ventilation controllers, and their connection to smart environments, is also examined. This thesis contributes to the integration of decentralized residential ventilation systems into the smart appliances world, aiming at increasing user acceptance, thus narrowing the gap between users and technology.

Based on the aspects mentioned above, the research questions can be defined as follows:

Research Question 1: *Which aspects should a residential ventilation control strategy consider to account for the occupant's needs?*

Research Question 2: *To what extent does the window opening behavior provide useful information for ventilation control strategies? How can this be represented?*

Research Question 3: *How do state-of-the-art control strategies for decentralized ventilation systems perform? Can innovative occupant-centered control solutions*

provide an improvement regarding energy consumption, hygrothermal comfort and indoor air quality?

Research Question 4: *How is the performance of innovative occupant-centered control strategies in a real-building implementation? Do they influence the acceptance of the user towards ventilation systems?*

1.4 Structure and methodology

The four research questions are answered from Chapters 2 to 5. The general methodology is condensed into Figure 1.4. In Chapter 2, the requirements for residential mechanical ventilation systems are analyzed by reviewing existing models and findings from the literature. The outcomes establish the foundations for designing occupant-centered solutions. In Chapter 3, the occupants' need for ventilation related to the window opening behavior is investigated. Window opening behavior as the need for fresh air is studied. A method to infer the ventilation preferences of the occupant without deploying extra sensors is proposed. The importance of the user feedback is therefore highlighted. Afterward, a user behavior model for the operation of mechanical ventilation systems is proposed. In Chapter 4, three multivariable occupant-centered control strategies are developed, based on the results obtained in the first two research questions. To evaluate them, models of building, occupant, and decentralized ventilation are developed, and simulation case studies are then performed. A sensitivity analysis of the results is also carried out. The best performing controller from these simulations is selected and implemented in a real building case study under a smart ventilation scheme in Chapter 5. An apartment is then equipped with decentralized ventilation systems and an IoT-based solution, to implement the selected user-centered strategy from the previous chapter. Results are collected to evaluate the performance of the controller, the ventilation system and to further investigate the occupant behavior regarding residential mechanical ventilation. Finally, Chapter 6 summarizes the findings of this thesis. Future recommendations for further research and potential application cases are discussed.

∞

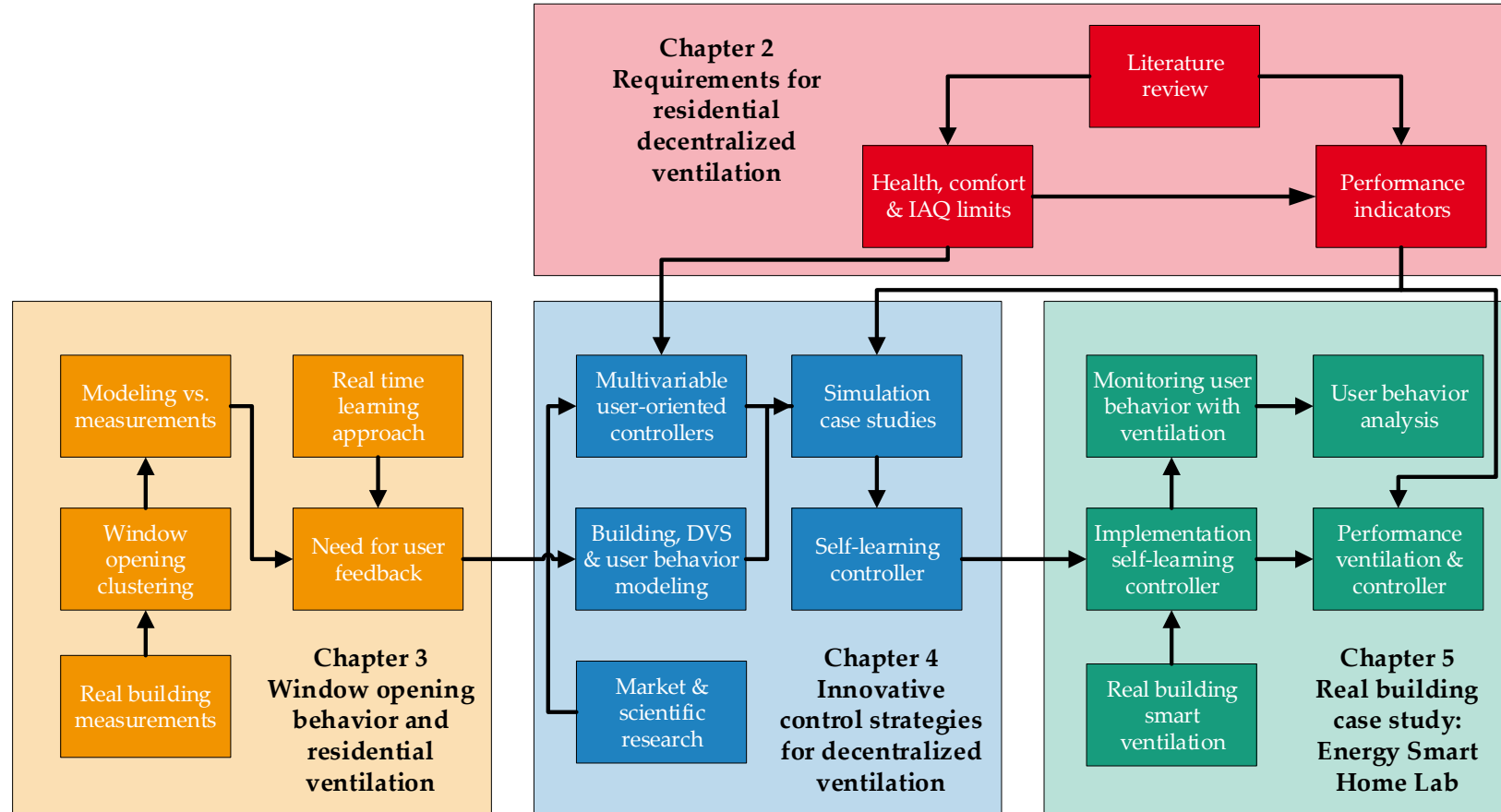


Figure 1.4: Flowchart of the thesis structure.

2 Requirements and evaluation of residential decentralized ventilation

The goal of this chapter is to discuss the different requirements to define an evaluation method for ventilation control strategies. Housing associations, manufacturers, and end users play different roles in this evaluation. In order to provide the foundations for this analysis, the considered variables are described from a scientific point of view. Following normative standards and current scientific research, performance indicators are selected to evaluate the performance of residential mechanical ventilation systems properly.

2.1 General aspects

Ventilation systems allow residential buildings to ensure an adequate air exchange when natural ventilation is not enough. As mentioned before, efficient control systems are relevant to ensure indoor comfort and air quality, while minimizing the energy consumption. Decentralized ventilation systems (DVS) allow a higher flexibility, given the possibility of controlling the airflow in every room.

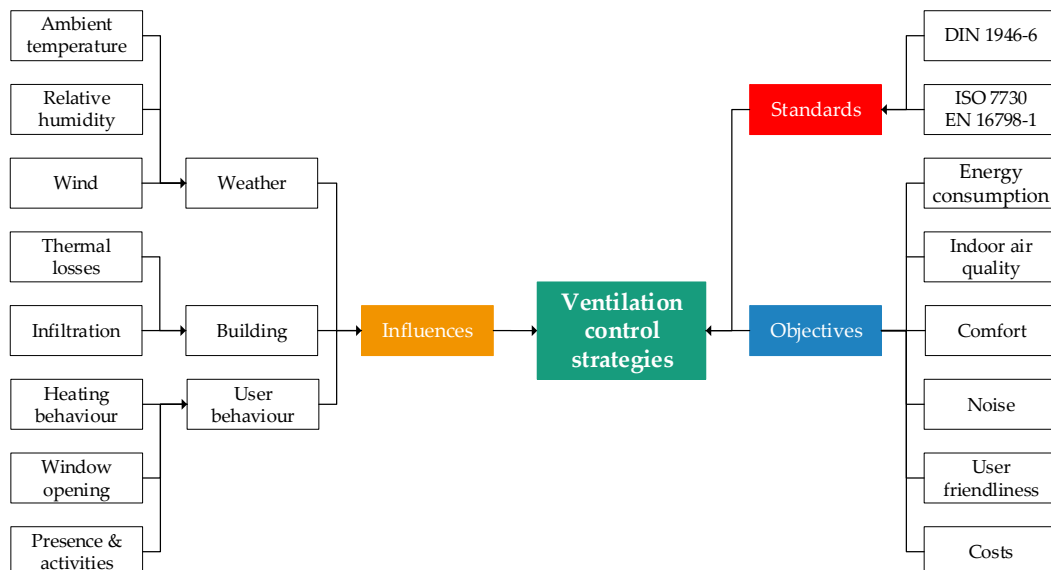


Figure 2.1: Overview of requirements for ventilation control systems.

Figure 2.1 shows an overview of the objectives, standards, and external influences of

control strategies for ventilation systems. The objectives and standards are further analyzed in this chapter. The influence of the occupant behavior on mechanical ventilation is studied in Chapter 3. The weather and building influences are tackled in Chapter 4.

In Germany, the standard DIN 1946-6 sets the requirements for air exchange in residential buildings [58]. This norm describes different scenarios in which the fresh air needs may be covered by natural ventilation as well as mechanical ventilation systems (MV) and the building infiltration. As a definition, the total supply volume flow rate of fresh air is the sum of the three aforementioned sources:

$$\dot{V}_{tot} = \dot{V}_{inf} + \dot{V}_{WO} + \dot{V}_{MV} \quad (2.1)$$

being \dot{V}_{tot} the total volume flow rate, \dot{V}_{inf} the volume flow rate due to infiltration, \dot{V}_{WO} the volume flow rate due to window opening, and \dot{V}_{MV} the volume flow rate due to mechanical ventilation systems [58, p. 28, s. 6.1.1]. For the selection and dimensioning of mechanical ventilation systems, the user-dependent volume flow rate (window opening) must not be considered.

Taking into account the dimensioning of ventilation systems, one of the key contributions of this norm is that it sets four different ventilation levels and their corresponding minimum outdoor airflow supply in different operating conditions:

1. Ventilation for moisture protection: the ventilation level is a function of the buildings' thermal characteristics and the dwelling area. The goal is to prevent structural damage due to mold growth. This ventilation rate must be guaranteed at any time independent of occupants.
2. Reduced ventilation: this level covers the minimum hygienic standards, in some cases by considering reduced humidity loads.
3. Nominal ventilation: ventilation to ensure the hygienic requirements as well as building protection during occupant presence.
4. Intense ventilation: required ventilation level to cover the peak internal loads (human activities) that might occur in residential indoor spaces. In this case, the user-dependent ventilation must be considered.

As stated before, the calculation of the necessary outdoor airflow includes the air exchange due to infiltrations and natural ventilation. This means the total fresh

air supplied by a mechanical ventilation system is the remaining air that was not provided by infiltration or window ventilation (for the infiltration estimation, wind load, and seasonal variation assumptions are made).

In addition, the standard defines different control strategies for room-specific ventilation systems [58, p .125, S I.3.4]: permanent operation, controlled by time or controlled by a specific sensor, such as temperature or relative humidity (*RH*). A permanent operation does not guarantee high humidity loads removal. On the other hand, a fixed time-dependent control strategy does not usually guarantee the building protection and is therefore undesired. According to the standard, only the relative humidity control strategy guarantees the removal of high humidity loads in the indoor environment. It is a goal of this thesis to assess to what extent different control strategies could optimize energy consumption, comfort, and indoor air quality in the residential sector. In the following sections, reference values and performance indicators regarding the objectives of a ventilation controller are discussed, selected, and defined.

2.2 Energy consumption

In decentralized ventilation systems decoupled from heating systems, heating and cooling energy is neglected, as these devices usually do not have such equipment. In that sense, the heating energy consumption is considered through the heat losses due to ventilation. Increasing the forced air exchange in a residential building will cause higher heating energy losses. The heat losses due to ventilation represent the highest energy consumption of residential mechanical ventilation systems [133]. To reduce these losses, ventilation systems are typically equipped with heat recovery systems (HRC), which provide a heat exchange interface between supply and exhaust air. The second highest consumption is the electrical power consumption of the fans.

2.2.1 Heat recovery

Heat recovery systems are designed and adapted to the different ventilation systems available on the market to reduce the heat losses due to ventilation. For example, continuous ventilation systems are typically equipped with recuperative counter flow heat exchangers which provide a heat transfer interface while at the same time avoiding contact between the air streams. In the case of decentralized reversible ventilation systems, most of them provide a regenerative heat storage system (typical

materials include ceramic, polymers, or metal) to store the heat in the exhaust phase and release it during the supply phase. In this thesis, only ventilation systems with heat recovery are examined. When considering the systems' efficiency, different definitions are used. A comparison of the different methodologies and their impact on the resulting efficiencies is available in the literature [49]. For example, heat recovery systems are mandatory in Passive House certification for ventilation systems [169]. Their requirement includes a minimum efficiency of 75%. Their definition of HRC efficiency is obtained by adding the heating energy required due to ventilation losses to the heat release of the fan to the room.

In the case of continuous decentralized ventilation systems, the degree of temperature change (*Temperaturänderungsgrad* in German) $\eta_{HRC,Cont}$ is usually adopted. This indicator only takes into account the heating energy losses due to ventilation and neglects others, such as enthalpy or fan power consumption. This indicator assumes that the supply and exhaust mass flow rates are balanced and that the average temperatures are equivalent. Even though this indicator is valid for balanced mechanical ventilation systems, the lack of normative foundations for alternating systems and the simplicity of the calculation procedure makes this definition of the heat recovery efficiency the most accepted one among manufacturers of DVS [149]. Coydon [49] developed a rule-based model to calculate the heat recovery efficiency for alternating ventilation systems. To calculate this efficiency, information about the status of the residential heating system is necessary, therefore it is impractical for laboratory measurements and manufacturers. In this thesis, the degree of temperature change $\eta_{HRC,Cont}$ is used, defined in Equation 2.2. Ambient, room, and ventilation supply temperatures are used.

$$\eta_{HRC,Cont} = \frac{T_{sup} - T_{amb}}{T_{room} - T_{amb}} \quad (2.2)$$

The total heating energy loss due to ventilation ($Q_{heat,vent}$) used in this work is calculated by integrating the heat flux losses due to ventilation after heat recovery over time, defined in Equation 2.3. As mentioned before, the heat recovery efficiency for continuous ventilation systems is used. The air properties are assumed constant for dry air ($\rho_{air} = 1.2 \text{ kg/m}^3$, $c_{p,air} = 1.005 \text{ J/kg} \cdot \text{K}$).

$$\begin{aligned} Q_{heat,vent} &= \int (\dot{Q}_{heat,vent} - \dot{Q}_{HRC}) \cdot dt = \\ &= \rho_{air} \cdot \dot{V}_{air} \cdot c_{p,air} \cdot (T_{room} - T_{amb}) \cdot (1 - \eta_{HRC,Cont}) \end{aligned} \quad (2.3)$$

2.2.2 Fan energy consumption

The fan power is usually system specific and therefore difficult to generalize [133]. The norm DIN 1946-6 [58, p. 66, Eq. 34] defines the specific fan power index (SFP) as the relationship between the nominal fan power ($P_{fan,nom}$) and the nominal volume flow ($\dot{V}_{fan,nom}$). The SFP is calculated in $\frac{W \cdot h}{m^3}$.

$$SFP = \frac{P_{fan,nom}}{\dot{V}_{fan,nom}} \quad (2.4)$$

According to the device certification procedure for ventilation systems of the Passivhaus Institute [169], the SFP should not be higher than 0.45. According to the literature, the values in decentralized ventilation systems range from 0.1 to 0.35 [49, 150]. In these devices, fans are usually small, and a constant SFP can be assumed. This assumption is not valid when considering centralized ventilation systems. Some manufacturers calculate the SFP for different fan speeds. Ideally, the hydraulic power of a fan varies with the cube of the rotational speed, according to the affinity laws of pumps, if a constant fan efficiency is assumed. This does not occur in reality, and models are available to calculate it for fans in centralized systems [7]. The fan power is available in this thesis through measurements of the SFP for different fan speeds (See Appendix A.3). Then, the energy consumption of the fan ($E_{el,fan}$) is calculated by integrating the instantaneous fan power over time, and neglecting the influence of the fan heat losses on the supply air:

$$P_{fan} = \dot{V}_{fan} \cdot SFP \quad (2.5)$$

$$E_{el,fan} = \int P_{fan} \cdot dt \quad (2.6)$$

2.2.3 Primary energy consumption

In this thesis, the total primary energy consumption due to ventilation $Q_{pe,vent}$ is calculated in kWh_{pe} , and defined in Equation 2.7. Assuming that the building is heated using a gas boiler, the system primary energy consumption is calculated given the heating energy losses due to ventilation ($Q_{heat,vent}$) and the electrical energy consumption of the fan ($E_{el,fan}$), together with the corresponding primary energy factors and heating system efficiency. The primary energy factors and heating system efficiency values are summarized in Table 2.1.

$$Q_{pe,vent} = f_{p,heat} \cdot \frac{f_{Hi/Hs}}{\eta_{heat,boil}} \cdot Q_{heat,vent} + f_{p,elec} \cdot E_{el,fan} \quad (2.7)$$

Variable	Definition	Unit	Value	Source
$f_{p,heat}$	Gas primary energy factor	$\frac{kWh, pe}{kWh, gas, Hi}$	1.10	[29]
$f_{Hi/Hs}$	Gas inferior-superior energy factor	$\frac{kWh, gas, Hi}{kWh, gas, Hs}$	1.10	[225]
$\eta_{heat,boil}$	Yearly mean boiler combustion efficiency	$\frac{kWh, heat}{kWh, gas, Hs}$	0.86	[225]
$f_{p,elec}$	Electricity primary energy factor	$\frac{kWh, pe}{kWh, el}$	1.47	[85]

Table 2.1: Assumed primary energy factors and heating system efficiency values.

2.2.4 Energy label

The European Commission implemented through the Commission Delegated Regulation 1254/2014 supplementing Directive 2010/30/EU of the European Parliament and the Council [71] an energy labeling method for residential ventilation units. To classify a certain product considering its energy consumption, the Specific Energy Consumption (SEC) is calculated according to the Annex VIII of the Regulation. This indicator is expressed in $\frac{kWh}{m^2 \cdot a}$, meaning the yearly energy consumed for ventilation per m^2 heated floor area of a dwelling or building. This indicator results in an energy label from A+ (most efficient) to G (least efficient). This label is usually informed together with nominal airflow and noise level protection.

This item becomes relevant due to its calculation: in the method, there is a non-dimensional control factor, which assumes a certain value according to the control system (from manual control to local demand control). This control factor affects significantly the variation of the SEC and, hence, decide if a unit is labeled “more energy efficient” simply by offering more sophisticated control strategies. For manufacturers, energy efficient control strategies can therefore become not only a tool to reduce operating costs, but also a powerful argument for marketing purposes. For example, a “manually regulated control” has an associated coefficient of 1, whereas a “fully automatic control” receives a coefficient of 0.65, enhancing the energy label

of a single device by one or two categories.

2.3 Indoor air quality

One of the key objectives of decentralized residential ventilation systems is to properly control the indoor air quality, in order to minimize the effects of contaminants on the occupants. This section describes the studied consequences of poor IAQ for humans and defines the target variables to measure it.

2.3.1 Mold growth protection

One of the key aspects of residential mechanical ventilation is ensuring protection against mold growth. As mentioned before in Section 2.1, the norm DIN 1946-6 [58, S. 8] establishes a minimum ventilation level for moisture protection, as a function of the characteristics of the building, to prevent mold growth. The growth of different kinds of fungi in residential buildings has severe negative effects both on the materials and the occupants' health, and building remediation does not eliminate molds [173]. From the side of the housing associations, mold growth protection is the most important feature of a residential ventilation system.

It is not a simple task to determine the critical moisture level for mold growth in building materials [117]. In the World Health Organization guidelines for indoor air quality [228], several authors and their investigations about mold growth in indoor spaces are listed. These authors conducted on-site as well as laboratory experiments to characterize the growth of several fungi species in different building construction materials. In all cases, it was observed that the presence of mold is related to the surface temperature of the material and the humidity content. Hence the importance of appropriate air exchange in residential buildings is highlighted. Viitanen et al. reported that mold fungi grow above an indoor relative humidity of 75% and within a temperature range of 5-40 °C [217]. This finding was confirmed later by Rowan et al. [187]. Sedlbauer [192] developed a model based on fungi germination time, as a function of the temperature and RH , defining characteristic curves for every type. In his publication, different fungi types are grouped into three main categories: highly pathogenic fungus, long exposure time pathogenic fungus, and economic fungus (where no health hazard is found, but economic damage to the building might be caused). The last two categories were found to have similar characteristic curves. In this publication, it was defined that a global value below 70% RH leads to a safe

mold-free building. This was confirmed by Moon and Augenbroe [156], who stated that a global 80% RH is considered a reasonable limit to prevent mold growth.

To summarize, in this thesis a global threshold of 75% RH is assumed to assess mold growth potential in humid rooms in residential buildings (such as bathrooms or kitchens).

2.3.2 Health effects

Preventing mold growth is not the only health-related issue for ventilation systems. In the last forty years, several studies reported that altering the indoor environmental quality can have different effects on the occupants' health and wellbeing.

In one of the first studies relating health and indoor environment, Arundel et al. [19] concluded that the indirect adverse health effects of relative humidity in buildings are minimized when it is kept between 40 and 60%. This is relevant especially in winter when higher air exchange rates can cause frequently a drop in the indoor RH to levels below 30%. Figure 2.2 shows a summary of different reported health effects and its dependency on the indoor relative humidity level. These results have been the basis of many health-related effects studies in the last 30 years.

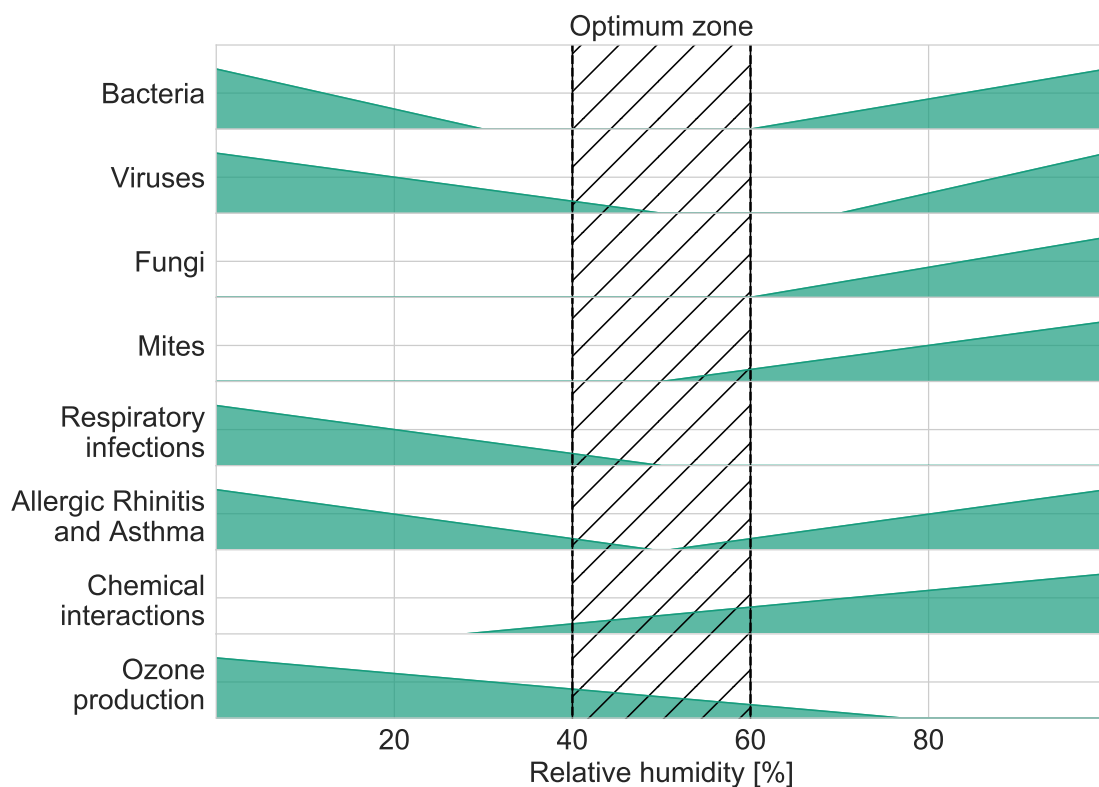


Figure 2.2: Relative humidity and health effects - adapted from [19, F. 1].

The relationship between bacteria and viruses and low relative humidities has been studied for more than 70 years. Dunklin and Puck [65] identified in 1948 that the slope of the atmospheric bacteria killing process is strongly influenced by the relative humidity. This means an indoor environment with 50% *RH* would much more quickly kill the airborne microorganisms than an environment with 20% or 80%. More recently, Lowen et al. [140] observed that Influenza virus has a varied sensitivity to relative humidity. They concluded that most virus particles are stable when relative humidity is below 30%, and transmission rate decays strongly around 50% *RH*. Ahlawat et al. [3] insisted on the strong correlation between the low *RH* in indoor spaces and the airborne transmission of COVID-19.

Additionally, Fisk et al. [81] reported strong evidence that poor indoor environments can significantly influence rates of respiratory disease (like allergy and asthma symptoms) and sick building syndrome (SBS). The sick building syndrome definition usually refers to a "collection of nonspecific symptoms including eye, nose and throat irritation, mental fatigue, headaches, nausea, dizziness and skin irritations, which seem to be linked with occupancy of certain workplaces" [227]. Although this concept was first studied in office buildings, it has also extended to residential buildings [88]. Besides the relative humidity, CO_2 concentration has been also typically correlated with the occurrence of sick building syndrome. For instance, Erdmann et al. [70] studied the relationship between carbon dioxide concentration and sick building syndromes in office buildings. Their findings suggest that an increase of 100 ppm in CO_2 concentration is significantly associated with a 10 to 20% higher probability of sore throat and wheeze symptoms. Other studies found associations between poor IAQ (represented by CO_2 and other contaminants) and other symptoms, like tiredness and exhaustion, headache, mood change, or anxiety [219].

Furthermore, a large number of potential contaminants have been studied to determine their contribution to poor IAQ. In addition to the *RH* and CO_2 concentration, other substances were reported (which could be dangerous), such as volatile organic compounds (VOC), particulate matter, formaldehyde, benzene, carbon monoxide, nitrogen oxides, or radon, among others [48, 1]. The main indoor pollutant sources are the occupant activities [212] as well as building or furniture materials [232]. In some cities, outdoor air pollution is also significant, and filtering the outdoor air is the main task of residential ventilation [40]. Ventilation control systems are only able to reach outdoor air quality without additional filtering or air cleaning.

These listed pollutants require mostly complex measurement systems and state-of-the-art sensors, to properly monitor their concentration in indoor environments. In

that sense, CO_2 has always been widely accepted as an IAQ indicator, due to the comparable lower measurement costs and its high correlation with other human-related contaminants [6, 70]. Establishing relationships between CO_2 concentration and health effects has always served this purpose.

Some authors studied the relationship between CO_2 concentration and bioeffluents or human odors as well. Haghghat et al.[97] compared the objective discomfort effects caused by different variables (such as indoor temperature and humidity) and contaminants (such as formaldehyde or VOC) to the human perception of this discomfort in an office building. Results suggested that the analyzed building presented "sick" symptoms objectively, but the occupants' complaints were associated with perceived IAQ rather than measured parameters. The perceived IAQ of the occupant is another key driver for actions regarding ventilation systems, and should not be neglected while studying control strategies.

2.3.3 Indicators

The Air, Infiltration and Ventilation Center (AIVC) [53] recognized CO_2 as an IAQ indicator because of its high correlation with other contaminants. The predicted percentage dissatisfied or simply percentage dissatisfied (PD) is used in most models to evaluate the user satisfaction with the indoor air quality. This concept was first introduced by Fanger to rate thermal comfort [76] and afterward extended to indoor air quality [77]:

Percentage dissatisfied: *"An estimation of how many people will find thermal comfort conditions satisfactory. Considering indoor air quality, the dissatisfied are those who found the air quality unacceptable."*

The European standard DIN EN 16798-1 takes into account the outdoor air pollution and suggests four IAQ categories based on the CO_2 concentration above outdoor level and the expected percentage dissatisfied, area, and type of room (bedroom and living room) [60, p. 50, T. B.2.1.4-1]. Table 2.2 shows these categories. This is an update of the standard DIN EN 15251 [59]. This standard has been extensively used in the last ten years and can still be found in several publications since it has not yet been updated at a European level. The air quality categories correspond to an associated expected percentage of dissatisfied occupants, based on different studies. Category IV is considered as inadmissible. Nevertheless, it should be mentioned that these corresponding categories are for energetic calculations in continuous ven-

tilation systems. A similar structure using North American guidelines can be found in the US-standard ASHRAE 62 [9].

Category	CO_2 above outdoors living room [ppm]	CO_2 above outdoors bedroom [ppm]	Expected PD [%]
I	550	380	15
II	800	550	20
III	1350	950	30
IV	>1350	>950	40

Table 2.2: Air quality categories from DIN EN 16798-1 [60, p. 51, T. B.2.1.4-2].

Furthermore, the IEA-EBC Annex 68 [1] reported long and short-term exposure levels for different contaminants and suggested using an aggregation of the DALY (Disability adjusted life year) and ELV (Exposure limit value) approach for multi-contaminant evaluation. The DALY indicator estimates the equivalent number of years lost from premature death and disability due to exposure to a certain contaminant, making it suitable for long-term exposure evaluation. On the other hand, the ELV presents a simple approach by comparing an instantaneous measurement of a contaminant with a certain threshold value, with only two possible outputs (below or above). Turner et al. [206] suggested to use the DALY approach, but monetarizing the outcome to compare the impact of different contaminants.

Coydon [49, p. 55, E. 76] used an absolute threshold for CO_2 (1000 ppm) and integrated over time the difference between the instantaneous concentration values and this threshold whenever it is exceeded. The time integration is also recommended by the Annex 68 [1] with the ELV approach. This approach is suitable to evaluate sudden peaks of high exposure and its relative impact in comparison to long exposure to slightly high concentrations. Therefore, it is used as the main indicator, although the value of the CO_2 threshold is further discussed.

This CO_2 concentration threshold varies according to the source. According to the AIVC [6], 100.000 ppm will lead to death. For occupational hygiene 5000 ppm is the absolute limit. For IAQ purposes, between 1000 and 1500 is recommended. The experts' commission of Annex 68 [1] concluded that a 1250 ppm short-term exposure is acceptable. The American standard ASHRAE 62 [9] takes 1000 ppm as a valid limit. The German Ministry of Environment (*Umweltbundesamt* [207]) states that 1000 ppm is hygienically safe, between 1000 and 2000 is elevated and above 2000 ppm is unacceptable. The DIN EN 16798-1 [60] suggests using 1350 ppm

in bedrooms and 1750 ppm in living rooms as the acceptability threshold (assuming 400 ppm as the outdoor concentration).

Nevertheless, the occupant discomfort with the indoor environment can also be related to perception, rather than to measured unhealthy environments. This means that an indicator related to this subjective perception should be included while considering ventilation control strategies. In that sense, Fanger [77] created an indicator of perceived IAQ related to bioeffluents and human odors. The used measurement unit is the *decipol* and was defined as "the pollution caused by one standard person (...) ventilated by $10 \frac{l}{s}$ of unpolluted air" [77, p. 3]. Fanger associated this perceived air pollution with occupant dissatisfaction (% percentage dissatisfied - PD) and ventilation rate. To build a relationship between discomfort and CO_2 , the *olf* unit must be related to the indoor concentrations, as shown in the European guideline for ventilation requirements [48]. Fanger fitted the PD values with the CO_2 concentration in a logarithmic equation, defined in Equation 2.8.

$$PD_{Fanger} = 395 \cdot \exp(-15.15 \cdot CO_2^{-0.25}) \quad (2.8)$$

Gunnarsen and Fanger [94] further studied the adaptation of the occupant to different indoor environments. They concluded that adaptation improves the acceptability of IAQ when it is polluted by human activities, though they might be neglected if sufficient ventilation is assured. They extended the decipol-model in adapted and unadapted environments.

Analogous to the decipol, Jokl [118] related human odor intensities with human CO_2 production in a new unit called *decicarbdiolx*. Its scale is also logarithmic, following the findings of Fanger [77]. Jokl introduced the concept of adaptation of the occupant to the environment, by creating two different functions that associate percentage dissatisfied and CO_2 concentration (Equations 2.9 and 2.10). A summary of the reviewed functions is shown in Figure 2.3.

$$PD_{Jokl,unad} = \exp\left(5.98 + \left(\frac{CO_2}{55833}\right)^{-0.25}\right) \quad (2.9)$$

$$PD_{Jokl,ad} = \exp\left(5.98 + \left(\frac{CO_2}{167353}\right)^{-0.25}\right) \quad (2.10)$$

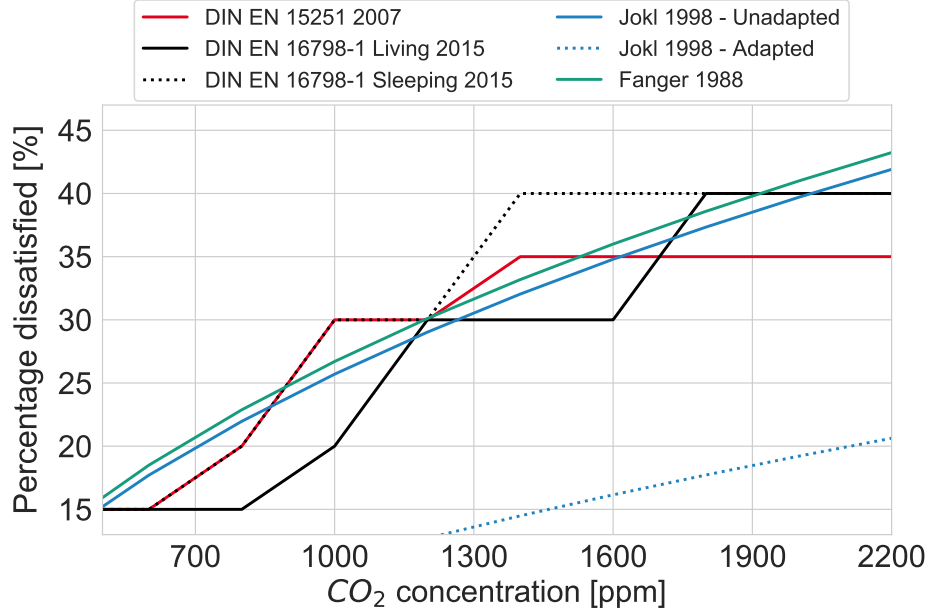


Figure 2.3: Comparison of available dissatisfaction models due to CO_2 concentration.

For unadapted persons optimal (PD=20%) and admissible (PD=30%) values are 1015 ppm and 1570 ppm. For adapted persons optimal (PD=20%) and admissible (PD=30%) values are 2420 ppm and 4095 ppm. These models that correlate CO_2 room concentration and user dissatisfaction are further referenced in chapter 4.3.

In this work, a general limit value of 1250 ppm is considered, following the recommendation of the experts' group in the Annex 68 [1], and used as the global threshold in the Equation 2.11. This value corresponds to the inflection point, where almost every studied model surpasses the 30% dissatisfaction threshold, which is usually acknowledged as the admissible limit. Equation 2.11 defines the ΔCO_2 indicator (in ppm), which is used to evaluate the performance of ventilation control strategies regarding indoor air quality. This indicator is only relevant when a room is occupied, thus the integration is done over the total time when a room is occupied (occ).

Indoor relative humidity arises as an additional health-related indicator, and the definition of the acceptability limits is explained in the next section together where the relationship between relative humidity and hygrothermal comfort is described.

$$\Delta CO_2 = \sum \frac{\max(0; CO_2 - 1250)}{occ} \quad (2.11)$$

2.4 Hygrothermal comfort

2.4.1 Influence of ventilation

Ventilation systems without HVAC integration are not primarily responsible for the regulation of the indoor room temperature in winter. In countries where the outdoor temperature is mostly below indoor temperature, summer night ventilation can help reduce cooling loads [193]. Extremely high indoor temperatures are not only responsible for discomfort, but also associated with sick building symptoms, as mentioned before in Section 2.3.2. Nevertheless, residential ventilation systems can contribute to improving the occupant's comfort. The effect of balanced ventilation systems with heat recovery on the indoor relative humidity is also considerable. In this section, some of the most relevant publications on the subject are reviewed.

High indoor RH may add sensitivity to temperature changes. In residential buildings without active cooling systems, the adaptive comfort model is suggested for the evaluation of indoor thermal comfort [60]. Research stated that the adaptive comfort model limits can be shifted when considering the relative humidity, suggesting that comfort temperatures are lower when humidity is high [214]. The difference in comfort temperatures between high and low humidity environments is as high as $4^{\circ}C$. In another publication [204], the upper humidity limits to prevent respiratory discomfort of occupants were studied (focusing more on summer conditions). The upper limits as a function of the indoor temperature and relative humidity are illustrated in Figure 2.4. This model includes air temperature and humidity (as vapor pressure) to predict the percentage dissatisfied, and it was obtained out of laboratory tests with occupants and their exposure to different conditions. Their findings report that a change of $1^{\circ}C$ had the same effect on acceptability as a change of 5% at $25^{\circ}C$. These findings were later confirmed in further studies [24, 119].

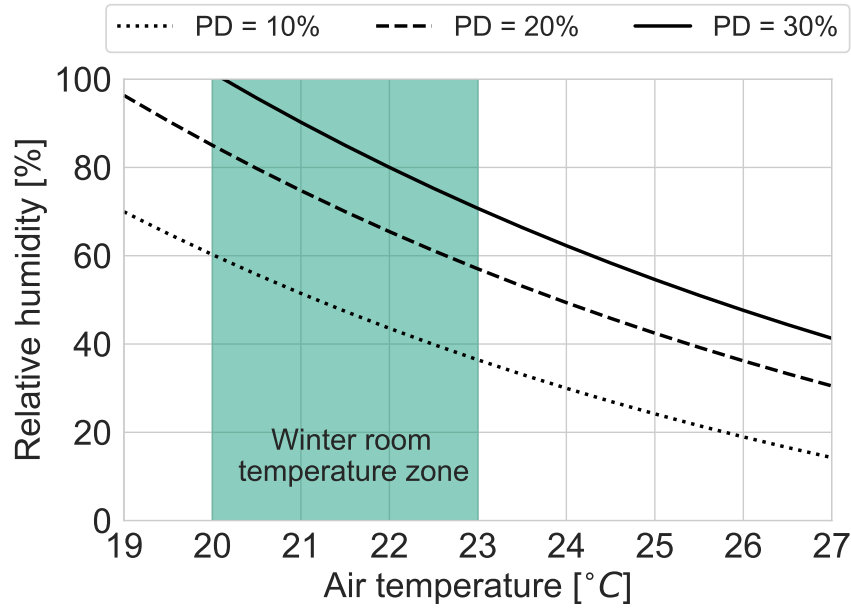


Figure 2.4: Upper limit relative humidity and discomfort - adapted from [204].

On the other hand, extremely low values of indoor relative humidity are often associated with discomfort in winter. For instance, Sunwoo et al. [200] studied the physiological response to low humidity values. Results showed that the dryness affects the human body significantly for a RH below 30%, and becomes critical around 10%. Besides, occupants felt colder when exposed to 10% RH than 30 or 50%, at the same room air temperature. This could have a direct effect on the manual control of heating systems. In another study, Wolkoff [226] illustrated the relationship between different symptoms associated with dry environments. According to their findings, dryness is present mainly in the throat, nose, eyes, and skin.

The incorrect design of ventilation systems can cause thermal discomfort to occupants. Jokl studied this phenomenon and defined it as "unwanted local cooling of the body. (...) Sensitivity to draft is greatest where skin is exposed at the head and ankles" [119, p. 21]. Draft basically depends on the temperature of the airflow, the mean air velocity, and the degree of turbulence. Therefore, the supply air temperature acquires relevance to avoid local discomfort issues. Draft is usually included in the international standards for thermal comfort and ventilation systems [11, 61]. For instance, in highly airtight buildings (i.e. passive houses) the occurrence of draft has already been registered and can have consequences not only to the comfort of the occupant but also economic consequences for landlords [55].

However, the focus of this thesis is on façade-integrated decentralized ventilation systems. Merckx et al. [148] compared the draft performance of three decentral-

ized ventilation units using computational fluid dynamic (CFD) simulations. He concluded that the draft risk is almost always low for decentralized ventilation systems, given the low air speeds in the room. These findings were later confirmed by Hörberg [107]. In her master thesis, air speeds and temperature were measured in a test chamber with two façade-integrated decentralized ventilation systems in winter conditions. It was found that draft risk can only occur at neck height (around 1.7 m), especially with cold supply air temperatures, but should not overcome the 10% dissatisfaction threshold. Wu et al. [229] also investigated the influence of the supply air temperature, who concluded that there was no significant vertical room temperature difference for mechanical ventilation systems, and confirmed that draft can be only expected at the neck. Hence, it can be concluded that the draft risk for decentralized systems is low, even for cold supply air temperatures, and will not be further considered in this thesis.

2.4.2 Indicators

Regarding indoor hygrothermal comfort, room air temperature and relative humidity are the essential indicators. However, residential ventilation systems are not responsible for controlling the indoor room temperature. In that sense, the RH is taken as the main comfort indicator in this thesis.

Coydon defines two equations for the upper and lower admissible humidity limits [49, p. 55, E. 74-75], where again the difference between the instantaneous value of the relative humidity is compared to a certain threshold, and integrated over the total time of an occupied room:

$$\Delta RH_{up,Coydon} = \sum \frac{\max(0; RH - 70)}{occ} \quad (2.12)$$

$$\Delta RH_{lo,Coydon} = \sum \frac{\max(0; 40 - RH)}{occ} \quad (2.13)$$

These equations are used in this thesis to analyze the performance of the ventilation systems in terms of the indoor RH , but with a redefinition of the selected threshold values. To define these threshold values, the RH influence on health (Section 2.3.2) must also be considered. The norm DIN EN 16798-1 defines three indoor air categories for the humidification of air in centralized HVAC systems (Table 2.3). Category IV is considered as inadmissible. Besides, the absolute humidity must be kept under $12 \frac{g}{kg}$. These results are the same in the standard ASHRAE 55 from the

United States [11].

Category	RH for dehumidification [%]	RH for humidification [%]
I	50	30
II	60	25
III	70	20
IV	>70	<20

Table 2.3: Categories for air humidification and dehumidification, according to DIN EN 16798-1 [60, p. 52, T. B.2.2-1].

Considering as well the mold growth protection and health issues (Section 2.3) associated with indoor RH values, two global acceptability thresholds are defined for this thesis: 25 and 75%. The final indicators are calculated by integrating over time the difference between these limits and the actual value as previously suggested. Equations 2.14 and 2.15 describe these indicators. The indicator ΔRH_{up} is relevant in the humid rooms (kitchen and bathroom), and the indicator ΔRH_{lo} in the dry rooms (bedrooms and living room) - in %. These indicators intend to consider the effects of the indoor relative humidity in every analyzed aspect: building protection against mold growth, health effects on occupants, and humidity influence on hygrocomfort.

$$\Delta RH_{up} = \sum \frac{\max(0; RH - 75)}{occ} \quad (2.14)$$

$$\Delta RH_{lo} = \sum \frac{\max(0; 25 - RH)}{occ} \quad (2.15)$$

The enhancement of thermal comfort in summer conditions through decentralized ventilation falls out of scope in this thesis and is not contemplated. Draft rate is also neglected in this study since the target of the ventilation control strategy would be to minimize the airflow rate (already considered in the minimization of the energy consumption), and is also strongly related to the dimensioning and positioning of the devices in the room.

2.5 Noise

Another central issue for decentralized ventilation systems is noise pollution. Manz et al. [145, p. 46] concluded that the "(...) most critical for successful applications of single room ventilation units are the acoustic properties. Indoor sound pressure levels of the investigated units are too high for many applications. Additionally, because of the transmission of outdoor noise through the units, the applications of the investigated units are limited to cases where a low (...) sensitivity of the building occupant for noise exists. If the requirements are higher, sound reduction in the units has to be increased". Mahler et al. [141] studied the performance of decentralized ventilation systems in 50 office buildings, and the highest number of complaints recorded were due to noise. Lai et al. [130] surveyed 46 apartments in China, discovering that high noise levels were the second most frequent reason not to use residential mechanical ventilation.

Noise pollution in residential buildings can have different sources. First, there is the noise produced directly by the fans of a ventilation device. This is usually due to high air speed in the ducts or a wrong position of the fans. In façade-integrated decentralized ventilation systems, the fan is close to the occupants, and therefore the risk of disturbance is considerably higher. If these change their direction periodically, the whole process is often annoying to the human ear [49]. On the other hand, using mechanical ventilation usually reduces the operation of windows, which is often associated with outdoor noise pollution, especially in big cities.

A model developed by Rasmussen et al. [181] associated residential ventilation noise levels with percentage dissatisfied. Noise levels over 30 dB(a) cause over 20% dissatisfaction (Table 2.4). In addition, the Passive House Institute defines a limit of 25 dB(a) in bedrooms and 30 dB(a) in living rooms for the certification of ventilation systems [169]. The standard DIN EN 16798-1 defines 40 dB(a) in living rooms and 35 dB(a) in bedrooms as the admissible limits [60, p. 55, T. 5-1].

Room class	A	B	C	D	E	F
Noise from building services [dB(a)]	<20	<24	<28	<32	<36	<40
Occupant dissatisfaction [%]	<5	5	10	20	35	>50

Table 2.4: Class limits for residential HVAC systems' noise [181].

Öhrström et al. [163] found significant differences in sleep disturbance for bedrooms with and without ventilation systems. Following that trend, Boerstra et al. [25]

measured noise levels over 30 dB(a) in 86% of the studied bedrooms with mechanical ventilation. The standard VDI 2081-1 calculates the sound pressure level (L_{W4}) of a fan proportionally to the logarithm of the volume flow [215, p. 19, E. 13]:

$$L_{W4}[dB(a)] = \propto \log(\dot{V}_{fan}) \quad (2.16)$$

This equation corresponds to the noise measurements of Manz et al. [145]. Active noise control is a task related to product development (design, shape, material selection, etc.), rather than to a controller. For a smart control system, noise control can only be related to the volume flow control, as suggested in Equation 2.16. Therefore, there will be no extra indicator that considers this aspect. Nevertheless, the noise is considered indirectly through the device volume flow. A smart control system aims at reducing the unnecessary air exchange rate, hence having an impact on every indicator related to it (such as energy consumption and noise pollution).

2.6 User-friendliness

The ongoing problems between occupant behavior and smart technologies have already been stated in Chapter 1.2. In that sense, user-friendliness is another requirement for ventilation systems and a key aspect of a successful technology.

In a report of the AIVC [208], some key points were outlined to consider the occupant's needs in residential ventilation devices:

- The device must not only provide a solution (i.e. to mold growth) but must be perceived by the user as useful.
- Fully automatic systems must adapt themselves to the current household. Service failures, system bugs, or unwanted behavior are decisive for its use.
- Even the most advanced systems must be operable. For example, if a user wants to turn the device off and it keeps running, the user will most probably block it.
- A suitable user interface and feedback are crucial. A study suggests that additional energy savings can be induced with adequate user feedback [45].

The industry focuses merely on meeting the requirements for building standards, and are typically technology-oriented. Then, poor results in terms of user-friendliness

can be expected. In general, there are insufficient studies about the relationship between user and ventilation systems in residential buildings [103, 208]. The occupant is not usually heard, and their needs might be different from the norm targets. For instance, a recent study in China concluded that mechanical ventilation system operation behavior differs greatly by resident and climate zone [235]. Maier [142] carried out a survey about residential ventilation in Germany and found out that several aspects are considered important to improve the user-friendliness: adjustability, multifunctionality, efficiency, low noise, and adequate user interfaces. In that sense, bringing technology closer to the everyday user is a challenge that will be further analyzed in this thesis.

2.7 Costs

The most relevant costs when designing residential mechanical ventilation systems are the initial investment (devices and installation), operating, and maintenance costs. Typically for mechanical ventilation systems, the heating energy losses due to ventilation are added, since they are usually higher than the fan energy consumption. Therefore, the annual operating cost can be defined (Equation 2.17) following the publication of Evola et al. [73].

$$cost_{op}[EUR] = cost_{heat} \cdot Q_{vent} + cost_{el} \cdot E_{fan} \quad (2.17)$$

- $cost_{el}$ is the electricity cost and $cost_{heat}$ the heating cost, both in $\frac{EUR}{kWh}$

In addition, Evola et al. [73] performed a sensitivity analysis of different variables in the operation costs of ventilation systems. To include all costs, the selected performance indicator was the payback period. The most sensitive variables for the cost structure are air exchange rate, price of natural gas (related to heating in Italy), and initial investment cost.

In another study, Coydon [49] defined a holistic evaluation method for ventilation systems, where the costs are one of the evaluated variables. Investment, maintenance, and operation costs are considered here as well. In this case, a system comparison was carried out, concluding that decentralized façade-integrated systems with a humidity-based control strategy have the lowest operating costs in Germany. Furthermore, Merzkirch [149] performed a cost analysis comparing centralized, decentralized, and semi-centralized (centralized system with decentralized fans) venti-

lation. Constant volume flow and demand-controlled ventilation are the considered control strategies. For an apartment of 80 m^2 in a multifamily building, a semi-centralized system with CO_2 -based control has the lowest primary energy consumption, followed by the decentralized systems. Volume flow, ventilation effectiveness, and heat recovery efficiency pose a high sensitivity for this value. The costs for these systems are high in comparison to a dwelling without ventilation. Merzkirch estimates a payback period of around 30 years for these facilities. In this work, the primary energy consumption of the ventilation systems was carefully studied, but annual hourly-profiles for the cost calculations are assumed. In contrast, Evola et al. [74] obtained different payback periods, of around two years for extract ventilation and four years for balanced ventilation systems in Italy. In this case, the authors simulated daily ventilation profiles, assumed a constant heat recovery efficiency, and neglected summer ventilation. This last assumption drastically reduces the annual costs associated with ventilation systems, therefore obtaining shorter payback periods than reported by Merzkirch. In both studies, the selection of a different controller only affects the operating costs.

A ventilation control strategy can only influence the operating costs. Similar to noise, the operating costs are directly associated with the primary energy consumption. Therefore, costs can be evaluated through the energy consumption and are not directly considered in this thesis.

2.8 Summary

Residential decentralized ventilation systems and their control strategies must account for the valid regulatory framework, the required targets, and the influence of the user at the same time. Through a literature review, the research question 1 can be answered as through the following points:

Research Question 1: *Which aspects should a residential ventilation control strategy consider to account for the occupant's needs?*

- A ventilation control strategy must fulfill several requirements of hygrothermal comfort, indoor air quality, and health. Energy efficiency must be ensured in the development of these systems. An energy-efficient system is not only interesting for the user due to potential savings, but also for the manufacturer, as an additional sales argument. In this thesis, the primary energy consumption ($Q_{pe,vent}$) related to the heat losses due to ventilation and the fan energy con-

sumption is considered as a suitable indicator to evaluate the energetic impact of a residential ventilation control strategy.

- Regarding health and indoor air quality, relative humidity. and carbon dioxide seem to be widely accepted indicators. RH is not only associated with building protection (mold growth risk) but was also found to significantly affect the propagation of viruses and bacteria outside certain ranges. Due to their high correlation with human bioeffluents, CO_2 concentration arises as a common solution for demand-controlled ventilation. Indoor room temperature is not controlled by a mechanical ventilation system in winter but becomes a relevant variable in summer to increase thermal comfort and reduce cooling loads.
- The integration over time of the values over a certain acceptability threshold is used to define the indicators to evaluate the performance of decentralized ventilation. These threshold values are:
 - RH must ideally be kept between 40 and 60%. The acceptable limits are 25% and 75%.
 - CO_2 concentration acceptability limit is set to be 1250 ppm.
- Other contaminants could be suitable variables to use in ventilation control strategies. However, there is still a need for development of reliable and affordable sensors, which could unlock new controlling technologies soon.
- Key aspects such as noise, user-friendliness, and costs should not be neglected, as they play a key role to narrow the gap between user and technology. When evaluating a controller, noise is proportional to the logarithm of the volume flow, and operating costs are directly related to the associated energy consumption.

3 Window opening behavior and residential ventilation

The goal of this chapter is to analyze the relationship between user and technology in the case of residential ventilation. Occupants have two main alternatives to ventilate a building: opening a window (natural ventilation) or operating a fan (mechanical ventilation). In that sense, window opening behavior could provide information about the user ventilation preferences to the mechanical ventilation control strategies without requiring direct feedback. Figure 3.1 shows a schematic flow chart of the research steps in this chapter.

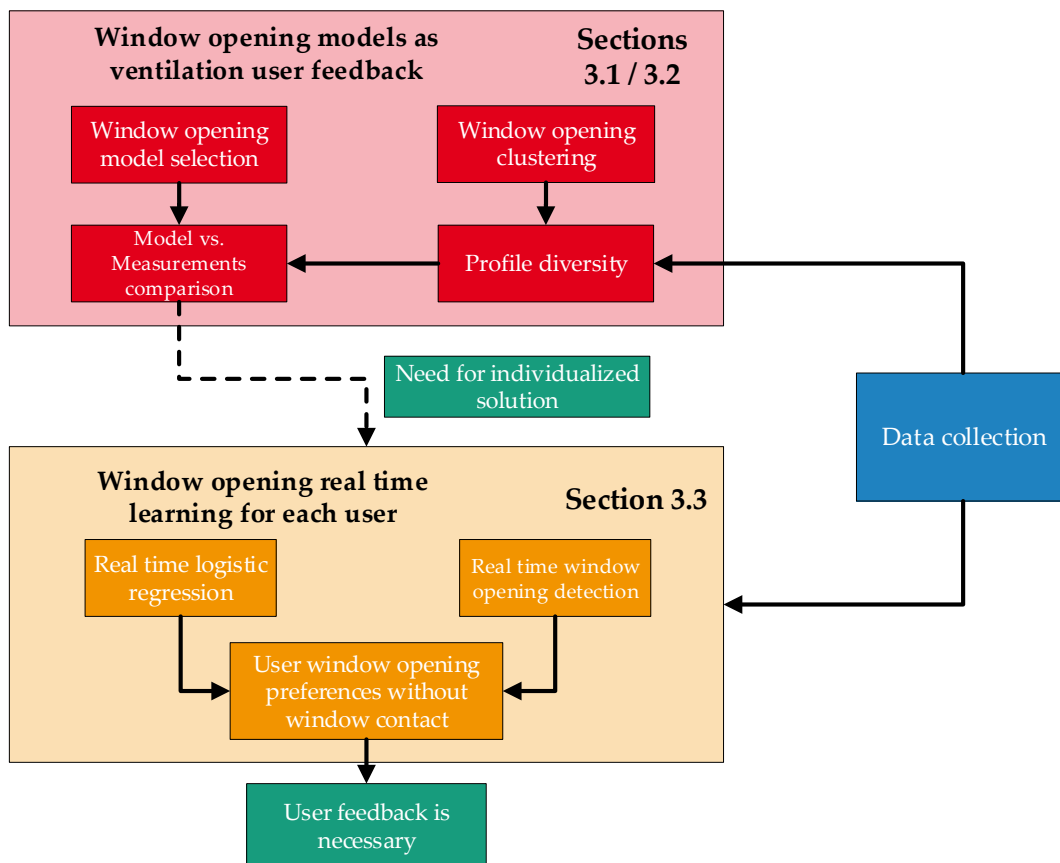


Figure 3.1: Schematic flow diagram of research method in this chapter.

Section 3.1 provides a literature review on the subject and describes the existing methods to model window opening behavior. In section 3.2, the representativity of available window opening models is investigated. The aim is to study the suitability of these models as a replacement for user feedback. A measurement campaign

was carried out, and the window opening behavior in two apartments (selected using a novel clustering method) is compared to the available models. As the need for individualized solutions arises, the possibility of learning the occupant ventilation preferences without requiring additional sensors is studied in Section 3.3. A real-time logistic regression scheme is proposed to identify window opening drivers, together with an algorithm to estimate a window opening action from the available indoor environmental sensors (as a potential replacement of window contacts). In the end, the need for user feedback to provide an occupant-centered control strategy is highlighted. The findings in this chapter are summarized in Section 3.4.

3.1 Modeling window opening behavior

This section deals with the occupant window opening behavior models. The occupant behavior concerning window opening has been studied in depth, both in residential and non-residential buildings. This section will summarize the most important publications and pick some models for further study. A complete review of window opening modeling techniques is available in the literature [51].

Researchers have been trying to model the occupant behavior using different approaches to integrate them into building performance simulation more realistically. The first efforts targeted office buildings. Fritsch et al. [84] developed one of the first published models. They simulated the occupants' window opening angle with a Markov chain. Nicol et al. [162] simulated window opening a logistic regression model dependent on the outdoor temperature. Besides, Herkel et al. [105] used also a logistic regression model, depending on the outdoor and indoor temperature, season, and occupancy patterns. The model developed includes the arrival and departure of occupants into office spaces and the length of the opening. In addition, Rijal et al. [185] developed a model regarding the adaptive thermal comfort algorithm, based on the indoor and outdoor temperature. Haldi et al. [100] studied several probabilistic approaches for window opening modeling. Their findings associated occupancy profiles with action probabilities and integrated Bernoulli processes with logit probabilities for window opening with Markov chains for occupancy. Moreover, Yun et al. [233] integrate user interaction frequency types (active, medium, passive) to categorize their opening probabilities.

Among the existing window opening models for residential buildings, a probabilistic model based on indoor and outdoor environmental variables is the most popular approach. For instance, Schweiker et al. [191] modeled the proportion of windows

open, taking into account indoor and outdoor temperatures. Furthermore, Andersen et al. [13] modeled opening and closing actions for building performance simulation, using multivariable logistic regression. Moreover, Calì et al. [32] developed a stochastic model to simulate opening and closing actions using data from over 300 windows. Jeong [115] studied the influence of different indoor activities (like cleaning or cooking) in the window opening behavior. In recent years, more complex modeling approaches were developed to improve the performance and generalization of the previous approaches [33, 99, 146, 154].

Since logistic regression is the most popular approach to model window opening behavior, three models using this technique in residential buildings are selected and compared. Logistic regression is a simple classification method [180] based on the concept of odds ratio (*OdR* - Equation 3.1). The odds ratio is defined as the probability of an event happening (p) over the probability of not happening ($1 - p$).

$$OdR = \frac{p}{1 - p} \quad (3.1)$$

The logarithm (or *logit*) of the odds ratio transforms an output of the range $[0, 1]$ into the entire real number range. When speaking of linearly separable data, the output of the logit function can be fitted with linear regression. Hence, Equation 3.2 defines the logistic regression function:

$$\log\left(\frac{p}{1 - p}\right) = \alpha + \beta_0 x_0 + \beta_1 x_1 + \dots + \beta_n x_n \quad (3.2)$$

- α is the intercept
- β_i is the regression coefficient of the explanatory variable x_i

Then, several different explanatory variables can be used to predict the state of the window in different scenarios using logistic regression. The selected models are described as follows, and their regression coefficients are listed in Table 3.1. They are valid for every season in renovated residential buildings.

1. Schweiker et al. [191]: this model calculates the probability of observing an open window, depending on the indoor and outdoor temperature. Measurements were collected in two apartments in Switzerland in 5-minute time intervals. The measured dwellings did not have any air-conditioning or mechanical ventilation. The published model includes only living room windows.

2. Andersen et al. [13]: in this case, window opening and closing actions were modeled independently. Several indoor and outdoor environmental variables were fitted to the model, as well as season or time. Measurements were collected in Denmark in 10-minute time intervals, distinguishing between owned or rented, with natural or mechanical ventilation. The obtained models are divided into four groups. In this thesis, the model corresponding to rented apartments with mechanical ventilation (group 4) is considered. The model distinguishes between living rooms and bedrooms.
3. Calì et al. [32]: window opening and closing actions were modeled independently. Measurements were taken in multifamily buildings in south Germany with 1-minute time intervals, with over 300 windows measured for three years in total. The only published coefficients correspond to the measurements in the living rooms of one particular section of a building (B2E1) during the day, where only exhaust ventilation was available.

Explanatory variable	Schweiker et al. [191] Neuchâtel	Andersen et al. [13] Group 4 Living	Calì et al. [32] B2E1
Intercept	0.711	-3.56	-7.795
T_{room} [$^{\circ}C$]	-0.3077	-0.38	0.134
RH_{room} [%]	n.a.	n.a.	n.a.
$CO_{2,room}$ *	n.a.	0.30	-551.15
T_{amb} [$^{\circ}C$]	0.3813	0.059	n.a.
RH_{amb} [%]	n.a.	0.029	n.a.
Solar rad. [W/m^2]	n.a.	0.35	n.a.
Solar hours [h]	n.a.	0.057	n.a.
Illuminance [lux]	n.a.	0.026	n.a.

Table 3.1: Logistic regression coefficients of window opening for each explanatory variable in three available models from the literature in winter (Solar rad. = solar radiation, n.a. = not available). *Room CO_2 concentration (Andersen et al. [13] in $[\log(ppm)]$ and Calì et al. [32] in $[ppm^{-1}]$).

Some of the key variables to predict window opening behavior used in these models are taken to study the sensitivity of these models to changes in the explanatory variables as follows. Only the variables present in more than one model are treated (indoor and outdoor temperature and room CO_2 concentration). The indoor RH is

not present in any of these models. For the other variables, the following values are assumed constant for the sensitivity analysis:

- Ambient $RH = 70\%$
- Solar radiation = $300 \frac{W}{m^2}$
- Solar hours = 7.5 hs
- Illumination = 100 lux
- Season = Winter

The following figures show the sensitivity of the models to the variation of the main variables. Figure 3.2 depicts a comparison of indoor room and ambient temperatures. CO_2 concentration is here assumed to be 750 ppm.

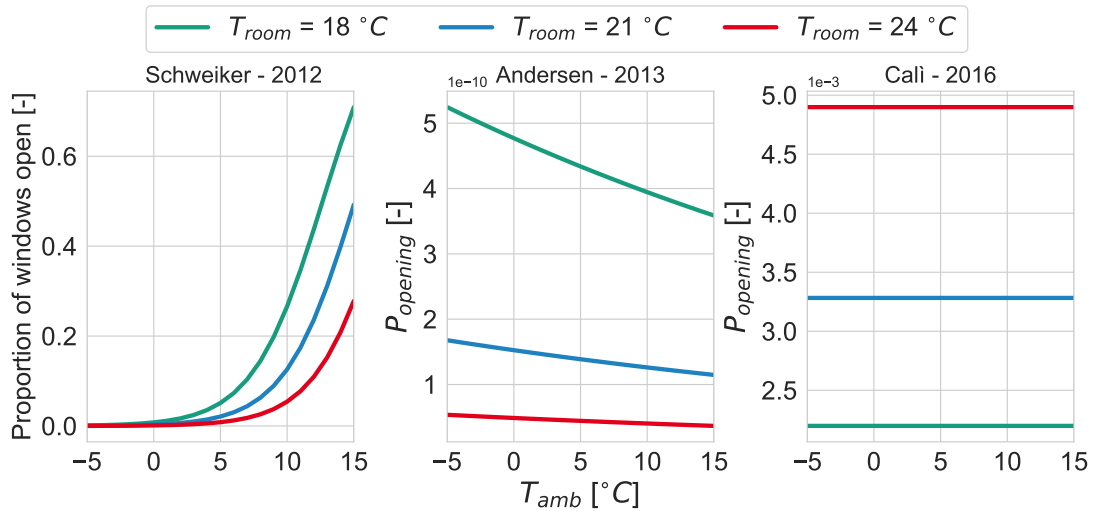


Figure 3.2: Dependence of the different window opening models on the ambient temperature at three different indoor room temperature levels.

The scales of the plot are widely diverse, being ambient temperature strongly relevant only in the model of Schweiker et al. For instance, given an outdoor temperature of 10 $^{\circ}C$ and an indoor temperature of 21 $^{\circ}C$, the model of Schweiker et al. shows a proportion of windows open of 0.14, and the other models an opening probability of 1.2 E-10 and 3.3 E-3. Besides, the shape of the curves is contrasting: Andersen et al. report a decreasing opening probability with increasing ambient temperature, Schweiker et al. the opposite, and Cali et al. constant values. Likewise, in the models of Andersen et al. and Schweiker et al., the window opening increases

when the room temperature decreases, while Cali et al. modeled exactly the contrary. The distinctive profiles repeat in Figure 3.3, for room temperature and CO_2 concentration. The ambient temperature is assumed to be $5\text{ }^\circ C$.

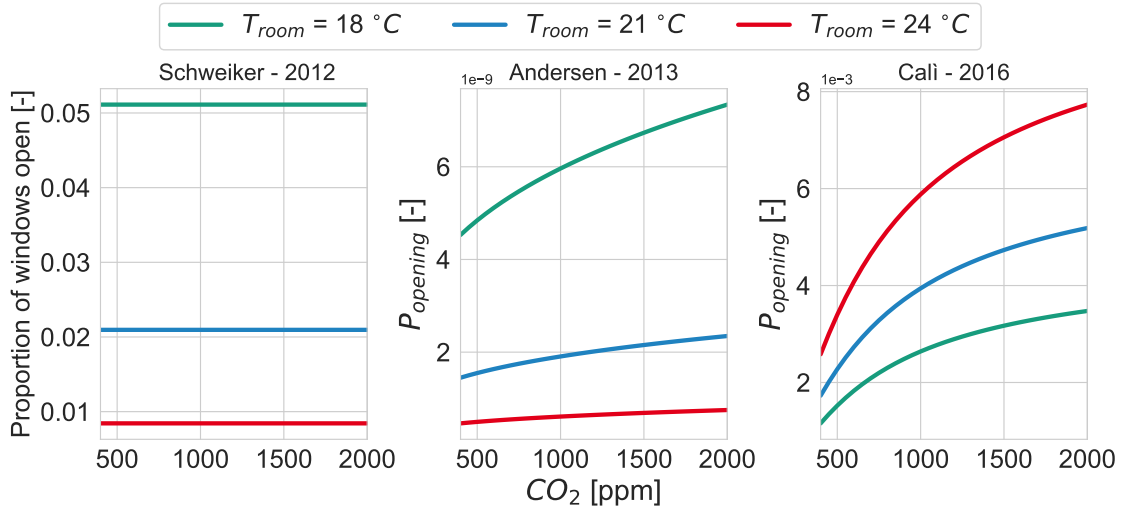


Figure 3.3: Dependence of the different window opening models on the CO_2 concentration at three different indoor room temperature levels.

These results might indicate that the obtained coefficients respond to a particular behavior. Nevertheless, the reported coefficients are so diverse that it appears difficult to define which models are the most representative. These studies were carried out in different countries in Europe, where different weather conditions may affect the obtained models, as well as cultural background and psychological differences. In the end, the models aim at providing a tool to integrate probabilistic window opening in building simulation, and it is the task of the researcher to select the suitable model for its purpose. Table 3.2 reflects a summary of the advantages and drawbacks of each evaluated model.

	Schweiker et al. [191]	Andersen et al. [13]	Calì et al. [32]
Advantages	<ul style="list-style-type: none"> • Simple model with two variables • Only temperature-dependent • Probabilistic opening angle 	<ul style="list-style-type: none"> • Opening and closing separated • 14 explanatory variables • Dwellings with MV included 	<ul style="list-style-type: none"> • Opening and closing separated • Over 300 windows measured • Time resolution high
Drawbacks	<ul style="list-style-type: none"> • Other influence factors ignored • No time-related intercept • Only living room model 	<ul style="list-style-type: none"> • More complex for BPS • Lower time resolution • Bathroom and kitchen ignored 	<ul style="list-style-type: none"> • Data from a single apartment • Presence data ignored • Time only as "day" or "night"

Table 3.2: Advantages and drawbacks of the evaluated window opening models (MV = mechanical ventilation. BPS = building performance simulation).

This review of available models creates a basis to compare to building measurements and helps to gain insight into the topic of window opening behavior in residential buildings. In the next sections, these models are compared to real window opening measurements to study the representativeness of different behaviors.

3.2 Representativeness of available models

This section aims at investigating the representativeness of the window opening models. The selected probabilistic models are compared with real building measurements. The data from different renovated apartments are clustered and diverse profiles are identified. These measured window opening profiles are compared to the selected window opening models from the previous section. The results of this section are published partially in a scientific article [38].

3.2.1 Data collection

Two measurement campaigns are considered for the study of the window opening behavior in residential buildings. The first one was carried out between 2011 and 2013 in a 16-story multifamily building in Weingarten Quartier (Freiburg, Germany), which was retrofitted to passive house standard [120]. This campaign was not carried out within the framework of this thesis. The window opening was particularly recorded in 27 dwellings over two years, in 6-minute time interval measurements. Other variables, such as indoor room temperature, thermostat control, and whole-dwelling power consumption, were also measured. The absence of data regarding relative humidity and CO_2 makes this data set inadequate to study the reliability of the window opening models. This data is used to train the proposed clustering algorithm in the next sections.

A second measurement campaign was carried out in winter 2018/2019 (138 days - from November 2018 to April 2019), also in Weingarten Quartier, Freiburg. In this case, ten apartments from retrofitted multifamily buildings were monitored, only where a mechanical balanced ventilation system was available. The dwellings' area range from 47 to 88 m^2 and have between one and three occupants. The design air exchange rate was $0.45 h^{-1}$. Sensors were placed in the dry rooms - bedroom and living room - to measure indoor temperature, relative humidity, and CO_2 concentration, and in the humid rooms - bathroom and kitchen - to measure only indoor temperature and relative humidity. Window contacts were installed in six of these ten apartments, resulting in a total of eighteen measured windows (six living rooms, seven bedrooms, three kitchens, one bathroom, and one storeroom). Table 3.3 summarizes the sensors' properties.

Sensor	Variable	Range	Accuracy
HOBO MX CO2	Temperature [$^{\circ}C$]	0-50	0.21
	Relative humidity [%]	1-90	2
	CO_2 [ppm]	0-5000	50
HOBO U12	Temperature [$^{\circ}C$]	0-50	0.35
	Relative humidity [%]	10-90	2.5
HOBO UX90-001M	State	0-1	-

Table 3.3: Sensors' properties for the second measurement campaign.

Figures 3.4 and 3.5 illustrate an exemplary floor plan of two of the measured apartments, which are analyzed in further sections as apartments 1 and 2 respectively,

used in Sections 3.2.4 and 3.3. Apartment 1 has the smallest area among the measured ones (47 m^2), and apartment 2 has the largest one (88 m^2). Figures 3.6 and 3.7 show an example of the sensor placement in these dwellings. This data is used to test the relationship of window opening behavior with other variables (such as RH or CO_2). The mechanical ventilation operation was not measured.

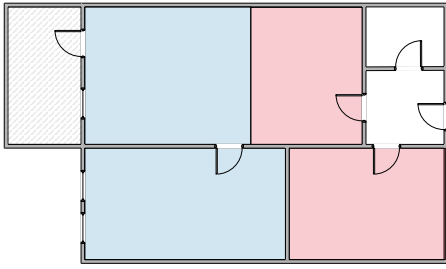


Figure 3.4: Schematic floor plan in apartment 1. Blue rooms are provided with supply air, and red rooms with exhaust air.

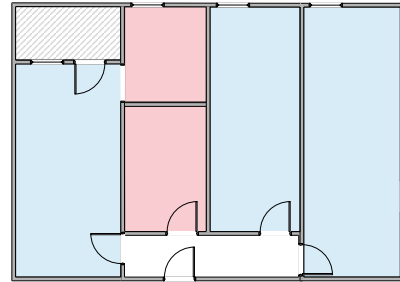


Figure 3.5: Schematic floor plan in apartment 2. Blue rooms are provided with supply air, and red rooms with exhaust air.



Figure 3.6: Window contact placement.



Figure 3.7: IAQ sensor placement.

3.2.2 Clustering method development

Clustering is the process of classifying data into different groups, aiming at finding similarities among them. A cluster is defined as a subset of objects in the database that belong to the same group. D'Oca et al. [63] concluded that clustering leads to an appropriate characterization of the occupant behavior regarding window opening. In this section, the window opening behavior of 27 measured apartments (first measurement campaign) over two years will be clustered as a time series, aiming at

obtaining distinctive behavioral profiles. This methodology is published in a scientific article [38]. The main strengths and challenges of clustering as a process are [153]:

- The attributes that differentiate one cluster from another are unknown and have to be estimated
- The data is unlabeled. This means there is no objective data on how to distinguish if one point belongs to a certain cluster or another one (except a priori knowledge provided by domain experts)
- The more data, the more complex the problem becomes
- Algorithms are influenced strongly by noisy data, missing values, and outliers. Hence the importance of an appropriate pre-processing of the data is highlighted

The innovation in this method lies on representing time series data with feature vectors, rather than data points, and its application to occupant behavior data in residential buildings. Instead of comparing a whole time series or an average profile (*shape-based* clustering), predefined indicators represent the data in a multidimensional space (*feature-based* clustering).

The shape-based process is faster (since only pre-processing of data is required to perform the clustering), although being usually more computationally expensive given the number of compared data points. On the other side, a feature-based approach compares feature vectors, reducing the number of data points. The best performing features are extracted typically from the a priori knowledge about the data and statistical indicators [95]. The main advantage of this method lies in the fast calculation process and its compatibility with other algorithms. A major disadvantage is the potential loss of information in case of not carefully selecting the mentioned features. Figure 3.8 shows the shape-based process with the whole time series, and Figure 3.9 illustrates an exemplary features-based representation using the same data.

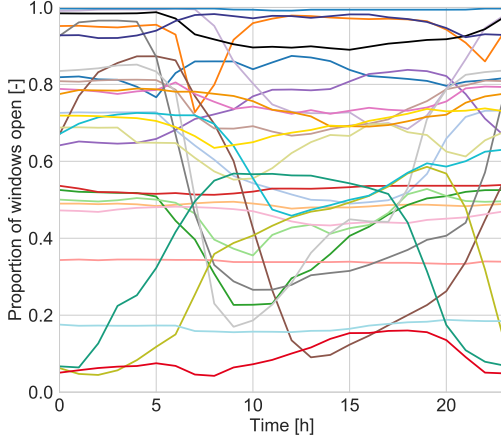


Figure 3.8: Daily mean observed window opening (proportion of windows open) profiles for the 27 apartments.

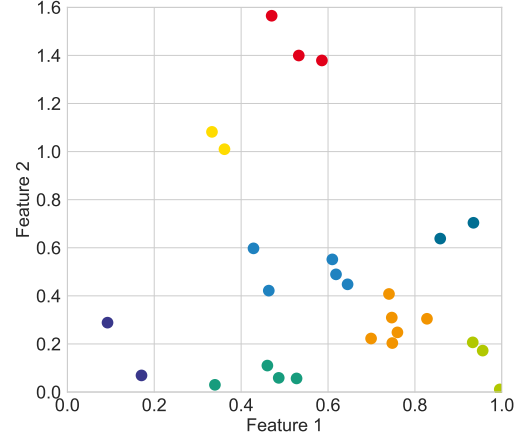


Figure 3.9: Features point representation of the 27 apartments.

Three types of features are considered: statistical (mean, standard deviation, kurtosis, and skewness, as defined in the literature [104]), time series decomposition-related (seasonality and trend [220]), and behavior-related features [96], listed in Table 3.4.

Feature	Definition
Weekend score (WkS)	$\sum \frac{\bar{X}_{week} - \bar{X}_{weekend}}{\bar{X}}$
Seasonal score (SS)	$\sum \frac{\bar{X}_{summer} - \bar{X}_{winter}}{\bar{X}}$
Day-night score (DNS)	$\sum \frac{\bar{X}_{day} - \bar{X}_{night}}{\bar{X}}$
Hour change score (HCS)	$\sum \frac{\bar{X}_{h+1} - \bar{X}_h}{\bar{X}_h}$
Average state changes (ACS)	$\sum \frac{StChg_h}{8760}$

Table 3.4: Definition of potential occupant-related features [96].

- \bar{X} is the average value of a variable X
- $StChg_h$ means changes of state per hour

To calculate the distance between the data points (features), the Euclidean distance is selected, mainly due to its simplicity and popularity (Equation 3.3) [109].

$$d(x, y) = \sqrt{\sum_{i=1}^n (x_i - y_i)^2} \quad (3.3)$$

Researchers established in the last years that the use of conventional algorithms in the clustering of static data generates results with acceptable quality and efficiency, in terms of time and accuracy [2]. In this proposed method, the centroid-based k-means algorithm was selected [180]. This algorithm is simple and understandable, but the number of clusters is an input parameter and must be known beforehand.

In addition, the goodness of clustering must be evaluated. The Dunn Index (DI - Equation 3.4) presents a widely-used measurement technique of cluster validity. The DI presents the best performance regarding the k-means clustering procedure [126].

$$DI = \min_{i=1..n_c} \left\{ \min_{j=i+1..n_c} \left\{ \frac{d(c_i, c_j)}{\max_{k=1..n_c} (diam(c_k))} \right\} \right\} \quad (3.4)$$

$$d(c_i, c_j) = \min_{x \in c_i, y \in c_j} \{d(x, y)\} \quad (3.5)$$

$$diam(c_i) = \max_{x, y \in c_i} \{d(x, y)\} \quad (3.6)$$

- n_c is the number of clusters
- $d(x, y)$ is the euclidean distance between two elements
- c_i is the centroid in cluster i

The Dunn index compares the distance between clusters (inter-comparison, to be maximized) and the diameter of every cluster (intra-comparison, to be minimized). Hence, a better clustering configuration means higher values of the Dunn index. The chosen implementation of DI compares the distance between the two closest points among clusters (minimum) with the maximum distance between cluster-centroids altogether, which does not collide with single-dwelling clusters whose diameter is zero. The working principle of this indicator is illustrated in Figure 3.10.

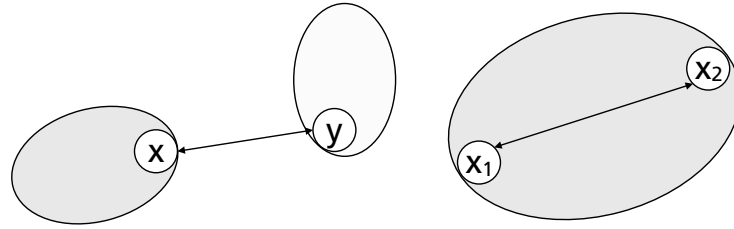


Figure 3.10: Dunn index - Intercluster (two different cluster points x and y) and intracluster (two points in the same group x_1 and x_2) comparison.

Finally, a feature elimination procedure is carried out for every considered variable. All possible combinations of features and number of clusters are tested. The result with the highest DI is selected as the optimum solution. The whole procedure is summarized in the following steps:

1. For a determined combination of features, calculate the minimal number of clusters that explain a selected threshold of 80% of the variance applying the k-means clustering method [180].
2. Calculate the Dunn index for the different number of clusters between the obtained minimum and an imposed limit of 12 clusters, as it was considered sensible for a total of 27 dwellings.
3. Selection of the best combination of features and number of clusters that result in the highest Dunn index – a priori defined features are preferred [95].
4. Analysis of results and final selection of optimal combination considering Dunn index, number of clusters, and number of features involved.

3.2.3 Clustering the measured window opening profiles

The clustering method was applied to monitoring data of the first campaign (Section 3.2.1). Window opening in the bedrooms is considered in 6-minute intervals. The data is divided into training and test data sets. The training data corresponds to the year 2013, and the test data to the year 2012 (the year 2011 was neglected due to measurement errors). The training data is used to obtain the representative features to characterize window opening behavior and validated using the test data. These features are applied to the measurements of the second campaign, and distinctive

behaviors in every room are selected and compared to the probabilistic window opening models.

Data pre-processing is key to the success of this procedure. Firstly, the data corresponding to absence periods was neglected by estimating the presence profile with the instantaneous power consumption [34]. Secondly, faulty data (sensor errors) were removed. Finally, the data is standardized by z-score normalization, using the module provided in the scikit-learn package [172].

After pre-processing the data, the data is clustered several times, using all possible feature combinations. The Dunn index was calculated iteratively for every possible combination of the number of clusters and features, and the highest values are presented in Table 3.5.

Features	Clusters	Dunn index
Mean, seasonality, skewness	3	1.8373
Mean, Hour-change score	8	1.8025
Mean, Hour-change score, Average state changes	8	1.7924
Mean, skewness	3	1.7773
Mean, seasonality, trend, skewness	3	1.7706

Table 3.5: Feature combinations with the highest Dunn index.

Results with fewer features are preferred for the sake of simplicity. The feature combination with the highest Dunn index was discarded since a minimum of four clusters was required. At least four clusters are needed to represent 80% of the variance. This is illustrated in Figure 3.11, where a comparison of the variance explained between whole time series and features-based clustering is presented for the second-best result in Table 3.5 (eight clusters). Therefore, the mean and hour-change scores were selected as the features to represent the window opening behavior. The resulting clusters with the training data set and the selected features are depicted in Figure 3.12.

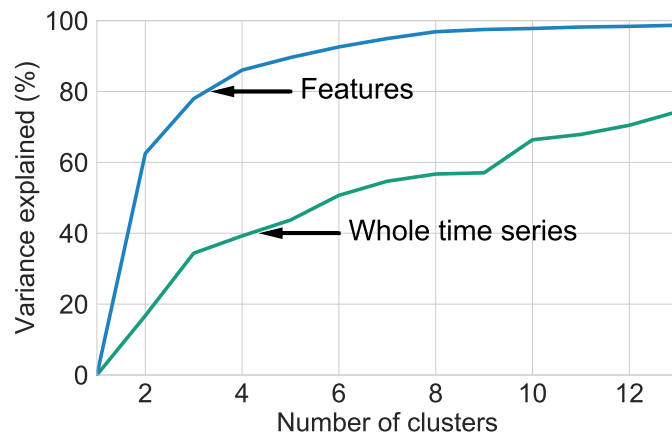


Figure 3.11: Percentage of variance explained with increasing number of clusters. Comparison between features (Mean and Hour-change score) and whole time series clustering procedure.

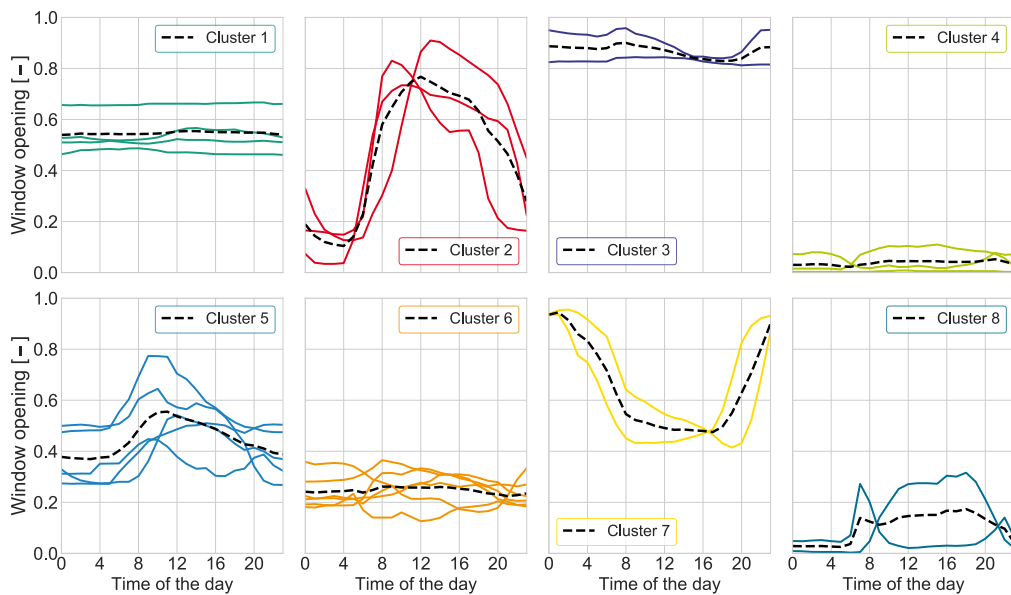


Figure 3.12: Cluster structure for training data set of observed proportion of windows open with features extraction. Dashed lines represent the daily mean profile of every cluster.

Eight distinctive profiles are obtained:

- Cluster 1: almost no changes during the day, with around 50% window opening (probably open in warm days and closed during cold ones).
- Cluster 2: open during the day and closed while sleeping.

- Cluster 3: almost always constantly open.
- Cluster 4: almost always constantly closed.
- Cluster 5: similar to Cluster 2 but with fewer changes between day and night profile, and higher night mean.
- Cluster 6: small changes and low mean value without a typical profile.
- Cluster 7: closed during the day and open while sleeping.
- Cluster 8: similar to Cluster 2 but with lower mean values during day.

The obtained cluster structure was labeled and learned using a supervised learning algorithm to evaluate the quality of the obtained clusters (Support Vector Machines classifier [26], described in the Appendix A.5). Given the training data where each point has a corresponding label (cluster number), the objective of the problem is to define a hyperplane that separates two points of different classes with a maximal possible margin. The test data is classified using this algorithm, and the resulting cluster structure is illustrated in Figure 3.13. Results showed that 19 out of 27 apartments were classified into the same category in training and test data sets, and those who changed presented as well a different profile, which is more compatible with the newly assigned clusters. The clusters' description with the training data set suits the test data set as well. The DI for the test set is 1.5086, which is lower than the original one (1.8025) as expected.

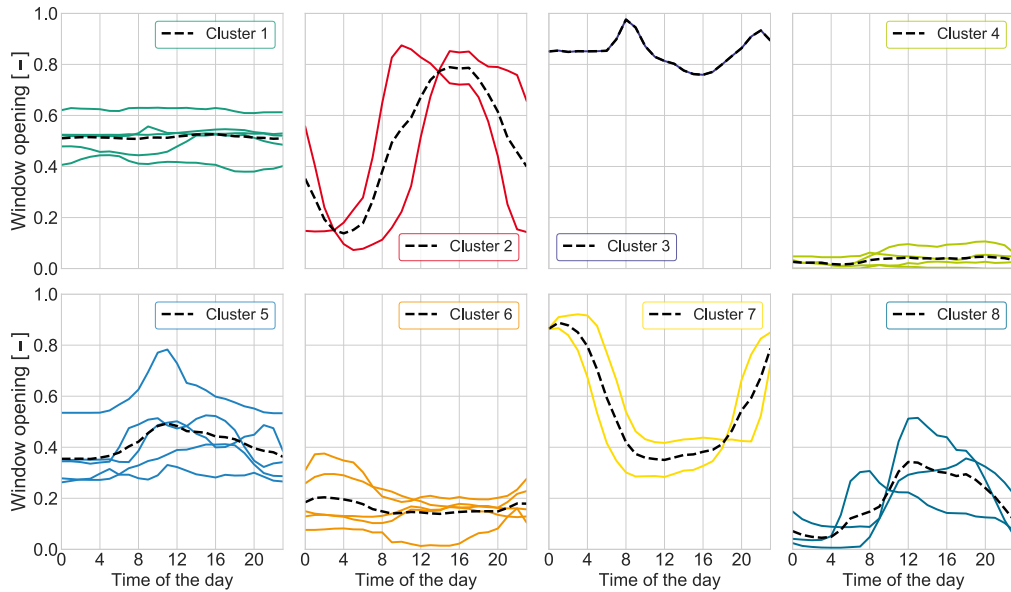


Figure 3.13: Cluster structure for test data set of observed proportion of windows open with features extraction and classification. Dashed lines represent the daily mean profile of every cluster.

On the contrary, the whole time series clustering method shows significantly lower Dunn index values. The highest Dunn index (1.0525) belongs to a six-cluster structure, which corresponds to 50% of the variance explained. Figure 3.14 shows the resulting cluster structure of the whole time series with six clusters. Two clusters are equivalent (Clusters 2 and 7 from features against Clusters 3 and 5 in whole time series), while Cluster 7 from features-based clustering was split into two single-dwelling categories (Clusters 3 and 4). The two remaining clusters present significant differences from each other, although Cluster 1 has lower mean values. Cluster 6 is highly diverse and appears difficult to understand.

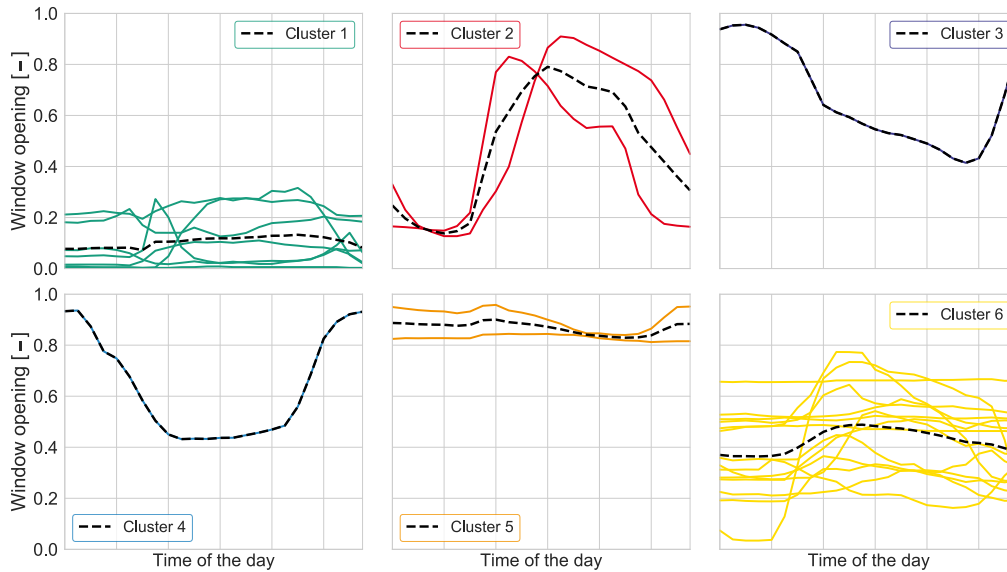


Figure 3.14: Cluster structure for training data set of observed proportion of windows open with whole time series. Dashed lines represent the daily mean profile of every cluster.

To summarize, the features clustering method presents the following advantages over a whole time series method:

- Higher clustering accuracy and prediction, given by the higher Dunn index.
- The variance explained is significantly higher in features clustering.
- Features clustering is more computationally efficient, due to dimensionality reduction.

In the following section, this procedure is applied to the second measurement campaign in Weingarten, to select three dwellings from different clusters, and compared to the probabilistic models described in Section 3.1.

3.2.4 Comparison of measurements and available models

In this section, the performance of probabilistic models is compared against measured building data. The data set belongs to the second measurement campaign described in Section 3.2.1. Following the clustering procedure from the previous section, the data from the living rooms are clustered. Two clusters in the living

room data are obtained, illustrated in Figure 3.15. The measured window opening profiles have lower average values than the ones from the first measurement campaign in Section 3.2.3. The difference lies in the monitoring period: the first campaign presents yearly measurements, while the second one only winter values, which are typically lower. The living room behavior is selected since two of the three analyzed window opening models report coefficients valid only for living rooms (Section 3.1). The selected apartments are highlighted for every cluster. The average measured indoor conditions in these rooms are illustrated in Figure 3.16. The diversity of the indoor conditions confirm the diversity of the occupant behavior.



Figure 3.15: Cluster structure for the daily average observed proportion of windows open in the living rooms in the second measurement campaign. The selected apartments are highlighted.

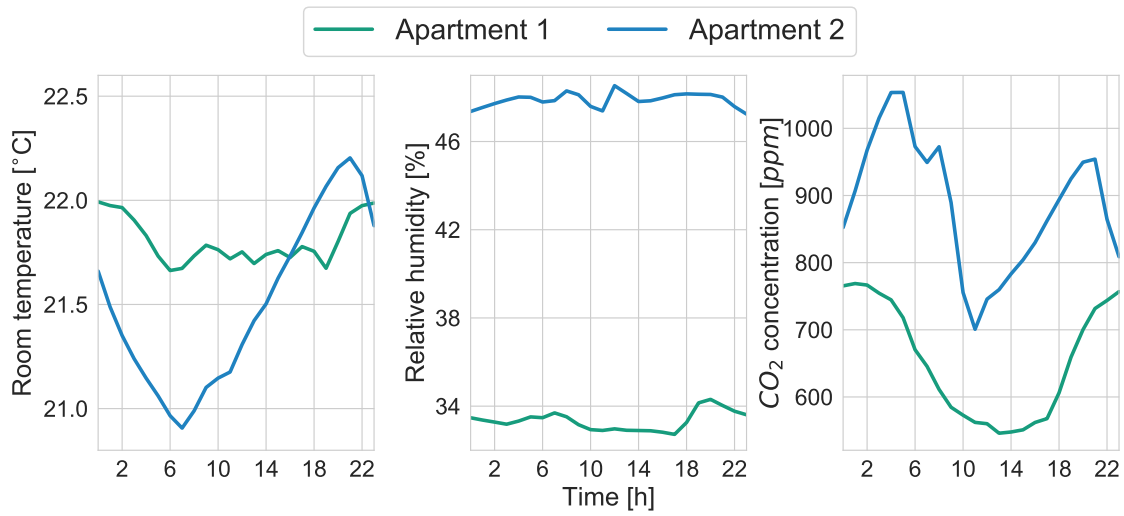


Figure 3.16: Measured daily mean indoor conditions in the living room for the two selected apartments.

Two different profiles were taken: the mean window opening (observed proportion of windows open) and the average opening action (1 for opening a window, 0 for no change), to be compared to the window opening models selected in Section 3.1. This comparison is depicted in Figure 3.17, along with the average output of the selected probabilistic models. The outdoor environmental variables for the probabilistic models are obtained using the Freiburg weather observations from the weather station of the German Weather Service (*Deutscher Wetterdienst*) in the same period [56].

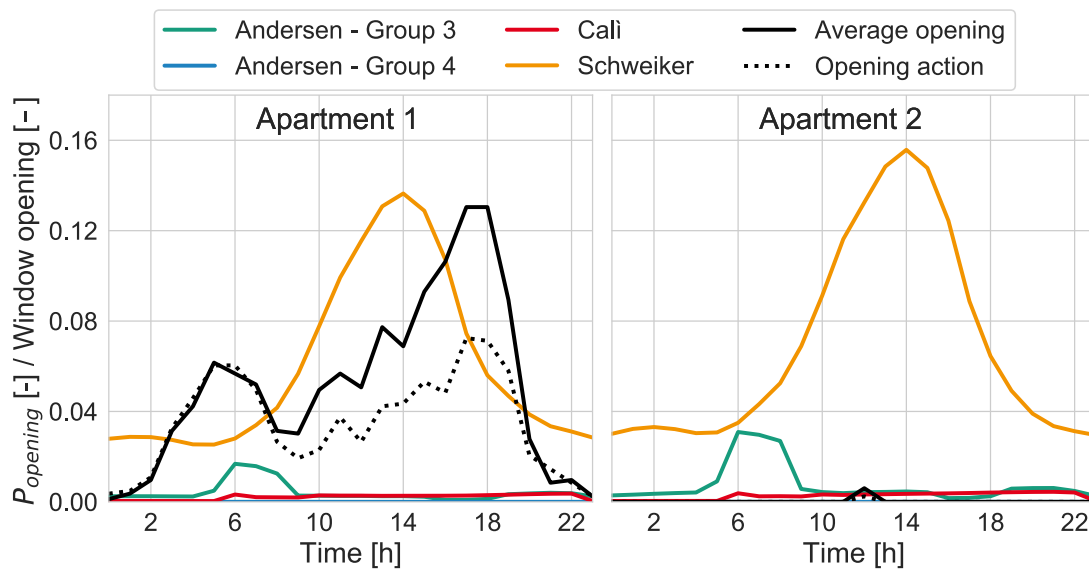


Figure 3.17: Window opening model and measurements comparison for the selected apartments. The opening probability $P_{opening}$ is used for the black lines, and the proportion of windows open (in %) for the colored lines.

The results of the probabilistic models are similar for both apartments, even though the indoor conditions profiles are different in the measured apartments. In apartment 1, a window opening in the morning is registered only by the model of Andersen et al. (Group 3 - rented apartment without mechanical ventilation), which is valid for naturally ventilated dwellings. The model of Schweiker et al. seems to predict well the detected openings in the afternoon in apartment 1. In apartment 2, the window was rarely opened during the measurement campaign. In this case, the models of Andersen et al. group 4 and Calì et al. are more suitable, given their low opening probabilities. For instance, the model of Andersen et al. group 4 yields between one and five openings in the whole measurement period (two openings were recorded in apartment 2).

Even though they simulate the stochasticity of the user, the probabilistic models depend strongly on the indoor and outdoor conditions (in the case of Schweiker et al. and Andersen et al.) and the time of the day (Andersen et al. and Calì et al.). This is the main reason why they usually fail to represent the diversity of the occupants. In the case of Schweiker et al., variables such as RH or CO_2 concentration were not measured, therefore ignored in the modeling process. The other authors found that the correlation between indoor environmental variables and window opening behavior was negligible and consequently excluded them.

This analysis could be extrapolated to other dwellings and other room types. Results show that these models sometimes fail to represent the wide spectrum of the occupant behavior. The studied window opening models are not developed to represent diversity, but to obtain a generalized model for building simulation, therefore they summarized data from several measurement campaigns into a single model. A possible solution could be to explore other modeling techniques [99]. In this section, it is concluded that the existing window opening models are not reliable to be used as user feedback models for residential mechanical ventilation systems, as they fail to represent the uniqueness of the user. In the next section, logistic regression is applied to window opening behavior to understand the drivers that motivate an opening act in every dwelling, rather than creating models suitable for its integration in building performance simulation.

3.3 Window opening behavior as user feedback for mechanical ventilation

In this section, the window opening behavior from the point of view of mechanical ventilation is explored. As stated by Hong et al. [106], drivers, needs, and actions are closely related to the occupant behavior, and the needs of the user in case of natural and mechanical ventilation are the same: obtaining fresh air. Figure 3.18 shows a flow diagram of the proposed analysis.

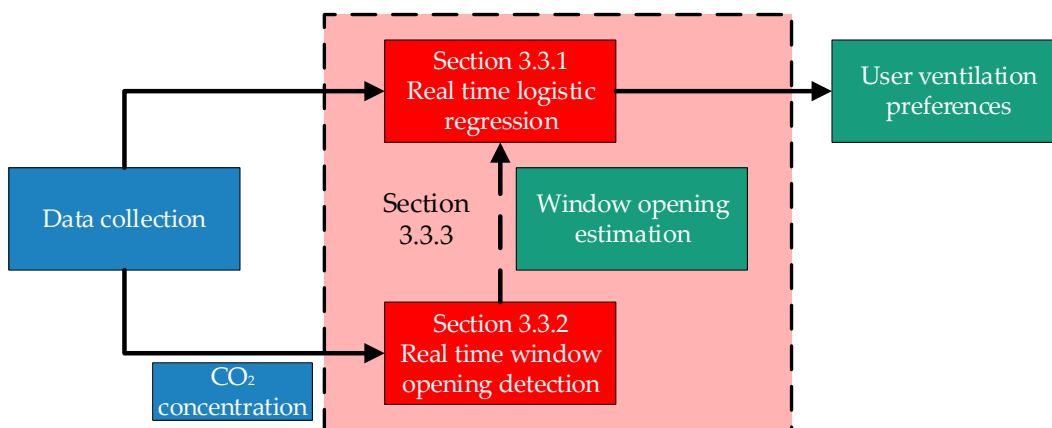


Figure 3.18: Schematic flow diagram of research method in this section.

The window opening models available in the literature can build different occupant profiles. However, they miss the singularity of the human, and even though there are tendencies to certain behaviors, each user is distinctive. As seen in the previous section, fitting an existing logistic regression model as user feedback for mechanical ventilation might be possible, but it would lose the nuances of individuals. In this section, a real-time logistic regression approach is presented to identify the drivers for window opening in every room. Besides, a window opening detection algorithm is proposed. The goal is to use available sensors in decentralized ventilation systems to detect when an occupant opens a window and then create user profiles. The result of the real-time logistic regression using the estimated window opening profile is relevant to obtain user-oriented solutions for mechanical ventilation systems, given that window contacts are usually not available in real buildings.

3.3.1 Learning preferences using logistic regression

In this section, logistic regression is used to quantify the relative importance of the different measured variables for the window opening behavior in residential buildings. This method was reported already in the literature for the window opening behavior in offices [63]. Models were fitted using the scikit-learn package in Python [172]. In this case, the model learns the window opening action related to indoor and outdoor environmental variables and time (represented by six dummy categorical variables), summarized in Table 3.6. For example, a dummy variable in the morning (6 - 10 AM) takes a value of 1 when time is in that range, and 0 outside it. The selected input parameters could be measured with the available sensors for decentralized ventilation systems.

Indoor parameters	Outdoor parameters	Time-related parameters [96]
Temperature	Temperature	Early morning (06-10)
Relative humidity	Relative humidity	Noon/Lunch time (10-14)
CO_2 concentration		Afternoon (14-18)
		Evening (18-23)
		Night (23-06)
		Weekend

Table 3.6: Explanatory variables (input parameters) for the real-time logistic regression.

The method consists of fitting a logistic regression every day at 00:00 hs during the whole measurement period and observing the evolution of the obtained regression coefficients. The main hypothesis in this method is that the absolute value of the regression coefficients stabilizes after some time, meaning that the user behavior is consistent. In this case, the window opening actions are learned to identify the occupants need for fresh air.

The whole measurement period consists of 138 days. The input variables are normalized to $[0,1]$, making the coefficients comparable to each other. In this section, an additional apartment from the second measurement campaign is analyzed (apartment 3). It belongs to the same cluster as apartment 1, meaning the average window opening profile is similar. Figure 3.19 shows the average window opening and opening actions profile for Apartment 3.

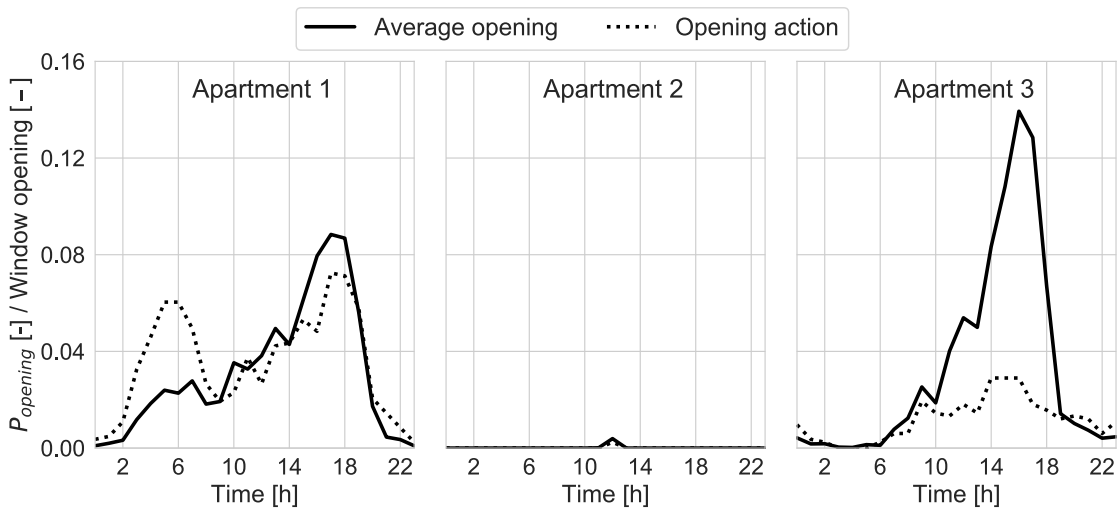


Figure 3.19: Daily average window opening and opening action profile for the Apartments 1, 2, and 3, respectively.

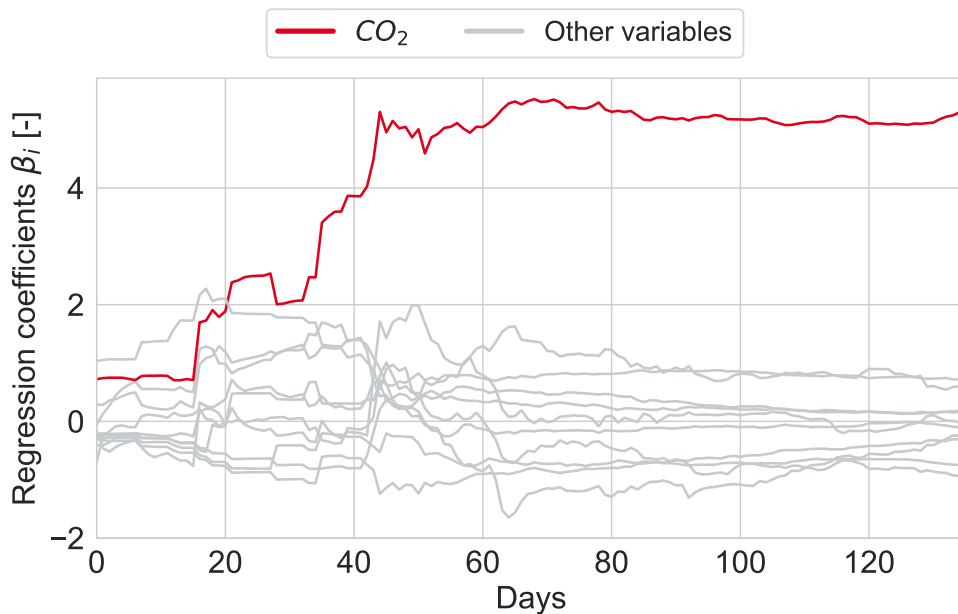


Figure 3.20: Real-time evolution of the logistic regression coefficients in Apartment 1. Complete figure in Appendix A.1.

Figure 3.20 shows the daily evolution of the regression coefficients for Apartment 1. It shows a strong influence of the indoor CO_2 concentration as a driver for window opening. All the other coefficients have a final absolute value below 1, while CO_2 is around 5. The regression coefficients become stable after day 50. From day 30 on, CO_2 concentration is the variable with the highest correlation with the window opening. When considering the window opening models, Andersen et al.

and Cali et al. considered CO_2 relevant to predict window opening actions, which is in agreement with these results.

In the case of Apartment 3 (Figure 3.21), the most important variable at the end of the measurement period is the outdoor temperature. In this case, coefficients show two stabilization levels: the first one after day 40, where the indoor RH has the highest coefficient. The second one happens after day 90, where the coefficients become reshaped, leading to changes in the final results. Indoor temperature becomes also more relevant after day 90. This occurs due to weather changes since available window opening models for summer present a stronger influence of the outdoor temperature (priority becomes cooling). Day 90 is February 12th, and in this particular year, outdoor temperatures above $20^\circ C$ were observed.

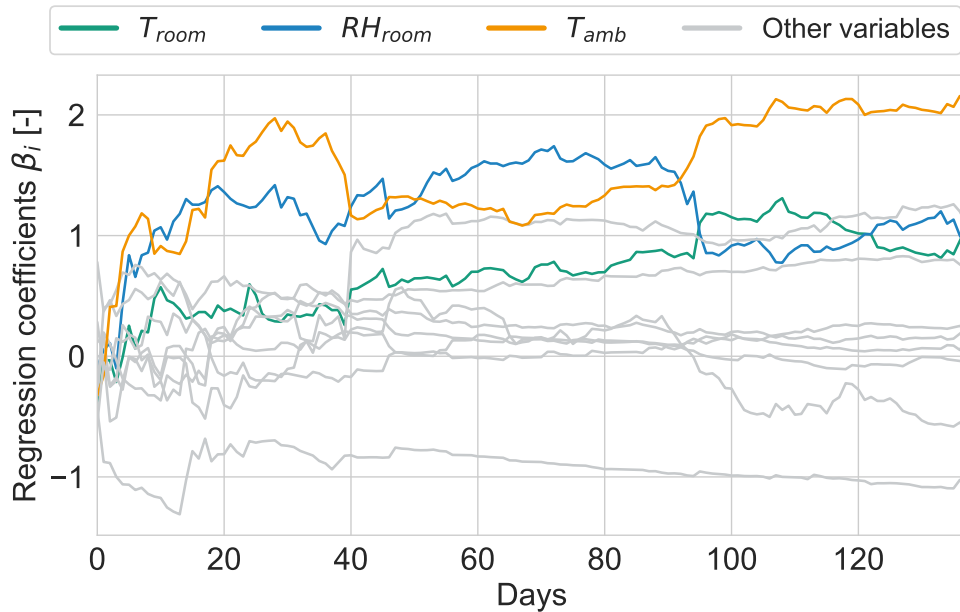


Figure 3.21: Real-time evolution of the logistic regression coefficients in Apartment 3. Complete figure in Appendix A.1

This proposed method helps to identify the drivers for opening a window in residential buildings. This information could be applied as a part of a mechanical ventilation controller, in which the controlled variable is defined by observing the main occupant drivers for window opening. This method is used in Section 5.4.1, where the occupant behavior towards the operation of mechanical residential ventilation systems is studied. The main limitation of this method is that a user feedback system (in this particular case, window contacts) are required, which are seldom available in residential apartments. The next section deals with this issue.

3.3.2 A real-time window opening detection algorithm

Window contacts are necessary to build a detailed profile of the opening behavior, but these sensors are hardly ever available in dwellings. Therefore, this section proposes a real-time window opening detection algorithm that could complement the logistic regression method.

Within the framework of a master thesis, Halden [98] proposed an innovative model to detect window opening using Hidden Markov Models (HMM). The algorithm is applied to a first order difference time series of the room absolute humidity or CO_2 concentration. Results show a better performance of using CO_2 than with absolute humidity, with total accuracies ranging from 89 to 96%. Yet this method has a limitation: it was tested only in apartments without mechanical ventilation. The impact of opening a window on the total air exchange rate is much higher without mechanical ventilation, and therefore a hidden Markov model can predict the window opening action. A study from Pereira et al. [174] detected different occupant actions in residences by combining several indoor environmental variables (namely, indoor and outdoor temperature, water vapor pressure, and CO_2 concentration). One of these detected actions is window opening, and accuracies higher than 99.5% are reached when using indoor and outdoor water vapor pressure as input variables. This study also presents some limitations: only one apartment was tested (no occupant diversity, which questions its potential generalization), and this dwelling had only mechanical extract ventilation. In addition, the two tested windows were located in the bathroom, where usually high punctual moisture loads are observed. The method was not applied to the "dry" rooms (bedroom and living room).

In this thesis, a peak-detection algorithm is applied in the window opening detection in apartments where residential mechanical ventilation is present, based on the smoothed z-score algorithm [28]. It is based on the principle of statistical dispersion [174]. The state change detection is created by comparing every new measured data point (real-time approach) with a certain calculated threshold. If this new point overcomes the calculated threshold, a state change is detected. The measurements are filtered with a moving average of the mean, and the threshold is calculated using the moving average standard deviation. In this case, the input data are the first order differences (FOD) of the room CO_2 concentration, and only window opening (not closing) signals are considered. The algorithm is described below in pseudocode.

Z-score peak detection algorithm

```
if ( $y[i] - meanFilter[i - 1]$ )  $\geq thr * stdFilter[i - 1]$  then  
     $window \leftarrow 1$   
     $y_{filt}[i] \leftarrow 0.6 * y[i] + 0.4 * y_{filt}[i - 1]$   
else  
     $window \leftarrow 0$   
     $y_{filt}[i] \leftarrow y[i]$   
end if  
 $meanFilter[i] \leftarrow mean(y_{filt}[i - lag : i])$   
 $stdFilter[i] \leftarrow std(y_{filt}[i - lag : i])$ 
```

The involved variables are:

- $y[i]$: the input variable (CO_2 concentration first order difference) at time i .
- y_{filt} : the filtered input (if there is a signal detection, the filtered input is considered as 0.6 of $y[i]$ and 0.4 of $y[i - 1]$).
- $meanFilter$: the mean of the filtered y_{filt} in the last lag periods.
- $stdFilter$: the standard deviation of the filtered y in the last lag periods.
- lag : the number of periods considered when calculating moving averages, and must be tuned for different signals.
- thr : the threshold number of $stdFilter$ that detect successfully a state change, and must be tuned for different signals.

Figure 3.22 presents the results of the detection algorithm on a sample day. The evolution of the CO_2 first order differences and the algorithm threshold are illustrated. The algorithm detected three openings, but only one was measured (the 6 AM opening is detected successfully). Two additional incorrect window openings are identified around 18 hs. These could be corrected by adjusting the threshold value thr , which will also affect the window opening detection on other days. The definition of the thr and lag values for different apartments are explained as follows.

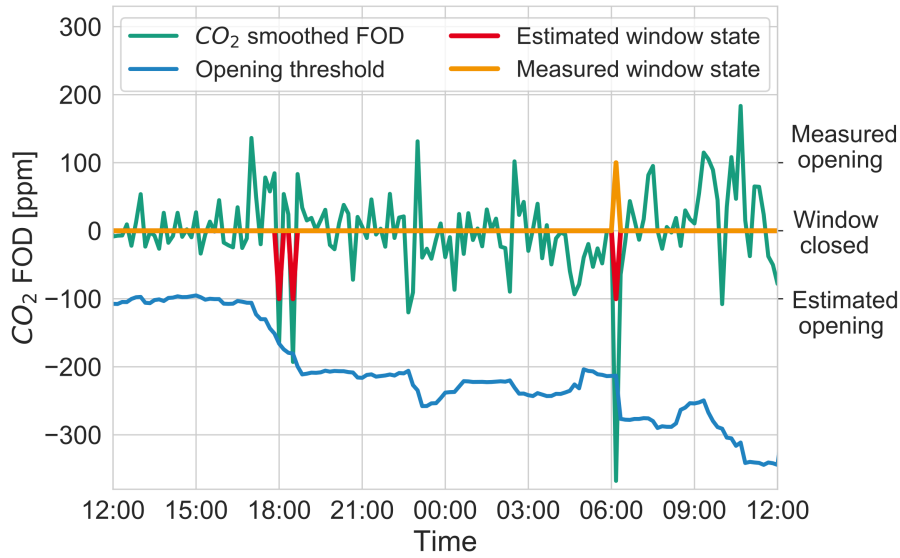


Figure 3.22: Sample day for real-time window opening detection algorithm, using the first order differences (FOD) of the CO_2 concentration as an input variable to detect the opening.

This algorithm was tested with data of the living room in the three apartments mentioned before. The thr and lag values were tuned to maximize the performance of the algorithm. A higher thr value means that higher CO_2 first order differences are required to detect an opening. A higher lag value means that the moving mean average is calculated using longer intervals, affecting the CO_2 first order differences as well as the moving threshold value. To evaluate the performance of the algorithm, indicators based on "true positives" (TP), "true negatives" (TN), "false positives" (FP) and "false negatives" (FN) are calculated [231]:

$$TPR = \frac{TP}{TP + FN} \quad (3.7)$$

$$Acc = \frac{TP + TN}{TP + TN + FP + FN} \quad (3.8)$$

$$PPV = \frac{TP + TN}{TP + TN + FP + FN} \quad (3.9)$$

$$Ind_{opt} = \frac{TP}{FP + FN} \quad (3.10)$$

TPR is the true positive rate, and Acc the overall accuracy. The predictive positive rate PPV evaluates the precision of the positive values obtained. The Ind_{opt} indicator (optimization indicator) was defined to evaluate the performance of the

algorithm, in terms of true prediction over errors committed. After testing the algorithm performance iteratively with different values of thr and lag , they are defined with the highest Ind_{opt} value. The results for the three tested apartments are displayed in Table 3.7.

Indicator	Apartment 1	Apartment 2	Apartment 3
Measured WO	698	2	236
Estimated WO	446	66	468
thr	3	5	3
lag	35	23	9
TPR	0.5318	0	0.1398
PPV	0.8251	0	0.1379
Acc	0.9798	0.9966	0.9679
Ind_{opt}	0.9154	0	0.0517

Table 3.7: Window opening (WO) real-time detection results in the three selected apartments.

Apartment 1 yields a much higher Ind_{opt} value than the other two. In the case of Apartment 3, the detection results are worse than for apartment 1. Apartment 2 shows the worst results, even having a null TPR (no correct window opening detections). The apartment with the lowest number of openings has the worst performance, and the apartment with the highest number of openings shows the best algorithm performance. However, this relationship does not follow a clear pattern when fitting other rooms or apartments. Observing the logistic regression plots from Section 3.3.1, the best results are the ones where the regression coefficient CO_2 was the highest. This emerges logically since the time series selected for the detection was the room CO_2 concentration (the selection of CO_2 relies on the property that its indoor concentration depends almost exclusively on occupants' breath release). In that sense, other variables should be considered as well when applying this algorithm.

Figure 3.23 depicts the estimated and measured average opening profiles, together with the average measured proportion of windows opened. Even though there were errors reported and low predictive values, the estimated opening action profiles match well with the average real estimated profiles. This was expected for apartment 1, where the best indicators were obtained. However, in apartment 2 or 3, the results appear to be also close to the real opening profile. This confirms the potential of this approach in building a residential real-time window opening profile, especially if the

occupants react to CO_2 concentration as a key driver. However, better statistical indicators should be achieved to confirm this potential.

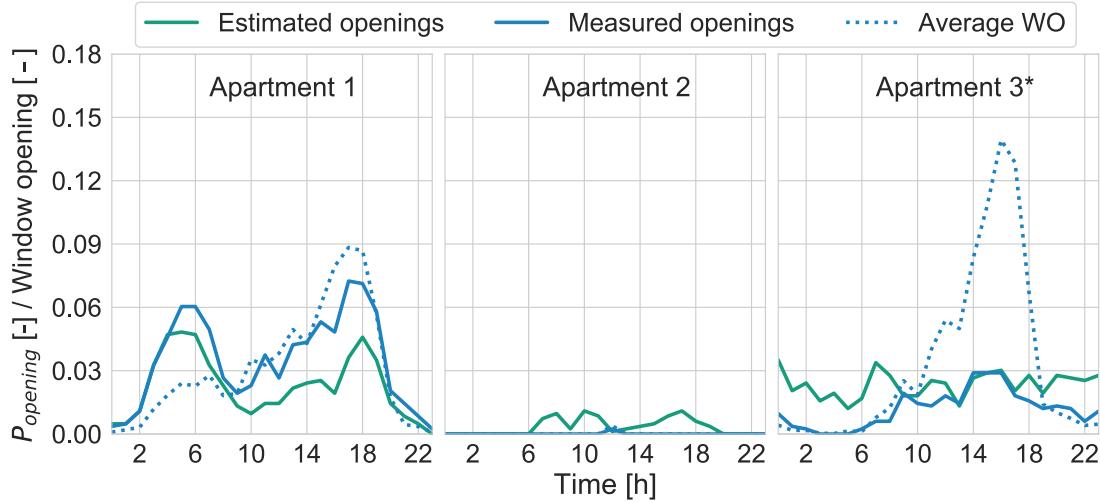


Figure 3.23: Real-time window opening detection results in the selected apartments and comparison with the measured window opening and opening action profile.

To summarize, results show that the detection success depends on the degree of correlation of the observed variable with the actual window opening (obtained through logistic regression coefficients). A limitation of this method is that the variables thr and lag must be tuned for a proper window opening detection. An implementation of a dynamic threshold coefficient could potentially improve the results, although it should be carefully studied to avoid overfitting to this particular data. A multivariable approach should be as well studied, as it could enhance the proposed model to yield higher accuracies.

3.3.3 A combination of detection and preference learning

In this section, the window opening detection algorithm is combined with the logistic regression scheme to learn the user preferences without needing window contacts. The aim is to study if this solution could provide potential information gain regarding user preferences for window opening replacing direct user feedback in residential mechanical ventilation systems (but also extendable to HVAC systems).

The results are shown only for the Apartments 1 and 3 but can be extrapolated to other apartments of the second measurement campaign. The real-time logistic regression, described in Section 3.3.1, is applied using the estimated opening profile, as a result of the detection algorithm from Section 3.3.2. The evolution of the re-

gression coefficients is analyzed. Figures 3.24 and 3.25 depict a comparison between fitting a regression with the real (left) and estimated openings (right) for Apartment 1. The estimated regression coefficients are very similar to the real ones. In this particular apartment, this method combination based on indoor environment monitoring without a window contact leads to similar regression coefficients, and the preferences of the user regarding the drivers to open a window in winter are successfully estimated.

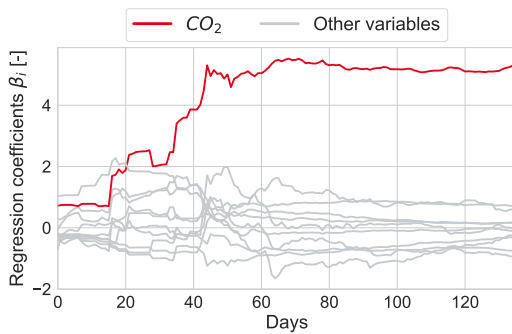


Figure 3.24: Real-time evolution of the logistic regression coefficients with measured window opening in Apartment 1. Complete figure in Appendix A.1.

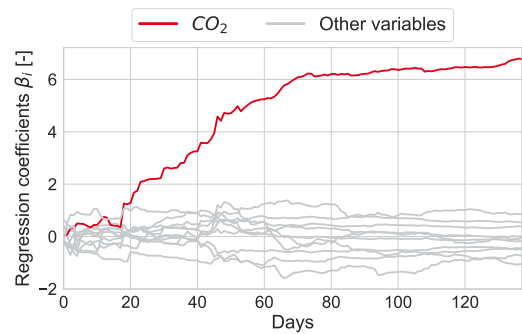


Figure 3.25: Real-time evolution of the logistic regression coefficients with estimated window opening in Apartment 1. Complete figure in Appendix A.1.

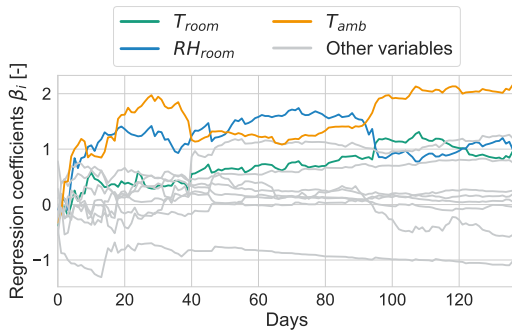


Figure 3.26: Real-time evolution of the logistic regression coefficients with measured window opening in Apartment 3. Complete figure in Appendix A.1

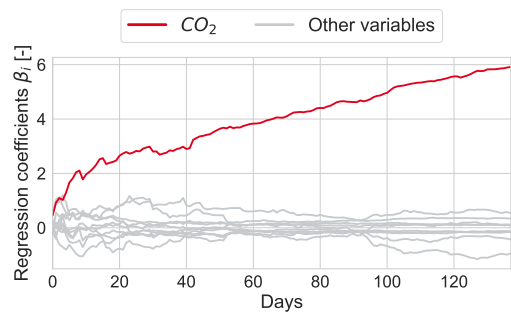


Figure 3.27: Real-time evolution of the logistic regression coefficients with estimated window opening in Apartment 3. Complete figure in Appendix A.1

Figures 3.26 and 3.27 depict a comparison between fitting a regression with the real (left) and estimated openings (right) for Apartment 3. In this case, the obtained regression coefficients to predict window opening differ strongly between measured and estimated opening actions. Similar to Figure 3.25, the estimated openings lead

to a high relevance of the CO_2 concentration in comparison to the other coefficients, as it is used as the variable to estimate window opening. Other regression coefficients are also affected: the indoor relative humidity and the outdoor temperature, which are the most relevant regression coefficients when fitting the measured opening profile, have negative coefficients when fitting the estimated profile. This means the influence of these variables when using estimated profiles is the opposite as when using measured profiles.

To sum up, the reliability of this approach with the presented methods is questionable. Information in advance about the occupants is needed to apply this method. For instance, if the occupant window opening behavior is correlated with CO_2 concentration (aApartment 1), this method can be successful. On the other hand, the occupant behavior is modeled incorrectly if other variables are more relevant (Apartment 3). This means the information obtained about the occupant ventilation preferences using this method is not reliable to replace user feedback. The improvement of the detection algorithm could lead to a reliable procedure to understand the window opening drivers of the occupant, and its applicability in mechanical ventilation systems.

3.4 Summary

The occupant behavior is distinctive and diverse. Until now, research has made little focus on its understanding and modeling regarding residential mechanical ventilation systems, therefore the chapter focuses on window opening behavior models (natural ventilation). Available probabilistic models are investigated and a method is proposed to obtain information about the ventilation preferences from the window opening behavior. Thus, the research question 2 can be answered as through the following points:

Research Question 2: *To what extent does the window opening behavior provide useful information for ventilation control strategies? How can this be represented?*

- There are different window opening models in the literature. The most popular ones propose an opening/closing action model based on logistic regression. The explanatory variables are usually related to the indoor and outdoor environment and time. Three models based on European residential buildings are selected and analyzed.
- To better understand the time-related window opening behavior, a novel clus-

tering method was developed, where features (based on statistical indicators) are calculated to represent the distinctive behaviors. This method was applied to measurements in renovated residential buildings, resulting in eight clusters. Using a second measurement campaign, two apartments of different clusters were selected and compared to the available probabilistic models. These models fail to represent the individual window opening behavior since they were designed to integrate the stochasticity of occupants into building simulation. Therefore, available probabilistic models are not suitable to be integrated as a replacement for user feedback in mechanical ventilation systems. These models are further used to represent window opening behavior in building simulation in the next chapter.

- A second approach was proposed using a real-time logistic regression-based driver learning method, to understand what are the key occupant drivers to open a window. The main assumption was that the regression coefficients should stabilize over time and could be used to infer the user preferences regarding ventilation. The evolution of the regression coefficients of three measured apartments was studied. In this study, the regression coefficients stabilize after day 40 and provide useful information about occupant window opening drivers. This method is reliable to evaluate user ventilation preferences and is further used in Chapter 5. However, the main limitation is the need for window contacts to measure window opening behavior. Therefore, a real-time window opening detection algorithm in absence of a window sensor is proposed. The developed method is based on a filtered z-score peak detection algorithm, in this case, applied to CO_2 concentration. The combination of this method with logistic regression could lead to a real-time estimation of the occupants drivers for window opening behavior. Results show high accuracy in apartments where room CO_2 concentration is a key driver to window opening, but poor results when the occupant behavior has a higher correlation with other variables. Thus, information in advance about the user preferences is required to obtain satisfactory results using this method.
- Consequently, user feedback collection is mandatory to develop occupant-centered solutions in residential ventilation systems. This is studied in the next chapter.

4 Innovative control strategies for decentralized ventilation

This chapter focuses on residential decentralized ventilation systems and their control strategies. In Section 4.1, current solutions on the market and science are reviewed, to gain an insight into how innovative controllers could impact this field. A novel co-simulation scheme is developed to test the control strategies, described in section 4.2. Moreover, in Section 4.3, three user-centered demand-controlled strategies are proposed and portrayed: a cost function, a fuzzy-based, and a self-learning scheme to represent the individualized needs of occupants. In Section 4.4, two simulation test cases are carried out to investigate the performance of the proposed occupant-centered control strategies regarding hygrothermal comfort, indoor air quality, and energy consumption in residential buildings. A summary of the findings in this chapter is available in Section 4.5.

4.1 State-of-the-art

In this section, the available control strategies for decentralized ventilation in the market and scientific publications are reviewed. The aim is to define typical present control strategies, which are used in the simulation as baseline cases to quantify the potential savings of the proposed solutions.

4.1.1 Market research

Within the frame of this thesis, a market research of control strategies in decentralized ventilation for residential buildings was carried out. Over sixty control systems from more than thirty companies in Europe were summarized, focusing on the German market, where decentralized ventilation has grown stronger than centralized systems in the last years. Sales in Euros of decentralized ventilation systems represented 17% of the total sales in 2012 and grew to 37% in 2018 [110]. The control strategies were taken into account only when room-individual control was available. The key findings of this market analysis are summarized in the following points:

- There are usually three to eight available airflow levels. Maximum airflow levels are between 30 and 60 $\frac{m^3}{h}$.

- Fully automated modes are often available as an option. The controlled variables are mostly indoor relative humidity (threshold between 65 and 80%) and CO_2 concentration (1000-1500 ppm). Room temperatures are often measured but not controlled.
- Other available modes:
 - Summer ventilation (by-pass without heat recovery)
 - “Party” mode (intense ventilation)
 - Long absence or holiday mode (minimum ventilation)
 - Sleeping mode (minimum ventilation or off, targeting noise reduction)

Every device on the market offer a manually adjustable fan speed, fixed at predefined levels. The first attempt to create an occupant-centric control for ventilation systems was to estimate the required air exchange rate on typical days, leading to predefined weekly programs. However, some occupants might have activity profiles or different habits, making the predefined control schedules not suitable for them. Hence, a closer user-technology relationship needs to be developed.

The automatic control strategies offered on the market are almost always an addition to decentralized ventilation systems. Most of them are commercialized under denominations like “smart control”, and together with smart home devices. These seldomly offer a connection between decentralized systems in different rooms. They usually focus on individual room airflow, depending on the current room conditions – the “demand-controlled ventilation” (DCV):

Demand-controlled ventilation: *”Demand-controlled ventilation is a feedback control method to maintain indoor air quality that automatically adjusts the ventilation rate provided to a space in response to changes in conditions such as relative humidity or carbon dioxide concentration.”*

The key advantage of DCV is that it regulates the airflow by controlling the speed of the fans, in contrast to most centralized systems, where dampers are usually present. This feature enhances its energy-efficiency. A hysteresis cycle is usually included to avoid sudden level changes surrounding a threshold value. An exemplary hysteresis cycle is illustrated in Figure 4.1. In this case, a hysteresis cycle is present for the control system when the relative humidity is between 45 and 50%. For instance, when indoor activities cause a release of moisture loads, the relative humidity in a room increases. When the relative humidity overcomes the threshold of 50%, a

higher airflow level is required. When the airflow is high enough to compensate for the moisture loads, the relative humidity starts decreasing. However, to avoid instabilities around the 50% threshold value, a hysteresis of 5% is included. The airflow level is reduced when the relative humidity is lower than 45%.

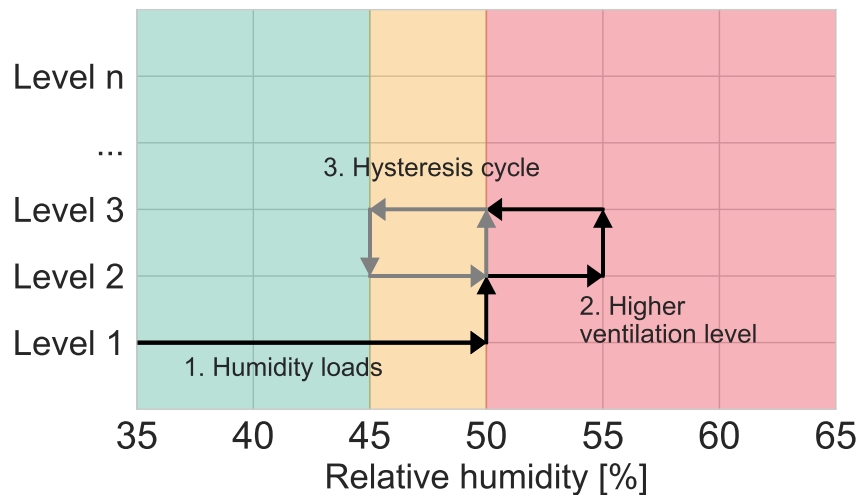


Figure 4.1: Working principle of a typical hysteresis cycle of a DCV in decentralized ventilation systems.

Other DCV solutions are also available, such as linear relationships between the volume flow and the target variable (for instance, RH or CO_2). Currently, there is a lack of innovation in decentralized control strategies. Most of the manufacturers still sell DCV strategies as smart ventilation, even though they have been on the market for more than ten years.

To summarize, two main gaps are identified from this research:

- Available smart DCV-based controllers handle only one variable at a time.
- User-centered solutions are represented in two forms: demand response to a certain load type (moisture or CO_2) or a preprogrammed strategy (such as "party" or "sleeping" modes). There is a clear lack of occupant-centric solutions in residential ventilation.

4.1.2 Scientific research

Twenty-nine scientific papers were reviewed, related to some extent to ventilation control strategies in the last twenty years. Ventilation systems with integrated

heating were also reviewed since innovative control strategies for decentralized ventilation have not yet been extensively studied (DVS were studied only in five of these twenty-nine publications). The controllers were developed in residential, commercial, or laboratory tests. The full table with the reviewed publications is in the Appendix A.4. Additional information about ventilation control strategies is available in scientific publications [160, 188, 195, 199, 218]

The controlled variables (output) for decentralized ventilation systems can be fan speed (or volume flow), damper position, or fan direction, depending on the analyzed system. The input of the controllers is usually related to indoor and outdoor environmental variables. Besides, sometimes these are used to predict the status of other correlated variables (for instance, CO_2 concentration in a room and occupancy status). Figure 4.2 illustrates the percentage of publications where the corresponding variable is controlled.

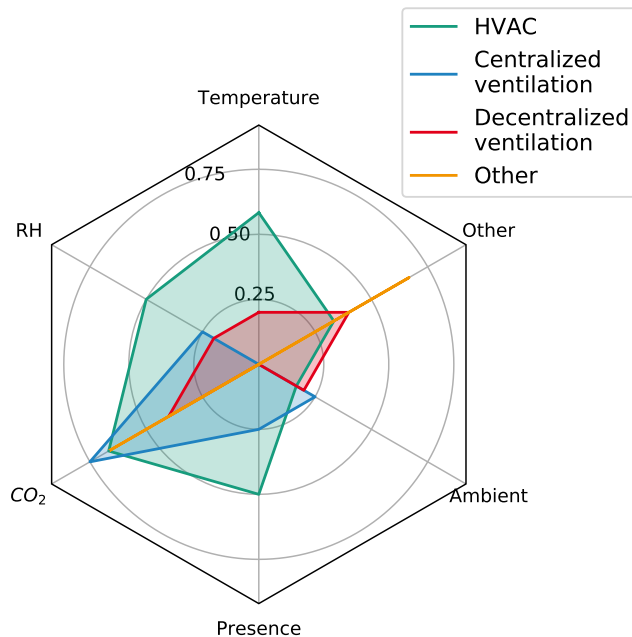


Figure 4.2: Proportion of publications that consider each input variable for different ventilation systems. The variable "Ambient" summarizes different outdoor environmental variables.

Regarding control strategies, decentralized systems seem to be always associated with DCV schemes. These DCV reviewed controllers usually react to relative humidity or CO_2 concentration. Other indoor contaminants (for instance, volatile organic compounds, or benzene) are considered, although these publications remark the need for better contaminant modeling. In this case, CO_2 is widely accepted

as it is correlated to the presence of the occupant. Other controllers are PI-based (Proportional-Integral), where the airflow is controlled to keep a certain CO_2 -based setpoint. Other controllers propose to predict the occupant exposure degree to other contaminants (for example, furniture contaminant release) and therefore minimize this exposure through load shifting, such as shock ventilation before the occupant arrives.

Centralized HVAC systems are a more frequent subject of study (because of their complexity and savings potential associated with heating and cooling). Recently, more advanced controllers, often machine learning-based, were developed. From the analyzed 29 publications, only five study directly and 22 are applicable to decentralized ventilation systems. Figure 4.3 depicts the studied controller types for different ventilation systems. Most of the publications that propose an advanced control strategy are simulation studies, and there is a lack of experimental studies.

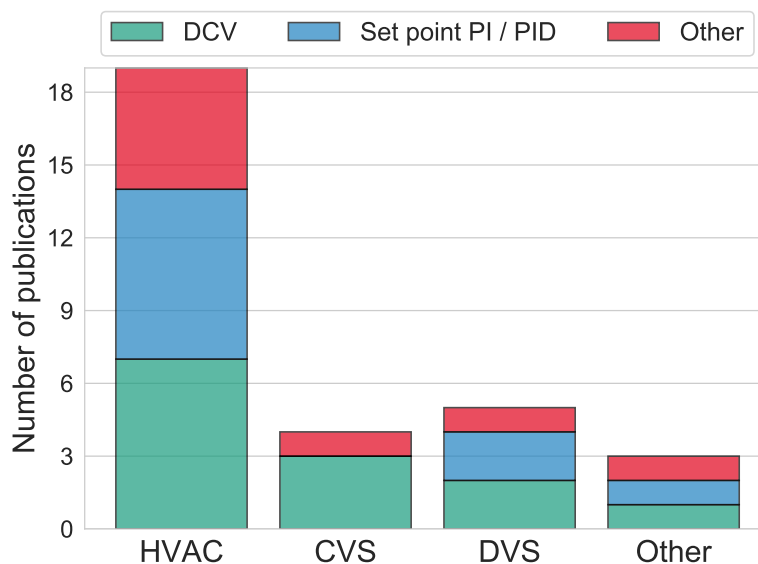


Figure 4.3: Number of publications reviewed for each controller type and ventilation system. Two publications review more than one system.

4.1.3 Reference control strategies

To conclude this review section about available control strategies for decentralized ventilation, two main reference strategies are derived as a comparison basis for innovative ventilation control systems.

1. A simple strategy, where the fan speed remains constant (around 0.4 air changes per hour - ACH - which corresponds to reduced ventilation level ac-

according to the DIN 1946-6 [58]), representing an unaware user who does not operate the ventilation system in residential multifamily buildings. The airflow may be affected by the pressure difference between the room and the façade.

2. A stepwise strategy, RH -controlled in humid rooms (bathroom and kitchen), and CO_2 -controlled for dry rooms (living room and bedroom), illustrated in Figure 4.4.

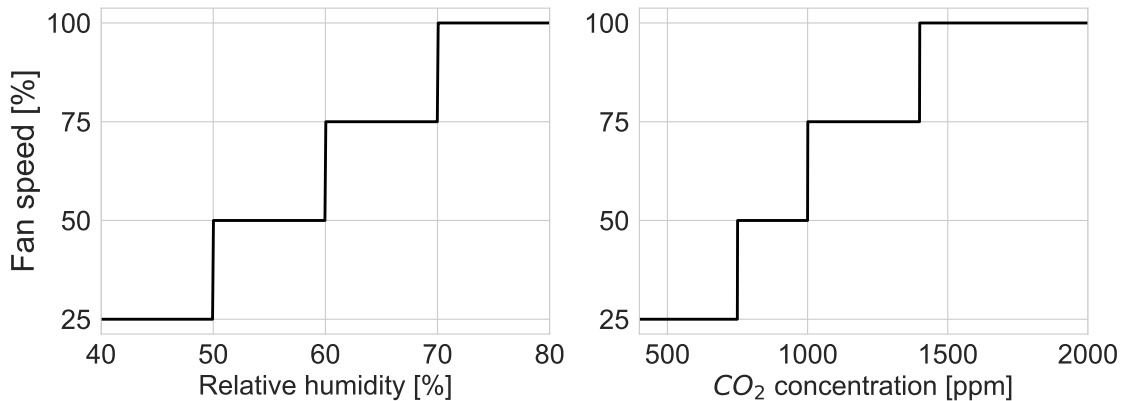


Figure 4.4: Baseline ventilation control strategy - "Steps".

4.2 Modeling and simulation

This section describes the approach to simulate the developed control strategies. A novel co-simulation scheme combines the strengths of different simulation environments. The included models (building, ventilation system, control strategy, and internal loads) are described. The introduced models in this section are already published in different scientific articles [34, 35, 36, 37].

4.2.1 Co-simulation

Different modeling techniques have their advantages and limitations. To properly simulate decentralized ventilation systems and the effectiveness of their control strategies, the following characteristics must be fulfilled by the selected models:

- A single apartment must be modeled with single-room controllers for every decentralized ventilation system.
- Air exchange between individual rooms and outdoor air must be simulated, including humid air and trace substances (CO_2).

- An alternating façade-integrated decentralized ventilation system with a reliable heat recovery model must be included.
- Wind pressure influence is not negligible in façade-integrated devices, and therefore must be considered [152]. The fan curve is therefore key to simulate the actual airflow as a function of the pressure difference.
- State-of-the-art and innovative control algorithms must be modeled and included.

There is no single simulation software available that fulfills all the requirements. Hence, a co-simulation approach is proposed, where the advantages of different environments are combined into a single simulation scheme. In this thesis, the building and weather data are modeled in EnergyPlus 8.9.0 [50], which has great capabilities regarding building physics. However, the modeling of independent façade-integrated ventilation systems (decoupled from heating and cooling) is not available. Therefore, the DVS was modeled in Modelica 3.2.2 [147]. The integration of advanced control systems takes place using Python 3.7 [209].

The models are connected through the Functional Mock-up Interface (FMI), where every model is exported as an individual Functional Mock-up Unit (FMU). These FMUs are afterward coupled in one particular environment or even through third-party environments, such as Python. An FMU comes along with a set of C-functions, according to the FMI standard (FMI Standard 1.0). The C-functions are provided as binaries and are responsible for the information exchange between the different simulation environments. The FMU coupling is performed in Python using the package PyFMI [15]. Figure 4.5 shows how the FMUs (slave models) interact with the master algorithm and with the additional models (external input data and control systems developed in python code). This coupling allows the integration of control algorithms developed directly in Python code. A disadvantage of this coupling is the lower simulation times.

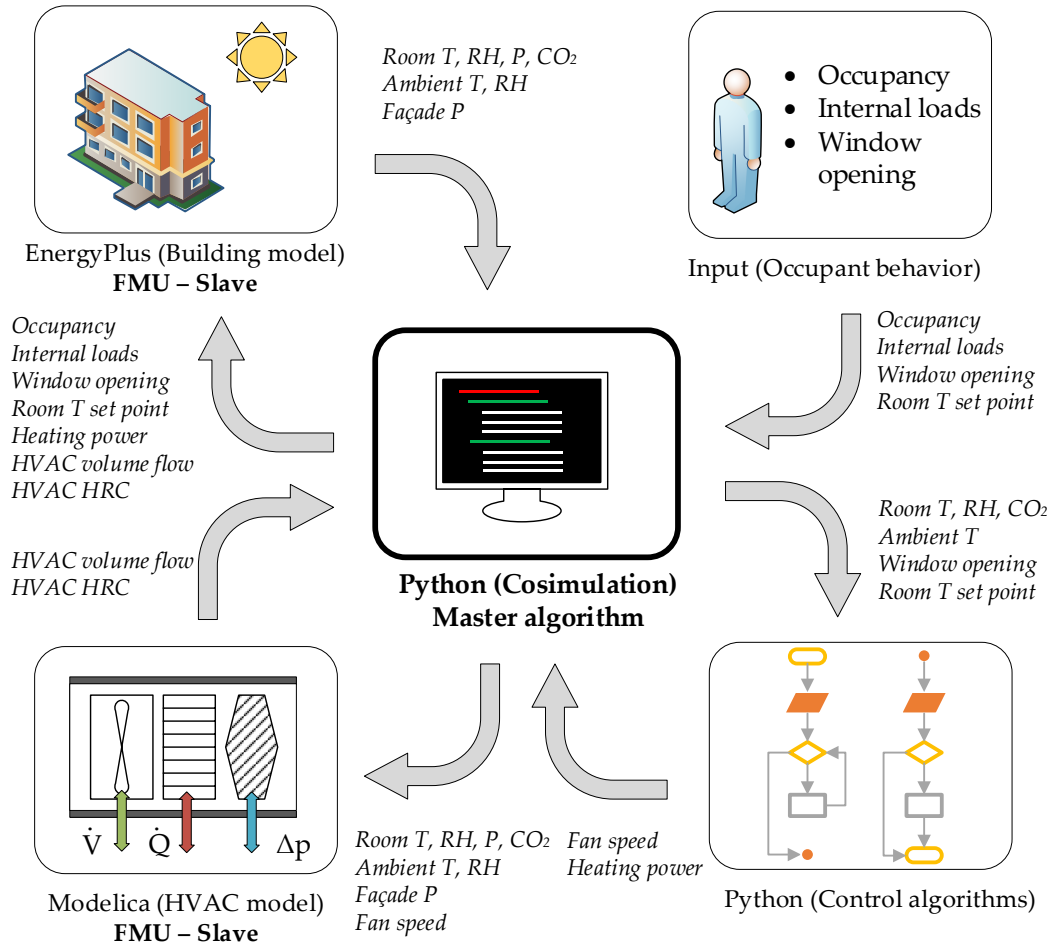


Figure 4.5: Co-simulation scheme developed for control algorithm testing.

4.2.2 Building model

A single dwelling of a typical German multifamily building (MFB) is proposed and modeled. The characteristics are assumed based on the investigation from the project "LowEx im Bestand" [68] and the interpretation of Rohrer [186]. Figure 4.6 illustrates the floor plan. The total area is 84.6 m^2 . The balcony was also considered, as it plays a role in shading (outdoor space). The dwelling is assumed to be 5 m above ground level.

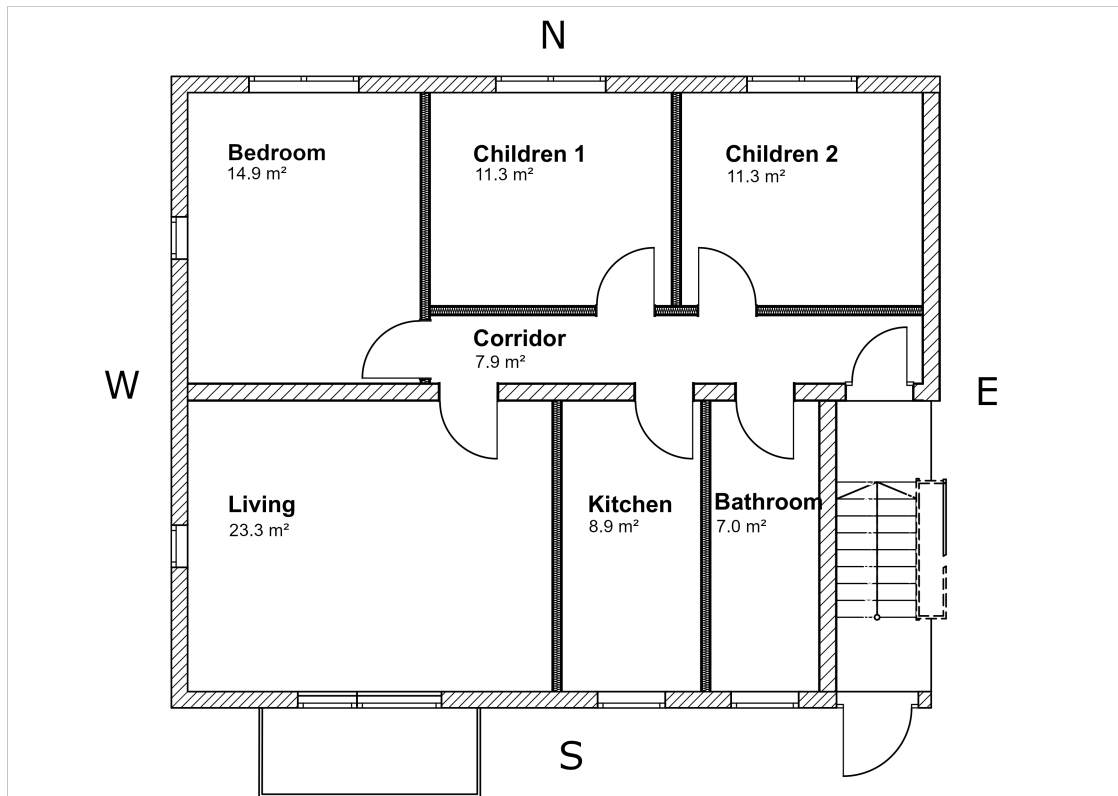


Figure 4.6: Floor plan of the simulated apartment.

Regarding the thermal simulation assumptions, floor and ceiling were modeled as adiabatic surfaces, as it is assumed that the stories below and above have similar room temperatures, neglecting the heat flow between them. The thermal characteristics are typical for a medium energy retrofitted building in Germany. Internal mass due to furniture is neglected, given that the impact on peak loads is less than 5% [179]. Table 4.1 summarizes the relevant thermal properties of the simulated reference dwelling.

Thermal properties of the dwelling	Unit	Value
Exterior wall	$\frac{W}{m^2 \cdot K}$	0.23
Interior wall	$\frac{W}{m^2 \cdot K}$	1.30
Windows U-value	$\frac{W}{m^2 \cdot K}$	1.30
Windows frame factor	-	0.80
Glazing SHGC	-	0.70
Wall/window proportion	-	4.17

Table 4.1: Simulated thermal properties of the dwelling.

The apartment is modeled with EnergyPlus 8.9.0 [50]. The air movement inside and

outside the dwelling, as well as the infiltration and wind pressure, were simulated applying the airflow network approach [27], illustrated on Figure 4.7, and already validated in previous studies [67]. Every room is modeled as a single node, as well as the air nodes on the surface of the external façades. Each node represents a closed volume, with air pressure as the state variable. Equivalent to an electrical circuit, the pressure difference between two nodes creates an air movement. The flow “resistance” determines the volume flow that is originated by this pressure difference, becoming an airflow path. Typical airflow paths are windows, doors, cracks (or any infiltration component), and orifices (including, for example, wall-integrated openings or ventilation systems). The flow resistances are modeled using the effective leakage area method [222] and using flow coefficients from the AIVC Technical Note 44 [164]. The outdoor nodes have static and dynamic (wind) pressure, which is modeled using the procedure developed by Swami and Chandra [201]. Details about the airflow network model and the selected coefficients are available in the Appendix A.2

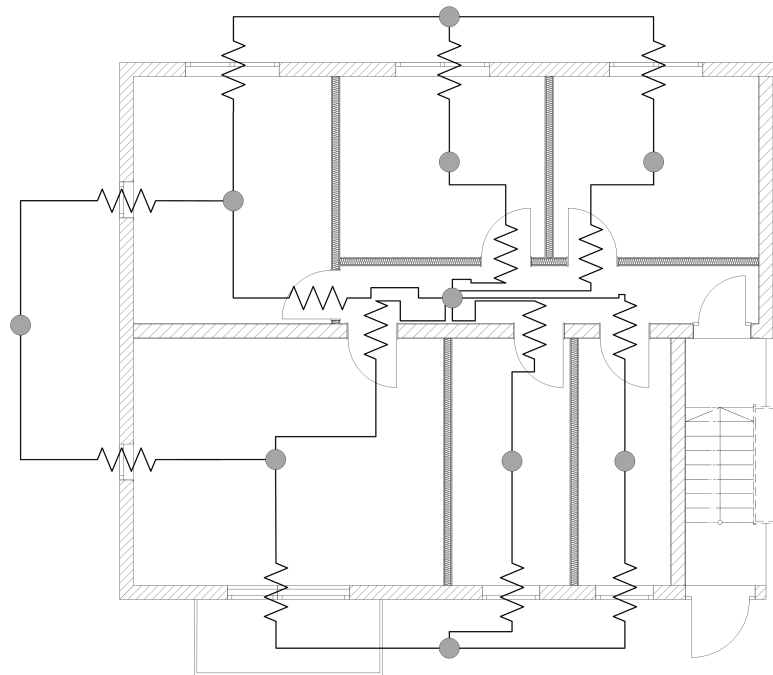


Figure 4.7: Airflow network model of the dwelling. The circles represent the nodes (room volumes or outdoor nodes) and the resistances (airflow paths) represent the air exchange between nodes.

Regarding the infiltration, the recommendation of the Passive House Institute is followed, suggesting a total air exchange rate of $0.5 h^{-1}$ when the pressure difference is 50 Pa [170]. The infiltration is distributed in every room and modeled using the

effective leakage area (ELA) method [10]. Furthermore, the ventilation concept for this dwelling is defined according to the norm DIN 1946-6 [58], explained in Section 2.1. The defined ventilation levels in the whole dwelling are:

- Humidity protection = $27.4 \frac{m^3}{h}$
- Reduced ventilation = $64.0 \frac{m^3}{h}$
- Nominal ventilation = $91.4 \frac{m^3}{h}$
- Intense ventilation = $118.9 \frac{m^3}{h}$

A total of eight decentralized ventilation systems are selected in the dwelling (two in the bedroom and living room, one per room in the rest). Besides, the airflow network model assumes a perfect air mixing (single node model) and ignores the impact of air distribution in the room and potential short circuits in different system configurations. Therefore, given that the ventilation systems are façade-integrated, a ventilation effectiveness profile as a function of the air exchange rate is considered [127], which directly affects the supply and exhaust volume flows in every room. The airflow network approach in EnergyPlus allows only balanced ventilation in every room, which is a known limitation. It neglects the direct impact of the ventilation supply and exhaust phases on the indoor conditions. The building model and its validation are commented on further in the Appendix A.2.

4.2.3 Decentralized ventilation system

A façade-integrated decentralized ventilation system with a reversible fan is modeled. As mentioned in Section 1.2, this device operates alternating periodically in supply and exhaust phase (60 seconds respectively) and usually consists of a reversible fan, heat storage, and filter. The ventilation system is modeled in Modelica [147]. Figure 4.8 illustrates the model of the mentioned device, with all the corresponding components (fan modeled as a double component for each flow direction, heat recovery, and pressure drop). The model outputs are the volume flow rate and heat recovered. These values are the result of a time integration over the simulation period in Modelica. The details about the thermal behavior of the model and its validation are described in the Appendix A.3.

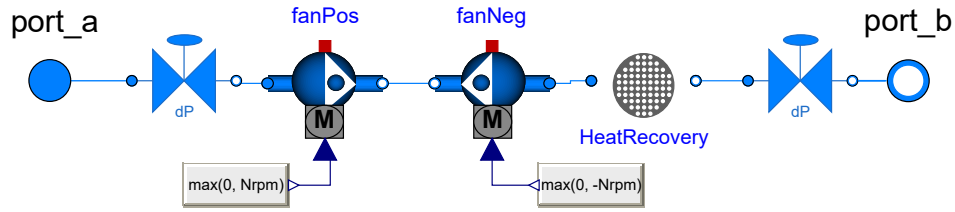


Figure 4.8: Decentralized ventilation system model in Modelica. The model includes pressure drop components, fan model and heat storage model. The details of this model are available in the Appendix A.3.

The modeled ventilation system can deliver up to $46 \frac{m^3}{h}$ at full speed (2750 RPM). The hydraulic modeling follows the data reported in the literature [57]. Three ventilation levels (associated with three different fan speeds) and the corresponding volume flow of the system were measured while varying the pressure difference on both sides of the fan. The four corresponding levels (for the reference steps DCV strategy) are calculated interpolating the given volume flow rates and the fan speed. The pressure difference between the façade and room affects the resulting airflows of these devices [152]. This model represents the supply and exhaust airflows properly by taking into account this pressure difference. Figure 4.9 depicts this mentioned influence. The corresponding levels are adjusted as required by every developed controller. The constant fan speed strategy corresponds to a 50% fan speed (corresponding to 0.4 air changes per hour in the apartment). A ceramic thermal mass represents the heat storage system. It has a cylindrical shape and a honeycomb structure that increases the heat transfer surface for a better heat recovery efficiency.

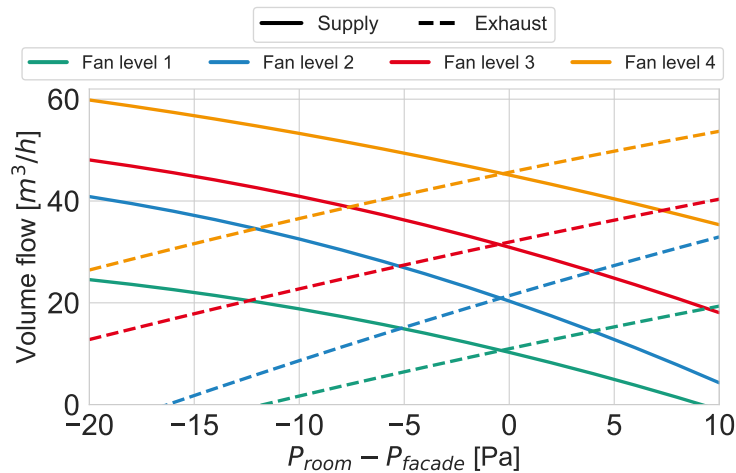


Figure 4.9: Supply and exhaust volume flow given the fan speed and pressure difference between room and façade.

The fan power as a function of the fan speed is also reported in the literature [57]. Three fan speeds were measured with their corresponding fan power. The pressure difference on both sides of the fan does not affect the power. Figure 4.10 shows the adopted values to calculate the fan power.

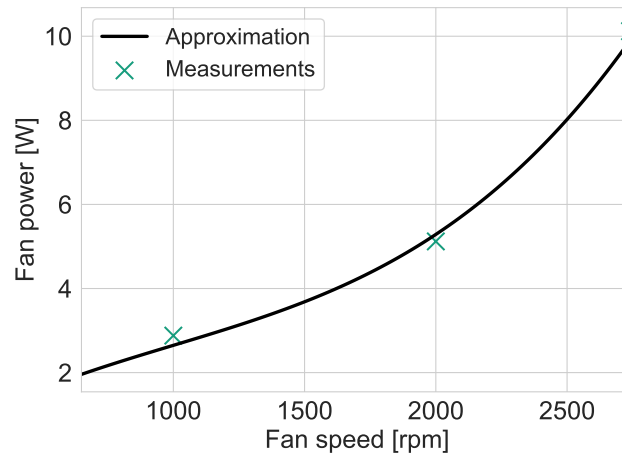


Figure 4.10: Interpolation of the fan power as a function of the fan speed. Measurements are indicated with crosses.

4.2.4 Occupant behavior

The representation of the occupant behavior can affect the results in building performance simulation largely. In this thesis, different methods are combined to obtain a suitable model to evaluate residential ventilation control strategies.

Within the framework of a master thesis, Halden [98] developed an internal loads model that includes heat, moisture, and CO_2 loads. The high resolution of the model (1-minute steps) allows testing the response of the ventilation system to rapid state changes in the dwelling. The loads are modeled for each room individually. The standard ISO 18523-2 [111] reports detailed occupancy and activity profiles for every room type. The heat release of the appliances (assumed to be 95% of the consumed power) is reported in the same source, and their use is assigned to the corresponding activities. The human heat loads are taken from the publication of Ahmed et al. [4]. The humidity release is also activity-dependent, and the values are taken from Firlag et al. [79]. The human moisture release is also included. The cooking and showering loads are adjusted and taken from TenWolde et al. [202]. Finally, the CO_2 human loads are described in the publication of Persily et al. [176]. Table 4.2 summarizes these values.

Category	Convective heat [W]	Humidity [$\frac{g}{h}$]	CO_2 [$\frac{l}{h}$]
1 Adult	79	45	14.4
1 Child	39	35	9
Lighting [$\frac{W}{m^2}$]	1.92	0	0
Washing machine	200	250	0
Dishwasher	200	0	0
Refrigerator	40	0	0
Cooking lunch	300	250	0
Cooking dinner	600	500	0
Showering	0	750	0
Plants	0	30	0

Table 4.2: Summary of the simulated internal loads.

The profiles are divided into weekdays and weekends. Figures 4.11, 4.12, 4.13 and 4.14 show the different internal loads profiles for a weekday. In simulation case studies where the simulated time is longer than one week, the weekly profiles are repeated periodically. The profiles are shifted slightly to simplify the visualization.

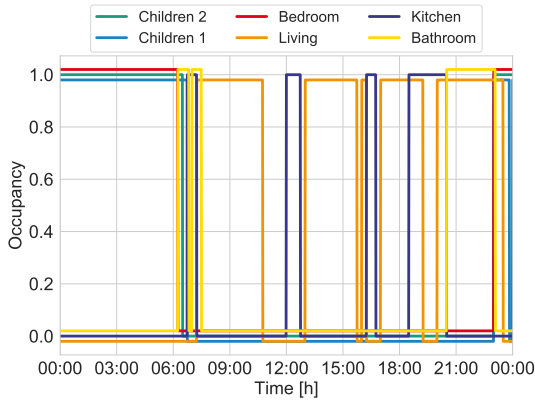


Figure 4.11: Occupancy daily profile.

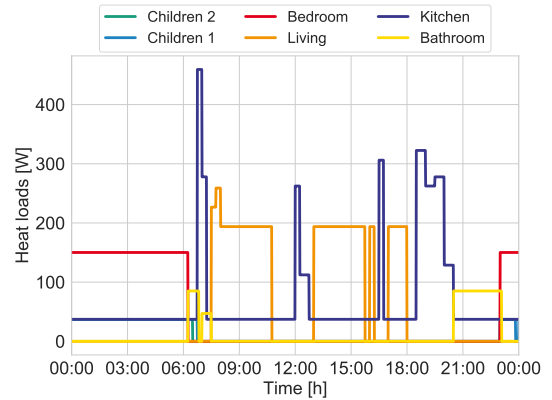


Figure 4.12: Heat loads daily profile.

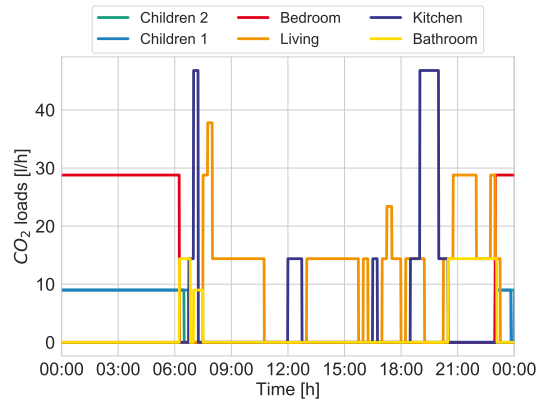


Figure 4.13: Moisture loads daily profile. Figure 4.14: CO_2 loads daily profile.

The window opening behavior is represented with two of the stochastic models that are discussed in Section 3.1. The window interaction probability in each room is modeled with logistic regression. The models of Schweiker et al. [191] and Andersen et al. [13] (group 4) are selected. The model of Andersen et al. is used in every room except the bathroom, where the model of Schweiker et al. is used. No model in the literature is valid for bathroom windows. The window state is updated depending on the output frequency of each model (5 minutes for Schweiker et al., and 10 minutes for Andersen et al.). Besides, the door opening is simulated with the occupancy status: every door remains open when the room is empty. This assumption leads to door opening ratios from 50 to 85%, which are consistent with the findings of the literature [208]. Window blinds are adjusted with an algorithm depending on the solar irradiation (closed if irradiation is above $192 \frac{W}{m^2}$) and the indoor temperature (closed if the room temperature is above $23^\circ C$ during the day, and under $23^\circ C$ at night) [18].

The heating system is not studied in this thesis and is modeled ideally and independent of the ventilation system. A PID-controller returns the required heat to maintain the desired temperature setpoints in every room (Table 4.3). The PID-controller is tuned so that it responds quickly to the heating needs (Equation 4.1). No manual adjustment of the heating system is considered. The heating setpoints are taken from the DIN 1946-6 [58], but the values in the bedrooms are adjusted to measured values in renovated buildings [31].

$$\dot{Q}_{heat}(t) = k_p \cdot e(t) + k_i + \int e(\tau) \cdot d\tau + k_d \cdot \frac{de(t)}{dt} \quad (4.1)$$

- \dot{Q}_{heat} is the instantaneous heat flow rate of the heating system

- $e(t) = T_{sp} - T_{room}(t)$ is the temperature difference between setpoint and room
- $k_p = 60$, proportional gain, non-dimensional
- $k_i = 30$, integral gain, non-dimensional
- $k_d = 1$, derivative gain, non-dimensional

Room	Day [7-22h]	Night [22-7h]
Bedroom and children rooms	21	18
Living	20	20
Kitchen	20	20
Bathroom	22	22

Table 4.3: Selected room temperature setpoints, in $^{\circ}\text{C}$ [58].

4.2.5 User interaction with mechanical ventilation

In this section, a novel user interaction model with residential decentralized ventilation systems and its integration in building performance simulation is described. Studies about the operation of mechanical ventilation systems are not widely available in the literature. This model aims to simulate the user response to different discomfort situations, in particular, to test the performance of occupant-centered control strategies.

There is only one publication that explicitly measured and investigated the occupant behavior with residential mechanical ventilation systems. Ren et al. [183] measured ten dwellings in the Netherlands for two years and inferred the user fan level selection from the fan power. They applied an exploratory analysis using clustering techniques to understand the key drivers that motivate occupants to operate mechanical ventilation systems. Results showed that there are four main groups: time-related operations, indoor environment-related, indoor and outdoor environment-related, and mixed factors-driven. Their conclusions are closely related to the results obtained in similar exploratory analyses for window opening behavior in residential buildings [63, 75].

4.2.5.1 Model assumptions and limitations

A user interaction model with mechanical ventilation is proposed, to represent the response of the occupants to discomfort with the indoor environmental quality as realistic as possible. According to Lai et al. [130], users might have different reasons to ventilate their dwellings. Therefore, there is a need to develop a model to consider the stochasticity of user behavior.

The main assumption under this model is that the user reacts only under uncomfortable conditions. The model neglects time-driven factors. Besides, the outdoor conditions influence the usage of energy recovery ventilators in cold climates [130]. This model is developed for building simulation in winter conditions but does not include weather-related variables as input.

Rather than providing a generalized validated occupant behavior model, this model intends to create a tool to simulate the stochasticity of the user regarding the manual operation of ventilation systems, focusing on its applicability in building simulation.

4.2.5.2 Artificial comfort profiles

As described in Section 2.3, the main variables used to control mechanical ventilation systems in winter conditions are the indoor relative humidity and the CO_2 concentration. The first step is to create artificial comfort profiles related to these variables. Table 4.4 shows a suggestion for four comfort profiles, following the results described on Sections 2.3.3 and 2.4.2. The profiles follow a normal probability distribution for the relative humidity and an inverted normal cumulative distribution for the CO_2 .

User comfort type	Mean RH (μ_{RH})	StdDev RH (σ_{RH})	Mean CO_2 (μ_{CO_2})	StdDev CO_2 (σ_{CO_2})
Norm	45	12	1300	250
Less air	60	8	1600	100
More air	30	8	1000	100
Distracted	45	35	1000	2000

Table 4.4: Definition of the artificial user comfort profiles. Mean (μ) and standard deviation (σ) characterize the probability distribution for each user type.

The “norm” profile follows the discomfort profiles suggested mainly in the DIN EN 16798-1 [60] norm. The “more” and “less” air profiles are deviations of the norm profile within the desired limits (relative humidity values under 25% and over 75% lead to unhealthy consequences). The lower standard deviation results in sharper profiles than the “norm” occupant. The “distracted” profile is associated with occupants who do not show a clear pattern and find themselves usually in comfortable conditions, having thus a higher SD. Figure 4.15 shows these profiles and the associated comfort probabilities.

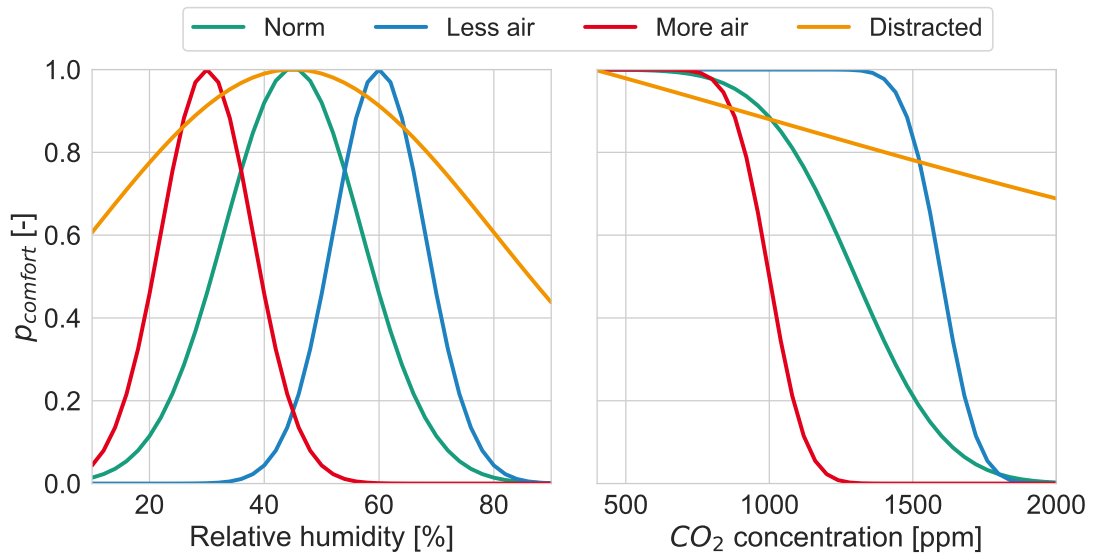


Figure 4.15: RH and CO_2 artificial comfort profiles given the probability distributions in Table 4.4.

4.2.5.3 User interaction algorithm

The interaction frequency of the user with the devices is also considered. A correct definition of this frequency is key for its application in building performance simulation. The interaction probabilities are obtained from the values reported in the literature [183]. Three profiles are modeled, following the scheme of Yun et al. [233]. The probability of interacting with the mechanical ventilation system is calculated by distributing the total interactions recorded in the present days (assuming thirty-five days of absence for holidays). Table 4.5 summarizes these values.

Frequency group	Total interactions	Daily interactions	10-min interactions
Passive	30	0.0455	3.1566E-4
Medium	200	0.3030	2.1043-3
Active	1150	1.7424	1.2100E-2

Table 4.5: Measured interaction frequencies with mechanical ventilation [183].

The user response is collected in votes, which are positive if the occupant wants a higher air exchange rate and negative if the occupant prefers a lower one. Five possible outputs are modeled, associating the user preference with a number:

- ”-2”: The user wants much less air exchange
- ”-1”: The user wants less air exchange
- ”0”: The user is comfortable and gives no vote
- ”+1”: The user wants more air exchange
- ”+2”: The user wants much more air exchange

For example, if a user votes a ”-2”, it is assumed that the user would want two ventilation levels less since the airflow is too high for this user at that moment where the vote is placed.

Then, a probabilistic approach comparing the interaction frequencies with random numbers was developed to simulate the interaction in every timestep. Figure 4.16 shows the structure of the model. In case of multivariable discomfort, a single vote is drawn for each variable, and then a random number is drawn, to consider which vote prevails (assigning an equal probability to each vote). A threshold of two standard deviations above the mean is selected since 95% of the values lie within two standard deviations in a normal distribution [104].

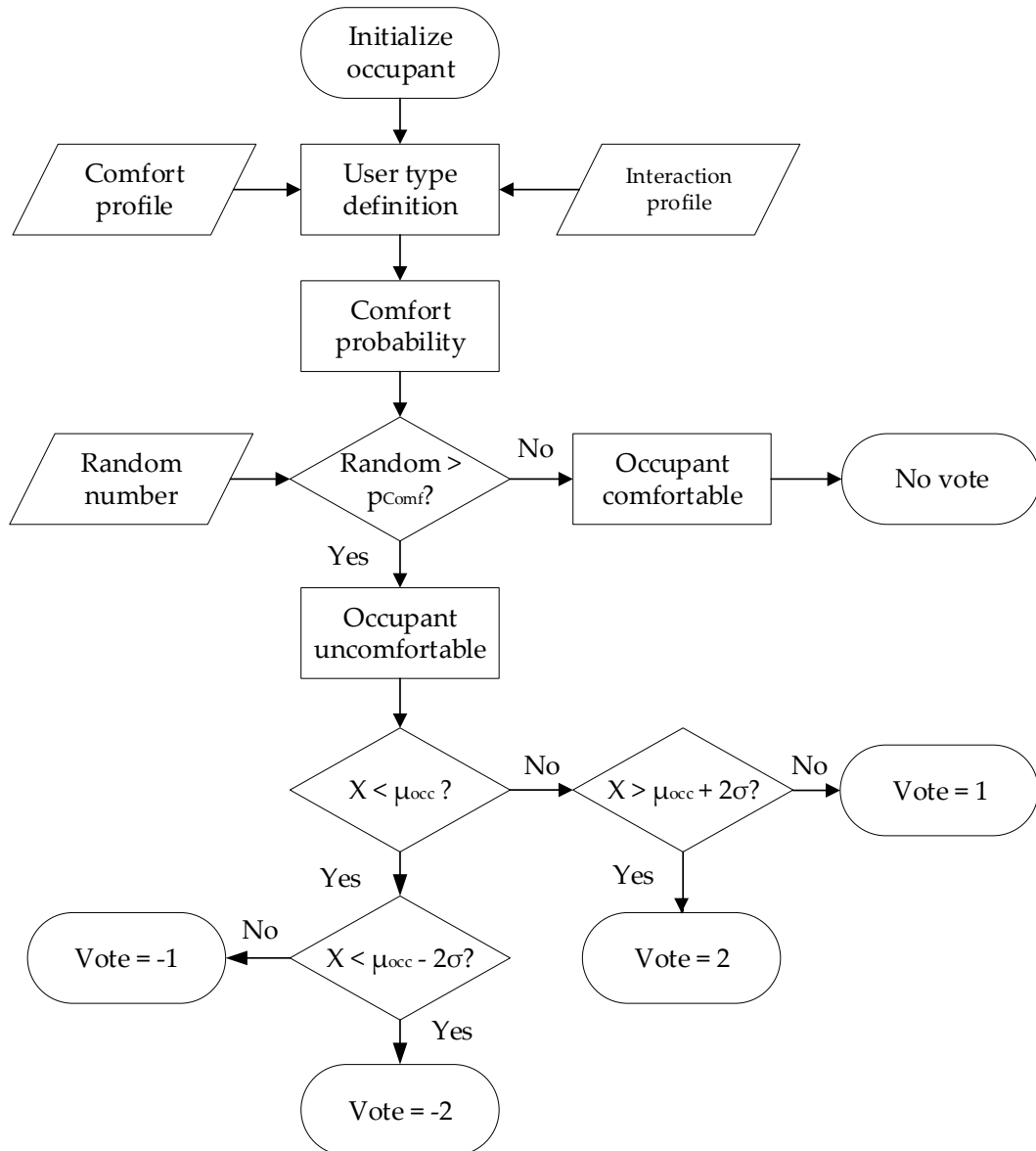


Figure 4.16: Flow chart of the proposed model to simulate the interaction between user and mechanical ventilation system, given the comfort profile.

The potential mechanical ventilation behavior in one measured building is simulated to test the proposed model. The measurements belong to the second measurement campaign reported in Section 3.2.1 during January 2019. The user votes were simulated, according to the different user comfort and activity profiles. Figure 4.17 shows the indoor RH and CO_2 values in this period used to simulate the occupant behavior towards mechanical ventilation.

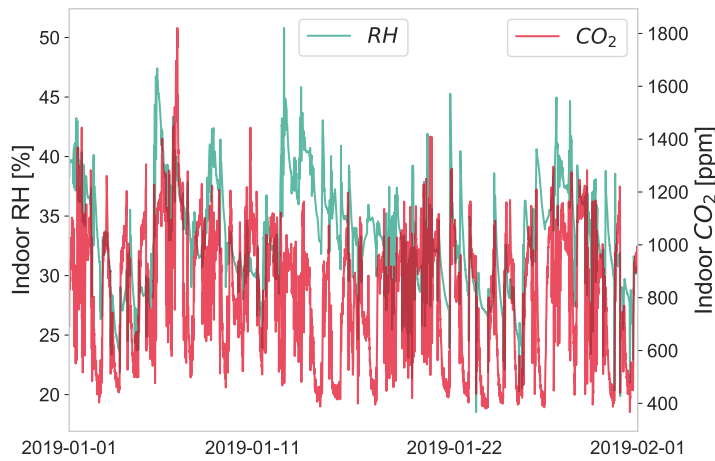


Figure 4.17: RH and CO_2 profile to test the proposed user interaction model.

Figure 4.18 left shows the comparison of an active, passive, and medium user, with a norm comfort profile. Figure 4.18 right illustrates the comparison of a "norm", "more air", and "less air" occupant, with a medium interaction frequency profile. In both cases, the model responds well to the defined artificial comfort profiles. This model serves as a basis to test different innovative control strategies for decentralized ventilation systems, especially in Section 4.4.2.

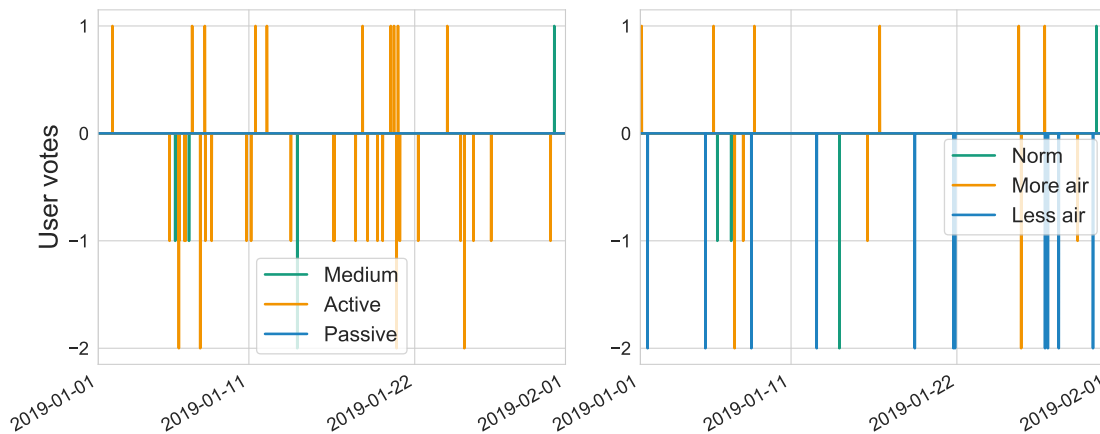


Figure 4.18: Simulated user votes given the interaction frequency (left) and RH and CO_2 comfort profile (right).

4.3 User-centered control strategies

In this section, three novel controllers for decentralized ventilation systems are described. They are tested in two simulation studies in Sections 4.4.1 and 4.4.2. The controllers in this section are already partially published in different scientific articles [36, 37]. The proposed solutions aspire to fill the gap identified in Section 4.1.1:

- Two fully automated multivariable DCV approaches are tested: cost-function and fuzzy-based.
- An occupant-centric learning DCV system is proposed.

4.3.1 Cost function DCV

The first attempt to tailor the needs of the occupants to a decentralized control strategy is to associate the dissatisfaction with the indoor RH and CO_2 with the system fan speed. The norm DIN EN 16798-1 [60] suggests acceptable values for both variables related to ventilation systems. For the RH , the norm defines ideal values between 30 and 50%, having its peaks under 20% and above 70%. This shape is approximated with a quadratic function. Furthermore, the acceptability values related to CO_2 concentration decrease with higher concentrations, and fits better the upper tier of a logit function. This approximation is as well in line with the CO_2 discomfort equations of Jokl [118].

The discomfort functions reported in the literature are converted into a DCV scheme. It is proposed that the dissatisfaction (D) due to the RH is approximated with a quadratic function. The CO_2 concentration fits better with the upper tier of a logit function. The Equations 4.2 and 4.3 define the proposed evaluation, and the figure 4.19 compares the state-of-the-art and new methods respectively. In these equations, RH is the relative humidity in % and CO_2 the carbon dioxide concentration in ppm. The coefficients are selected to fit the dissatisfaction curve to the same shape as the reported curves in the literature.

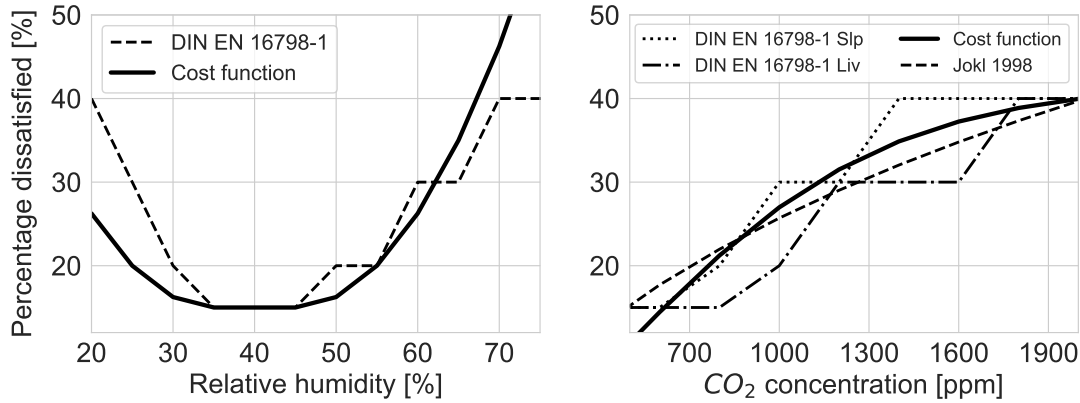


Figure 4.19: Percentage dissatisfied (PD) functions for relative humidity (left) and carbon dioxide concentration (right). Comparison of the proposed cost function and the reviewed models in Chapter 2.

$$D_{RH} = 0.05 \cdot \max(0; \text{abs}(RH - 40) - 5)^2 \quad (4.2)$$

$$D_{CO_2} = -24 + \frac{66}{1 + \exp\left(1 - \frac{CO_2}{450}\right)} \quad (4.3)$$

These approximations are integrated into a demand-controlled ventilation scheme. The control strategy in each room is lead by the variable with the highest dissatisfaction (Equation 4.4). For instance, when the dissatisfaction due to relative humidity is higher than due to CO_2 , the DCV is RH -driven, and vice versa. This controller is named the cost function strategy (*Costfun* in the plots) since the fan speed is calculated following the highest discomfort cost. Figure 4.20 shows a comparison of this strategy with the previously defined reference steps function. This DCV scheme is tested in a simulation study in Section 4.4.1. Additional key points of this controller are:

- 100 % fan speed is selected with over 75% relative humidity, to increase the importance of mold growth protection.
- Minimum fan speed is selected with below 20% relative humidity, to highlight the relevance of health-related issues with dry environments.
- No dissatisfaction is registered when CO_2 is under 750 ppm.

$$D(RH, CO_2) = \max(D_{RH}(RH), D_{CO_2}(CO_2)) \quad (4.4)$$

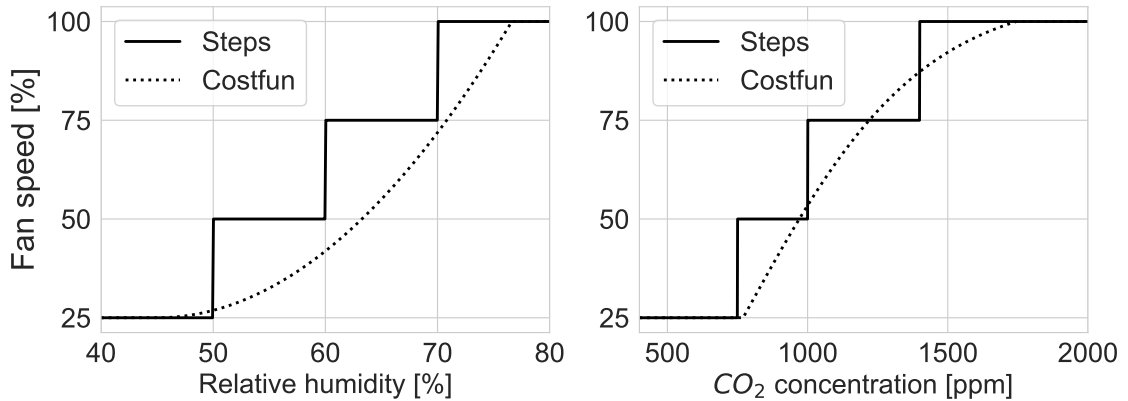


Figure 4.20: Cost function DCV strategies for RH (left) and CO_2 (right).

4.3.2 Fuzzy logic control

Another option is to control the fan speed by combining the values of RH and CO_2 into a single control strategy. Fuzzy logic is an approach to input processing that allows for multiple variables to be processed at the same time and to obtain a single output variable. Controllers based on fuzzy logic appear as a suitable solution when the system cannot be easily modeled or controlled using classical control methods due to the modeling complexity. A fuzzy approach is proposed, to seek a solution to this three-cornered problem between energy consumption, hygrothermal comfort, and IAQ.

Dounis et al. [64] developed already a thermal comfort-based fuzzy controller twenty-five years ago to control natural ventilation depending on the outdoor temperature. Besides, Kolokotsa et al. [125] designed a multivariable fuzzy system to optimize thermal and visual comfort at the same time. Molina Solana et al. [155] controlled a whole smart home system using fuzzy logic. Fuzzy controllers were also used to control IAQ. For instance, Pitalúa-Díaz et al. [177] reduced benzene concentrations when using a fuzzy-controlled exhaust ventilation system. Jaradat et al. [113] developed a multipollutant fuzzy-based control strategy. Jazizadeh et al. [114] proposed an approach to learn the thermal occupant preferences and individualize the heating system control using a self-adaptive fuzzy controller. Nevertheless, fuzzy controllers have not been considered yet for residential ventilation devices.

The controller must foremost keep the indoor environment outside the unacceptable range values, defined in Chapter 2. Figure 4.21 shows a workflow of the proposed controller, where the instantaneous measurements are compared to the previously defined limits. If these are outside those limits, then the control system must be

overridden, so that the ventilation system reacts immediately and tries to keep them. The imposed thresholds are:

- If $RH > 80\%$, then fan runs at full speed
- If $RH < 20\%$, then fan runs at minimum speed
- If $CO_2 > 1800$ ppm and $RH > 25\%$, then fan runs at full speed

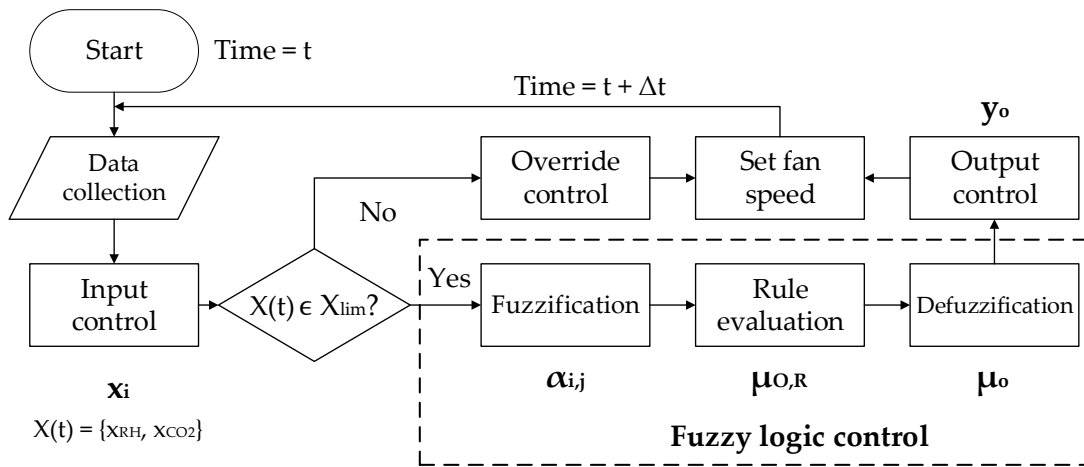


Figure 4.21: Fuzzy controller workflow.

These limits are slightly more flexible than defined in Chapter 2, because they define the segment of action of the fuzzy controller. Then, if the values are within those limits, the fuzzy controller is enabled. Even though there are recommended values for the acceptance of the indoor environmental variables, the well-being of the occupant is subjective and individual. Then, the controlled variables have a fuzzy nature. The proposal of a fuzzy controller aims at bringing a mathematical formulation of the problem rather than a unique optimal solution. Membership functions for every variable are used to determine the degree of association of a certain variable with a previously defined linguistic term (such as ‘warm’ or ‘cold’, when representing thermal sensation). Fuzzy inference rules are necessary to build a relationship between the different memberships. These and the corresponding fuzzy rules are defined through expert knowledge of the dynamic behavior of the system. The linguistic terms of every input variable (RH or CO_2) are associated with the controlled variable (fan speed) through fuzzy rules. The measured input variables (in this case, RH and CO_2 concentration) are normalized (CO_2 concentration between

400 and 1800 ppm) and fuzzified through their previously developed membership functions. The crossing points of the membership functions are selected:

- *RH*: 30 and 70%
- *CO*₂: 825 and 1250 ppm
- Fan speed: 33 and 67%

Each domain is described using three linguistic labels: “low”, “medium” and “high”, for the indoor *RH*, and “excellent”, “acceptable” or “poor” for the room *CO*₂ concentration. The fuzzification process calculates consequently the membership degree $\alpha_{i,j}$ (probability of belonging to a certain category j for each input measurement x_i) using the sigmoid function (Equation 4.5). A sigmoid shape allows the fuzzy control field to be smoother than using sharp-edged shapes, such as trapezoids.

$$\alpha_{i,j} = \frac{1}{(1 + e^{-a(x_i-c)})} \quad (4.5)$$

The fan membership function, necessary to calculate the fan output speed, is trapezoidal and divides the whole normalized fan speed range into three equal parts (low, medium, and high). Figure 4.22 illustrates the three membership functions of the controller.

The fuzzified inputs are interpreted based on a set of rules, which compose the fuzzy inference engine. As explained before, fuzzy rules aim at describing the relationship between the fuzzified linguistic terms of the input and output variables. In this thesis, an expert knowledge-based system of rules is implemented, summarized in Table 4.6. Because keeping the relative humidity inside the healthy limits (defined in Chapter 2) is the first task of the controller, the *CO*₂ concentration is neglected when the *RH* is not in its admissible range.

IF <i>RH</i> is Low OR (<i>RH</i> is Acceptable and <i>CO</i> ₂ is Excellent) THEN <i>FS</i> is Low
IF <i>RH</i> is Acceptable AND <i>CO</i> ₂ is Acceptable THEN <i>FS</i> is Medium
IF <i>RH</i> is High OR (<i>RH</i> is Acceptable and <i>CO</i> ₂ is Poor) THEN <i>FS</i> is High

Table 4.6: Fuzzy rules for every fan output (*FS* = Fan speed).

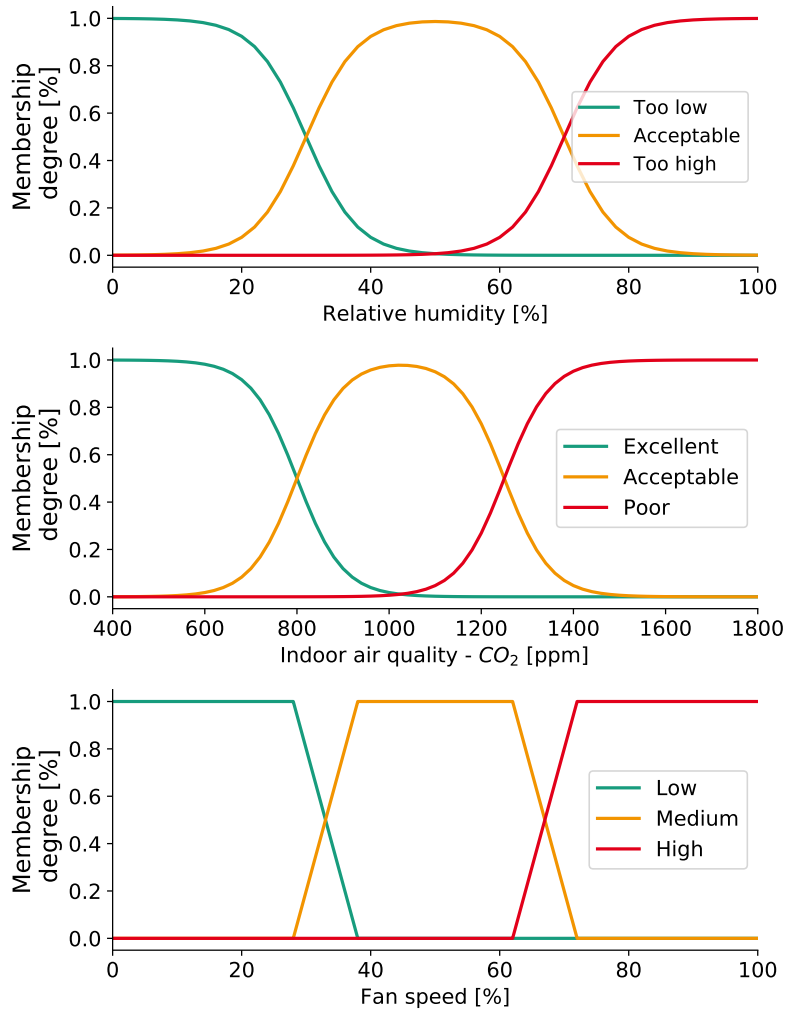


Figure 4.22: Membership functions for the fuzzy controller. RH and CO_2 are the input variables x_i and the fan speed is the output variable y_o .

The minimum number of rules is the number of linguistic terms used to define the output variable. The level of detail of these rules depends on the number of categories used to describe the input and output variables [69]. Furthermore, the inference engine interprets the degree levels of the inputs for each rule (μ_R) and calculates the degree levels of each output (fan speed) category. In this case, the used inference engine is the Mamdani max-min method [144]. The *AND* operator is represented with the minimum and the *OR* operator with the maximum. The fuzzy output of each rule ($\mu_{o,R}$) and the final aggregation (μ_o) are calculated. The following equations describe, as an example, the calculation for fan speed low and the final aggregation of the three fan categories:

$$\mu_{R_1} = \max(\alpha_{RH,low}, \min(\alpha_{RH,Acc}, \alpha_{CO_2,Exc})) \quad (4.6)$$

$$\mu_{o,R_1} = \min(\mu_{RH,low}, \alpha_{Fan,Low}) \quad (4.7)$$

$$\mu_o = \max(\mu_{R_1}, \mu_{R_2}, \mu_{R_3}) \quad (4.8)$$

Once the output degree for the three fan speed categories $\mu(o, R)$ is obtained, the normalized fan speed y_o is calculated using the centroid defuzzification method:

$$y_o = \frac{\sum Y_j \cdot \mu_{o,j}(Y_j)}{\sum \mu_{o,j}(Y_j)} \quad (4.9)$$

being $Y_j \in [0, 1]$ the normalized fan speed, j the number of evaluated points in the output domain, and $\mu_{o,j}(Y_j)$ the membership degree at each point of the output variable domain. The outcome of the whole process is illustrated in a 3D control field in Figure 4.23. In principle, this field can be predefined, which makes the fuzzy controller another variation of a DCV scheme, and highlights its robustness and reliability. Together with the cost function controller, the fuzzy-based DCV is tested in a simulation study in Section 4.4.1.

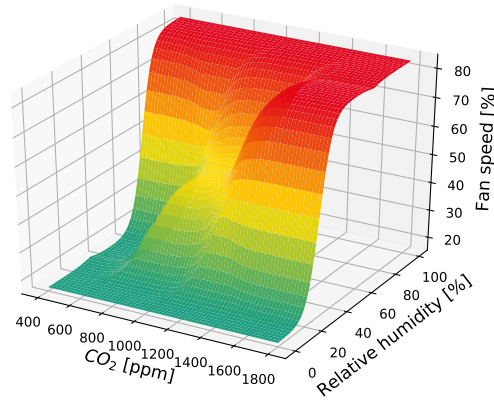


Figure 4.23: Fan speed control field resulting of the fuzzy control strategy.

4.3.3 Self-learning DCV

In this section, an innovative learning control strategy for residential ventilation systems is presented. This strategy is based on a DCV scheme, which can tailor itself to the needs of the occupant. The control uses a comfort profile and a supervised learning algorithm (requires training data) to predict the user vote by taking into account the indoor environmental conditions.

Learning systems gained popularity in the scientific world around buildings in the last ten years. The primary optimization target has been the heating energy consumption. For instance, Kastner et al. [121] developed a system that learns an occupancy schedule for office buildings and uses it to optimize the heating energy consumption with an artificial neural network. Daum et al. [52] defined a new method to represent the thermal occupant preference, using curves based on logistic regression. They concluded that the thermal preference could be learned successfully between 40 and 60 user feedback votes. Carreira et al. [39] simulated the optimization of an HVAC system that learns the occupants thermal preference using a clustering algorithm. Results indicate that the system could successfully learn and adapt itself to this individualization of the occupants' preferences. Xu et al. [230] developed a scheme to differentiate the individual thermal preferences in a multi-occupant environment to tailor the HVAC controller. Learning schemes are implemented already in real cases. Gunay et al. [93] developed a learning scheme to optimize the temperature setpoint of a heating system. Commercial systems that learn the thermal occupant preference and optimize the heating setpoint are already available [161].

Other building systems have been studied as well and controlled with learning algorithms. For example, Cheng et al. [44] created a satisfaction-based learning controller for integrated light and blind control to tailor the illuminance levels to the needs of the user. Park et al. [167] created a self-learning lighting controller. Vazquez Canteli et al. [213] used a learning algorithm to adapt the demand response behavior of residential electricity consumption to reduce energy costs. Lastly, Ghahramani et al. [89] developed a learning algorithm for the occupant interaction with their workspace (for example, working alone or with other people) using a combination of wearable and environmental sensors.

Until now, no publication covers the application of learning systems to a residential ventilation system. The next sections provide a full description of the proposed control strategy.

4.3.3.1 Default comfort profile

The default comfort profile for the control system was built following the norm comfort profile for the occupant behavior model, described in Section 4.2.5. This profile should represent an average comfort profile for both RH and CO_2 , while at

the same time keeping the flexibility to adapt itself to new incoming data points from the user feedback.

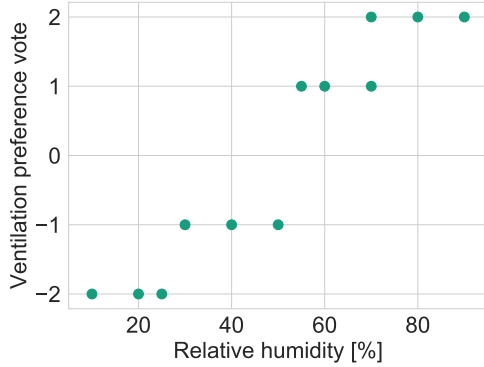


Figure 4.24: RH ventilation preference votes for the default comfort profile.

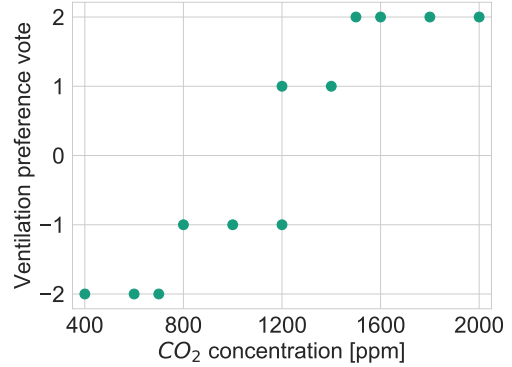


Figure 4.25: CO_2 ventilation preference votes for the default comfort profile.

Twelve ventilation preference votes for each variable were arbitrarily defined, to build the comfort and IAQ profile. These votes give a total combination of 144 default artificial user votes. These are shown in Figures 4.24 and 4.25, and the resulting comfort profile is seen in Figure 4.26. This profile is considered the starting point of the learning control strategy.

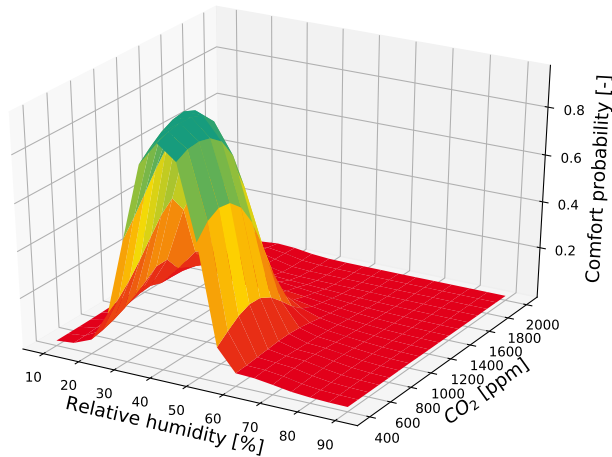


Figure 4.26: Resulting 3D field for the default comfort profile.

4.3.3.2 Algorithm selection

A key step to a successful learning DCV is the algorithm selection. With the help of machine learning, the user preferences can be successfully captured and provide

a proper solution to achieve better comfort, enhance the acceptance, and meet the energy efficiency targets [39].

In this section, six popular classification algorithms are picked and compared. The performance in terms of computational resources and the ability to learn the desired profiles are tested. The best algorithm is then selected and applied in the learning DCV scheme. The preselected algorithms are:

- Logistic regression (LogR)
- Support vector machines with radial basis function kernel (SVM)
- Gaussian naïve Bayes (NB)
- Gaussian process classifier with Matérn kernel (GPC)
- Decision tree classifier (DT)
- Random forests (RF)

The comparison was performed using the python package scikit-learn [172]. The first approach was to learn the default comfort profile and to observe the resulting predictions after learning. The performance indicators are accuracy (Acc), true positive rate (TPR), and positive predictive value (PPV), recommended in the literature for the evaluation of learning algorithms [89]. These indicators are already defined in Section 3.3.2. Accuracy evaluates the overall degree of closeness of predictions with the actual labels. However, in algorithm tuning and selection in the context of occupant behavior, the goal is to maximize the PPV while at the same time keeping the TPR in an acceptable range. Table 4.7 summarizes the results.

Algorithm	Acc	TPR	PPV
LogR	0.7783	0.7701	0.7525
SVM	0.9022	0.9011	0.8875
NB	0.7918	0.8138	0.8150
GPC	0.8694	0.8832	0.8825
DT	0.9000	0.8985	0.8825
RF	0.8856	0.8945	0.8875

Table 4.7: Selection of DCV algorithm: comparison of performance indicators for every classification algorithm.

From the table, support vector machines shows the best performance in comparison to the other five algorithms. However, the difference in the values between support vector machines and others is marginal. The logistic regression and naive Bayes classifiers are discarded due to their poor performance, and a second comparison was carried out. Daum et al. [52] suggested using the overlapping surface as a learning indicator, being only valid for a single variable. This indicator is called the learning rate (LR) and is defined by Equation 4.10. A value of one indicates perfect learning of the comfort profile. The average of the learning rate is calculated to combine both variables. Before entering the calculation procedure, the learned profiles are rescaled so that the maximum comfort probability is always one.

$$LR(X) = 1 - \int |p_{comf,user}(X) - p_{comf,learn}(X)|dX \quad (4.10)$$

$$LR = \frac{\sum LR(X_i)}{n} \quad (4.11)$$

A simulation was carried out using the four artificial occupant comfort profiles for RH and CO_2 . The goal was to calculate the learning rate for the four preselected algorithms and to compare them. The simulation was performed until the 150th vote took place since it was assumed as a reasonable limit for a stabilized learned profile. Table 4.8 shows the values of the learning rate for the indoor RH and CO_2 comfort profiles and the time consumption of the algorithm.

Algorithm	Norm	Less air	More air	Distracted	Time [s]
SVM	0.8499	0.7334	0.7530	0.7374	9.95
RF	0.8472	0.6119	0.6436	0.6024	3.92
DT	0.6974	0.7611	0.6298	0.6003	1.70
GPC	0.7835	0.6796	0.7487	0.8153	234.45

Table 4.8: Selection of DCV algorithm: Combined learning rate results for every tested classification algorithm for the learning DCV controller.

Two out of four learning indicators were best when using support vector machines (SVM). This result discards the usage of random forests (RF) and decision trees (DT) as possible learning algorithms, as their learning rate is significantly lower than the other two. When comparing the computational resources, the support vector machines took almost ten seconds to learn the profile, while the Gaussian process classifier (GPC) procedure lasted almost four minutes. Hence, the support vector machines (SVM) was selected to develop the DCV learning scheme. Figure

4.27 shows the combined learning rate for this algorithm when simulating the four synthetic profiles. The stabilization (the point where the value of learning rate stays fairly constant) occurs between 60 and 80 user votes. This result agrees with the publication of Daum et al. [52]. A detailed explanation of the mathematics behind this algorithm is described in the Appendix A.5.

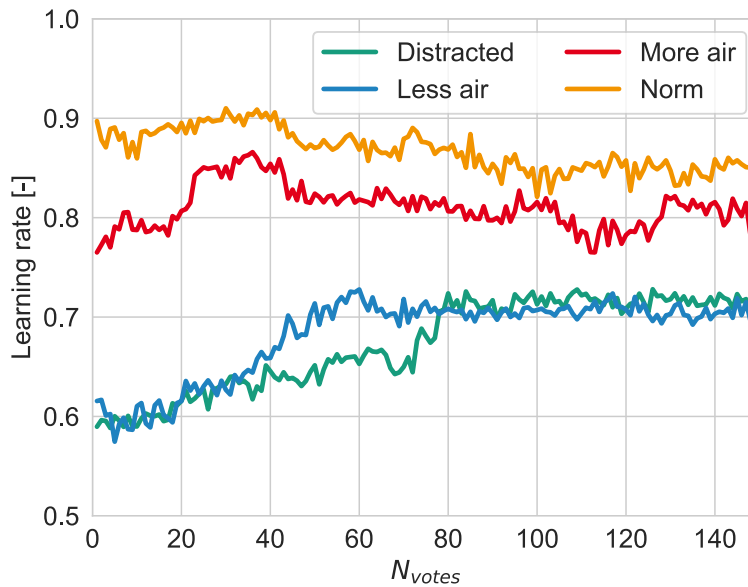


Figure 4.27: Evolution of the combined learning rate using SVM.

4.3.3.3 Learning DCV process

Once the algorithm is selected and tuned, and the starting profile is defined, the learning procedure can take place. The learning process is executed as follows:

1. Initialize the algorithm and create the default comfort profile
2. If there is a new user vote, collect it together with the instant values of RH and CO_2
3. Append new votes to the previous ones
4. Check the date of the votes and erase the oldest ones
5. Check that the votes are inside the healthy limits. If not, correct them.
6. Update comfort profiles for control

7. Continue until new votes come

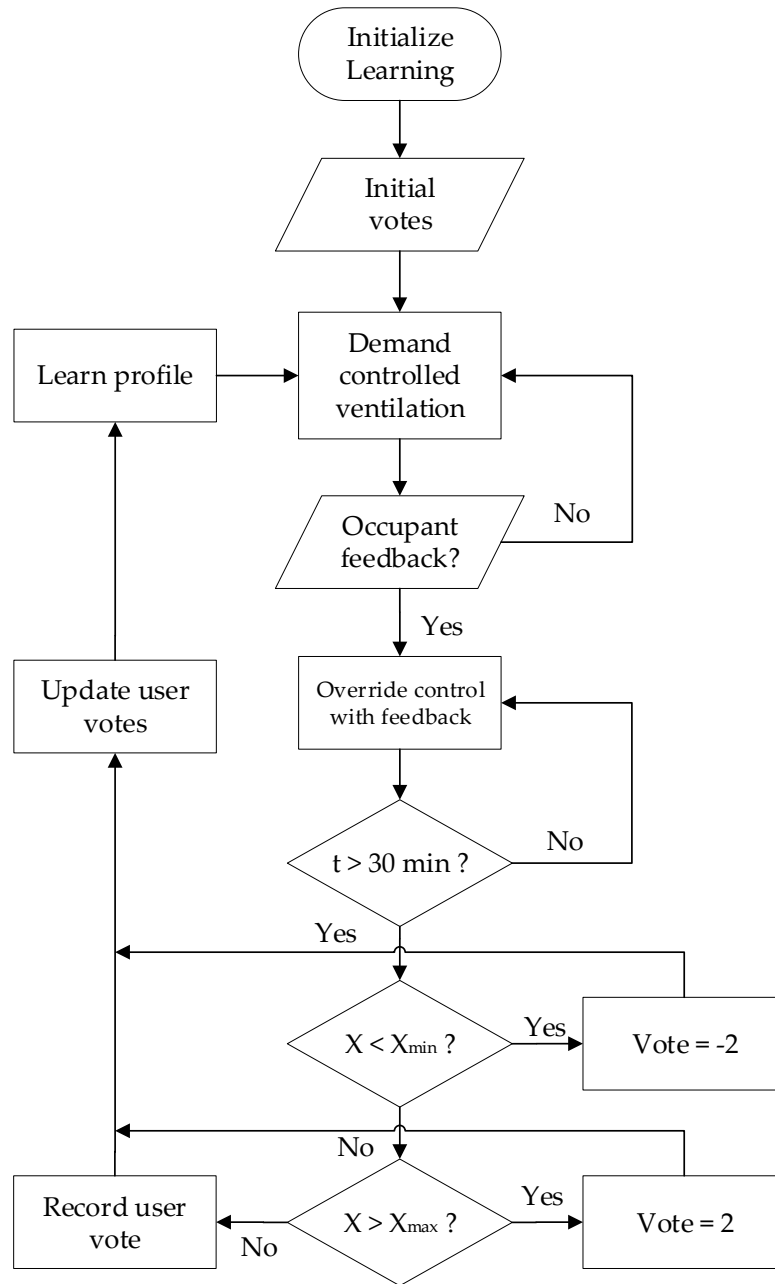


Figure 4.28: Workflow of the self-learning controller.

Figure 4.28 shows a flow chart of the learning scheme. A vote limit of 150 votes was imposed, in line with the results of the previous section. Limiting the number of votes creates a slower response of the system to the learning process when the vote count reaches its limit. Because the oldest user votes are erased when reaching the

vote limit, the learning process will never cause the comfort zone to be extremely far away from the default profile. On the one hand, this reduces the possible individualization of the control to “extreme” occupant preferences. On the other hand, this limits possible inconsistencies of the user votes due to their stochastic nature and non-desired comfort zones (such as too dry air or too humid air, which can cause adverse health effects or promote mold growth in the dwelling). In addition, analogous to the fuzzy controller, “healthy limits” are imposed, to avoid having indoor environmental conditions which are rated as unacceptable by the norms and the literature:

- If $RH > 80\%$, then fan runs at full speed
- If $RH < 20\%$, then fan runs at minimum speed
- If $CO_2 > 1800$ ppm and $RH > 25\%$, then fan runs at full speed

When the user gives feedback to the ventilation system, the control is overridden for 30 minutes, and the airflow level is determined by the user’s choice. Otherwise, the control system tries to predict the occupant comfort according to the learned profiles and adjusts the airflow levels respectively. The whole sequence is described in four steps:

1. Collect the instantaneous value for the controlled variables (RH , CO_2)
2. Predict the ventilation vote of the user according to the learned comfort profiles
3. Adjust the fan level according to this vote
4. When the occupant votes, adjust the fan level for 30 minutes to the voted fan level

The resulting default control profile is illustrated in Figure 4.29. The colors are associated with user vote predictions.

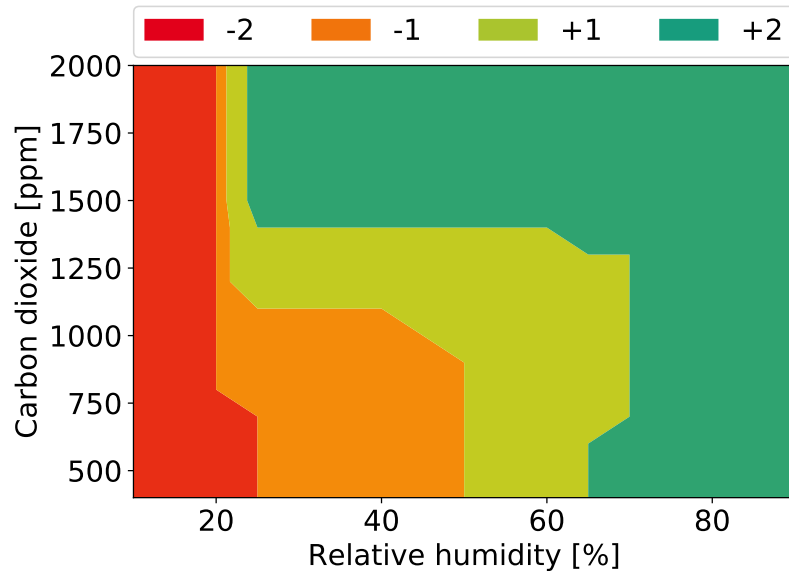


Figure 4.29: Default control field of the self-learning controller. The colored areas represent the prediction of the user vote.

Moreover, learning the artificial user profiles and their impact on the DCV control field are illustrated in the Appendix A.6. The pictures represent the learning process from 10 to 200 votes. An additional complete random profile shows the resilience of the learning to random user profiles, highlighting its ability to keep the predefined control shape.

4.4 Simulation case studies

In this section, two simulation studies are carried out.

1. A comparison of fully automated control strategies, to analyze the performance of the proposed cost function and fuzzy logic controllers.
2. A simulation of the learning DCV scheme under different user comfort and interaction frequency profiles.

The selected climate is representative of a European temperate climate without a dry season and with warm summer (Cfb classification type [175]). This thesis focuses on the performance of ventilation control strategies in winter conditions. The selected simulation weeks are detailed in every subsection. All selected strategies are applied in the co-simulation scheme (Section 4.2.1), taking advantage of the models in Section 4.2.

The performance indicators are already defined in Chapter 2. The energy consumption is evaluated through the primary energy consumption $Q_{pe,vent}$ (Equation 2.7), which takes into account the heating losses due to ventilation and the electricity consumption of the fan. The indoor air quality is evaluated through the CO_2 concentration using the indicator ΔCO_2 (Equation 2.11). The health-related issues and humidity comfort are evaluated through the relative humidity, using the indicators ΔRH_{up} (Equation 2.14) and ΔRH_{lo} (Equation 2.15).

4.4.1 Multivariable fully automated control strategies

4.4.1.1 Methodology

In this section, the proposed user-centered fully automated multivariable control strategies (cost function and fuzzy logic) are tested in a simulation case study. These are compared to the control systems defined as baseline cases (constant fan speed and steps DCV). These results are published partially in scientific articles [36, 37].

For the first analysis, a single week is simulated due to computational reasons since the internal loads profile is modeled only for this period. In Section 4.4.1.2, the performance of four fully-automated controllers in an average winter week is compared. In Section 4.4.1.3, two controllers (steps and fuzzy-based DCV) are selected, and the sensitivity to the ambient conditions is studied. Merzkirch [150] concluded that the two variables that influence the most the primary energy consumption in ventilation systems are the heat recovery efficiency and volume flow rate. From the definition of the heat recovery efficiency in Section 2.2.1, and since the heat storage is modeled component-based, the only variable left that affects the heat recovery efficiency is the ambient temperature. Thus, cold and warm winter weeks are taken into account as well. Besides, different algorithms control the fan speed. However, the actual volume flow is sensitive to the wind pressure [152]. In this case, windy and calm winter weeks are simulated. The mean ambient conditions in the whole winter period are summarized in Table 4.9, together with the mean value of the ambient conditions of every simulated week. Figure 4.30 shows the selected weeks for the sensitivity analysis. Lastly, the results are discussed in Section 4.4.1.4.

	Unit	Winter season mean	Average week mean	Warm week mean	Cold week mean	Windy week mean	Calm week mean
T_{amb}	$^{\circ}C$	3.60	2.70	6.40	-5.28	3.08	3.41
RH_{amb}	%	80.15	67.76	80.41	71.64	81.51	87.19
AH_{amb}	$\frac{g}{kg}$	3.91	3.22	5.05	1.89	4.17	4.47
WS	$\frac{m}{s}$	3.09	3.40	3.01	1.89	7.00	1.06

Table 4.9: Mean values of the weather conditions (ambient temperature, relative humidity, absolute humidity and wind speed - WS) in the selected weeks for the sensitivity analysis.

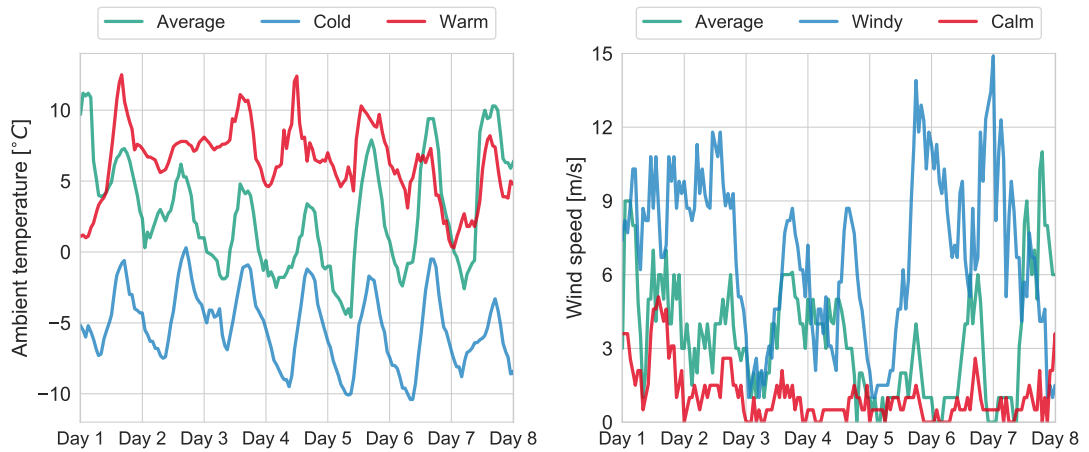


Figure 4.30: Ambient conditions (left: ambient temperature, right: wind speed) in the selected weeks of the winter season for the sensitivity analysis.

The sensitivity to internal loads is also investigated. In this study, the loads are reduced and increased by 50%. A discussion of the obtained results is included at the end of the section.

4.4.1.2 Results for an average week

Figure 4.31 illustrates the total air change rate in the dwelling on a single day. The wind influence is observed in the constant speed strategy, which does not deliver a constant airflow. Although the three DCV approaches are not equivalent, the general trend of the required air exchange rate coincides, as it follows the simulated RH and CO_2 internal loads profiles. The cost function strategy presents the smoothest airflow rate changes. The piecewise steps control strategy is sometimes unstable around the equilibrium point (threshold value between two different steps), even

when including a hysteresis cycle. This instability is a disadvantage against the other DCV controllers, which provide smooth airflow levels. The resulting air change rates are within the typical values for renovated German multifamily buildings [68], which are around 0.4 ACH.

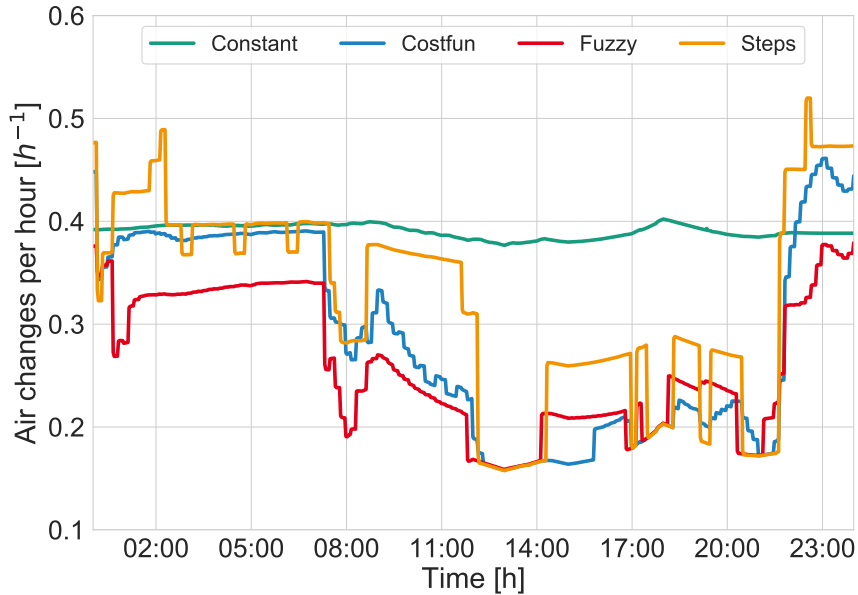


Figure 4.31: Total air exchange rate in a single day for the four controllers.

Some rooms of particular interest are selected to illustrate the comfort and IAQ results. Figure 4.32 depicts the cumulative distribution of indoor RH and CO_2 concentration during occupancy. The high humidity values during showering in the bathroom are present in the four cases. In the kitchen and bathroom, the constant airflow strategy offers more extreme values on both sides (below 25% and above 75%). In the dry rooms, a similar pattern is observed in both RH and CO_2 plots. During occupancy, the bedroom has high CO_2 internal loads, which results in a higher airflow for the three DCV strategies, but also keeps these rooms drier. The constant strategy fails to keep the CO_2 concentration in the desired range in this room. In the living room, the constant airflow strategy has values below 25% 30% of the time. The three controllers reach the equilibrium state in a range of 1250-1500 ppm in the bedroom, as around 60% of the values during occupancy are in this range (the fuzzy controller performs worse than the other ones in this room). In the living room, the fuzzy strategy presents around 5% higher relative humidity values on average than the steps controller. The CO_2 concentration in the living room is similar for the four analyzed controllers.

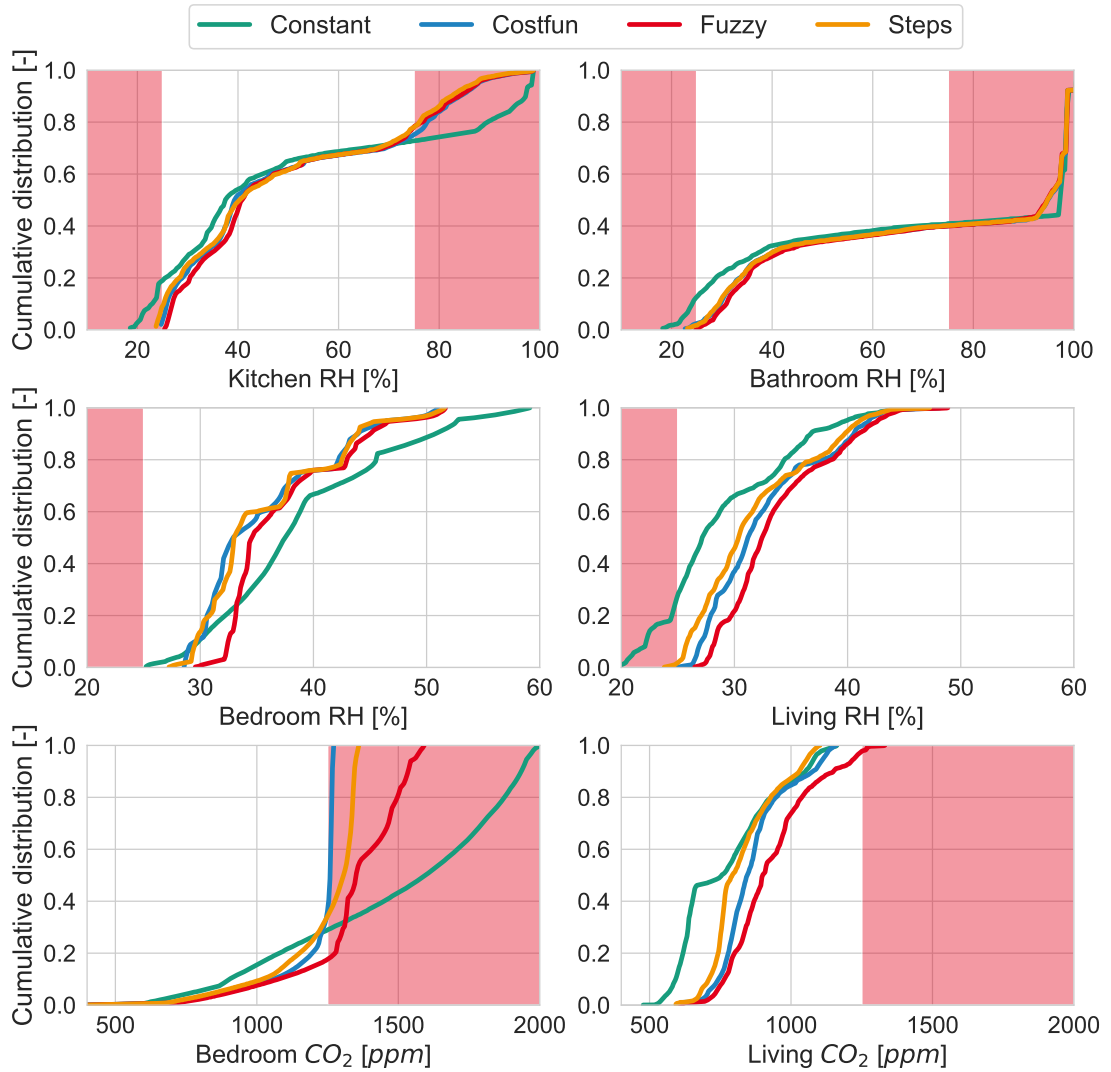


Figure 4.32: RH and CO_2 cumulative distribution plots in selected rooms.

Table 4.10 summarizes the results of the key performance indicators for each simulated control strategy. The fuzzy controller has not recorded any instant of RH below 20%, which highlights the importance of the imposed “healthy limits” rule for the multivariable controllers. Even though the steps controller reacts to CO_2 concentration in the “dry” rooms, there are almost no registered points below the 25% threshold. In this particular case, the four controllers perform well regarding dry environments.

Control	ΔRH_{lo} [%]	ΔRH_{up} [%]	ΔCO_2 [ppm]	$Q_{pe,vent}$ [kWh]
Constant	1.16	9.47	120.59	65.42
Costfun	0.01	7.89	31.78	52.11
Fuzzy	0.00	7.76	58.49	46.53
Steps	0.05	7.67	41.74	56.25

Table 4.10: Summary of performance indicators for the simulated control strategies.

Moreover, the constant strategy overcomes more often the RH_{up} threshold, as expected (10% above the acceptable limit), but the reported values for the other strategies are close (around 7.5%). These values are reduced to 1.5% when also considering the absent period in the humid rooms (kitchen and bathroom), meaning that the actual mold growth risk in the simulation is low. Besides, the duration of the high RH values is never longer than an hour. A constant airflow strategy in this case ensures mold growth protection successfully. Despite the differences, the three DCV solutions are set to full speed when the indoor relative humidity is over 75-80%. The resulting window opening is never over 0.1%, therefore neglecting its influence on the results. The three DCV strategies outperform slightly the constant airflow strategy regarding the relative humidity.

The outcome for the ΔCO_2 is analogous. The constant strategy has an integrated overshoot of almost 120 ppm against the considered threshold. This is also a consequence of the chosen “unaware” fan level speed. The three DCV controllers improve the IAQ performance significantly, being the cost function the best in this case.

Figure 4.33 shows the primary energy consumption associated with ventilation and the potential savings related to the constant airflow strategy. When considering the ventilation primary energy consumption, the fuzzy controller presents a saving of 29% in comparison to the worst-case scenario (constant airflow). In comparison to the smart state-of-the-art controller (steps), the cost function strategy provides around 9% total primary energy savings, and the fuzzy controller reaches 18% savings (fan primary energy savings are 20%). However, the reported performance indicators can be affected by different weather conditions or internal loads. The next sections provide further insight into this topic.

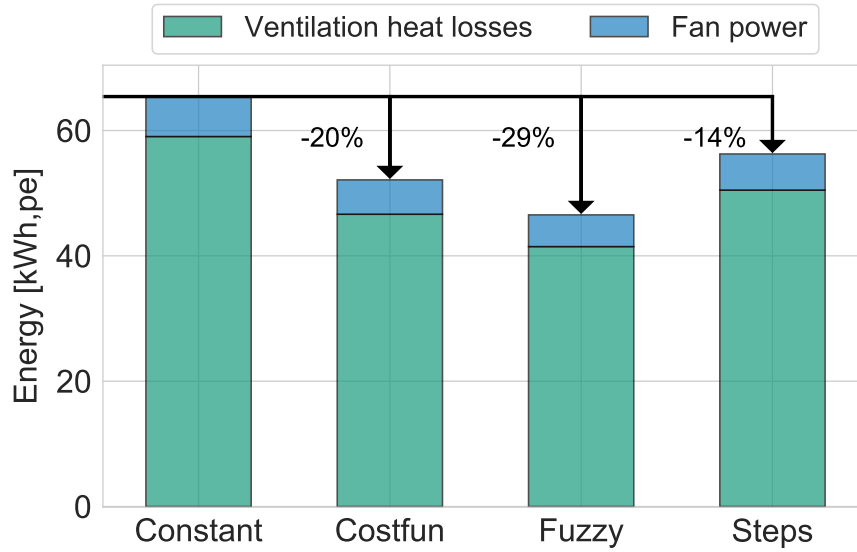


Figure 4.33: Primary energy savings of the proposed ventilation controllers. Constant airflow strategy is taken as baseline case.

4.4.1.3 Sensitivity analysis

In this section, the results of the sensitivity analysis are presented, only comparing the state-of-the-art smart steps strategy with the fuzzy-based DCV. Table 4.11 shows the results for the five simulated weeks regarding weather conditions. The relative humidity indicators do not vary strongly between the simulated weeks, and the difference between the controllers is minimal. The warm week presents a higher ambient absolute humidity (see Table 4.9), and therefore the mold growth risk increases for both controllers. Mold growth protection becomes relevant especially in the humid days of the winter season. Dry environments are slightly present only in the cold week for the steps strategy. The CO_2 indicator is also not strongly affected, and mostly stays in the range of the values presented in the last section (30-60). In the warm and windy weeks, the fuzzy controller increases the air exchange rate in comparison to the steps strategy, resulting in almost identical values for the CO_2 indicator. In the cold week, the fuzzy controller has a higher value (reducing the air exchange rate to avoid dry environments) but is still considerably lower than the value presented for the constant strategy in the last section (120 - see Table 4.10). These results are a consequence of a general low sensitivity of the air exchange rate. In the five simulated weeks, the mechanical air exchange rate remains fairly constant, as well as the fan speed. In the windy week, the average fan speed is lower, as the system takes advantage of the additional pressure difference, which causes

higher volume flow rates at lower fan speeds. Baldini et al. [23] already identified this advantage as a potential energy-saving strategy in decentralized ventilation. The lower CO_2 concentration in the windy week is explained through an increased infiltration rate, as the mechanical air exchange rate remains fairly constant. The fuzzy strategy provides energy savings in the five simulated weeks.

	Control	Average week	Warm week	Cold week	Windy week	Calm week
ΔRH_{up} [%]	Fuzzy	7.76	10.01	7.30	9.30	8.04
	Steps	7.67	9.89	7.23	9.12	7.91
ΔRH_{lo} [%]	Fuzzy	0.00	0.00	0.23	0.00	0.06
	Steps	0.05	0.00	2.92	0.00	0.76
ΔCO_2 [ppm]	Fuzzy	58.49	38.21	85.95	33.35	57.92
	Steps	41.74	39.38	48.45	33.77	46.16
$Q_{pe,vent}$ [kWh]	Fuzzy	46.53	36.86	58.82	47.08	46.25
	Steps	56.25	43.28	75.60	52.08	55.61
$FanRPM_{av}$ [%]	Fuzzy	900	928	873	898	924
	Steps	1035	1057	1050	989	1059
ACH_{mech} [h^{-1}]	Fuzzy	0.21	0.22	0.20	0.23	0.22
	Steps	0.27	0.27	0.28	0.27	0.28

Table 4.11: Summary of performance indicators in the different simulated weeks for the weather sensitivity. In addition, average fan speed ($FanRPM_{av}$) and total mechanical air exchange rate (ACH_{mech}) are considered.

This similarity among the obtained fan speeds lies on the importance of the indoor environmental conditions for the controller behavior. Figure 4.34 illustrates the discomfort in every room on a single day for the average week. The discomfort is represented by the dissatisfaction functions, developed for the cost function strategy in Section 4.3.1. In every room except the bathroom, the discomfort is almost always higher due to CO_2 concentration than to relative humidity. The resulting indoor CO_2 levels are independent of the ambient conditions, where a constant concentration of 400 ppm is assumed. The ambient humidity levels can have an additional influence, especially on dry days, where the rooms with lower internal loads present a low relative humidity, dropping under the acceptable threshold and increasing the discomfort. Therefore, the sensitivity of the results to the internal loads must be studied.

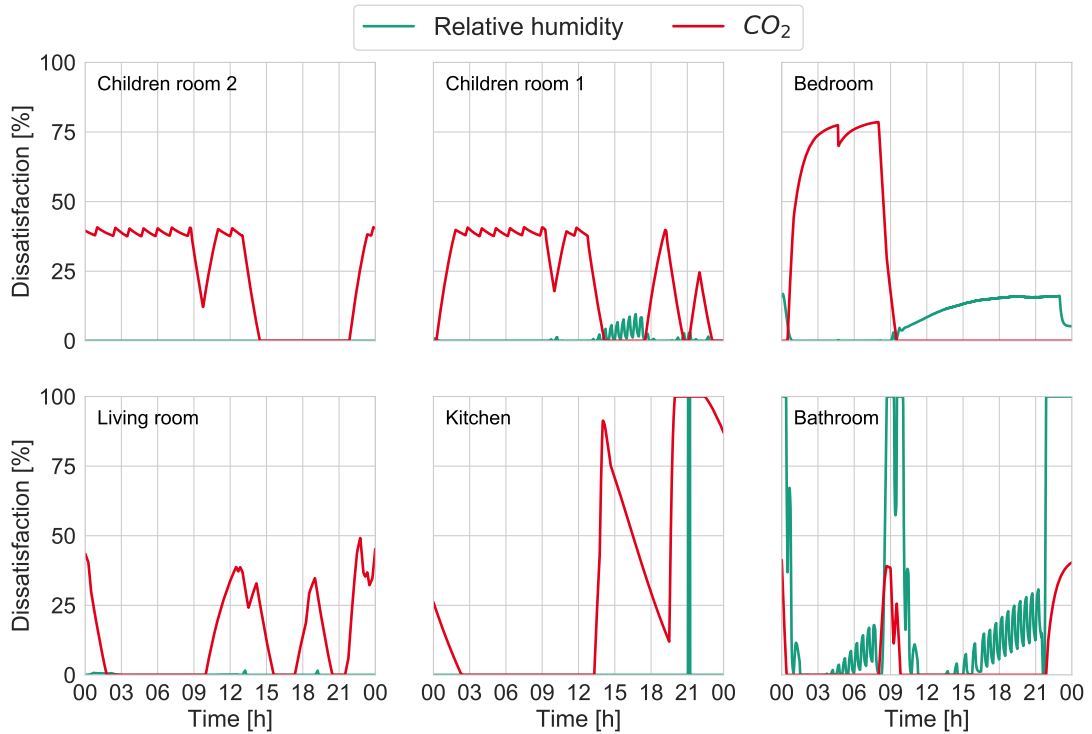


Figure 4.34: Discomfort values due to RH and CO_2 in every room in a single day of the average week.

Three simulations of the average week with a global variation of the internal loads (-50% and +50%) are performed. Table 4.12 summarizes the results. In this case, every indicator in the table is strongly affected by the internal loads variation. The relative humidity and CO_2 indicators become worse than the constant strategy when the loads are increased or become negligible when the loads are reduced. The average fan speed and resulting air exchange rate are also strongly affected, which highlights the importance of the correct dimensioning of residential ventilation systems, adjusting it to the needs of the occupants if possible. The performance difference between both strategies for the RH indicator remains similar. The CO_2 indicator is more sensitive to internal loads variations. The fuzzy controller can perform better than the steps strategy when the loads are reduced. In addition, the fuzzy controller provides primary energy savings in the three simulated scenarios, which are further analyzed.

	Control	- 50% Internal loads	No change	+ 50% Internal loads
ΔRH_{up}	Fuzzy	3.49	7.76	10.52
	Steps	2.95	7.67	10.48
ΔRH_{lo}	Fuzzy	0.34	0.00	0.00
	Steps	0.63	0.05	0.01
ΔCO_2	Fuzzy	3.69	58.49	166.56
	Steps	5.77	41.74	106.83
$Q_{pe,vent}$	Fuzzy	37.54	46.53	54.13
	Steps	41.87	56.25	67.71
$FanRPM_{av}$	Fuzzy	771	900	1005
	Steps	825	1035	1194
ACH_{mech}	Fuzzy	0.16	0.21	0.26
	Steps	0.18	0.27	0.35

Table 4.12: Summary of performance indicators in the different simulated weeks for the internal loads sensitivity. In addition, average fan speed ($FanRPM_{av}$) and total mechanical air exchange rate (ACH_{mech}) are considered.

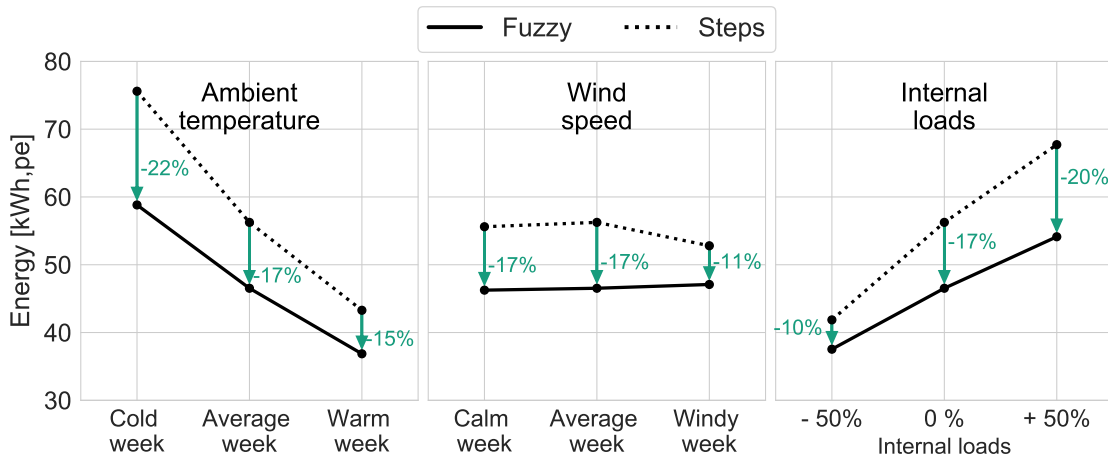


Figure 4.35: Sensitivity of the primary energy savings of the fuzzy controller against the steps controller for different simulated conditions.

Figure 4.35 shows the sensitivity of the primary energy consumption for the different weather conditions and internal loads variation. In any case, the primary energy savings of the fuzzy controller reported in the last section remain. These potential savings are strongly affected by the ambient temperature and the internal loads and are less sensitive to wind speed variations. Colder ambient conditions increase the

savings potential, highlighting the importance of heat recovery to minimize heat losses due to ventilation. Colder environments do not affect the fan power. The fuzzy controller has almost a constant primary energy consumption in windy or calm weeks (where the ambient temperature is similar). The internal loads have a direct impact on the resulting air exchange rate, therefore affecting both heat losses and fan power. Reducing the internal loads undermine also the potential energy savings of the fuzzy controller. Lower loads require lower average fan speeds, for both analyzed controllers. The next section discusses the obtained results.

4.4.1.4 Discussion

Adequate ventilation is necessary to ensure good IAQ and comfort in renovated residential buildings, as well as minimizing energy consumption. Comfort-oriented ventilation strategies do not only improve comfort, but also bring a significant energy saving potential without compromising IAQ. At first glance, the cost function strategy fits slightly better with the comfort standards, especially regarding the ΔCO_2 indicator. This result appears logical since this controller was designed considering occupant discomfort curves from Chapter 2, while the proposed fuzzy controller only takes into account specific threshold values. The individualization of the occupant preferences can significantly impact the indoor environmental quality since the acceptability of indoor conditions is subjective. This could be achieved by redefining the fuzzy membership functions [199]. Thus, these results open the door to learning DCV systems, which are evaluated in the next section.

Furthermore, other acceptability thresholds for RH and CO_2 could be taken into account. However, the shape of the dissatisfaction equations as well as the membership functions in the fuzzy controller were defined according to the limits reviewed in Chapter 2. A redefinition of these functions must come together with a redefinition of the performance indicators. This means the actual performance of the developed controllers is relative to the proposed performance indicators in this thesis, which are based on previous studies.

A known limitation of the present case study is that only winter conditions during one week are tested. The sensitivity to ambient conditions confirmed that the fuzzy controller provided in any case at least 10% energy savings in comparison to the conventional smart steps controller, while the relative humidity and CO_2 indicators are slightly worse as a consequence of lower air exchange rates. The resulting dissat-

isfaction levels in every room (Figure 4.34) indicate that the assumption of a smart state-of-the-art strategy, based on RH in the humid rooms and on CO_2 in the dry rooms is correct. The steps strategy provides most of the potential primary energy savings while simultaneously improving the comfort and air quality indicators.

Moreover, the sensitivity analysis regarding internal loads confirms that the fuzzy controller can provide energy savings with higher and lower loads. Other factors, such as indoor temperature setpoints and window opening behavior, might affect the obtained results. Raising these setpoints would correspondingly increase the heating energy losses due to ventilation and would also produce lower indoor RH values. Furthermore, occupant attitudes towards window opening are heterogeneous, hence leading to high dissimilarities in measured profiles, as studied in Chapter 3. This diversity could influence the indoor environment and the resulting fan speed profile. In this particular study, the windows are open less than 1% of the time. Other window opening models could be considered, which can lead to higher opening rates.

A question arises around the results for the calm and windy weeks. Mikola et al. [152] concluded that the influence of pressure differences on the performance of decentralized ventilation systems is not negligible. The results of the sensitivity analysis for the wind speed show the contrary, as the windy week has the lowest primary energy consumption for mechanical ventilation. This is a consequence of the selected modeling approach. The airflow network approach in EnergyPlus models room-individual balanced ventilation and adds infiltration to compensate for the system disbalance. This results in lower pressure differences between room and façade. Thus, the effect of an advanced control strategy could be undermined as the total air exchange rate in the dwelling would be dominated by the air movement due to pressure difference. Besides, this additional infiltration caused by the disbalance increases heat losses. In the windy week, the apartment needs for every simulated strategy around three times higher heating energy to keep the selected room temperature setpoints. Alzade investigated the impact of unbalanced airflow rates in the performance of decentralized ventilation systems within the framework of a master thesis [8]. He concluded that the energy savings of balanced decentralized ventilation systems can reach up to 20%. In addition, unbalanced decentralized ventilation results in higher supply airflow rates and lower supply temperatures, where draft could become an issue. In this case, other modeling techniques should be considered, where the air room distribution is investigated. A modeling approach where individual supply and exhaust airflow rates are modeled individually could be suitable to investigate the impact of unbalanced decentralized ventilation in every

room. Methods based on computational fluid dynamics (CFD) might also be an appropriate tool for the assessment of room air distribution and its impact on draft [203].

Fuzzy systems are a well proven technology and have been widely implemented in other fields [114, 125, 155]. Therefore, the implementation of the proposed fuzzy scheme in a real building is technically feasible but not included in this thesis.

4.4.2 Learning DCV using different user profiles

4.4.2.1 Methodology

In this section, a simulation case study about the proposed self-learning DCV strategy is carried out. The analysis focuses on four key points:

- Section 4.4.2.2: Automatic control strategies performance (constant speed, steps, fuzzy logic, and self-learning DCV) assuming a single user type. The cost function strategy is left out, since its performance is worse than the fuzzy logic, as concluded in the previous section.
- Section 4.4.2.3: Learning performance with different user comfort profiles, against automatic strategies. The user comfort profiles and interaction model are described in Section 4.2.5.2.
- Section 4.4.2.4: Influence of user interaction frequency profile: learning performance with an active, medium, or passive user. These frequency profiles are defined in Section 4.2.5.3.
- Section 4.4.2.5: Influence of a mixed comfort profile ("more air" in humid rooms, and "less air" in the rest) on the performance of the self-learning DCV.

The simulation is implemented in the co-simulation scheme (Section 4.2.1), using the models described in Section 4.2. The decentralized ventilation heat storage model is replaced with a constant heat recovery efficiency of 70% to reduce the simulation time. In this case, a period of three months is simulated (winter). The ambient conditions are illustrated in Figure 4.36. The simulation time was selected as a previous analysis of the implementation of this controller in Chapter 5. The analysis of results is performed using the same indicators from the previous section,

defined in Chapter 2. A discussion of the results in this analysis is included in Section 4.4.2.6.

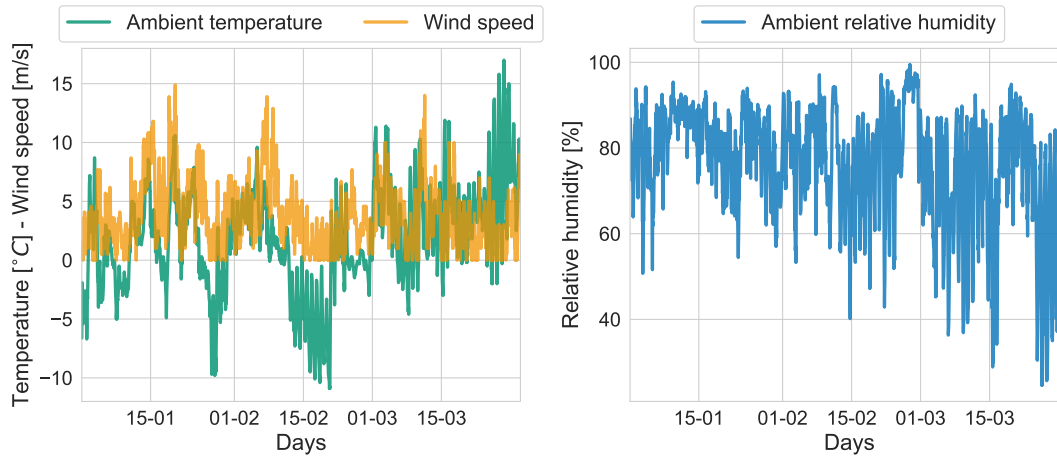


Figure 4.36: Ambient conditions in the selected months for the simulation of the self-learning control strategy.

4.4.2.2 Control results for a single user type

The simulation results of four different automatic controllers are presented in this section. The selected user comfort profile for the learning controller is a "norm" user with medium interaction frequency. Figure 4.37 illustrates the total air exchange rate in the dwelling. The profile is analogous to the previous section (Figure 4.31), where the constant speed strategy shows an almost constant air exchange rate, and the DCV controllers allocate the speeds according to the values of RH and CO_2 .

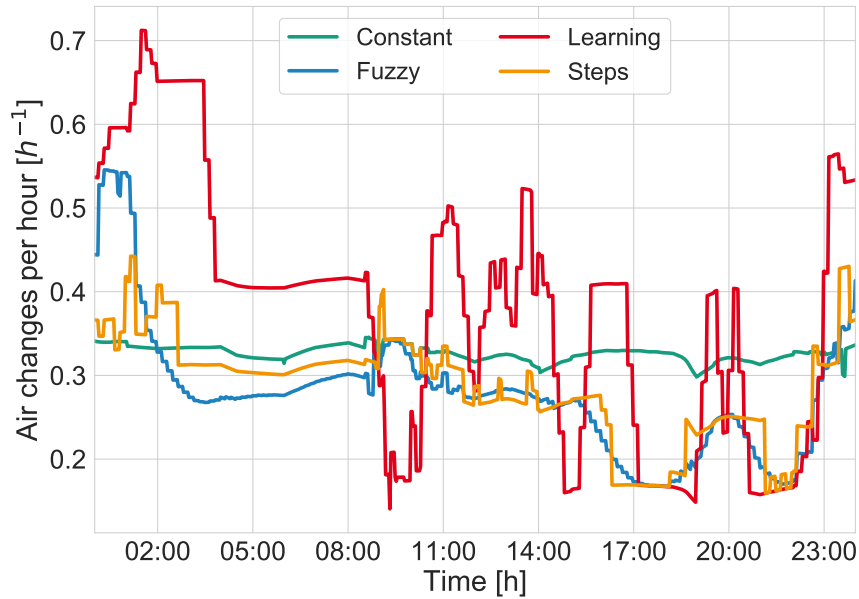


Figure 4.37: Total air exchange rate in a single day, after 75 days of learning.

Table 4.13 presents the simulation performance indicators. The four controllers perform similarly considering the RH indicators. The learning strategy outperforms somewhat the other two DCV controllers in IAQ, but significantly the constant speed strategy. These results are in line with the previous analysis in Section 4.4.1.2.

Control	ΔRH_{lo} [%]	ΔRH_{up} [%]	ΔCO_2 [ppm]	$Q_{pe,vent}$ [kWh]
Constant	2.54	3.24	70.84	447.85
Fuzzy	2.16	1.82	19.46	369.15
Learning	2.10	1.31	8.72	390.73
Steps	2.27	1.59	14.58	383.23

Table 4.13: Summary of performance indicators for every simulated controller.

Furthermore, the results are analyzed further through the cumulative distribution of the relative humidity and CO_2 concentration during occupancy, where the unacceptable range is highlighted in red (Figure 4.38). As expected, the steps and fuzzy strategies deliver almost identical distribution profiles since the resulting air exchange profiles are similar. In the kitchen, the four controllers perform similarly. In the bathroom, the constant speed strategy has a RH above 85% for 20% of the occupied time, while the other controllers present almost no values above this threshold. This value highlights the inability of the constant airflow strategy to deal with high RH peak values since it is not demand-based. However, the values shown in the cumulative distribution plot are when the rooms are occupied. In the

bathroom, this occurs only 15% of the time, which means that the real mold risk due to high RH is not high, even for the constant airflow strategy. Besides, the four controllers keep the RH mostly above the lower limit. In the case of CO_2 concentration, the performance in the bedroom is diverse. The cumulative values above the 1250 ppm threshold are 0, 25, 50, and 75% for learning, steps, fuzzy and constant speed, respectively. In this case, the learning strategy outperforms the other ones.

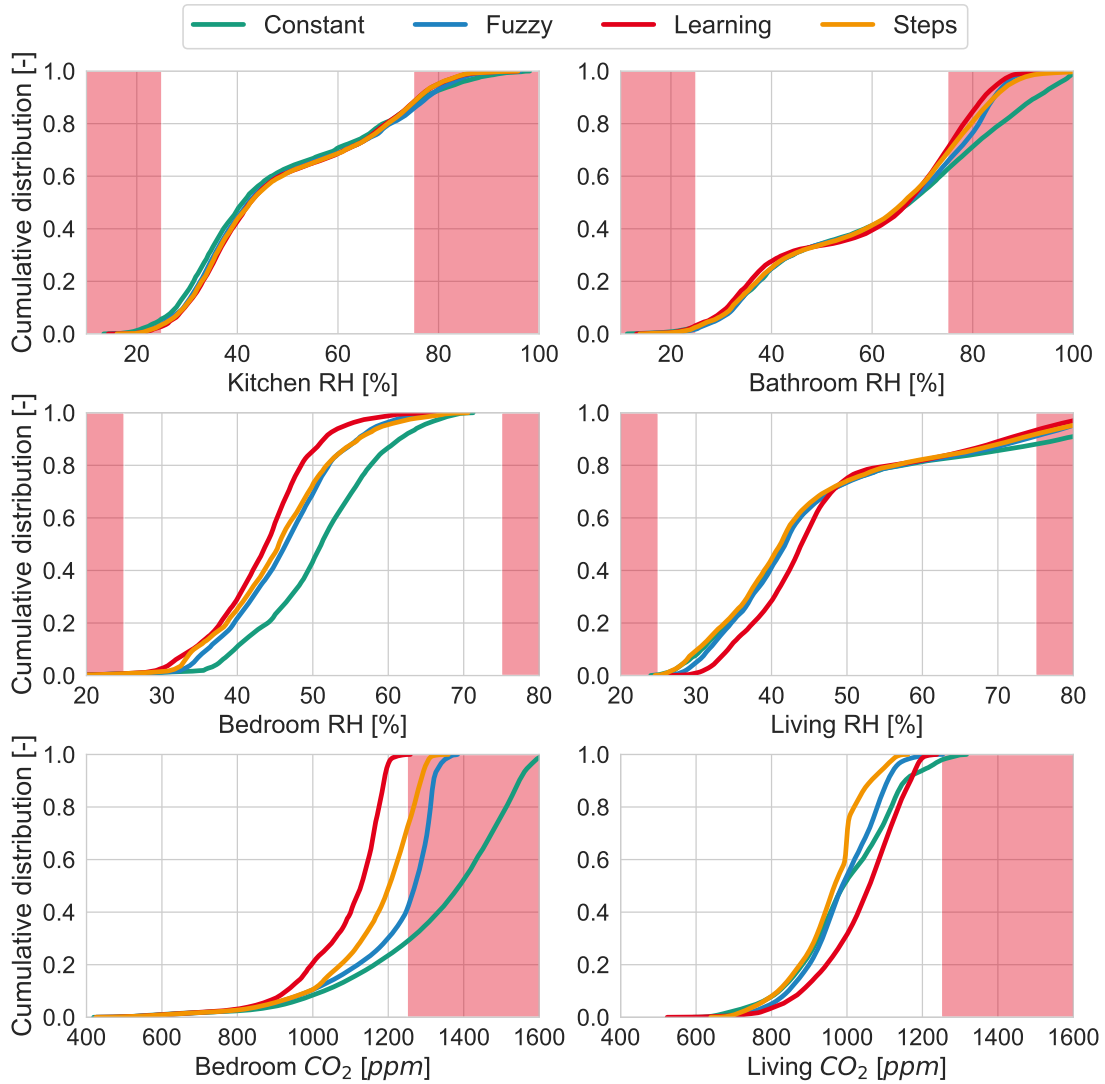


Figure 4.38: RH and CO_2 cumulative distribution plots in relevant rooms for the different simulated control strategies.

The fuzzy controller presents the lowest primary energy consumption. In this scenario, the potential savings of the fuzzy and the learning controller with a "norm" user are almost negligible in comparison to a steps controller. The three DCV

controllers provide between 16% and 19% primary energy savings compared to the constant airflow strategy.

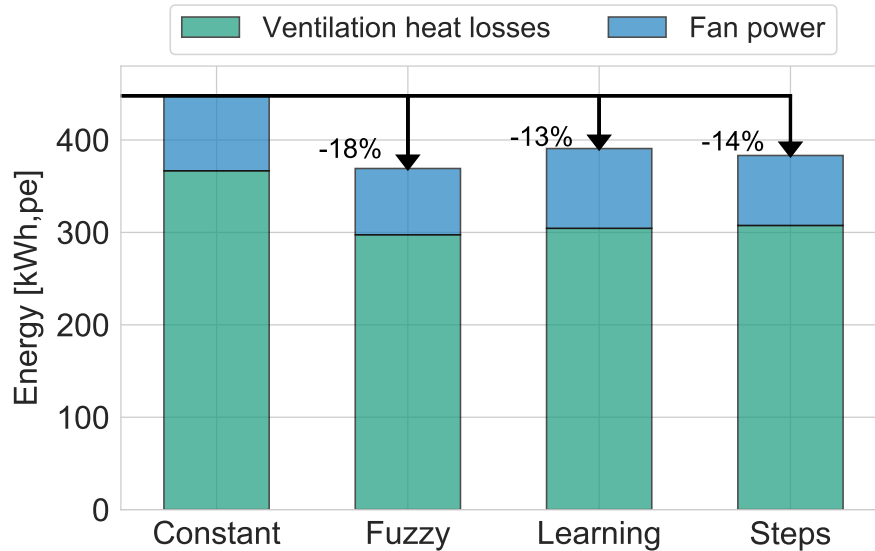


Figure 4.39: Primary energy savings of the proposed controllers. Constant airflow strategy is taken as baseline case.

To sum up, results show that smart control strategies in decentralized ventilation systems have a significant impact on hygrothermal comfort, IAQ, and energy consumption. The proposed controllers have the potential to improve the indoor environmental conditions without compromising the primary energy savings of the state-of-the-art steps DCV. The learning DCV strategy has besides the possibility of adapting itself to different occupant profiles, which is studied in the following sections.

4.4.2.3 Learning results for different comfort profiles

The performance of the same four automatic controllers with different user comfort profiles is characterized in this section. The selected user interaction frequency profile is medium. The goal is to show how the learning system adapts itself to the needs of the different users and to quantify (through performance indicators) the degree of adaptation. The learning process is decentralized, which means that user preferences are learned individually in every room.

Table 4.14 reveals the distribution of votes in every room for each simulation. In Section 4.3.3.2, it was estimated that the learning process stabilizes after 60 votes.

Taking into account the four user comfort profiles and the individual rooms, the living room of the norm profile presents the highest number of votes (20), which has not learned yet a stable profile. The total number of votes in each dwelling is around 50, suggesting that a whole-dwelling learning approach might be suitable to accelerate the learning process.

Votes	Child 2	Child 1	Bedroom	Living	Kitchen	Bathroom	Total
Distracted	4	8	12	14	4	5	47
Less air	16	16	8	11	5	1	57
More air	17	11	5	11	7	4	55
Norm	8	12	5	20	5	4	54

Table 4.14: Number of votes per room and user comfort profile, with medium interaction frequency.

Therefore, the simulation is carried out again with decentralized ventilation and single-room DCV controllers, but a whole-dwelling learning scheme. The whole-dwelling learning takes place under the assumption that there are no deviations in the user preferences given the room type (for instance, this assumes that the comfort profile in bedrooms and bathrooms are equivalent). Figure 4.40 shows the different resulting air exchange rate profiles and Table 4.15 shows the performance indicators.

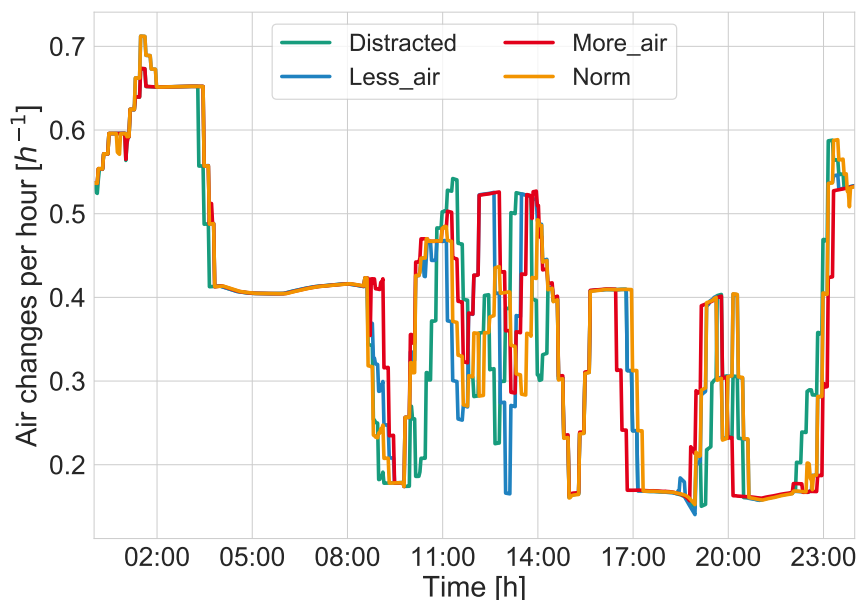


Figure 4.40: Total air exchange rate in a single day with whole-dwelling learning algorithm, after 75 days of learning.

Control	ΔRH_{lo} [%]	ΔRH_{up} [%]	ΔCO_2 [ppm]	$Q_{pe,vent}$ [kWh]
Distracted	2.16	1.30	8.50	399.28
Less air	2.00	1.52	25.92	359.25
More air	2.28	1.13	7.23	434.02
Norm	2.11	1.36	14.95	372.85

Table 4.15: Performance indicators for the learning DCV strategy with all user comfort profiles and a whole-dwelling learning process.

Similar to the single-room learning results, the four controllers can handle the values of the RH indicators independent of the different user comfort profiles. Low RH values are mostly absent in all four cases. Larger differences are observed in the CO_2 concentration and primary energy consumption. Figure 4.41 illustrates the cumulative distribution for CO_2 in different rooms for the simulated user profiles.

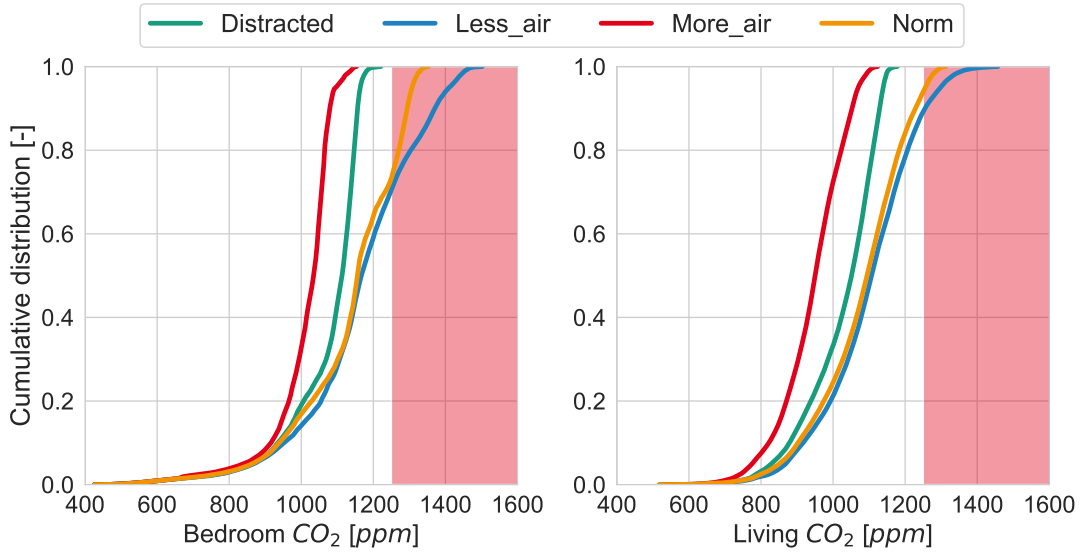


Figure 4.41: CO_2 cumulative distribution plots in selected rooms with centralized learning scheme for the different user comfort profiles.

The cumulative distribution of the CO_2 concentration reflects the impact of the learning scheme: the "less air" profile (especially in the bedroom) shows considerably higher values than the others, even reaching 1500 ppm, while the "more air" profile has a peak value of almost 1100 ppm.

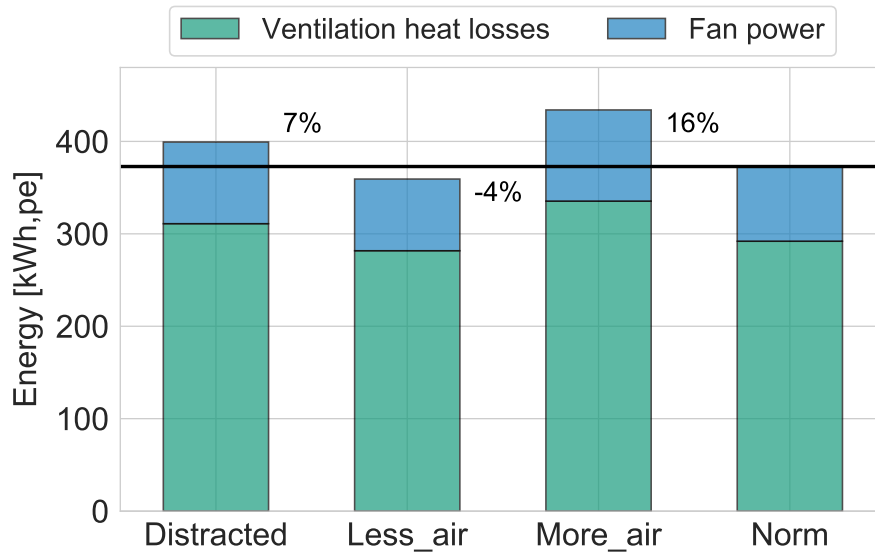


Figure 4.42: Primary energy consumption due to ventilation for the selected user profiles. "Norm" user is taken as baseline case.

The primary energy consumption of each selected user profile is distinctive for each case (Figure 4.42): the resulting air exchange rate has a huge impact. The "less air" comfort profile consumes 20% less energy than the "more air". A distracted user appears to consume 7% more than the norm profile. The relative differences among user profiles for the fan energy consumption are similar to the relative differences for the heating energy losses due to ventilation.

The differences of the performance indicators are due to the different learned DCV control fields. Figures 4.43, 4.44, 4.45 and 4.46 show the finally learned profiles for each user comfort type after the whole simulation period (90 days) in the whole dwelling. The profiles are in this case distinctive and well-defined. To summarize:

- the distracted user has a larger area of single-level changes (-1, +1).
- the less air user has a larger area of double negative changes (-2).
- the more air user has a larger area of single and double positive changes (+1,+2).
- the norm user has a similar profile to the default profile (Figure 4.29).

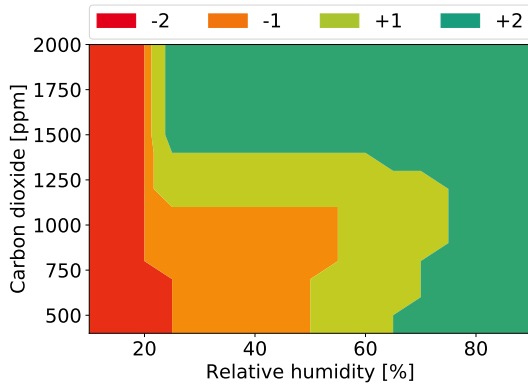


Figure 4.43: Learned profile for the "distracted" user with whole-dwelling learning approach.

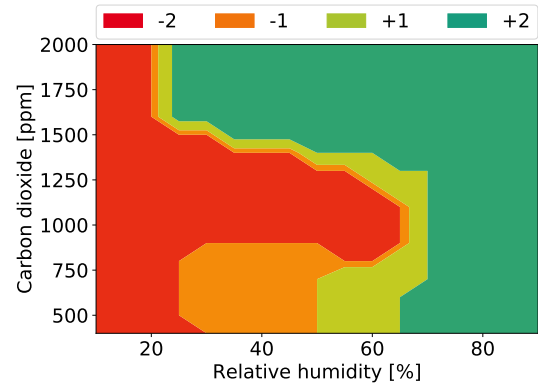


Figure 4.44: Learned profile for the "less air" user with whole-dwelling learning approach.

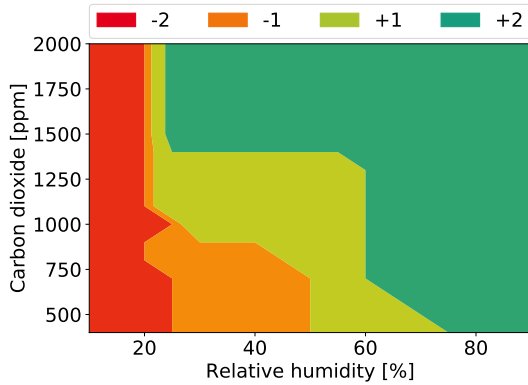


Figure 4.45: Learned profile for the "more air" user with whole-dwelling learning approach.

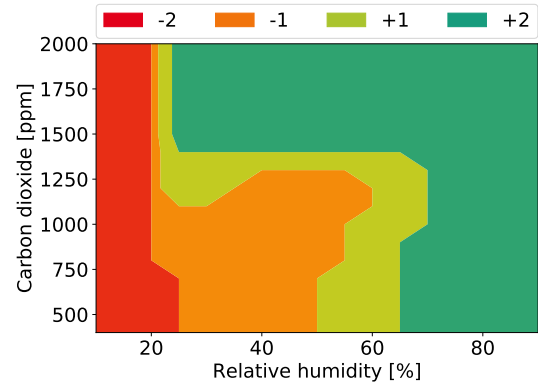


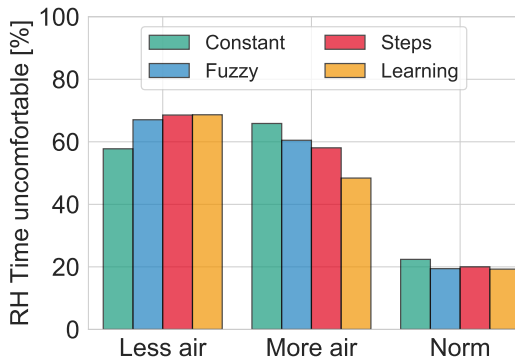
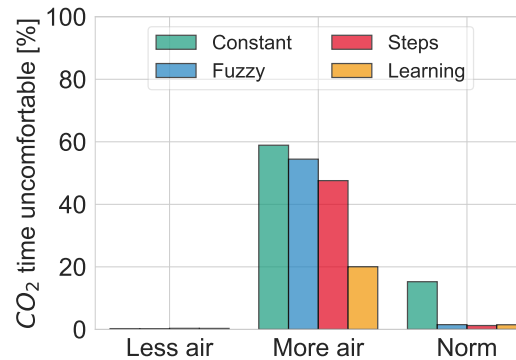
Figure 4.46: Learned profile for the "norm" user with whole-dwelling learning approach.

These learned DCV controllers gained information about the comfort status of the occupant. However, the performance indicators (Table 4.15) are calculated with global discomfort threshold values from the literature. For instance, the "less air" profile presents peak values of 1500 ppm, which is classified as uncomfortable (threshold of 1250 ppm) but is within the assumed comfort range for this particular user. Hence, assuming an admissible threshold of 30% PD (as seen in Section 2.3.3), the discomfort time (defined as the percentage of the time outside the comfort limits) is recalculated using the individual threshold values that lead to a comfort probability of 30%. Table 4.16 shows the results for every comfort profile. The comfort profile for the "distracted" user covers the whole measurement spectrum and is therefore excluded from this analysis.

User profile	RH_{lo} [%]	RH_{up} [%]	CO_2 [ppm]
Norm	26.22	63.78	1431
Less air	47.54	72.46	1652
More air	17.65	42.36	1052

Table 4.16: 30% PD threshold values for the artificial user comfort profiles.

Figures 4.47 and 4.48 show the discomfort time considering the individual profiles for each control strategy. For the "more air" profile, the learning strategy provides a substantial reduction of the time where the occupant is exposed to uncomfortable conditions. The "less air" profile feels comfortable in higher RH values than the other profiles (48 to 72%). The indoor RH is expected to have lower values in winter conditions, resulting in a higher discomfort of the "less air" user. In the humid rooms (kitchen and bathroom), the upper comfort threshold is briefly surpassed when the resulting RH is high due to occupant activities. The "norm" profile performs similarly for all the demand-based controllers. This appears logical, since the default profiles for these controllers are based on literature values for comfort and IAQ. The comfort limits are slightly tighter than the indicators defined in Chapter 2, but do not shift the control field from the default one strongly. The results for the three user comfort profiles confirm the success of the learning strategy. This adaptation could be also translated to the membership functions in the fuzzy controller, which can improve its performance regarding norm-defined comfort and indoor air quality profiles. These results are independent of the indoor temperature since the same setpoints are defined for every control strategy.

Figure 4.47: Percentage of time outside the RH comfort range.Figure 4.48: Percentage of time outside the CO_2 comfort range.

To summarize, the self-learning DCV control strategy has the potential to adapt itself to the different requirements of the user. In the next section, the influence of

user interaction frequency is studied.

4.4.2.4 Influence of interaction frequency

The number of user votes influences the performance of the learning algorithm strongly. In this section, three different user interaction frequency profiles are compared, where the "more air" comfort profile is simulated with active, passive, and medium users. It is expected that the control profile (and performance indicators) of the passive user are closer to the "norm user" since the number of votes would not be enough to learn a clear "more air" profile. On the other hand, the "active" and "medium" users should have a control field where the "+2" area is larger as a result of the higher number of positive votes.

Table 4.17 exposes the number of votes in every room for each simulated profile. Similar to the previous section, the centralization of the learning algorithm plays a key role in the success of the learning DCV strategy. Given the number of votes, it is expected that the single-room learning is only successful for the active user. Moreover, the medium user should somewhat present distinctive profiles for the rooms but can learn the comfort profile properly when performing a whole-dwelling learning algorithm. The passive user has only six total votes, which is not enough to obtain a shifted profile from the default one in any case, and similar results to the distracted profile are expected for single-room learning. However, a whole-dwelling learning algorithm can lead to better individualization for the medium interaction profile since the total number of votes is close to the stabilization value of 60.

Votes	Child 2	Child 1	Bedroom	Living	Kitchen	Bathroom	Total
Active	65	56	54	69	21	26	291
Medium	17	11	5	11	7	4	55
Passive	1	0	2	3	0	0	6

Table 4.17: Number of votes per room and user interaction frequency for the "more air" comfort profile.

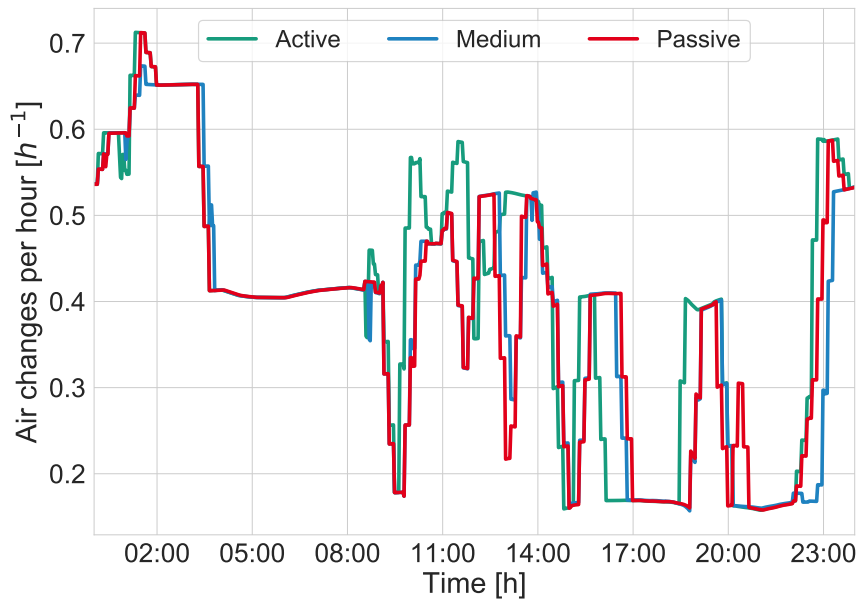


Figure 4.49: Total air exchange rate in a single day with whole-dwelling learning, after 75 days of learning.

Thus, the simulation is performed using a whole-dwelling learning approach. Figure 4.49 shows the daily air exchange profile after 75 simulation days. The active user presents a higher air exchange rate profile than the other two in this case.

Figures 4.50, 4.51 and 4.52 illustrate the final profiles of the whole-dwelling learning process. In this case, the three develop a bigger ”+2” area, meaning better learning of the selected user comfort profile (”more air”). In this case, the medium profile could shift the threshold values of the relative humidity between vote areas to the left of the plot, meaning that the user wants a higher air exchange at lower relative humidity values than a ”norm” user (used to define the default control field). The unorthodox shape for the active user in Figure 4.50 is explained by the lack of user feedback points where the dark green area seems incomplete (around 50% and 1250 ppm). The passive user shows only a slight deviation from the default profile.

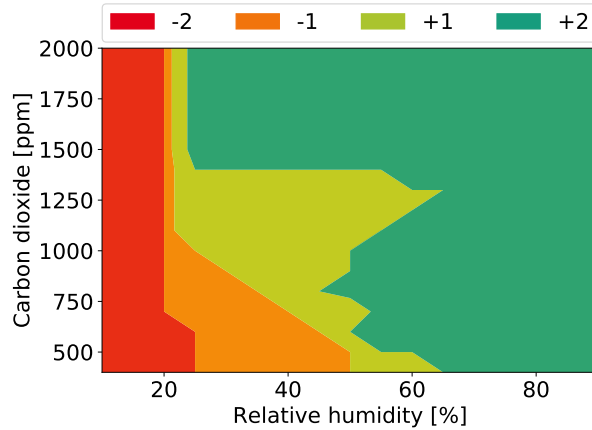


Figure 4.50: Learned control field for the active user with whole-dwelling learning.

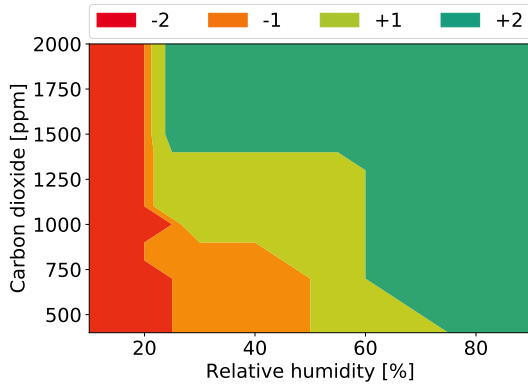


Figure 4.51: Learned control field for the medium user with whole-dwelling learning.

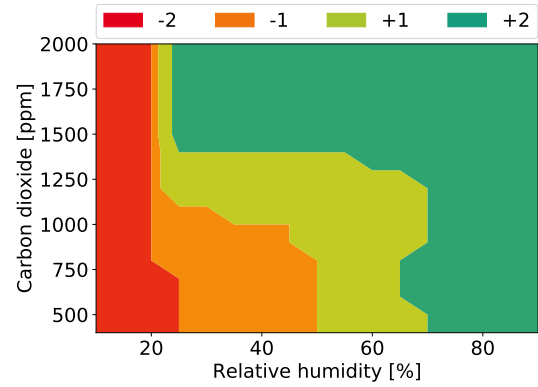


Figure 4.52: Learned control field for the passive user with whole-dwelling learning.

Table 4.18 displays similar performance indicators for the RH and CO_2 in every user frequency type. The whole-dwelling learning process enables a faster reaction to a well-defined profile. The lowest energy consumption is obtained with the passive profile, as expected since a well-defined "more air" profile results in higher air exchange rates (Section 4.4.2.3). The difference between an active and passive user is around 10%. The three profiles present the highest energy consumption of all the user comfort and frequency profiles analyzed in this section but remain somewhat lower than the constant speed strategy (Table 4.13). This shows that even the passive profile gained some information about the user comfort profile and that providing just a few votes may be enough to approximate the tendency of the user preferences. This introduces the analysis in the next section, where a mixed comfort profile is simulated, and the impact of single-room and whole-dwelling learning schemes is analyzed.

Control	ΔRH_{lo} [%]	ΔRH_{up} [%]	ΔCO_2 [ppm]	$Q_{pe,vent}$ [kWh]
Active	2.35	1.03	6.15	460.20
Medium	2.28	1.13	7.23	434.02
Passive	2.20	1.22	7.93	416.63

Table 4.18: Summary of performance indicators for the learning DCV strategy with every user interaction frequency profile.

4.4.2.5 Learning results for a mixed comfort profile

In the last section, it was concluded that a whole-dwelling approach might provide a faster solution to adapt the control field to the occupant's needs. However, consistent comfort and interaction profiles were assumed in every room. In this section, two different comfort profiles for this dwelling are considered: the humid rooms (kitchen and bathroom) have a "more air" profile, whereas the rest of the rooms present a "less air" profile. An active user is assumed. The votes are simulated only once and used in both cases. The contrast of these profiles and the influence on the self-learning DCV control field is analyzed. Besides, the obtained results comparing single-room and whole-dwelling approaches are described.

Table 4.19 shows the number of votes per room and type for the mixed comfort profile. As expected, the "more air" profile causes a higher number of positive votes in the humid rooms, and the "less air" profile causes a higher number of negative votes in the rest. The time an occupant spends in the humid rooms is less than in the rest, therefore resulting in a lower total number of interactions.

Votes	Children 2	Children 1	Bedroom	Living	Kitchen	Bathroom
+2	0	0	0	8	9	16
+1	0	3	1	0	7	5
-1	2	4	9	0	3	1
-2	54	58	49	79	2	0

Table 4.19: Number of votes per room and type for a mixed comfort profile.

Table 4.20 shows the performance indicators for both simulations. The prevalence of negative votes in the dry rooms causes a higher result in the ΔRH_{up} indicator for the whole-dwelling approach. In this case, the single-room scheme has a better performance in humid rooms. The same results are observed for the indoor air

quality indicator ΔCO_2 and the primary energy consumption. The presence of "more air" profiles in two rooms causes higher energy consumption and a lower ΔCO_2 value for the single-room scheme.

Learning scheme	ΔRH_{up} [%]	ΔRH_{lo} [%]	ΔCO_2 [ppm]	$Q_{pe,vent}$ [kWh]
Single-room	1.59	1.94	45.17	365.79
Whole-dwelling	3.23	1.72	153.72	335.61

Table 4.20: Performance indicators for the mixed comfort profile using single-room and whole-dwelling learning schemes.

Figures 4.53 and 4.54 show two exemplary learned control fields, obtained in the single-room simulation scheme. They belong to the bedroom and bathroom, respectively, which have different comfort profiles. The influence of the selected user profiles is recognized in every room, although the bathroom profile is not shifted extremely from the default profile (there are only 16 "+2" votes in the bathroom).

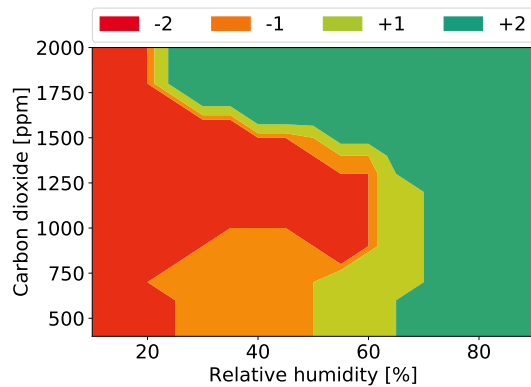


Figure 4.53: Learned control field for the single-room scheme in the bedroom.

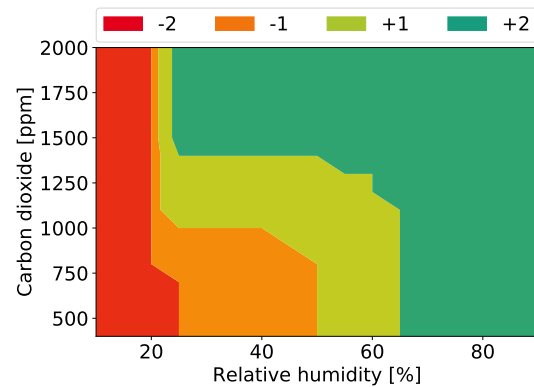


Figure 4.54: Learned control field for the single-room scheme in the bathroom.

On the other hand, Figure 4.55 illustrates the learned control field obtained in the whole-dwelling simulation scheme. This profile appears as an extreme version of the "less air" profile, also studied in previous sections. This control field is a result of a conflict between the two comfort profiles and the mixed learning scheme. Figure 4.56 illustrates the resulting learned comfort profile. In this case, two comfort zones are identified: the first one with low CO_2 and RH values, corresponding to the "more air" profile, and a second one for higher RH and CO_2 values, corresponding to the presence of the "less air" profile. Even though the "less air" user is simulated in more rooms and has more votes, the "more air" profile is closer to the starting profile and therefore has a bigger comfort probability. This analysis emphasizes the

importance of a single-room learning scheme, even if it takes longer to learn the desired profiles. The next section discusses the results obtained for the different comfort and interaction user profiles.

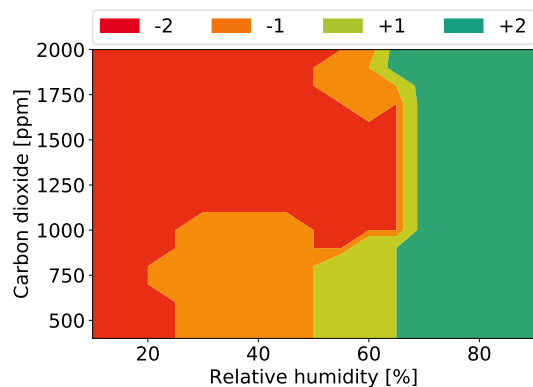


Figure 4.55: Learned control field for the whole-dwelling scheme.

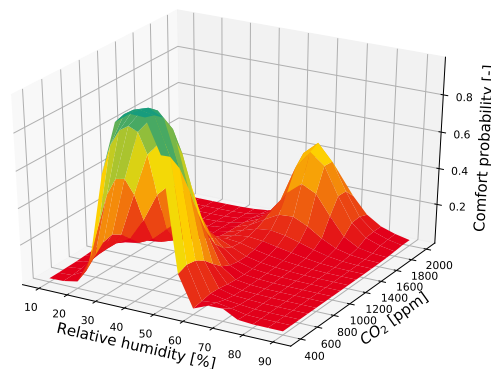


Figure 4.56: Learned 3D comfort profile for the whole-dwelling scheme.

4.4.2.6 Discussion

As reported in Section 4.3.3, some learning algorithms have already been applied to different HVAC and building systems to address the trade-off between occupant comfort and satisfaction, indoor air quality, and energy consumption. In that sense, the proposed learning DCV control strategy is a first approach to tailor a residential mechanical ventilation system to the needs of the occupants.

The building simulation scheme has some limitations, as discussed in Section 4.4.1.4. In this section, constant heat recovery efficiency is assumed. In comparison to Section 4.4.1, the potential energy savings of the fuzzy controller in comparison to the steps controller are significantly lower, which is a consequence of the simplification of the heat recovery modeling. In that sense, the self-learning DCV with the default control field provides primary energy savings in the same range as the fuzzy and steps controllers.

The limitations of this study are explained in this paragraph. The four considered user profiles are not only artificial but also well-defined. This leads to well-defined learned DCV schemes, which may be an uncommon case in reality. The lack of data about user feedback in residential ventilation systems hinders the possibility of studying it reliably. Furthermore, the assumed human diversity creates some wasteful profiles as well, which result in relatively high energy consumption (for instance, the "more air" user consumes more energy than the smart DCV baseline

controller). In addition, the winter simulation strongly affects the learning process since the most comfortable area of some user profiles never occurs. A "less air" user feels most comfortable at a RH of 60%, a value that is seldomly reached in the living or bedrooms during the whole simulation period. The algorithm will not obtain any feedback regarding comfortable areas in this particular case, influencing the learning performance.

A fundamental point is that all user profiles began with the same default learning DCV control field. This means there is a period where the controller was not fully individualized during the three simulated months, given the lack of votes. Longer simulation periods will increment the difference between the performance indicators for every user type, emphasizing the potential of the learning DCV strategy. Another option would be to perform the same simulation study changing the starting DCV profile with the learned one for every single user. However, this section aims to assess the individualization of the learning DCV controller. This controller shows resilience to complete random user profiles, highlighting its ability to offer an individual solution for every user without compromising mold growth protection and potential health-related issues. These results are available in the Appendix A.6.

Moreover, a big question arises concerning whole-dwelling or single-room learning. The first one can provide a faster learning scheme, under the assumption that the occupant's preferences are consistent in every room of the apartment, although room singularities would be lost. Single-room learning might result in slower learning processes but can capture the different profiles for different rooms. Assuming that an occupant in a highly uncomfortable state is probably more willing to operate the available control systems (HVAC), a single-room learning scheme is more suitable to be tested in a real-building implementation. Results in Section 4.4.2.5 highlight the importance of applying a single-room learning scheme on the modeling of mixed comfort profiles. In this thesis, artificial comfort profiles were defined to test the learning algorithm, under the assumption that an occupant would only operate the mechanical ventilation system in uncomfortable indoor conditions. These profiles are unlikely to be crisply well-defined in real buildings. The diversity of the occupant behavior in different circumstances turns the single-room scheme into a suitable approach to preserve the individual preferences of the occupant in every room. This suitability does not only apply to the behavior of different occupants (for example, two bedrooms) but also for rooms with other purposes: kitchen, living room, and bathroom. It is expected that the whole-dwelling approach is also not suitable when considering diversity: number of occupants, different comfort profiles, even consider-

ing different personality traits and psychological aspects. Within the framework of a master thesis, Maier [142] analyzed the different ventilation needs through a survey, confirming this diversity. A validated occupant behavior model geared towards mechanical ventilation is needed to gain further insight into this topic.

Finally, the proposed self-learning user-centered solution has not yet been implemented in a real building. A question arises regarding the occupant's comfort profiles (if they are crisply well-defined, as the user model proposes) or if they have a more random characteristic. Thus, the study of the real building implementation of the learning DCV controller is addressed further in the next chapter.

4.5 Summary

Defining proper control strategies is a key to the success of decentralized ventilation systems. Within the framework to integrate occupant-centric control strategies in residential buildings, this chapter evaluates the performance of present and novel controllers for residential decentralized ventilation, including the occupant interaction with the systems. Simulation studies provide an insight into the optimization of these systems before developing a real building application. Hence, the research question 3 is answered through the following points:

Research Question 3: *How do state-of-the-art control strategies for decentralized ventilation systems perform? Can innovative occupant-centered control solutions provide an improvement regarding energy consumption, hygrothermal comfort and indoor air quality?*

- A market and scientific research was carried out. As a result, two baseline control strategies were defined, one with constant fan speed and a second one representing current smart ventilation technologies (stepwise DCV). Two main weaknesses were identified: only one variable at a time is controlled (either RH or CO_2) and there is a confirmed lack of occupant-centered strategies, where diversity and individual preferences are considered.
- In contrast to the available DCV solutions, two innovative fully automated controllers were developed, with the aim of looking for multivariable controllers where both RH and CO_2 are considered together. The first one was a cost function DCV, where the fan speed is determined by the variable which has the highest dissatisfaction, given literature-related values. The second one was a fuzzy-based DCV. Membership functions are as well defined with literature

discomfort values. Both solutions provide primary energy savings compared to the baseline strategies (29% compared to the constant airflow strategy and 18% compared to the steps strategy, in an average winter week). A state-of-the-art steps strategy already provides a significant improvement in energy efficiency, hygrothermal comfort, and indoor air quality. Fuzzy DCV provides higher energy efficiency while keeping the IAQ and hygrothermal comfort results among the same values of the other DCV studied. A sensitivity analysis regarding weather conditions confirmed the primary energy savings potential of the fuzzy-based DCV in different winter scenarios. The resulting air exchange rate is more sensitive to the occupant's indoor activities than to external conditions. Another simulation approach is necessary to properly evaluate the impact of high wind speeds on the resulting air exchange rate and draft. Fuzzy logic controllers are already a well-proven technology and have been implemented successfully in several control systems across different areas.

- Tackling the lack of user-oriented solutions, a learning DCV strategy was proposed, where the user comfort profile regarding RH and CO_2 is learned through a supervised learning algorithm. Default comfort profiles were defined using the literature methods reviewed in Chapter 2. To test the user diversity for mechanical ventilation in building simulation, four different user comfort models (with RH and CO_2 as input variables) and three user interaction models (active, medium, and passive) were developed and integrated into a probabilistic model, which allows having a time-dependent occupant behavior model that simulates the manual selection of the ventilation level. This user model for the operation of residential ventilation systems was applied to the learning strategy to characterize its performance and learning capabilities. The learning stabilizes for all user types after 60 votes. In almost every case, this controller achieves an individualized comfort improvement without resigning energy-efficiency. Single-room and whole-dwelling learning schemes were tested. Whole-dwelling learning provides a faster response for passive and medium users (interaction frequency) but loses the potential behavior diversity in different room types when assuming a mixed comfort profile. Given the artificial comfort profiles, different comfort types affect the potential primary energy consumption up to 20% without compromising the RH and CO_2 indicators. The learning DCV provides a solution for occupant-centered residential decentralized ventilation controllers that can adapt itself to different user profiles. Its real-building implementation is covered in the next chapter.

5 Real building case study: Energy Smart Home Lab

This chapter reports the implementation of the self-learning demand-controlled ventilation strategy in a real building, which is a living lab. A brief description of the selected building is first provided in Section 5.1. The planning and implementation are also detailed in Section 5.2. Moreover, different hypotheses and test analyses are presented. The performance of the proposed self-learning controller is analyzed in Section 5.3. In addition, a lessons-learned section is included with general recommendations about field implementations of occupant-centered strategies in decentralized ventilation. In Section 5.4, the interaction between occupant behavior and decentralized ventilation systems is studied. A summary of the findings in this chapter is available in Section 5.5.

5.1 General aspects

In this study, the self-learning DCV controller was implemented and investigated for three months in a test apartment in Karlsruhe, Germany. In the literature, some studies already covered the implementation of self-learning systems for other technologies, but not yet for ventilation systems [44, 93, 167]. The apartment is called Energy Smart Home Lab (ESHL) and was built within the framework of the MeRegioMobil Project [182]. It has two bedrooms, a main room (combining the living room and kitchen), and a bathroom, with a total area of 60 m^2 . An additional room contains the technical systems, but the occupants do not have access to this room. Figures 5.1 to 5.4 show the test facility.



Figure 5.1: Living room area.



Figure 5.2: Bedroom 1.



Figure 5.3: Kitchen area.



Figure 5.4: Outdoor view.

Two students (25-30 years old, one male, one female) occupied the apartment from the 02.03.2020 to 31.05.2020. Decentralized ventilation systems were installed in the dwelling, together with a special user interface. Each device switches the airflow direction every 60 seconds and has a ceramic heat recovery system, as explained in Section 4.2.3. The study aims to implement the proposed learning DCV control strategy and to study the occupant behavior regarding mechanical ventilation in residential buildings. The proposed ventilation concept fits the definition of the AIVC regarding smart ventilation systems mentioned in Chapter 1 [66].

5.2 Implementation and design

5.2.1 Ventilation concept

Decentralized alternating ventilation systems were installed in the test environment, with the following properties:

- Fan nominal speed = 2750 RPM
- Fan maximum airflow = $41 \frac{m^3}{h}$
- Ceramic heat regenerator ($\eta_{HRC,eff} = 0.81$)
- Reversible DC Fan ($SPI = 0.17 \frac{W \cdot h}{m^3}$)
- Direction change every 60 seconds

The ventilation requirements of the dwelling were calculated applying the norm DIN 1946-6 [58], as described in Section 2.1. The total ventilation requirements depend on the total dwelling area (A_{Dw}):

$$\dot{V}_{tot} = f_{LSt} (-0.002A_{Dw}^2 + 1.15 + A_{Dw} + 20) \quad (5.1)$$

- f_{LSt} is a coefficient to define each ventilation level, in $\frac{m^3}{h \cdot m^2}$

In addition, the infiltration is estimated ($6 \frac{m^3}{h}$), since there were no previous measurements available, following table 10 in the norm [58, p. 29, T. 10]. Having a conservative approach by neglecting natural ventilation, the factors f_{LSt} were obtained from table 6 [58, p. 25, T. 6] for a building with high occupancy (low occupancy is for single-family houses). The four ventilation levels were obtained subtracting the infiltration from the total air requirements (Equation 5.1). Given the floor plan of the apartment, it was decided to install one device per room (living area and kitchen were considered separately), having a total of five devices. Since the bathroom fan would only operate at its lowest level and in full exhaust speed when the light is turned on, the required ventilation levels were divided over four devices. These levels are defined for continuous ventilation systems. In alternating ventilation systems, half of the fans are supply phase, and the other half in the exhaust phase. Thus, each device must contribute half of the requirements at every level. Besides, there is a limitation: the minimum airflow rate is higher than the calculated one for humidity protection, and the maximum airflow rate is slightly lower than the dimensioned one for intense ventilation. A summary of these calculations is available in Table 5.1.

Ventilation level	Total required \dot{V}_{flow}	Mechanical ventilation \dot{V}_{flow}	DVS \dot{V}_{flow} from DIN 1946-6	DVS installed \dot{V}_{flow}	Fan speed [%]
Humidity protection	22.2	16.2	8	10	20*
Reduced ventilation	51.8	45.8	23	23	50*
Nominal ventilation	74.0	68.0	34	34	75*
Intense ventilation	96.3	90.3	45	41	100

Table 5.1: Ventilation levels (in $\frac{m^3}{h}$) defined according to the system dimensioning procedure in DIN 1946-6 [58].*The bedrooms had additional 5% speed in level 2 and 3 to compensate the pressure losses of the extra sensors installed.

Figure 5.5 shows a floor plan of the dwelling with the placement of the ventilation devices, the central controller, and user interfaces.

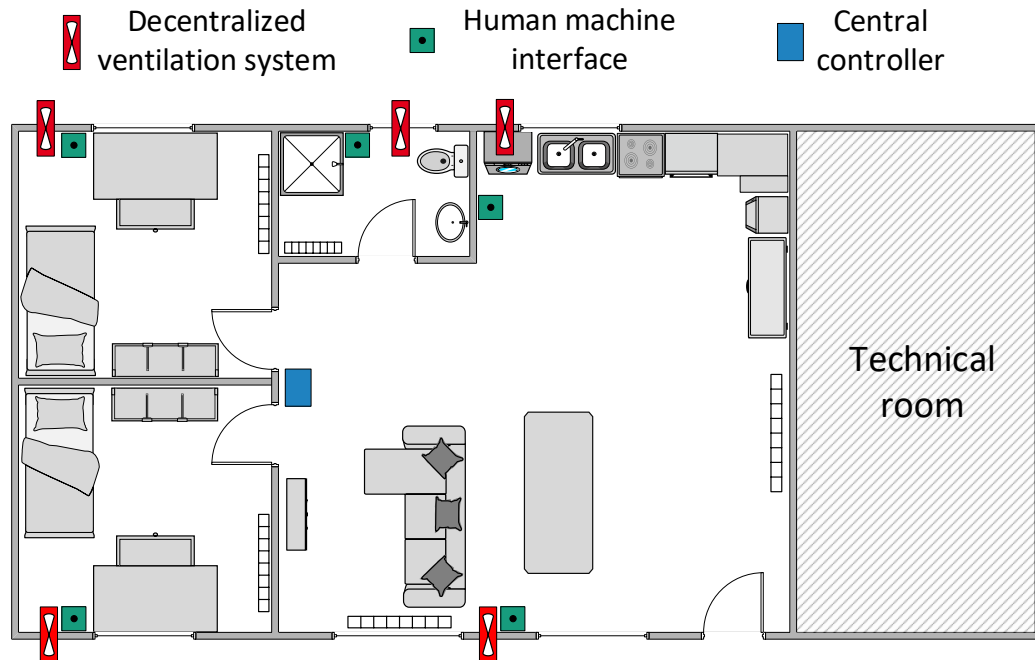


Figure 5.5: Floor plan of the Energy Smart Home Lab. The placement of the DVS, user interfaces and central controller is indicated.

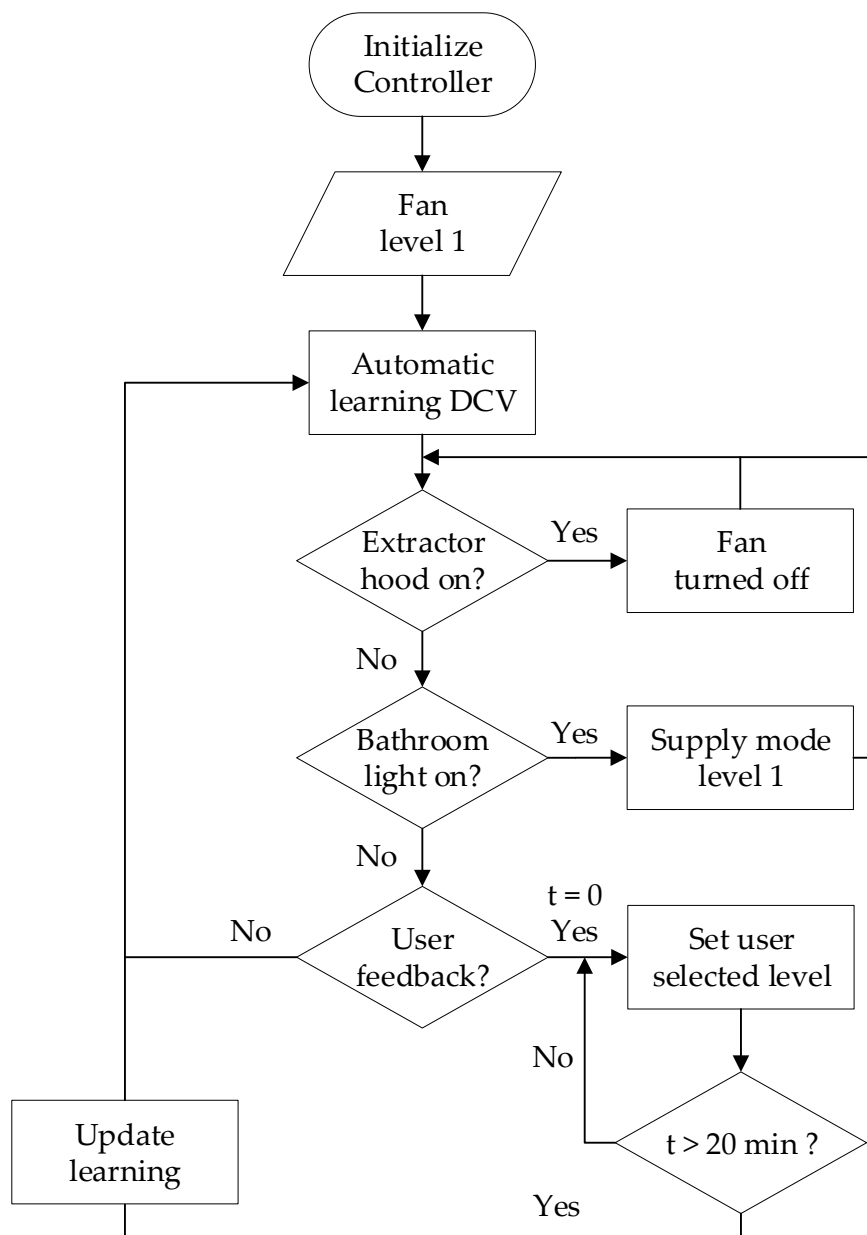


Figure 5.6: Flow diagram of the implemented controller.

As this experiment aims to test the field implementation of the learning DCV scheme, a special rule-based controller was developed. The workflow is illustrated in Figure 5.6. In automatic mode, the same controller as described in Section 4.3.3 was implemented, where a classification algorithm (support vector machines) predicts the user preferences towards the airflow levels. The user operation data are

collected, and the algorithm learns how the occupant behaves concerning the indoor relative humidity and CO_2 concentration. The fans provide a minimum air exchange rate (humidity protection) and cannot be switched off. The controller is applied individually in every room, to grasp the different user preferences. The controller is overridden in three scenarios:

- When the kitchen extractor hood is on, the fans are turned off to avoid fan damage (the exhaust airflow rate of the hood is the double of the sum of all ventilation systems)
- When the bathroom light is on, the bathroom fan operates in full speed exhaust mode, and all the other fans operate in 25% speed and supply mode, to avoid spreading of odors in the dwelling.
- When the user operates the system, the selected fan level stays for 20 minutes. The user can override this selection again.

5.2.2 Electronic set up and monitoring

The installation of the devices must be complemented with an adequate electronic set up for a successful implementation of a machine learning-based controller. In this case, an IoT-based approach was chosen. As defined by Walker et al. [218], "smart ventilation allows building managers or homeowners to integrate information from many sources to make informed and intelligent decisions about efficient and effective ventilation". IoT-based systems allow this information integration and have the potential to implement intelligent ventilation controllers efficiently [132]. The general scheme is depicted in Figure 5.7.

Every device has a human-machine-interface (HMI), where the fan, user interface, and environmental sensors are connected. A microcontroller (Node MCU ESP32[®]) collects the data from installed indoor environmental sensors and user interface, and sends the control signal to the fan. This communication procedure happens every minute or when the user operates the fan. The microcontroller communicates with the central controller (Raspberry Pi 4B[®]) through WiFi, whereas the room-individual controller operates as a service. The Raspberry Pi receives the data from the decentralized microcontroller, stores it, runs the control algorithm, and returns the decision to the microcontroller, which then sends the corresponding signal to the fan. The whole centralized controller is programmed in python 3.7 [209]. The

data exchange takes place every minute, although the learning only occurs every ten minutes. Figure 5.8 illustrates the developed board.

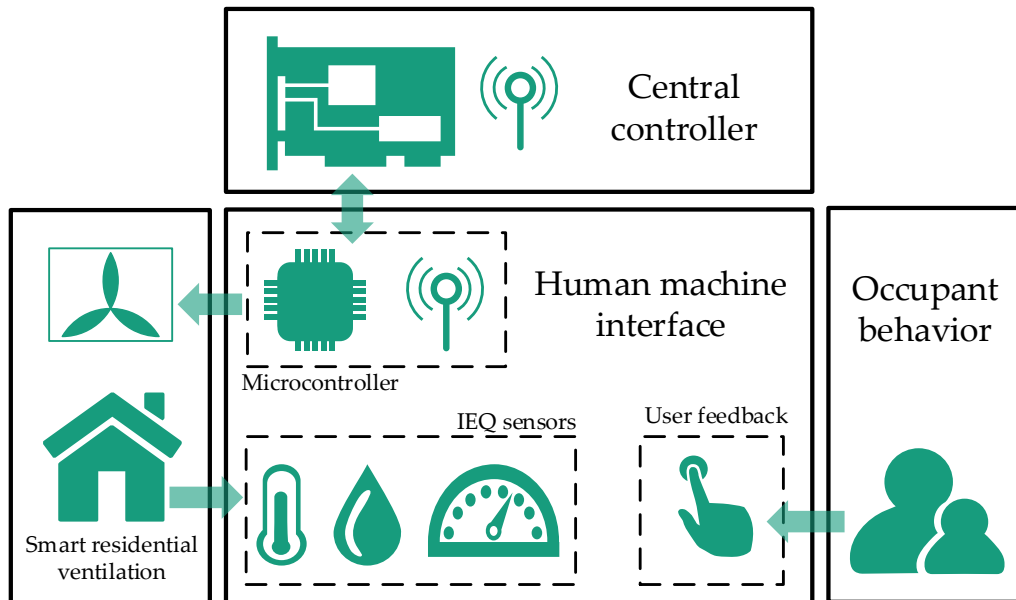


Figure 5.7: IoT Scheme for the learning controller implementation.

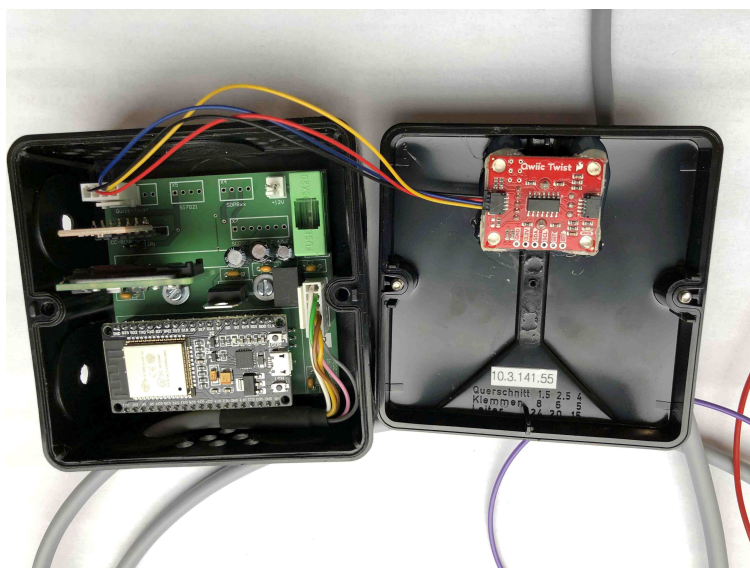


Figure 5.8: Developed board for the learning controller implementation.

Several indoor environmental sensors were installed to collect data every minute, which are connected to every microcontroller. These sensors are positioned within the user interface at chest height (1.5 m), close to the ventilation device in every

room. The measured variables include room temperature, relative humidity, CO_2 (combined in a single sensor), and VOC concentration, together with the rotary encoder for the user feedback. Due to the positioning, the heat released by the microcontroller altered the room temperature and relative humidity readings, which required a sensor calibration (the indoor room temperature was measured with an offset of around $7^\circ C$). In addition, both bedrooms have a second small board integrated into the fan, which collects the data from sensors placed inside the ventilation device. These include a temperature and humidity sensor on the outdoor cover, a temperature, RH , and CO_2 sensor on the indoor cover, and a pressure difference sensor integrated to the channel, which measured the pressure drop along with the whole ventilation device. Table 5.2 summarizes the properties of the installed sensors.

Sensor	Variable	Unit	Range	Precision
Sensirion SCD30	T	$^\circ C$	-40 - 70	$0.4+0.023(T-25)$
	RH	%	0-100	3
	CO_2	ppm	0-40000	30
Silicon Labs Si7021*	T	$^\circ C$	-10 - 85	0.4
	RH	%	0-100	3
AMS CCS811	VOC	ppb	0 - 1187	**
	$eqCO_2$	ppm _{eq}	400 - 8192	**
Sensirion SDP810*	Pressure	Pa	0 - 50	0.35
PEL12T Rotary encoder	State	-	0 - 24	-

Table 5.2: Sensor properties for the monitoring concept.*Additional sensors for the bedrooms.**Accuracy not reported.

5.2.3 User interface

A user-friendly interface was developed. Maier [142] carried out two surveys about residential ventilation. In the first one, participants were interviewed and asked about the characteristics and functionalities of user interfaces for residential ventilation systems. The central findings are summarized in three points:

- The interface must be intuitive and understandable
- The user must be able to identify the ventilation levels
- The interface must be understandable for users without a technical background

Besides, the participants were asked to define their ideal interface in her study, having some existing examples available on the market as a reference. Findings revealed that users prefer mostly rotary interfaces, if excluding integrated HVAC controllers (the heating system worked independently from the ventilation system), thus it was decided to build a rotary encoder to collect the user feedback. Plus, a color field was included (red-green-blue) to facilitate the interpretation of the rotation (the occupants received information about this before the experiment), illustrated in Figures 5.9 and 5.10. A green light indicates no level change, a blue light means decreasing the fan level, and a red light means increasing the fan level. As seen before in Figure 5.6, when the user selects a certain ventilation level, the controller is overridden for 20 minutes. The user's choice is collected into four possible votes (-2, -1, +1, or +2), according to the difference between the selected and the previous fan level, which are then learned by the controller.



Figure 5.9: Operable user interface - decreasing level color (blue).



Figure 5.10: Operable user interface - increasing level color (red).

5.3 Results

General aspects of the indoor environmental quality, the performance of the ventilation system, and the proposed learning controller are investigated and presented in this section.

5.3.1 Performance indicators

The general results are presented in this section. The performance indicators regarding relative humidity and CO_2 concentration defined in Chapter 2 are calculated as well, together with the performance of the decentralized ventilation system. Figure

5.11 illustrates the mean average outdoor conditions during the whole measurement period. Although this experiment was designed for winter conditions, most of the days with an outdoor average temperature below 5°C are in the first month. In late April, typical weather conditions of mid spring were observed. This influenced the results of the experiment strongly.

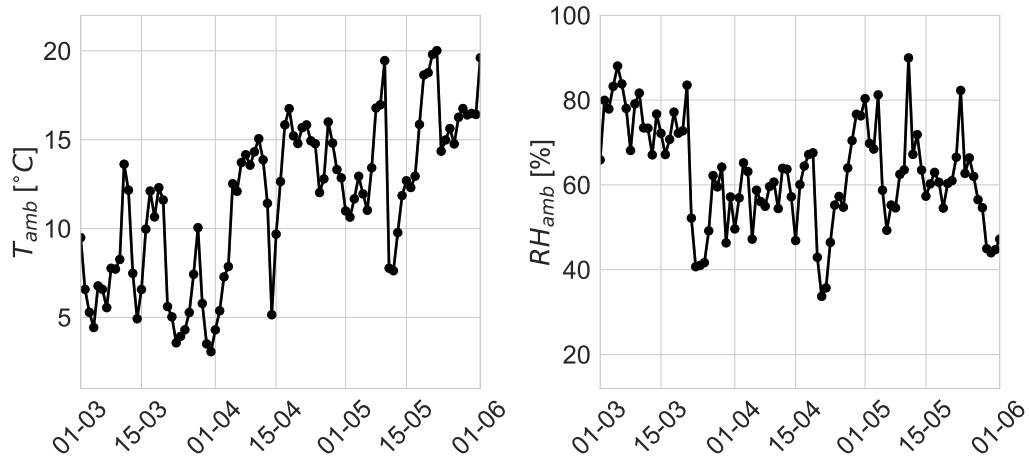


Figure 5.11: Daily mean ambient conditions during the measurement period.

Figures 5.12 to 5.15 show the boxplots of the indoor measurements in every room. Indoor temperatures stayed between 22 and 24° usually. The high internal loads (due to the smart devices of the house) and elevated temperature setpoints caused these high temperatures. As a result, lower indoor relative humidities were observed (almost always between 25 and 50%). Only the bathroom presented high humidities, probably when the occupants were taking a shower. The controller kept the CO_2 concentrations in every room below the desired threshold of 1250 ppm usually. Both bedrooms present higher upper quartile values, reaching around 1600 ppm (mostly during sleeping). The VOC concentration reveals slightly higher indoor contaminants in the kitchen area.

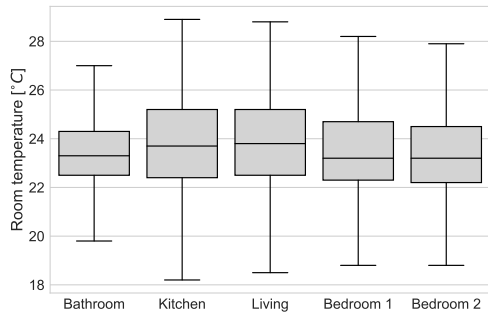


Figure 5.12: Indoor room temperature boxplot.

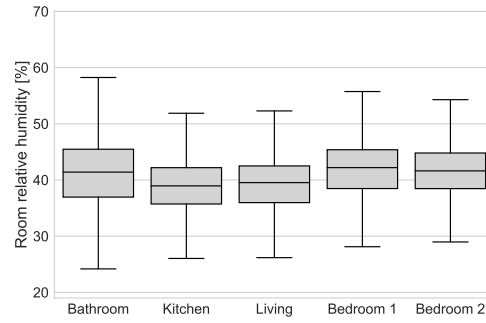


Figure 5.13: Indoor relative humidity boxplot.

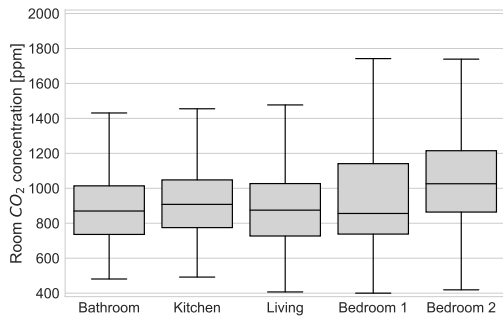


Figure 5.14: Indoor CO₂ concentration boxplot.

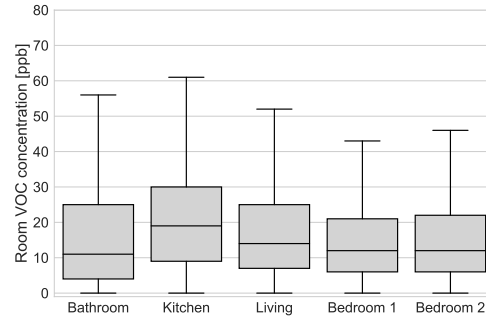


Figure 5.15: Indoor VOC concentration boxplot.

Similar to the simulation results in Chapter 4, Figure 5.16 shows the cumulative distribution of the two most relevant variables during the measurement period. The highest exposure to high humidities happens in the bathroom, even though only for short periods. The highest exposure to elevated CO₂ concentration occurs in the bedrooms, during sleeping. In this case, the considered points for the cumulative distribution are not filtered with the presence of the occupant. This indicates at first glance that the designed ventilation concept was adequate for the dwelling.

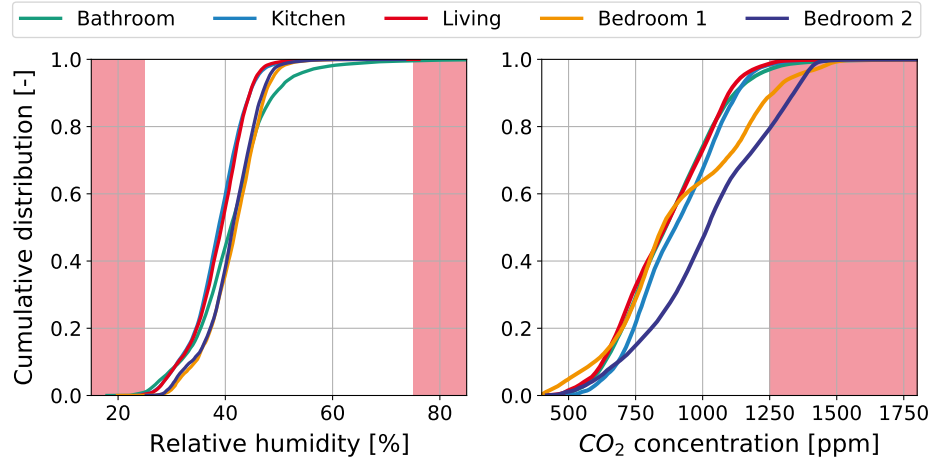


Figure 5.16: Cumulative distribution of RH and CO_2 concentration in every room.

Table 5.3 summarizes the performance indicators for the whole measurement period. Indicators regarding comfort and indoor air quality present values closer to zero, confirming that the ventilation concept and the learning control strategy were successful. CO_2 concentration presents an overshoot of around 35 ppm for both bedrooms, which is considered negligible (almost inside the accuracy range of the sensor). As both the heat recovery efficiency and fan power could not be measured, the energy consumption of the ventilation system cannot be properly evaluated. Therefore, the heat losses due to ventilation were estimated assuming a heat recovery profile following the results of the laboratory measurements of the device [35], which is shown in Figure A.20 in Appendix A.3. Besides, the fan power was estimated using the datasheet of the fan, as shown in Figure 4.10. The total energy consumption due to ventilation ($Q_{pe,vent}$) was 71.84 kWh. This result is not comparable to the simulations in Chapter 4, since the boundary conditions are extremely different (climate conditions and time of the year, building floor plan, number of occupants).

Control	ΔRH_{lo} [%]	ΔRH_{up} [%]	ΔCO_2 [ppm]
Bathroom	0.04	0.11	13.03
Kitchen	0.01	0.00	3.72
Living	<0.01	<0.01	3.71
Bedroom 1	<0.01	0.00	34.16
Bedroom 2	0.00	0.00	37.20

Table 5.3: Performance indicators in every room for the measurement period in the ESHL.

During the measurement period, the installed ventilation device provided an average air exchange rate of around 0.22 h^{-1} . The average theoretical profile is depicted in Figure 5.17. This plot shows a theoretical profile, as the mass flow was calculated using the fan speed and not measured. Pressure differences between indoor and outdoor and high wind speeds can deviate the real airflow rate from the theoretical one in a decentralized ventilation system. The peaks are due to the automatic clock that turned off the fans for ten minutes five times a day to prevent a memory overflow in the microcontrollers. The temperature correction in the board caused an overestimation of the relative humidity every time it was restarted, which resulted in a short increase in the volume flow.

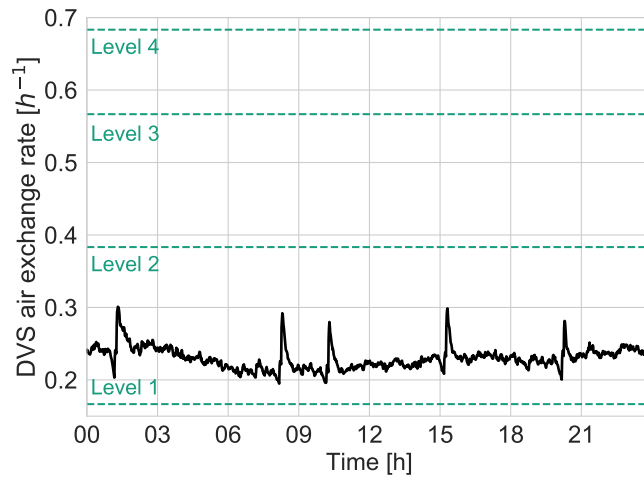


Figure 5.17: Total daily mean theoretical air exchange rate profile in the measurement period.

Besides, Figure 5.18 shows the fan level frequency in every room. The fans operated almost always at the extreme levels (1 and 4). The kitchen and living room are the only rooms with more than 10% of higher fan levels. This reacts not only to the basis ventilation controller but also to the learned profiles. The influence of the user on the ventilation levels is discussed in the next sections.

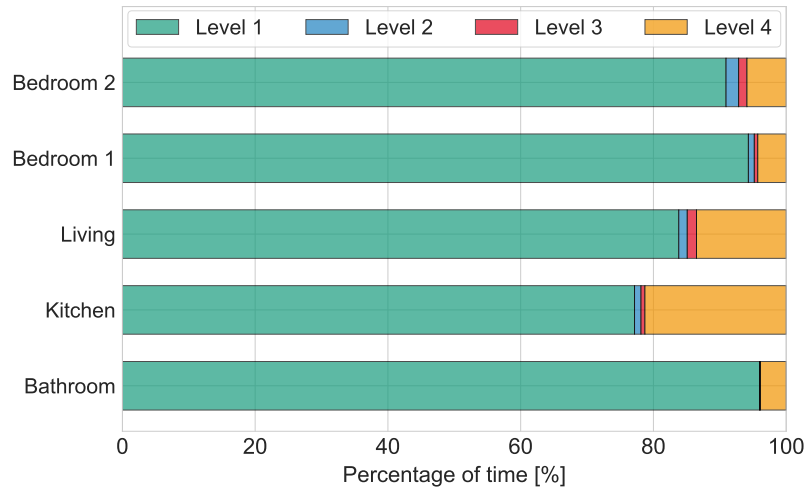


Figure 5.18: Fan level frequency in every room in the measurement period.

5.3.2 Performance of the learning controller

In this section, the performance of the implemented self-learning DCV controller is analyzed. As seen before, the ventilation concept developed for this application was successful considering norm-related values of acceptability of indoor relative humidity and CO_2 concentration. In this section, the influence of the occupant on the performance of the DCV is studied and the learning process of the controller is described.

Table 5.4 shows the time progression of the user votes in the three measured months. The kitchen and both bedrooms had more than 40 user votes, meaning that the learning process may be close to the stabilization. The living area and bathroom had significantly fewer interactions, meaning the resulting learned profiles could still present potential differences. The total number of votes in 3 months was around 200, which means that the occupants operated actively the ventilation system [183]. This can be also a consequence of the Covid-19 pandemic outbreak, as the students spent more time indoors than expected. More than half of the votes occurred in the first month, where the occupants were probably still experimenting with the devices. Only the kitchen area presented over ten interactions in the last month.

Month	Bedroom 1	Bedroom 2	Living	Kitchen	Bathroom	Total
March	29	28	14	27	10	108
April	8	14	5	13	5	45
May	8	3	7	16	7	41
Total	45	45	26	56	22	194

Table 5.4: Number of votes per room and month in the measurement period.

Table 5.5 shows the distribution of the user votes in every room given its vote type. The occupants almost always operated the fans by changing the desired volume flow strongly, resulting in extreme votes (-2 or +2). This could be also a consequence of the designed user interface, even though the occupants were instructed on how to operate it. A clear trend is observed, as the users voted often less airflow in the bedrooms and more airflow in the other rooms. As discussed in Section 4.4.2.6, the occupants might have different requirements or comfort profiles in the different rooms, and the shape of the votes in these measurements confirm this. Therefore, a whole-dwelling learning approach would lose those room-individual profiles.

Votes	Bedroom 1	Bedroom 2	Living	Kitchen	Bathroom	Total
+2	6	6	15	26	18	71
+1	2	0	0	4	1	7
-1	0	3	2	10	2	17
-2	37	36	9	16	1	99

Table 5.5: Number of votes per room and type in the measurement period.

In this analysis, bedroom 1 and kitchen are taken as reference. The rest of the rooms do not show a distinctive profile from these two or were not relevant for the learning (user behavior plots in those rooms are in the Appendix A.7). Figures 5.19 and 5.20 illustrate the votes of the occupants in relationship to the measured relative humidity and CO_2 concentration, as proposed for the learning algorithm. In bedroom 1, a strong presence of negative votes (-2) is observed, and there is no clear pattern between the RH , the CO_2 concentration, and the resulting user vote (Pearson's R correlation coefficient [180, p. 282] is -0.012 for RH and -0.008 for CO_2). In the case of the kitchen, a predominance of positive votes (+2) is detected, although the distribution of the votes is more balanced. Once again, no correlation was found in the variables (Pearson's R Coefficient is 0.005 for RH and -0.004 for CO_2). Higher RH and CO_2 values are typically expected in the kitchen, usually

during cooking time. The user interface containing the sensors was placed over 1.5 m away from the cooking field (main pollutant source), registering then lower values [236]. This could potentially establish a different correlation between the user vote and the measured values.

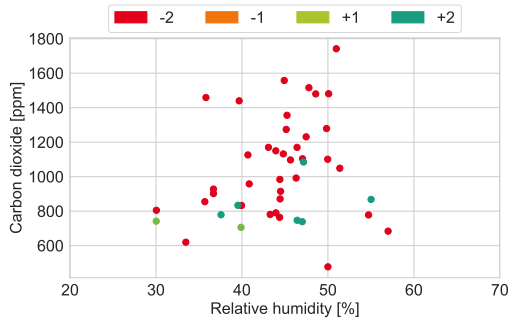


Figure 5.19: User votes dispersion as a function of RH and CO_2 in the bedroom 1.

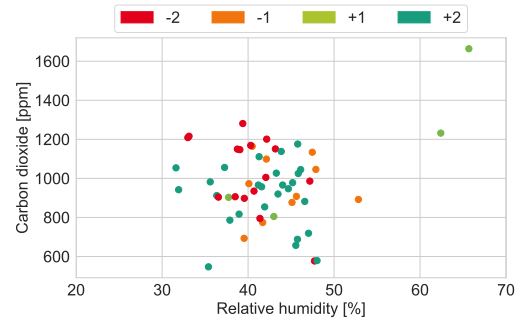


Figure 5.20: User votes dispersion as a function of RH and CO_2 in the kitchen area.

Figure 5.21 shows the default learning DCV control profile. It was the starting point for every room and shifted to the individual chosen preferences after the measurement period. Figures 5.22 and 5.23 illustrate those resulting profiles for the bedroom 1 and kitchen, respectively. These reflect the user votes distribution previously analyzed. The main changes in the control field occurred between 30 and 60% relative humidity and 500 to 1500 ppm CO_2 concentration. This is primarily because the measured points in the indoor environment were seldom in extreme values, given the air exchange of the installed ventilation system and the outdoor conditions.

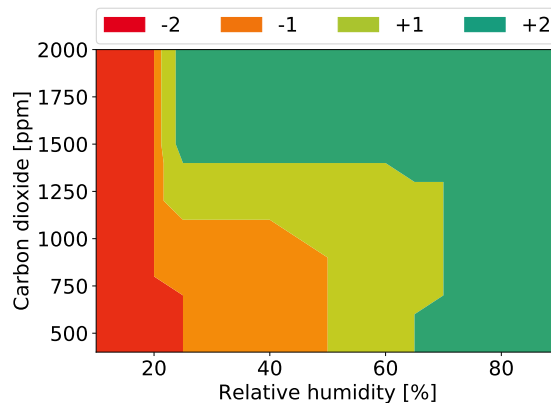


Figure 5.21: Starting control profile.

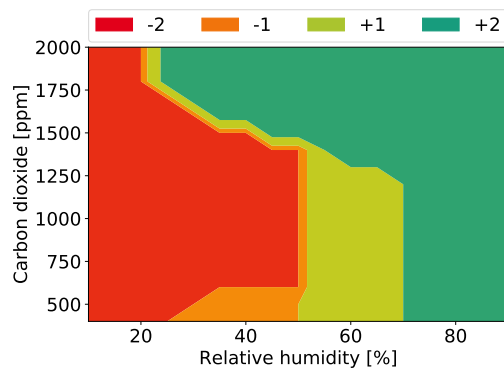


Figure 5.22: Bedroom 1 control field after learning.

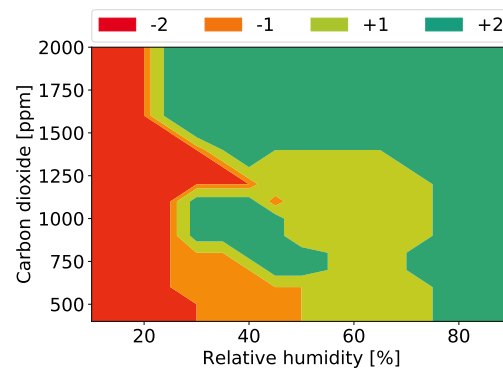


Figure 5.23: Kitchen control field after learning.

Providing a whole-dwelling learning scheme can speed up the adaptation of the control field to the occupant's votes, as concluded in Section 4.4.2.6. However, this could result in a loss of room-individual preferences. Figure 5.24 shows the learned control field if a whole-dwelling approach had been used. As expected, the formerly reported differences, for instance, between bedroom 1 and kitchen, would disappear under this scheme.

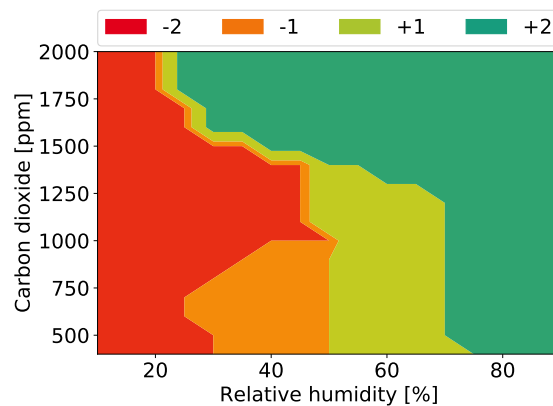


Figure 5.24: Whole dwelling potential control field after learning.

Moreover, the impact of the learning controller is analyzed. Figures 5.25 and 5.26 show the differences in the fan level frequencies in the first and last month of the measurement period. For instance, compared to the overall frequencies in Figure 5.18, bedroom 1 had more time in level 4 in the first month than in the last one, as a result of the negative user votes, wanting less airflow in this room. On the contrary, the kitchen showed significantly more time in level 4 in the last month, given the positive votes.

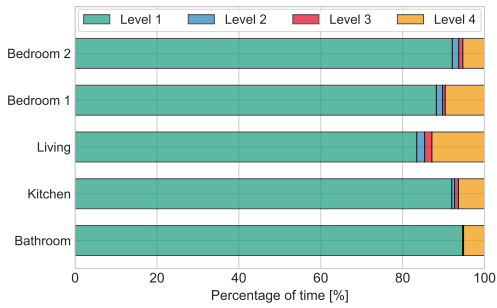


Figure 5.25: Fan level frequencies in the first month.

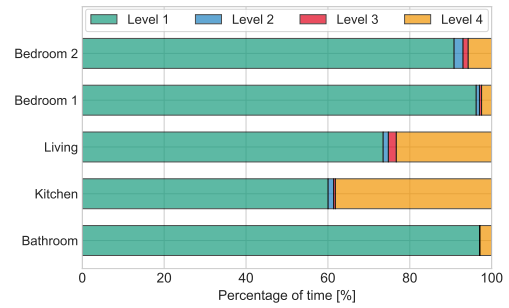


Figure 5.26: Fan level frequencies in the last month.

Figures 5.27 and 5.28 depict the fan speed on two sample days (at the beginning and end of the test phase) together with the relative humidity and CO_2 concentration for bedroom 1 and kitchen. Even though both days show similar RH and CO_2 profiles, the fan speed profile is distinctive in each case, reflecting the influence of the learned control field. Fan speed is lower on the last day for bedroom 1 as a result of the user votes, and the opposite effect occurs in the kitchen, where the fan speed is significantly higher on the last day.

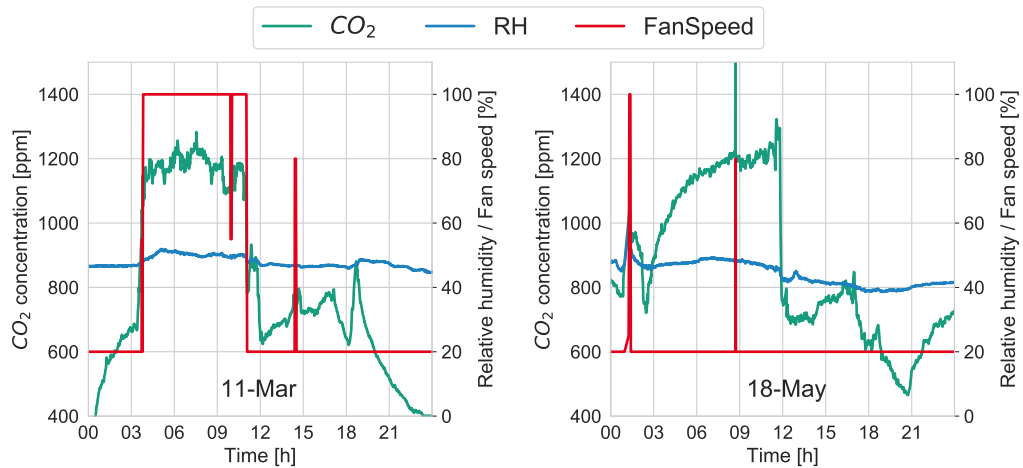


Figure 5.27: RH , CO_2 and fan speed daily profile for the bedroom 1.

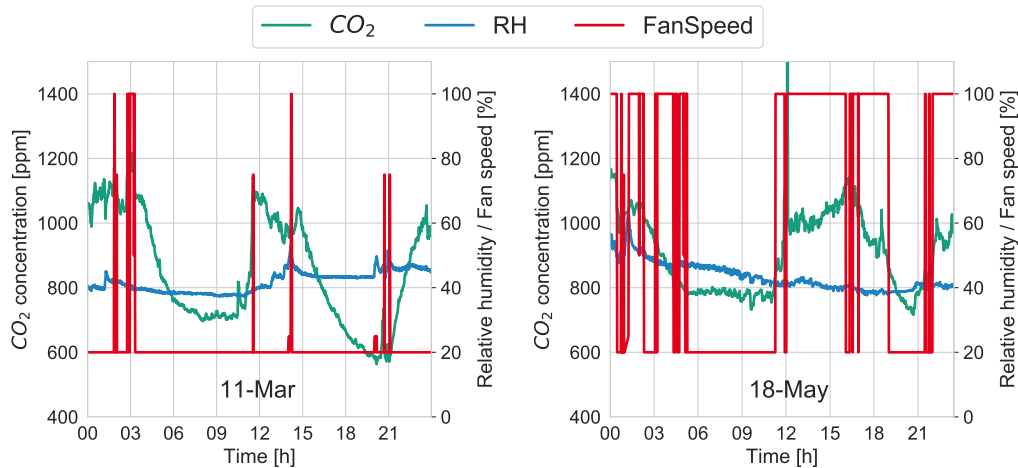


Figure 5.28: RH , CO_2 and fan speed daily profile for the kitchen.

5.3.3 Practical lessons learned from the field

The field implementation of a machine learning-based smart ventilation system using decentralized push-pull devices was successful. This confirms that the further development of smart IoT-based technologies in residential buildings can be applied also to ventilation systems.

Angsten et al. [16] described the advantages and drawbacks of decentralized ventilation systems against centralized systems. Lessons learned around the complete process of commissioning, installation, and operation of decentralized systems in residential buildings are summarized in Table 5.6, complementary to the mentioned study.

Advantages	Disadvantages
<ul style="list-style-type: none"> • Simple commissioning and installation process • Easy individual room control through user interface • Controlled air exchange rate in the whole dwelling 	<ul style="list-style-type: none"> • DVS placement can lead to draft (Bedroom 2) • Shifted direction change critical for unbalances • High fan speed causes noise pollution

Table 5.6: Advantages and disadvantages of decentralized ventilation, as a result of the field implementation.

Furthermore, issues with the IoT system were identified. In the first place, the selected microcontrollers communicated with the fan, the sensors, and the central Raspberry Pi, resulting in sometimes a memory overflow, which leads to a failure on the individual room board. This system failure was unluckily detected after the installation, and when the occupants were already living there. The problem was troubleshot during the first occupancy week. A reset clock function was included that shut down the entire system for ten minutes to prevent memory overflow and data losses. This function ran five times a day, corresponding to the air exchange peaks in Figure 5.17. Table 5.7 shows the total time down of the system in every room.

Failure time [%]	Bedroom 1	Bedroom 2	Living	Kitchen	Bathroom
Average	10.5	10.9	8.4	13.2	7.7

Table 5.7: Average system failure time during the experiment.

Although the system presented technical disadvantages and improvement potential by the implementation, this experiment can conclude that the employment of machine learning-based techniques is as well possible in residential ventilation systems. This opens the door for future developments in this field, considering as well the integration with IoT-based systems and smart building technologies.

5.4 Occupant behavior analysis

5.4.1 Analysis of user behavior and mechanical ventilation

An exploratory analysis of the occupant behavior regarding the operation of mechanical ventilation is performed in this section. Following the methodology described in Section 3.3.1, the coefficients of a logistic regression model can evaluate the occupant preferences towards mechanical ventilation.

Regarding the explanatory variables, VOC, previous fan speed, and supply temperature (measured only in bedrooms) are added in comparison to the window opening analysis. Since the noise produced by the fan is proportional to the logarithm of the volume flow (Section 2.5), the previous fan speed represents noise pollution as an additional variable to interpret the user behavior. In contrast to the window opening behavior which has only two possible states (open or closed), the occupants' votes are grouped in four possible outputs (-2, -1, +1, and +2), plus a no-change value. For this analysis, this was reduced to three outputs (less air, grouping -1 and -2,

more air, joining +1 and +2, and no change as 0). Models were fitted again using the scikit-learn package in python [172], using a "one-versus-rest" method, in which the model is fitted individually for each class different than 0, taking the rest as points that do not belong to this class. Thus, two models arise, one for increasing the fan level and another for reducing it. The resulting coefficients for every room are shown in Tables 5.8 and 5.9 respectively. Both tables highlight the most relevant variables in every model.

Variable	Bedroom 1	Bedroom 2	Living	Kitchen	Bath
Intercept	-9.58	-10.14	-10.34	-9.95	-10.29
T_{Room}	-0.22	-0.02	0.57	0.17	-0.53*
RH_{Room}	0.17	-0.19	0.60*	1.56*	2.36*
$CO_{2,Room}$	-0.46	0.22	-0.56*	0.23	2.55*
VOC_{Room}	-0.02	-0.01	-0.02	0.05	0.34
T_{Sup}	0.15	0.30	n.a.	n.a.	n.a.
$FanRPM_{Prev}$	0.47	0.05	-0.61	0.10	0.61
T_{amb}	0.18	0.03	0.62	0.83	0.10
RH_{amb}	0.13	0.11	0.73	0.37	0.54
06-10	-0.63	-0.50	-0.75	-0.69	-0.33
10-14	0.93	0.09	-0.24	-0.43	1.30
14-18	0.33	1.18	-0.24	0.29	0.48
18-23	-0.21	-0.03	1.52	0.78	-0.45
23-06	-0.43	-0.75	-0.29	0.05	-0.99
Weekend	-0.12	-0.30	-0.14	0.67	-0.12

Table 5.8: Logistic regression coefficients for increasing mechanical ventilation volume flow in every room (n.a. = not available, * = p-value<0.05).

There is no clear pattern in the dry rooms between the explanatory variables and the action of increasing the fan level. In all of them, time-related actions are observed, with coefficients ranging from 0.9 to 1.5. This result might be due to the low number of positive votes (below 10), especially in the bedrooms. In both bedrooms, all the coefficients are not significant, while in the living room only the CO_2 coefficient explains the occupant behavior. In the humid rooms (kitchen and bathroom), the indoor relative humidity plays a significant role. Relative humidity and CO_2 concentration are correlated (especially in the bathroom), resulting in similar regression coefficients, which are both positive and significant (moisture loads are only activity-related). Hence, the users wanted to remove the excess of humidity in

these areas. In these rooms

Variable	Bedroom 1	Bedroom 2	Living	Kitchen	Bath
Intercept	-8.26	-6.84	-9.00	-8.13	-10.79
T_{Room}	-1.31	-0.66	-1.24	-1.57*	-0.37
RH_{Room}	0.40	-1.13*	0.60	0.86	0.38
$CO_{2,Room}$	0.04	-0.62	0.42	0.72	0.40
VOC_{Room}	0.11*	0.05	<0.01	-0.02	<0.01
T_{Sup}	0.35*	-0.50	n.a.	n.a.	n.a.
$FanRPM_{Prev}$	2.86*	1.80*	1.93*	1.16*	0.68
T_{amb}	-1.28*	-1.51	-1.07*	-1.57*	-0.38
RH_{amb}	0.50	0.54	-0.13	1.07	-0.12
06-10	-0.46	-1.14	-0.59	-0.58	-0.30
10-14	0.49	0.14	-0.57	0.39	-0.30
14-18	-0.43	-0.16	0.75	0.55	0.92
18-23	-0.62	-0.02	0.73	-0.15	-0.40
23-06	1.03	1.18	-0.31	-0.20	-0.07
Weekend	-0.08	-0.41	0.46	0.27	0.64

Table 5.9: Logistic regression coefficients for decreasing mechanical ventilation volume flow in every room (n.a. = not available, * = p-value<0.05).

Noise (represented by the previous fan speed) seems to be the main reason to turn down a fan in the dry rooms, reporting strong positive and significant coefficients (1.8 - 2.9). In the kitchen, the indoor and outdoor temperatures have the highest influence (with noise in the second place). However, in the bathroom, there is no clear indicator (no significant coefficients), as a consequence of having only three total negative votes. This analysis reinforces that noise is a critical point in decentralized ventilation and that this is an issue that should be addressed further in future developments [145]. Besides, the outdoor temperature is significant in almost every room. This is also interesting when observing the evolution of the regression coefficients during the measurement period. Taking again bedroom 1 and kitchen as examples, Figures 5.29 and 5.30 illustrate the coefficient evolution of the negative and positive votes in the former, and Figures 5.31 and 5.32 in the latter respectively.

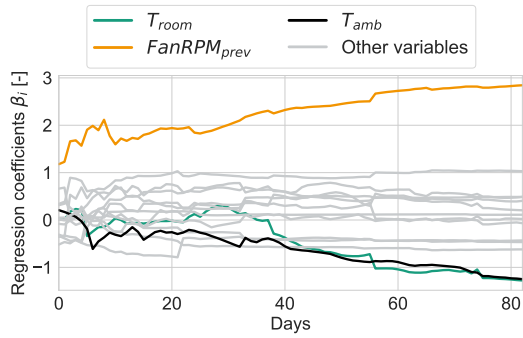


Figure 5.29: Evolution of logistic regression coefficients for decreasing fan level in bedroom 1.

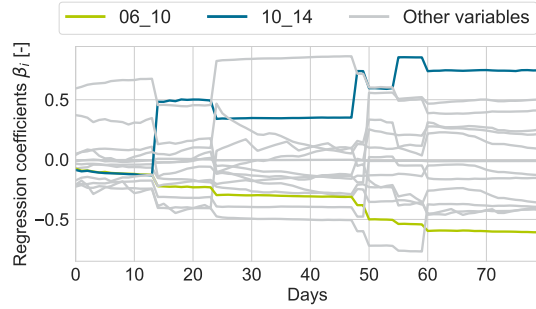


Figure 5.30: Evolution of logistic regression coefficients for increasing fan level in bedroom 1.

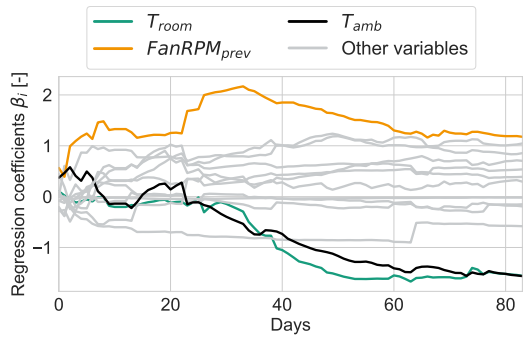


Figure 5.31: Evolution of logistic regression coefficients for decreasing fan level in the kitchen.

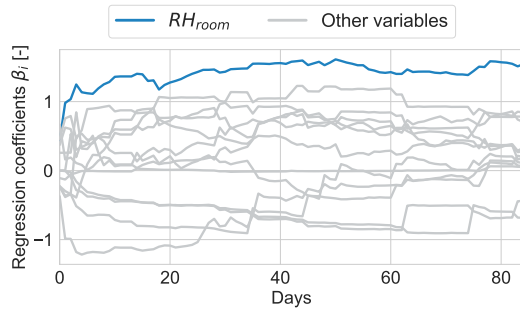


Figure 5.32: Evolution of logistic regression coefficients for increasing fan level in the kitchen.

For decreasing the fan speed, in both rooms, the importance of the previous fan speed is observed from the beginning. In the case of the bedroom, where occupants can be more sensitive to noise, this trend remains until the end of the experiment. Following Figure 5.11, after day 40 (around April 10th), there is a substantial increase in the mean outdoor temperature, which reflects in the occupant behavior regarding mechanical ventilation. From this day on, the influence of the indoor and outdoor temperature increases steadily, becoming the most important explanatory variables for the decreasing fan level in the kitchen and second place in bedroom 1. The coefficients are negative, meaning that a higher temperature reduces the probability of decreasing the fan level. The higher the temperatures, the higher the airflow that the occupants needed to satisfy their comfort requirements.

The occupant behavior for increasing the fan speed does not show a clear pattern, as in the decreasing case. In bedroom 1, the few recorded votes result in no significant regression coefficients. In the kitchen, the RH established itself from the

beginning as the strongest explanatory variable. Besides, the variation of the indoor temperature coefficient is identified as being high during the first month (negatively correlated) and weakening its effect by the end of the measurement period. The profiles for the other rooms are available in the Appendix A.7.

5.4.2 User satisfaction

Complementary with the previous results, the two occupants were surveyed after the experiment. The questionnaire was the same as the one developed by Maier [142]. The duration was around 30 minutes, where the participants had to answer questions regarding natural ventilation (window opening) as well as mechanical ventilation. Different topics were asked, such as the motivation to ventilate an indoor space, evaluation of mechanical ventilation devices, user interface design, and improvement suggestions. The most relevant results for this study are described in this section.

The main reason to ventilate is to get fresh air, according to the occupants. However, they also suggest that ventilating an indoor space is not associated necessarily with improving the indoor climate. Besides, humidity and smells are recognized as triggers to ventilate, mostly in the kitchen and bathroom. When considering summer, indoor temperature becomes a relevant variable, which is consequent with the results obtained in Section 5.4.1. Ventilation routines were asked as well. After showering has the strongest association with ventilation, emphasizing the importance of removing the humidity excess. On cold days, ventilation before leaving the apartment is also reported as relevant, whereas night ventilation is preferred on warm days.

The evaluation of mechanical ventilation systems was also included in the survey. In the first place, the occupants highlighted that the installed devices met their requirements and perceived the resulting air exchange successfully. Although Angsten et al. [16] reported critical issues regarding ventilation effectiveness and air short-circuiting, the occupants were satisfied with the provided fresh air. Another positive aspect was the developed user interface, evaluated as intuitive and understandable, especially considering the color field. On the other hand, this simplicity was also criticized, given the lack of programmability of the system. Another complaint was the loudness of the devices at night, which caused some sleep problems at the beginning. This confirms the previous analysis, where the noise of the device was identified as key to decrease the fan level. This result is independent of the selected controller since the loudness of the system was reported in levels 3 and 4.

Finally, the occupants provided suggestions, which could improve the relationship between the user and technology. Programmability and remote control options (mainly through a smartphone app) are recognized as a key for the individualization of the operation. It is worth mentioning that both occupants have a university degree in a technology-related field, which increases their affinity to these solutions [142]. Besides, the user interface could be enhanced with direct feedback (for example, room temperature and humidity). A sleeping mode could be included as well (which is typically present, as described in Section 4.1.1).

In general, the smart controller was perceived as useful but not crucial for the acceptance of the system. A comparison with other controllers should be carried out to study properly the acceptance. The users could realize the intelligence of the system; however, the lack of flexibility was sometimes perceived as a negative issue. Even though both occupants have a similar background and lived together during the measurement period, their answers are different in some aspects, especially considering the drivers to ventilate a room and the perception of the IAQ.

5.5 Summary

Smart ventilation acquired more relevance in the residential sector in the past years. Research has been focusing mostly on different demand-controlled controllers since the implementation of this technology is already proven. In Chapter 4, an innovative self-learning DCV controller is proposed, and the implementation in a real building was covered in this chapter. Thus, the research question 4 is answered through the following points:

Research Question 4: *How is the performance of innovative occupant-centered control strategies in a real-building implementation? Do they influence the acceptance of the user towards ventilation systems?*

- The implementation of a self-learning DCV controller in decentralized ventilation systems was successful. A field study in a smart home apartment was carried out where two occupants lived for three months. An Internet of Things scheme was developed along with a user interface, that the occupants used to operate the ventilation systems as desired. The controller learned through the user feedback to adapt itself to the occupants' needs.
- The installed decentralized ventilation system performed convincingly, providing enough air exchange to keep the performance indicators regarding relative

humidity and CO_2 concentration in the desired range. Energy consumption was not measured but estimated. The proposed learning DCV strategy was implemented satisfactorily, as the rooms presented highly diverse control fields after the measurement period. The influence of the user in every field was recognized, shaping the air exchange rate profile given the different user votes. The votes distribution profile was distinctive in every room, which confirms the suitability of single-room learning schemes against a whole-dwelling approach (as concluded in Section 4.5). Even though longer learning periods should be considered, a single-room learning scheme can grasp the singularities of the occupant behavior in every room correctly. However, a room-individual control would require a balancing procedure in case a single decentralized system is installed per room, as different airflow levels are required in different rooms at the same time. Other learning variables, such as fan noise or outdoor temperature, should be considered since there is no clear pattern in some rooms regarding RH and CO_2 concentration.

- User behavior was analyzed through data analysis using logistic regression, to understand the user motivation to ventilate. For increasing the fan level, in the humid rooms (kitchen and bathroom) RH was the most important explanatory variable, and in the other rooms, time-related coefficients (routines). For decreasing the fan level, noise (represented by previous fan speed) was identified as the most important explanatory variable in the dry rooms. The humid rooms had indoor and outdoor temperature, noise being the second most important. The influence of weather change during the experiment could be seen, as the temperature variables gained relevance through time in every room. These findings were supported later by the user survey, carried out after the experiment. Occupants were satisfied with the performance of the installed devices and highlighted the user interface development. On the other hand, noisy environments in bedrooms and lack of programmability were criticized. Smart residential ventilation systems are perceived as useful but are not the only aspect that the user considers for its acceptance. The combination of the logistic regression analysis and user survey concludes that the motivations and preferences of the occupants regarding mechanical ventilation can be extremely different, even when sharing an apartment. This highlights the importance of the individualization of the user preferences when proposing innovative user-centered ventilation controllers.

6 Conclusions and outlook

Main findings

This thesis provides an insight into residential decentralized ventilation control strategies. The relationship between users and ventilation systems is complex and must be understood properly within a context that targets health and comfort without disregarding energy efficiency. Understanding this relationship is a key to narrow the gap between technology and the user. The increasing market share regarding decentralized ventilation in Germany, mainly due to the retrofit of residential buildings, is driving the attention of scientific research to these devices.

The requirements for residential decentralized ventilation systems have been investigated. Owners and housing associations are primarily interested in minimizing investment costs, reducing maintenance efforts, and avoiding mold growth. In different standards, mechanical ventilation is compulsory only when a minimum humidity-protection air exchange rate is not achieved with infiltration, and in humid rooms without windows. From the industry perspective, energy-efficient devices are considered as an additional sales argument. The latest trend in research is to prioritize indoor air quality and health effects. Even though many contaminants are present in indoor environments, CO_2 is still the most accepted variable to control in dry rooms. In extreme values (below 25% and over 75%), relative humidity also has a direct impact on human health. In that sense, higher air exchange rates become more attractive. Other variables, which can be directly hazardous for occupants, are usually not considered since the monitoring technology is too complex for a commercial device. In times of a worldwide pandemic, health can also turn into a highly compelling argument for the installation of residential ventilation systems [205]. From the perspective of the occupant, the sense of fresh air is one of the main targets, while at the same time minimizing the energy costs. Relative humidity and CO_2 concentration are targeted in winter since they are highly correlated with indoor occupant activities. Different acceptability thresholds were found in the literature because occupants have vastly different definitions of the concept of "fresh air". Other aspects, such as noise pollution caused by the system itself and user-friendly interfaces, are crucial for the success of these technologies.

Furthermore, occupant behavior models related to residential ventilation were compared and discussed. Available data about user behavior towards residential mechanical ventilation is limited and mostly acquired through surveys. Thus, window

opening behavior was analyzed, as a reaction to the need for fresh air. Three popular models from the literature based on logistic regression were tested and compared. The outputs of the models are highly diverse, showing potential overfitting to the training data. Available real window opening data was used to tune a novel clustering method, to identify distinctive user behavior patterns. The existing probabilistic models represent only reliably a few profiles, as a result of generalized modeling, missing the individual preferences in some cases. A real-time logistic regression is proposed and tested with collected data from renovated apartments with mechanical ventilation, to understand the occupants' drivers to open the window. This has the potential to understand the occupants' preferences targeting the individualization of mechanical ventilation control strategies (analogous to a previous study [183]). Results indicate that occupants operate windows mostly due to time habits or as a consequence of indoor and outdoor environmental variables. To integrate this into a residential ventilation controller, a peak detection algorithm was applied to identify window opening without using window contacts. High accuracies in apartments where CO_2 concentration is a key driver to window opening were observed. Otherwise, the accuracy strongly decreases. An improvement in this method could lead to a tailored scheme that detects the user ventilation needs and implements it directly in a controller.

Simulation has become a necessary tool for the development of different technologies and their evaluation before implementation. Existing models do not meet all the requirements to assess control strategies for decentralized ventilation in residential buildings. The Airflow Network modeling principle is crucial to evaluate the impact of these controllers in room-individual models, where heat, moisture, and CO_2 values could be evaluated. Reliable heat recovery and fan models were developed and validated, given their high impact on the buildings' energy performance. A co-simulation scheme was proposed, which combined the strengths of different environments, to obtain reliable results for the evaluation of the developed controllers.

Since assessing a real-time user preference detection was not feasible, other occupant-centered solutions were explored. A thorough market and scientific state-of-the-art analysis regarding ventilation control strategies identified the lack of multivariable controllers and occupant-centric solutions in this field. In this regard, two fully automatic controllers were developed, which return the desired fan speed as a function of the relative humidity and CO_2 concentration. Both cost function and fuzzy-based controller provide energy savings in comparison to traditional demand-controlled strategies, without compromising hygrothermal comfort or indoor air quality. How-

ever, the state-of-the-art steps strategy already provided more than half of the potential energy savings and achieved significantly better performance indicators. These results confirm that the lack of innovation in ventilation control strategies lies in the capabilities of the current state-of-the-art controllers, which can achieve already an acceptable performance against manual controllers. The sensitivity to different weather conditions concluded that the primary energy savings potential is higher in colder climates and that ambient conditions do not strongly impact the resulting fan speeds, which coincides with previous studies [91, 150]. The sensitivity to internal loads resulted in greater fan speed differences. In any case, a fuzzy-based DCV has a primary energy savings potential ranging from 10 to 25% in comparison to a state-of-the-art stepwise demand-controlled ventilation strategy, without compromising the health and air quality indicators.

However, occupants need a certain degree of control over the systems to improve their acceptance [208]. In that sense, an innovative self-learning DCV scheme was proposed, to learn the user preferences towards RH and CO_2 . Hence, a user behavior model regarding mechanical ventilation was necessary. Four user profiles were developed and exposed to the self-learning DCV in a simulation scenario. The selected learning algorithm is the Support Vector Machines (SVM). The algorithm was tested regarding learning rate, room-individual or whole-dwelling learning, user comfort, and activity profile. The self-learning DCV performed satisfactorily, tailoring its shape to the predefined user profile from the beginning, and stabilizing after around 60 user votes. This solution achieved an individualized comfort improvement, without resigning energy-efficiency. The whole-dwelling approach could learn the well-defined user comfort profiles more quickly, but failed to build a reliable solution when occupants present distinctive comfort profiles in the different rooms. Hence, a single-room approach is preferred. Different user comfort profiles were tested, which directly influence the potential primary energy savings of the proposed controller. In this case, validated user comfort profiles are required to properly assess the influence of the occupant behavior on the performance of residential ventilation systems. In this thesis, the four artificial comfort profiles affected the potential energy savings within a range of 20%. Comfort and indoor air quality indicators are not sensitive to the different user profiles, as the ventilation controller adapts the resulting air exchange rate to the occupants' needs.

In contrast to fuzzy-based solutions, the implementation of a self-learning DCV system had not yet been investigated. The developed controller was installed and tested in the Energy Smart Home Lab, a living lab facility in Germany. Decentralized ven-

tilation systems were installed together with an IoT-based solution, which collects data and runs the self-learning controller. A Human-Machine-Interface with a rotary encoder was developed to collect user feedback and make the operation simple and understandable. From the ventilation side, the performance indicators showed a correct dimensioning and operation of the installed system. Additionally, the learning algorithm could follow the occupants' preferences in almost every room. Nevertheless, there are no clear patterns between the independent (RH and CO_2) and dependent (Fan speed) variables. Analyzing the votes with a real-time logistic regression confirmed this later. It highlighted the need for quieter environments in bedrooms and moisture removal in wet rooms. The developed approach provided an individualization that the occupants remarked as effective. On the other hand, the user survey and logistic regression analysis show that there are potentially other variables, that could be more suitable for tailoring the system to the user preferences, rather than the selected ones. For instance, indoor and outdoor temperature gained importance in the last month of the measurement period, mainly because the outdoor conditions were closer to summer conditions. Moreover, the occupants perceived the operation of the ventilation systems as useful. Some improvement suggestions emerged regarding control flexibility, scheduling, and noise.

Limitations

The thesis limits itself to the analysis of decentralized ventilation systems in residential multifamily buildings. The behavior models and weather conditions were defined for a Central European zone. In that sense, further work to expand the validity of these results to other ventilation systems, building, and climate types should be considered.

The selected simulation approach presents some limitations. The building model represents a generic multifamily apartment and was validated against measurements in real apartments with different floor plans but similar thermal characteristics. The influence of higher wind speeds could not be assessed properly, as the selected simulation scheme compensates the pressure difference between room and façade with infiltration. The additional infiltration results in a higher heating energy consumption, meaning that a proper assessment of the impact of unbalanced decentralized ventilation in comfort and indoor air quality requires other modeling techniques [203]. Besides, the decentralized ventilation model was developed and validated following laboratory measurements, as field measurements were not available. Regarding the

occupant behavior, deterministic (internal loads) and probabilistic (heating setpoint, window opening and ventilation operation) were combined into a single simulation model. D'Oca et al. [62] studied that heating setpoint and window opening behavior must be simulated with stochastic models to lower the discrepancy between predicted and actual energy consumption. The combination of different occupant behavior models should be further studied.

A central limitation concerns the single-room learning approach. As seen in the simulation study in chapter 4, having different comfort profiles learned in a single room can be problematic. These should not be an issue in multifamily residential buildings, where usually the number of occupants is rather low in comparison to other building types. However, when extending the proposed method to other buildings such as office buildings (where workers share open spaces), the clash of the different comfort profiles can become critical. Comparable to the results for the whole-dwelling learning scheme, the self-learning controller would deliver unstable control fields in shared open spaces. Other solutions should be explored to achieve an individualized solution in these multi-occupant spaces.

The analysis of the occupant behavior towards mechanical ventilation at the ESHL has a main limitation: only two occupants operated the system. Besides, the exchange students come from South America (different climate zone), which might result in different behaviors than Central European countries. In this thesis, it was preferred to have the same occupant behavior for three months to evaluate the potential of the self-learning controller. To properly study the occupant behavior, data from different occupants should be collected, including control groups. Therefore, this experiment could be repeated with different occupants to lower the bias of the results towards a specific behavior.

Outlook

This thesis is expected to gain relevance for the development of control strategies in the forthcoming years. The residential ventilation market is growing steadily, and decentralized systems are increasing their market share every year. More than ten years ago, Hasselaar [103] described one of the main reasons for a residential ventilation crisis as the poor relationship between user and technology. Since that publication, several health effects related to poor indoor environments have been investigated, once again emphasizing the relevance of residential ventilation. In this thesis, these effects were represented by the indoor relative humidity and CO_2

concentration. When extending this method to other buildings (such as office buildings), the relevance of the relative humidity as a contaminant is limited, and other pollutants are more relevant, such as VOC. These other pollutants were not modeled in this thesis due to their complexity [1]. Besides, pollutant monitoring in the field is currently limited, since it requires an advanced sensor deployment. In general, a lack of cost-effective solutions can be identified. A few studies [149, 54] analyzed the suitability of VOC as a target variable for DCV. Overventilated apartments were observed, given the sensitivity of VOC to activity-related contaminants. Further research is needed on this topic, to obtain a more reliable indoor air quality indicator than CO_2 alone. The proposal of other indicators could enhance the performance of the self-learning scheme.

Concerning decentralized ventilation systems, noise is a key unresolved issue. Sleep disturbance was observed in the implementation of facade-integrated ventilation systems in chapter 5, confirming previous studies [163]. If the fan operates at its lowest levels, the occupants reported high acceptability. One of the key advantages of decentralized ventilation is the simple installation process and its compactness. Axial fans allow changing the direction of the volume flow but are sensitive to pressure changes. The use of radial fans could provide a solution where the fans are louder but able to overcome noise reduction measurements and keep an acceptable ventilation efficiency. Summarizing, the market for residential ventilation expands every year, and tackling the noise problem is key to the prosperity of this technology.

The proposed real-time logistic regression method provides a reliable data-based interpretation of the occupant needs. An improvement of the detection algorithm, together with its application in real case studies, could provide further insight into the adaptation of ventilation control strategies to the user preferences. As described in chapter 3, the occupants' drivers to operate a residential mechanical ventilation system are still not sufficiently investigated. Ren et al. [183] emphasized the need to develop better user behavior models for building performance simulation. In that sense, more measurement campaigns in real buildings regarding the operation of mechanical ventilation are needed. Psychological and cultural aspects should not be neglected in future research, in order to further understand the potential of self-learning systems in multi-occupant spaces. The application of self-learning systems in shared spaces should be studied both in residential and non-residential buildings.

The simulations performed in this thesis focused on the winter operation of ventilation systems. As a direct consequence of climate change, summer outdoor temperatures increase steadily, causing frequent summer overheating in the last years.

This increased the interest in summer ventilation. The proposed strategies could be extended as well to summer operation, considering an extension regarding the occupant-related variables. Indoor and outdoor temperatures and the reduction of cooling loads, as well as thermal comfort, should be primary objectives. Although the implementation of the self-learning controller was designed for winter conditions, part of the experiment took place under early summer weather. This field implementation confirmed that the temperature variables gained relevance throughout time in every room. In that sense, some work related to fuzzy controllers and summer residential ventilation is already available in the literature [92].

The development of self-learning control strategies, as well as the field implementation, is covered in this thesis. The installation of the device in the real building was simple, however the development of an electronic concept for the deployment of the smart controller was necessary. With the investment in additional hardware and sensors, the start-up procedure could require IT experts in the field, losing the simplicity of the installation process. Chiesa et al. [46] suitably explained the advantages and challenges of IoT platforms for smart ventilation systems.

Smart technologies have received more attention in the research community. In July 2020, the International Energy Agency approved the new Annex 86 - "Energy-efficient smart IAQ management for residential buildings", confirming the direction of the technology towards the optimization of ventilation systems [5]. Some publications already cover the impact of big data on ventilation systems [139]. Schieweck et al. [190] explained that the acceptance of smart home technologies (including ventilation) depends on several factors, although users mostly see their benefits and perceive the advantages in terms of energy savings and comfort improvement. In addition to a cost-effective offer, fears towards new technologies should cease. In that sense, endeavors from research, industry, and users must join together for the prosperity of these technologies.

A Appendix

A.1 Real-time logistic regression for window opening

In this section, the plots with the time evolution of all regression coefficients from the logistic regression analysis are presented, as described in section 3.3.

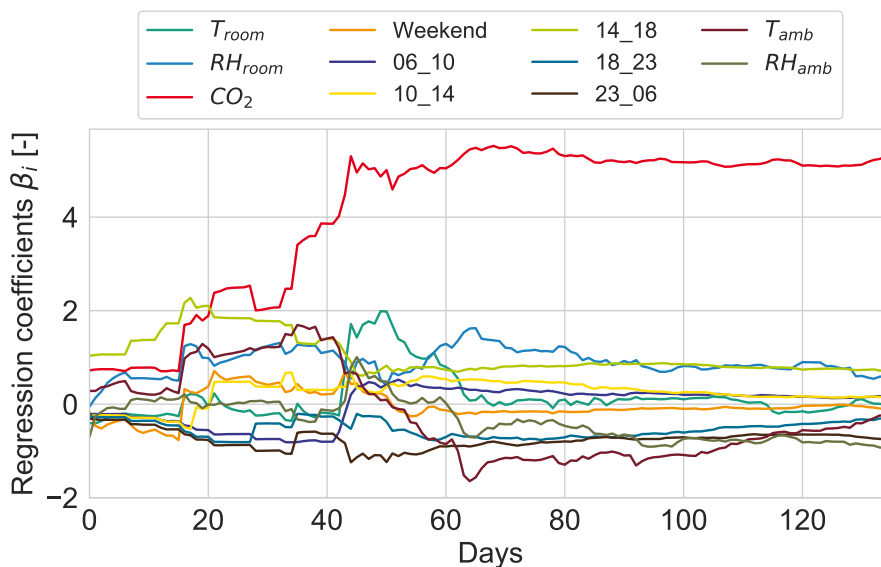


Figure A.1: Real-time evolution of the logistic regression coefficients with measured window opening in the apartment 1.

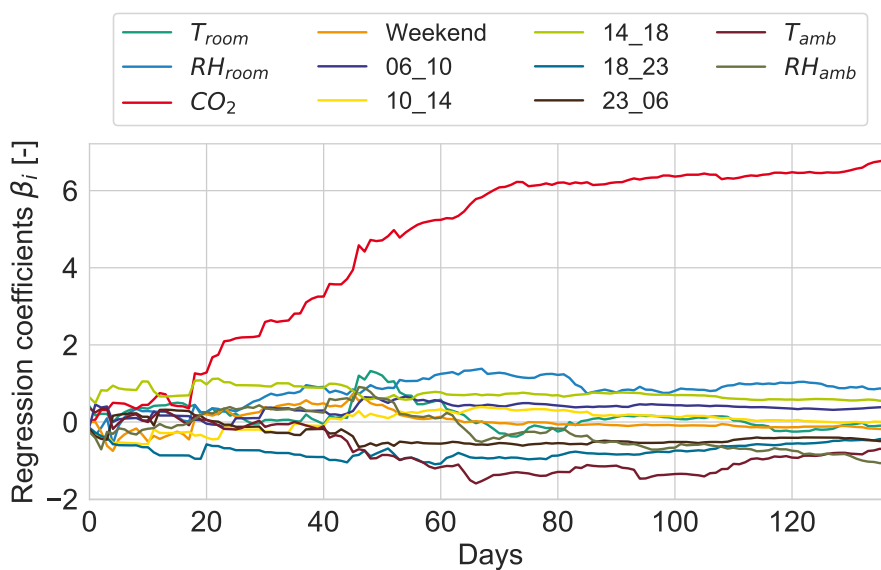


Figure A.2: Real-time evolution of the logistic regression coefficients with estimated window opening in the apartment 1.

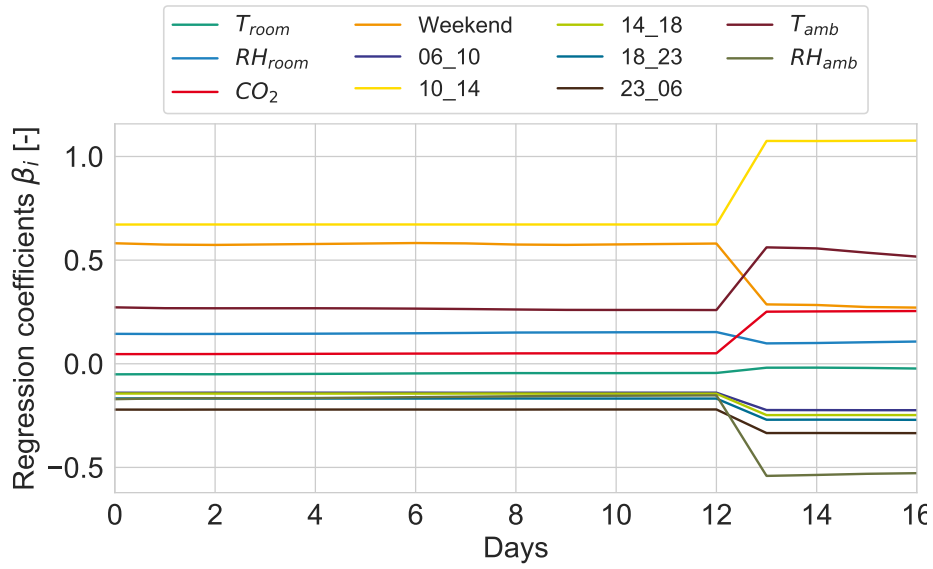


Figure A.3: Real-time evolution of the logistic regression coefficients with measured window opening in the apartment 2.

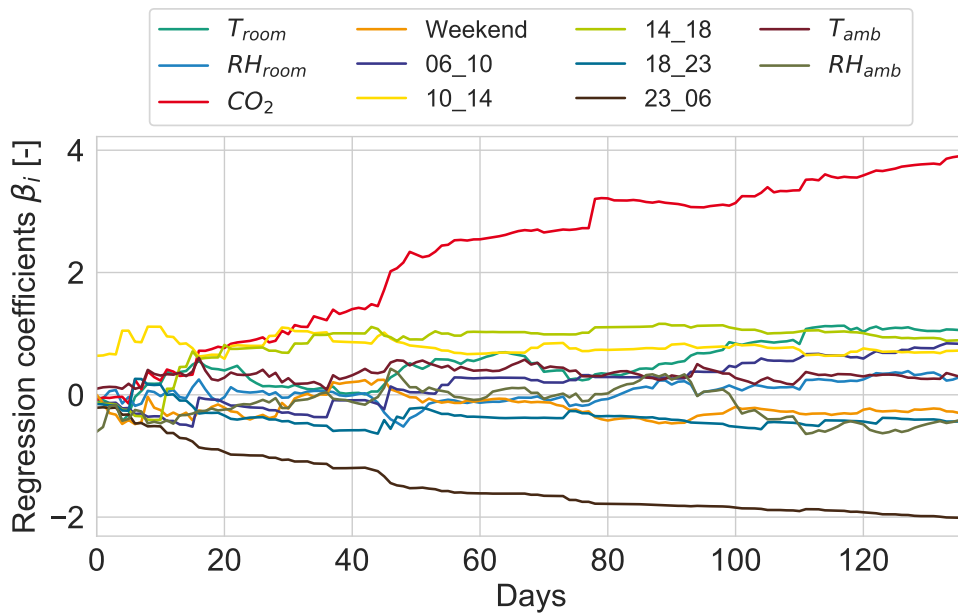


Figure A.4: Real-time evolution of the logistic regression coefficients with estimated window opening in the apartment 2.

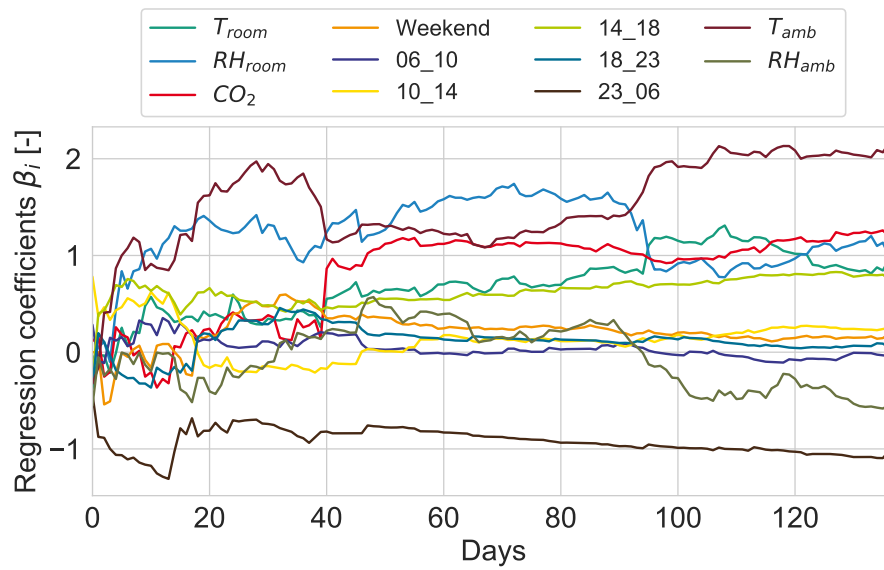


Figure A.5: Real-time evolution of the logistic regression coefficients with measured window opening in the apartment 3.

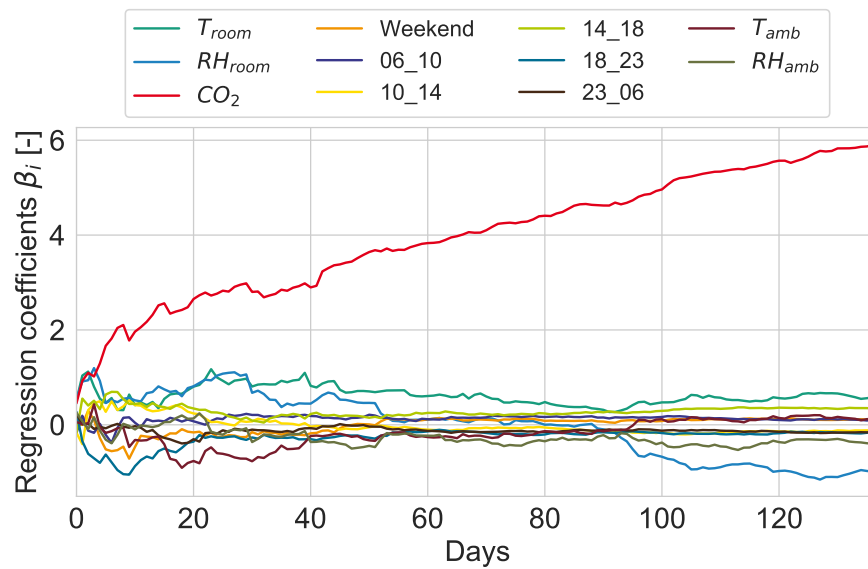


Figure A.6: Real-time evolution of the logistic regression coefficients with estimated window opening in the apartment 3.

A.2 Multifamily building model

This section addresses further details of the proposed building model (Section 4.2.2) and its validation. As mentioned before, the building is modeled with EnergyPlus 8.9.0 [50]. The air movement inside and outside the dwelling, the infiltration, and wind pressure are simulated by applying the airflow network approach [27].

Every room is modeled as a node, where pressure is the associated state variable. A pressure difference between two nodes causes an air movement. This happens through air paths (equivalent to electric resistances). Thus, the air movement is calculated using the power law [21].

$$\dot{V} = C_d \cdot A \cdot \left(\frac{2 \cdot \Delta P}{\rho_{air}} \right)^m \quad (\text{A.1})$$

- \dot{V} is the resulting volume flow in $\frac{m^3}{h}$.
- ΔP is the pressure difference between two nodes in Pa.
- ρ_{air} is the air density in $\frac{kg}{m^3}$, assumed 1.2.
- C_d is the non-dimensional discharge coefficient.
- A is the opening area in m^2 .
- m is the mass flow exponent (0.5 for turbulent, 1.0 for laminar flow), non-dimensional.

To model the airflow through small openings (cracks, doors, closed windows), the Technical Note 44 of the AIVC suggests using the flow coefficient k [164]:

$$k = C_d \cdot A \cdot \left(\frac{2}{\rho_{air}} \right)^m \quad (\text{A.2})$$

Assuming a C_d of 0.6 and a mass flow exponent m of 0.667, the mass flow coefficient k was measured in different countries and building schemes in Technical Note 44 of the AIVC [164]. For windows, a value of $k_w = 1.5\text{E-}04$ was used, and for doors $k_d = 4.4\text{E-}04$. The window value is valid for German multifamily buildings, whereas the door value is measured in the United States for residential doors since the source does not report values for Germany.

Regarding the infiltration, the recommendation of the Passive House Institute is followed, which suggests a total air exchange rate of 0.5 h^{-1} when the pressure difference ΔP_{ref} is 50 Pa [170]. The infiltration is distributed in every room and modeled using the effective leakage area (ELA) method [10]:

$$ELA = \dot{V}_{ref} \cdot \left(\frac{\rho_{air}}{2 \cdot \Delta P_{ref}} \right)^m \cdot C_d^{-1} \quad (\text{A.3})$$

- ELA is the effective leakage area in m^2 .
- \dot{V}_{ref} is the reference volume flow in $\frac{m^3}{h}$.
- ΔP_{ref} is the reference pressure difference in Pa.
- ρ_{air} is the air density, assumed $1.2 \frac{kg}{m^3}$.
- C_d is the non-dimensional discharge coefficient, assumed 0.6 [164].
- m is mass flow exponent, assumed 0.667 [164].

Table A.1 illustrates the distribution of the outdoor surfaces in every room in the building model. The calculated effective leakage area (in m^2), assigned proportionally to the outdoor surfaces, is shown in Table A.2. The air exchange due to infiltration is calculated also using the power law (Equation A.1).

Room	Volume [m^3]	EW_N [m^2]	EW_W [m^2]	EW_S [m^2]
Children 2	28.04	8.91	0	0
Children 1	28.04	8.91	0	0
Bedroom	36.98	8.6	10.75	0
Living room	57.94	0	10.75	13.48
Kitchen	22.04	0	0	5.13
Bathroom	17.2	0	0	4.00

Table A.1: Summary of exterior wall surface properties for the modeled building (N = north façade, W = west façade, S = south façade).

Room	ELA_{total} [m^2]	ELA_N [m^2]	ELA_W [m^2]	ELA_S [m^2]
Children 2	3.43E-04	3.43E-04	0	0
Children 1	3.43E-04	3.43E-04	0	0
Bedroom	4.53E-04	2.01E-04	2.52E-04	0
Living room	7.10E-04	0	3.15E-04	3.95E-04
Kitchen	2.70E-04	0	0	2.70E-04
Bathroom	2.11E-04	0	0	2.11E-04

Table A.2: Summary of ELA properties for the modeled building (N = north façade, W = west façade, S = south façade).

To calculate the wind pressure on the façade, the wind pressure coefficients were calculated using the equation of Swami and Chandra [201]. Results for the three used orientations and wind angles are presented in Table A.3.

$$C_p = C_p(0) \cdot \ln \left[1.248 - 0.73 \cdot \sin \left(\frac{\theta}{2} \right) \cdot 1.175 \cdot \sin^2(\theta) + 0.131 \cdot \sin^3(2G\theta) + 0.769 \cdot \cos \left(\frac{\theta}{2} \right) + 0.07 \cdot G^2 \cdot \sin^2 \left(\frac{\theta}{2} \right) + 0.717 \cdot \cos^2 \left(\frac{\theta}{2} \right) \right] \quad (\text{A.4})$$

- $C_p(0)$ is the reference wind pressure coefficient (suggested 0.6), non-dimensional.
- θ is the wind angle (0 at north, advances clockwise) in *rad*.
- $G = \ln(\frac{W}{L})$ is the natural logarithm of the building width and length relationship, non-dimensional.

Wind angle [<i>deg</i>]	North	West	South
0	0.603	-0.415	-0.260
30	0.469	-0.599	-0.308
60	0.123	-0.308	-0.599
90	-0.415	-0.260	-0.415
120	-0.599	-0.308	0.123
150	-0.308	-0.599	0.469
180	-0.260	-0.415	0.603

Table A.3: Summary of wind pressure coefficients for every façade.

Furthermore, the ventilation concept for this dwelling must be defined. The four ventilation levels according to the norm DIN 1946-6 [58], explained in Section 2.1,

are dimensioned for the building model. The total ventilation needed \dot{V}_{tot} is defined in Equation A.5:

$$\dot{V}_{tot} = f_{LSt} \cdot (-0.002 \cdot A_{Dw}^2 + 21.15 + A_{Dw}) \quad (\text{A.5})$$

- f_{LSt} is a coefficient for each ventilation level, in $\frac{m^3}{h \cdot m^2}$
- A_{Dw} is the dwelling room surface (84.6 m^2)

Following Equation 2.1, the mechanical ventilation requirements are defined by the total air exchange requirements, subtracting the infiltration and natural ventilation. Neglecting the window opening (conservative assumption), the infiltration \dot{V}_{inf} is calculated using Equation A.6.

$$\dot{V}_{inf} = e_z \cdot V_{Dw} \cdot n_{50} = 4.5 \frac{m^3}{h} \quad (\text{A.6})$$

- e_z is a coefficient for placement and size of the whole building for each ventilation level, nondimensional (0.04)
- V_{Dw} is the dwelling volume (311.5 m^3)
- n_{50} is the air exchange rate at 50 Pa pressure difference (0.5 h^{-1} [170])

Hence, the ventilation levels are defined. Six devices are planned a priori (one in every room). Table A.4 summarizes the total air requirements and the distribution in every ventilation system, together with the modeled fan speed.

Ventilation level	Total \dot{V}	\dot{V}_{DVS} minimum	\dot{V}_{DVS} modeled	Fan speed [%]
Humidity protection	27.4	8	10	25
Reduced ventilation	64.0	20	21	50
Nominal ventilation	91.4	29	32	75
Intense ventilation	118.9	38	45	100

Table A.4: Ventilation requirements (in m^3/h) according to DIN 1946-6 [58].

Additional conditions must be fulfilled [58, T. 16, p. 48], such as:

- Kitchen and bathroom when showering or cooking = $40 \frac{m^3}{h}$
- Toilet nominal ventilation = $20 \frac{m^3}{h}$
- Bedroom ventilation = $15 \frac{m^3}{h}$ per person

Thus, nominal and intense ventilation levels must be raised in the humid rooms to comply with this regulation. Besides, the bedroom (two persons) must deliver twice the airflow in nominal ventilation. In this case, a second device will be added to the bedroom. A second ventilation device is included in the living room as well to balance the dwelling. A total of eight devices are planned. Moreover, the airflow network model assumes a perfect air mixing (single node model) and ignores the impact of air distribution in the room and potential short circuits in different system configurations. Given that the ventilation systems are façade-integrated, the ventilation effectiveness η_{vent} can be modeled as a function of the air exchange rate (Equation A.7)[127]. This assumed effectiveness affects the volume flow in every room.

$$\eta_{vent} = -0.244 \cdot \left(\frac{\dot{V}_{sup}}{V_{room}} \right)^2 + 0.376 \cdot \left(\frac{\dot{V}_{sup}}{V_{room}} \right) + 0.732 \quad (A.7)$$

- \dot{V}_{sup} is the supply volume flow rate in $\frac{m^3}{h}$
- V_{room} is the volume of the room in m^3

The validation is performed by comparing a baseline case with measured indoor environments. The fan speed was set to 2000 RPM, which provides an air exchange rate of $0.4 h^{-1}$, analogous to the observed values in the measured apartments (Section 3.2.1). Apartment 2 of the measured data is compared to the simulation results since it is the closest floor plan from the measured apartments ($88 m^2$, two bedrooms, renovated to the medium energy standard). The following figures illustrate a histogram comparison of indoor temperature, RH , and CO_2 concentration values (CO_2 was not measured in the kitchen and bathroom). Energy consumption was not measured in the apartments. Since the heating and cooling energy consumption is not considered in the analyses of this thesis, this was not a part of the validation process.

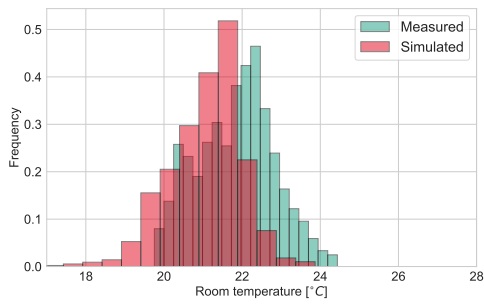


Figure A.7: Histogram comparison for indoor temperature in the bedroom.

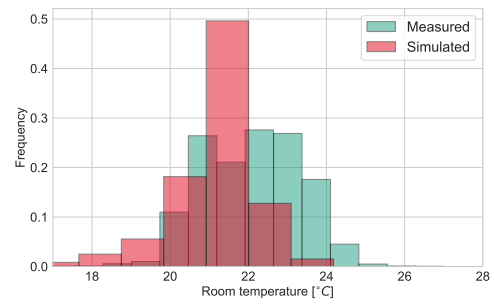


Figure A.8: Histogram comparison for indoor temperature in the living room.

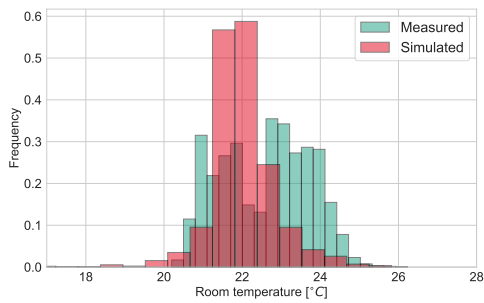


Figure A.9: Histogram comparison for indoor temperature in the kitchen.

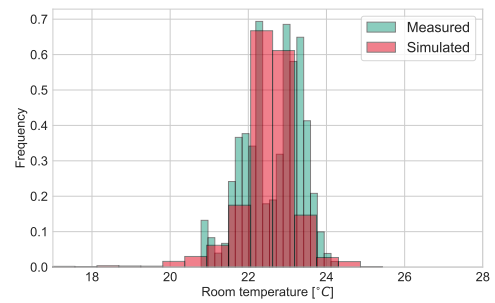


Figure A.10: Histogram comparison for indoor temperature in the bathroom.

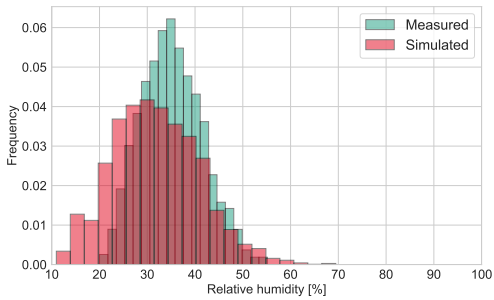


Figure A.11: Histogram comparison for indoor RH in the bedroom.

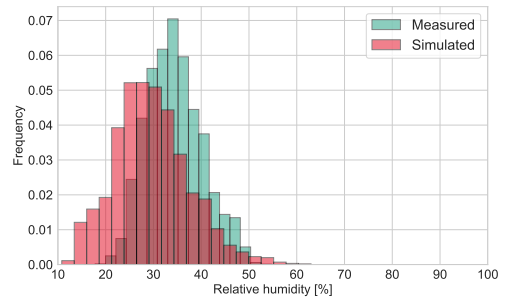


Figure A.12: Histogram comparison for indoor RH in the living room.

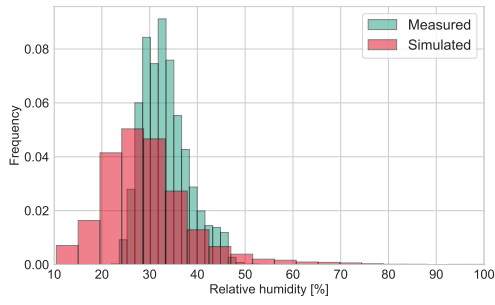


Figure A.13: Histogram comparison for indoor RH in the kitchen.

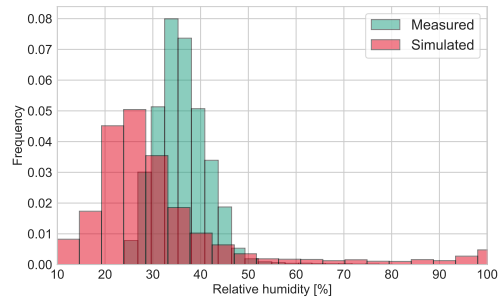


Figure A.14: Histogram comparison for indoor RH in the bathroom.

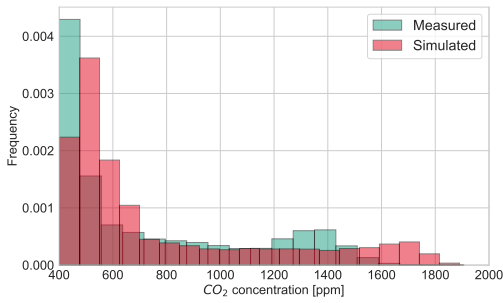


Figure A.15: Histogram comparison for indoor CO_2 in the bedroom.

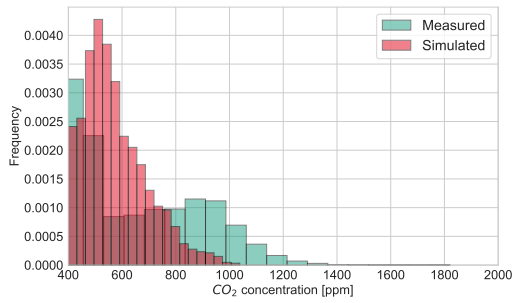


Figure A.16: Histogram comparison for indoor CO_2 in the living room.

A.3 Decentralized ventilation system model

The proposed decentralized ventilation model (Section 4.2.3) is detailed and validated in this section. The decentralized ventilation system is modeled with Modelica 3.2.2 [147]. The thermal and hydraulic modeling and validation process are published already in a scientific article [35]. Figure A.17 shows the structure of the heat recovery system (HRC). Table A.5 summarizes the properties of the ceramic heat storage.

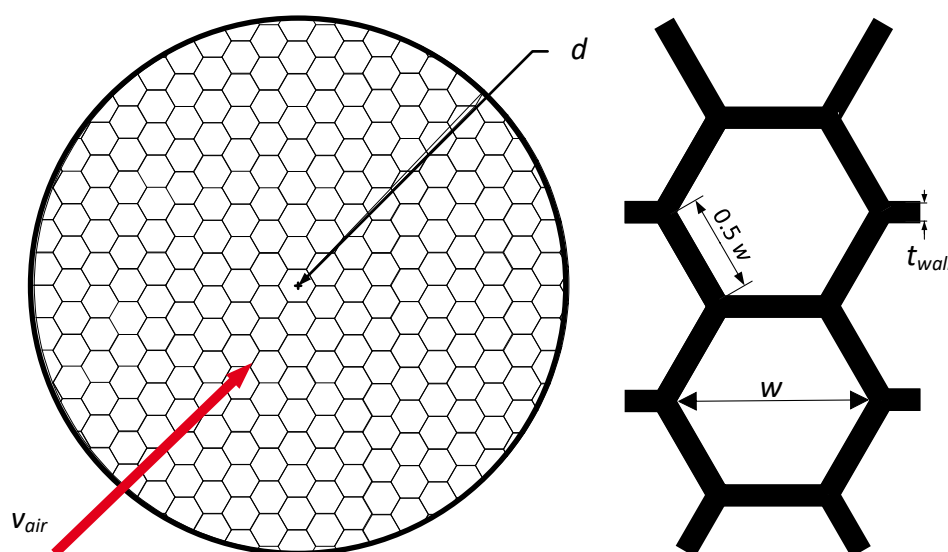


Figure A.17: Honeycomb regenerator, front view (left) and channel (right) [35].

Variable	Definition	Unit	Value
w_{chan}	Channel width	m	0.004
l_{chan}	Channel length	m	0.15
d_{cyl}	Cylinder diameter	m	0.142
m_{cyl}	Mass	kg	2.32
C_{solid}	Heat capacity solid	$\frac{kJ}{kg}$	2034
ρ_{solid}	Density solid	$\frac{kg}{m^3}$	2700
k_{solid}	Thermal conductivity solid	$\frac{W}{m \cdot K}$	0.026
n_{chan}	Number of channels	-	1000
t_{wall}	Wall thickness	m	0.001

Table A.5: Heat storage properties.

The heat exchange between the air and the heat storage is assumed as a pure convection case (temperature rise due to radiation between surfaces in comparison to convection is around 3% [87]). Equation A.8 was obtained applying the first law of the thermodynamics in a control volume of the heat exchanger:

$$\dot{Q}(t) = \rho_{air} \cdot \dot{V}_{air} \cdot c_{p,air} \cdot \frac{\partial T_{air}}{\partial x} = \frac{h_{air} \cdot A_{ht} \cdot dx}{L_{ht}} (T_{air} - T_{solid}) = C_{solid} \cdot \frac{dx}{L_{ht}} \frac{dT_{solid}}{dt} \quad (\text{A.8})$$

- \dot{Q} is the heat transfer rate between the fluid and the HRC surface, in W.
- ρ_{air} is the dry air density, in $\frac{kg}{m^3}$, assumed 1.2.
- \dot{V}_{air} is the air volume flow rate, in $\frac{kg}{s}$.
- $c_{p,air}$ is the dry air specific heat capacity, in $\frac{J}{kg \cdot K}$, assumed 1.005.
- T_{solid} is the temperature on the surface of the solid, in K.
- T_{air} is the air temperature, in K.
- h_{air} is the specific convection coefficient, in $\frac{W}{K \cdot m^2}$.
- C_{solid} is solid heat capacity, in $\frac{kJ}{kg}$.
- A_{ht} is the heat transfer area, in m^2 .
- L_{ht} is the heat transfer length, in m .

The specific convection coefficient is calculated using Equation A.9.

$$h_{air} = \frac{Nu \cdot k_{air}}{d_h} \quad (\text{A.9})$$

- Nu is the non-dimensional Nusselt number.
- d_h is the hydraulic diameter, in m.
- k_{air} is the thermal conductivity of dry air, in $\frac{W}{K \cdot m}$, assumed 0.025.

Therefore, the heat stored is modeled as a capacity that absorbs or releases heat on each time step, depending on the temperature difference and the Nusselt number. The hydraulic diameter d_h is calculated using Equation A.10.

$$d_h = \frac{\sqrt{3}}{2} \cdot w \quad (\text{A.10})$$

Since the flow through the channels is laminar ($Re < 2300$), an empirical correlation for Nusselt number was used (Equation A.11) [136]. The non-dimensional numbers of Reynolds (Re) and Prandtl (Pr) are necessary to calculate it [194].

$$Nu = 3.61 + \frac{0.0668 \cdot \left(\frac{d_h}{l}\right) \cdot Re \cdot Pr}{1 + 0.04 \cdot \left[\left(\frac{d_h}{l}\right) \cdot Re \cdot Pr\right]^{\frac{2}{3}}} \quad (\text{A.11})$$

Concerning the geometrical modeling approach in Modelica, the heat transfer through the hexagonal channels is modeled as a heat transfer in a circular pipe. The equivalent diameter of this pipe is calculated with the corresponding cross-section area during the heat transfer. The equivalent cross-section in the simulated pipe must be the same as in the channels. Equation A.12 shows the geometrical transformation.

$$d_{eq,pipe} = \sqrt{\frac{3 \cdot \sqrt{3} \cdot w^2 \cdot n_{chan}}{2 \cdot \pi}} \quad (\text{A.12})$$

Besides, the heat storage model is discretized to represent better the temperature progression across the heat exchanger. Along with the higher accuracy, the computational time increases. Figure 4.8 in Section 4.2.3 shows the model in Modelica. For the model validation, two indicators are used: the root mean squared error (RMSE) and mean average percentage error (MAPE) [17], which are applied to the supply temperatures on the room side of the heat exchanger. The RMSE has the unit of the measured variable, while the MAPE is expressed in percentage.

$$RMSE = \sqrt{\frac{\sum_n (X_{sim} - X_{meas})^2}{n}} \quad (\text{A.13})$$

$$MAPE = \frac{\sum_n \left| \frac{X_{sim} - X_{meas}}{X_{meas}} \right|}{n} 100 \quad (\text{A.14})$$

A key parameter of the model is the number of nodes of the discretization. Figure A.18 shows the calculated RMSE between simulated and measured supply air temperatures as a function of the number of nodes for the simulation with an alternating

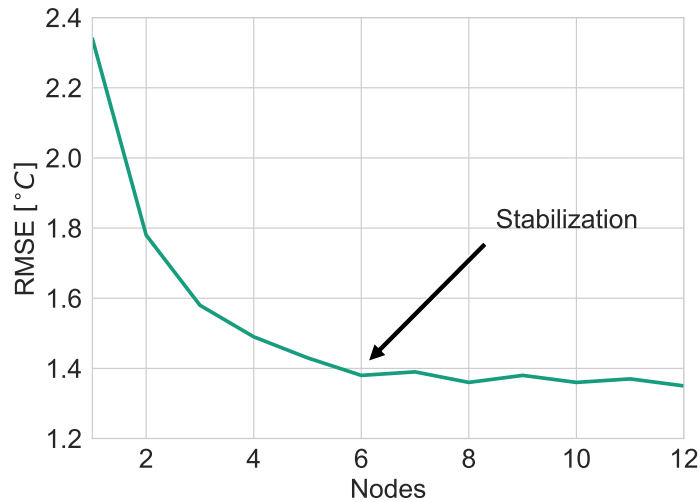


Figure A.18: RMSE for the supply air temperature as a function of the number of nodes [35].

period of 60 seconds and nominal fan speed. The error stabilization occurs for the models with six or more nodes. Therefore, simulations are carried out by modeling the regenerator with six nodes.

Table A.6 presents the simulation results for the quasi steady-state cycles of every parametric case. As expected, higher air speeds mean a higher heat exchanged in both phases. Besides, a higher air speed means a lower heat recovery efficiency. Shorter periods lead to a lower mean heat exchanged but higher efficiencies. The principle is the same as in the analysis of the air speed: a longer cycle means that the regenerator is closer to its heat saturation in both phases, leading to a lower average air supply temperature, therefore a lower efficiency.

Period	60 s		180 s				
	Control	η_{HRC} [%]	\dot{Q}_{sup} [W]	η_{HRC} [ppm]	\dot{Q}_{sup} [W]	v_{air} [$\frac{m}{s}$]	Re [-]
50% Speed		0.77	25.3	0.76	30.6	0.40	94
100% Speed		0.71	46.7	0.63	59.0	0.89	204

Table A.6: Average simulated supply heat exchanged and heat recovery efficiency.

Figure A.19 compares the measured and simulated air temperature profiles for the 180 seconds cycle length. Asadov [20] carried out laboratory measurements of regenerative decentralized ventilation systems, used in this thesis for the validation process. The temperature profiles on both sides of the regenerator display an overall adequate agreement. The initial temperature on both phases shows a slight jump

and then a linear behavior, mainly because of the direction change of the fan and the inaccurate modeling of the flow. These temperature gaps affect the simulated heat exchange between the airflow and the regenerator. However, the obtained results are acceptable for the model. The achieved relative errors (MAPE) are under 10% in every simulated case, for both fan speeds. Additionally, the model neglects radiation, thermal conductivity in the heat storage, and the air velocity profile. Table A.7 summarizes the performance indicators for the supply temperature. The model simulates ten periods (1800 seconds) in 0.17 seconds.

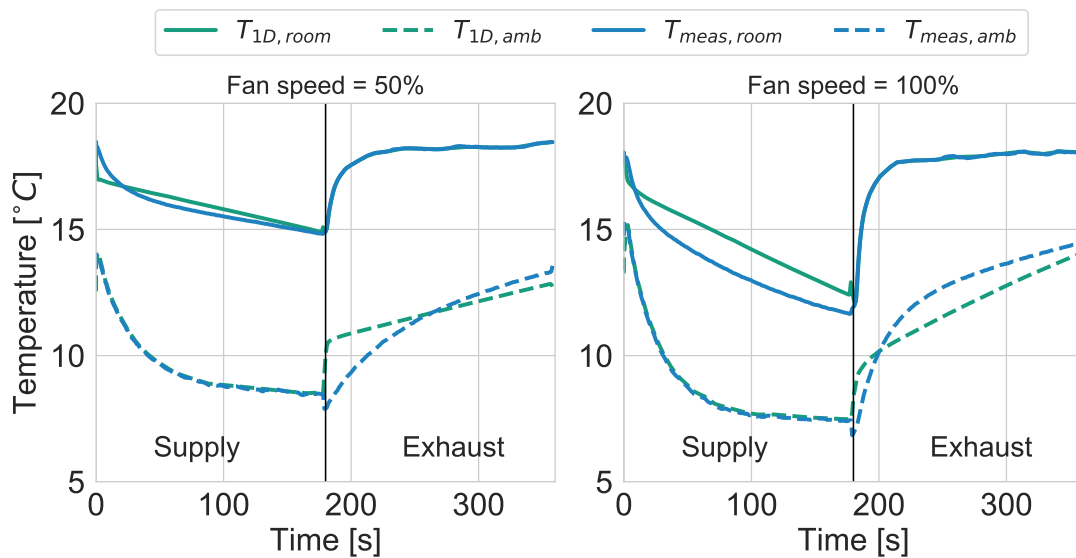


Figure A.19: Supply and exhaust temperatures for a 180 second period. Measured and simulated profiles are compared [35].

Period	60 s		180 s	
	RMSE [°C]	MAPE [%]	RMSE [°C]	MAPE [%]
50% Speed	0.57	2.26	0.31	1.61
100% Speed	1.06	6.91	1.05	7.64

Table A.7: RMSE and MAPE concerning the average supply air temperature.

To estimate the energy consumption due to ventilation in Chapter 5, an estimated heat recovery efficiency as a function of the ventilation volume flow is simulated. A curve is then fitted using an exponential approximation. The curve is illustrated in Figure A.20.

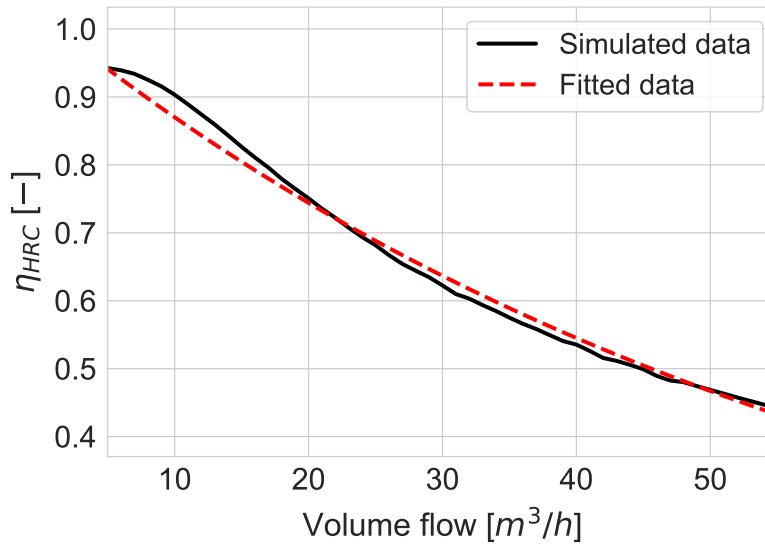


Figure A.20: Approximation of the heat recovery efficiency as a function of the ventilation volume flow.

Regarding the fan model, the data reported in the literature [57] is followed. Three ventilation levels (associated with three different fan speeds) are given, and the volume flow of the system was measured while varying the pressure difference on both sides of the fan (Figure A.21). The curves in Figure 4.9 are a result of the linear relationship between fan speed and volume flow, shown in Equation A.15. Together with the curve, the fan is assumed to have a rising time (time to reach 99.6% of speed) of 25 seconds. The applied fan model is available in the Buildings library [223].

$$\frac{n_{fan}}{n_{fan,nom}} = \frac{\dot{V}_{fan}}{\dot{V}_{fan,nom}} \quad (\text{A.15})$$

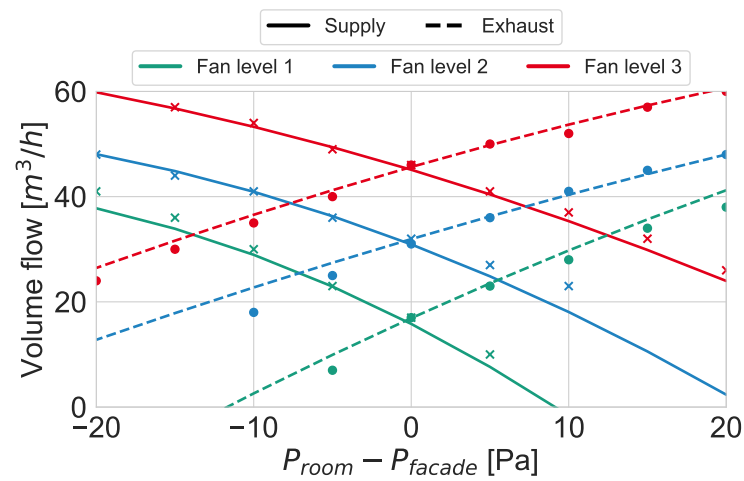


Figure A.21: Supply and exhaust volume flow given the fan speed and pressure difference between room and façade. Circle points are measured supply airflow rates and crosses are measured exhaust airflow rates [57].

A.4 Market research

29 scientific publications related to innovative ventilation control strategies in the last twenty years were reviewed. The search was extended to other HVAC systems as well where the airflow rate is controlled, to obtain a better overview of the latest developments applicable to ventilation systems. Table A.8 summarizes the key properties of every paper.

- VS = ventilation system (CVS = centralized, DVS = decentralized)
- SCVS-IF = semicentralized ventilation system with individual fans.
- CAV = constant air volume, VAV = variable air volume.
- MPC = model predictive control.
- MDP = Markov decision process.

VS	Control			Inputs			Outputs	
	Ref.	Scheme	Algorithm	Indoor	Outdoor	System	Ventilation	Others
	[12]	DCV	-	T, RH, Presence	-	Power	Volume flow	Supply air T
	[14]	Robust control	-	-	-	Supply and exhaust air T	Volume flow, damper	Supply air T, power
	[42]	PID	Artificial neural networks	T, RH, CO_2	-	-	Fan speed, damper	Supply air T
	[90]	Set point; State feedback; MPC	-	T, RH, Presence	T, RH	Volume flow	Volume flow, damper	Supply air T
Centralized HVAC	[122]	Comfort range optimization	-	T, RH, CO_2	-	Light	Volume flow	Power, humidifier
	[128]	On-off; PID; State-feedback	Genetic algorithm	T, RH, CO_2 , Presence	-	-	Fan speed	-
	[129]	State-feedback	-	CO_2 , Presence	-	-	Volume flow	-
	[131]	Decentralized control	Markov decision process	T, RH, CO_2 , Presence	-	Volume flow, light	Fan speed	Power, lighting
	[134]	DCV	-	CO_2	CO_2	-	Volume flow	-
	[135]	DCV	Load shifting	T, Presence	T	Volume flow	Volume flow	On-off
	[137]	PI	Artificial neural networks	T, PMV	-	-	Volume flow	Power
	[155]	Fuzzy	-	T, RH, CO_2	T	-	Volume flow	Power, window opening, lights

Continued on next page

Table A.8 – continued from previous page

VS	Control			Inputs			Outputs	
	Ref.	Scheme	Algorithm	Indoor	Outdoor	System	Vent.	Others
Centralized HVAC	[157]	DCV	-	Emission rate, Presence	-	-	Volume flow	-
	[158]	Set point	Genetic algorithm	T, RH, CO_2	-	Volume flow	Volume flow	Supply air T
	[159]	Robust control	-	CO_2	-	-	Volume flow	-
	[165]	DCV	-	T	-	-	Volume flow	T set point
	[171]	DCV	-	RH, CO_2	-	-	Volume flow	-
	[189]	PI-based DCV	-	CO_2	-	-	Dampers	-
	[230]	MPC	-	T, thermal vote	-	-	Fan speed	-
CVS	[47]	Dynamic control	Load shifting	Presence	-	-	Fan speed	-
	[133]	DCV	-	RH, CO_2	-	-	Volume flow	-
	[196]	DCV	Load shifting	CO_2	-	Volume flow	Volume flow	On-off
DVS	[23]	CAV	-	-	Wind speed	-	Fan speed	-
	[22]	PID	-	P	Wind speed	-	Fan speed	-
	[108]	PI	-	T, RH, CO_2 , VOC	-	T set point	Fan speed	Power

Continued on next page

Table A.8 – continued from previous page

VS	Ref.	Control		Inputs			Outputs	
		Scheme	Algorithm	Indoor	Outdoor	System	Vent.	Others
DVS	[197]	DCV	-	RH	-	-	Volume flow	-
SCVS-IF	[124]	Set point	-	CO_2	-	-	Fan speed	-
CVS; DVS; SCVS-IF	[150]	DCV	-	CO_2 , VOC	-	-	Fan speed	-
Extract	[177]	Fuzzy	-	VOC, Benzene	-	-	Fan speed	-

Table A.8: Summary of scientific literature review.

A.5 Support vector machines

Support vector machines (SVM) is one of the most popular supervised learning algorithm, developed by Vapnik [211]. This classification algorithm is already extensively used in different disciplines, such as text categorization [116], heart disease diagnosis [101], building energy consumption [234], wind speed forecasting [138], or thermal comfort prediction [78]. In this section, the algorithm and its capabilities are briefly introduced, following the explanation of Burges [30] and Vanderplas [210].

Let x_i, y_i be the training data, $x_i \in R^d$. d is the dimension of the training data and $i = 1, \dots, n$ are the number training of data points. For the sake of simplicity, the training points are bidimensional ($d = 2$). The classification has only two possible outcomes and, therefore $y_i \in -1, 1$. The data is linearly separable, as illustrated in Figure A.22.

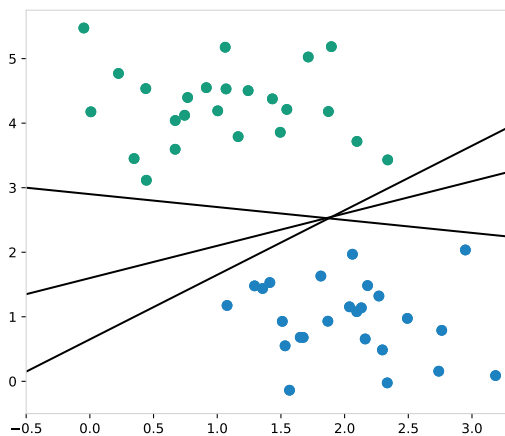


Figure A.22: Linearly separable data.

Suppose the data can be linearly separated by a hyperplane, having on each side the positive and negative (green and blue) classifications of the training data. The vector w_v , perpendicular to the hyperplane, and the constant b are defined, such as the points x on the hyperplane satisfy $w_v^T x + b = 0$. There are infinite hyperplanes that can be defined under this condition. The “margin” is defined as the distance between the hyperplane and the closest point of each side. The SVM method looks to obtain the optimal hyperplane by maximizing the margin. For the points that lie on the positive and negative margin, the following constraint applies:

$$y_i \cdot (w_v^T \cdot x_i + b) - 1 = 0 \quad (\text{A.16})$$

$\frac{|b|}{\|w_v\|}$ is the minimum distance from the hyperplane to the origin. Since both margins are taken into account, the algorithm pursues the maximization of the margin, which is defined as $\frac{2}{\|w_v\|}$. Therefore, the following optimization applies:

$$\min \frac{1}{2} \|w_v\|^2 \tag{A.17}$$

$$\text{subject to } y_i \cdot (w_v^T \cdot x_i + b) - 1 \geq 0 \tag{A.18}$$

The expected solution is illustrated in Figure A.23. The points that lie on both margins are the calculated limits of the solution, and their presence affects directly the obtained hyperplane. These are called the support vectors. In his publication, Burges [30] explains in full detail the development of the mathematics of the method.

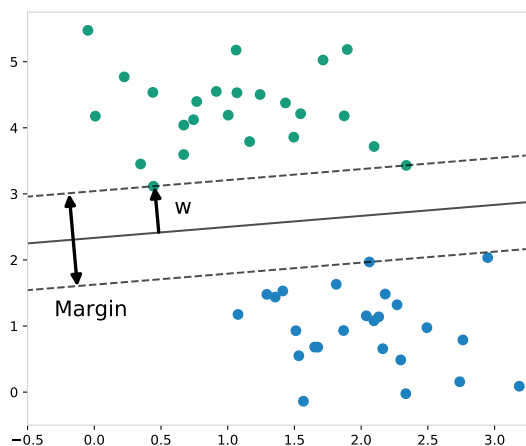


Figure A.23: Classification after maximization of margin.

Yet in most cases, the data cannot be linearly separated. In that sense, the target function requires a certain cost coefficient C together with the creation of slack variables ξ_i , which helps to relax the constraints but only up to a certain point. The larger the parameter C becomes, the higher the penalty associated with the committed errors. Figure A.24 illustrates an example with two different values of this coefficient. Equation A.17 becomes Equation A.19 for the optimization process. $\frac{-\xi_i}{\|w_v\|}$ becomes the minimum distance between the point i and the obtained hyperplane.

$$\min \frac{1}{2} \|w_v\|^2 + C \sum_i \xi_i \tag{A.19}$$

$$\text{subject to } y_i \cdot (w_v^T \cdot x_i + b) \geq 1 - \xi_i, \xi_i \geq 0 \tag{A.20}$$

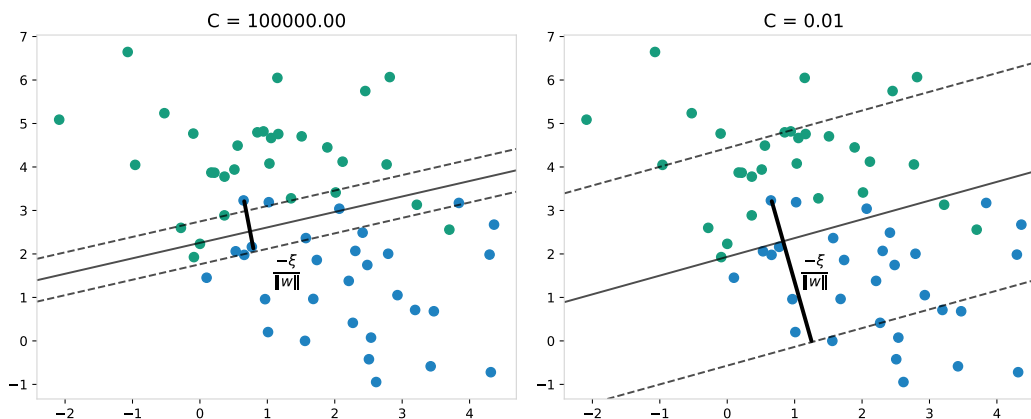


Figure A.24: Algorithm sensitivity to the cost coefficient C .

In some other cases, the points can show a clear pattern, which can only be poorly separated by a linear hyperplane. Figure A.25 shows an example of this case.

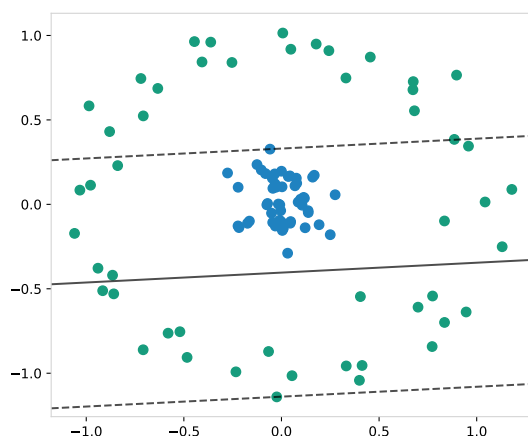


Figure A.25: Non-linearly separable data.

According to Burges [30], the procedure is to apply a kernel function to transform data into a linearly separable case. One of the most popular solutions in combination with SVM classification algorithms is the gaussian radial basis function (RBF) kernel. The Equation A.21 shows the transformation of the data, depending on the parameter γ , which is called the Kernel coefficient. This coefficient must be positive and can be defined by the user, to determine the degree of the transformation.

$$k_{RBF}(x_i, x_j) = \exp(-\gamma \|x_i - x_j\|^2) \quad (\text{A.21})$$

Figure A.26 shows a 3D plot of the transformation of the data after applying RBF

and the results of the classification algorithm over the transformed data. The effect of the kernel shows that the new classification results much more accurate than the previous one.

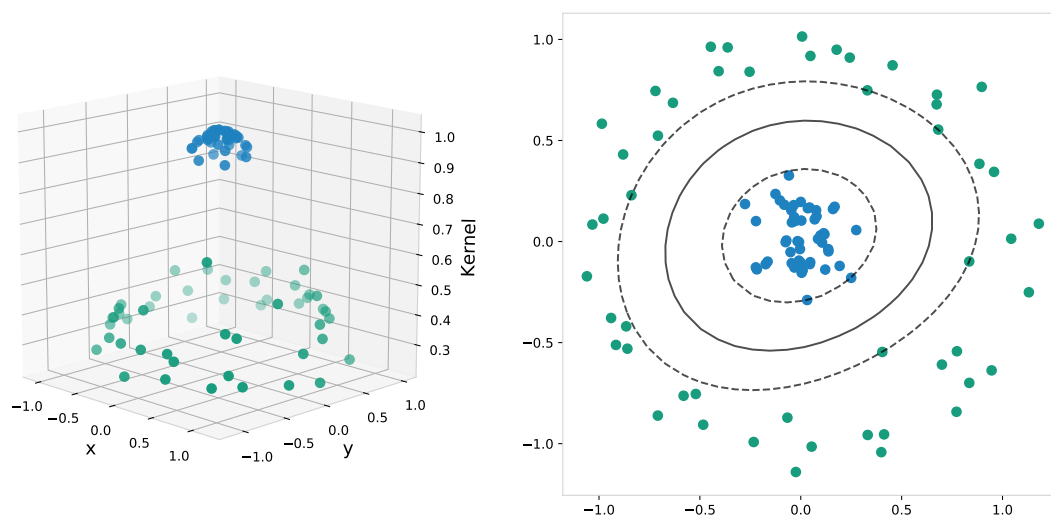


Figure A.26: Data classification after RBF kernel.

In this study, the employed SVM method was taken from the LibSVM library [41], which includes all the parameters already described. The library expands this classification method to multiclass labels using the “one-against-one” method by Knerr et al. [123]. This strategy consists of constructing one SVM learning procedure per class. Each one is trained to classify the samples of one class against all remaining classes together. The probability of being classified as a certain class is calculated following the description of Platt [178], who fits a sigmoid function into the class-conditional probability density and calculated the associated probability using Bayes’ rule.

The coefficients C and γ were tuned using a grid search cross-validation process [172]. The results obtained were $C = 1000$ and $\gamma = 1$, which are used for the user preferences learning process.

A.6 Learned user artificial comfort profiles

The following plots illustrate the progression of the learned control fields for the four artificial user comfort profiles.

Distracted user

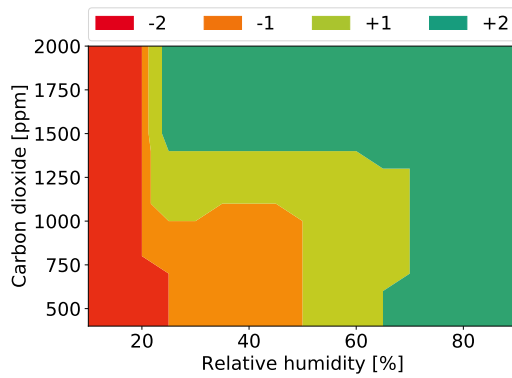


Figure A.27: Learned profile for the "distracted" user after 10 votes.

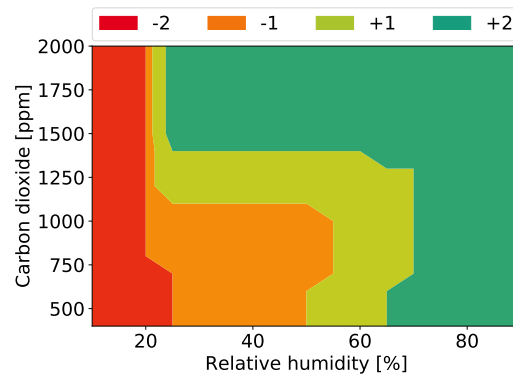


Figure A.28: Learned profile for the "distracted" user after 30 votes.

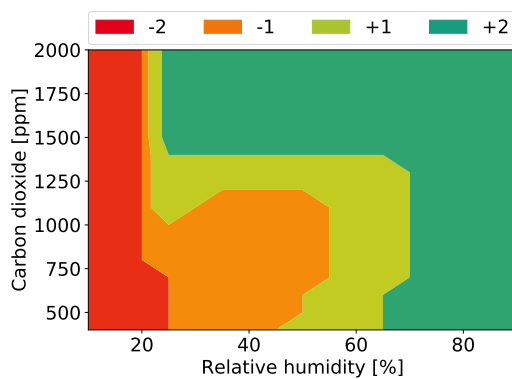


Figure A.29: Learned profile for the "distracted" user after 50 votes.

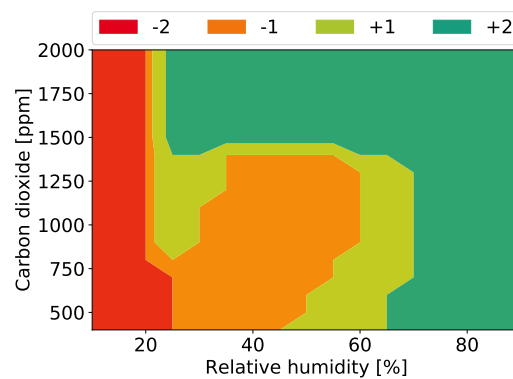


Figure A.30: Learned profile for the "distracted" user after 100 votes.

Less air user

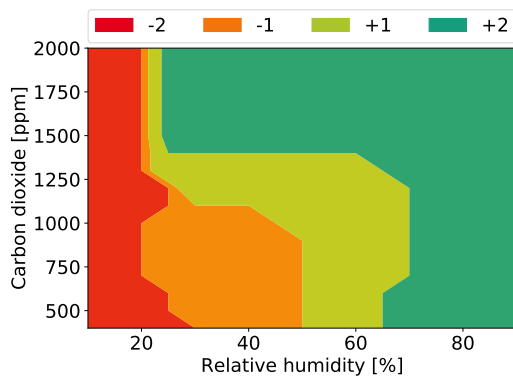


Figure A.31: Learned profile for the "less air" user after 10 votes.

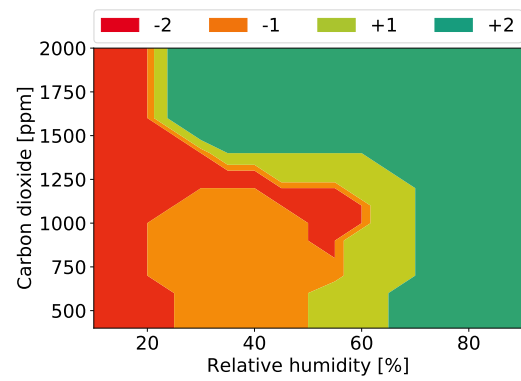


Figure A.32: Learned profile for the "less air" user after 30 votes.

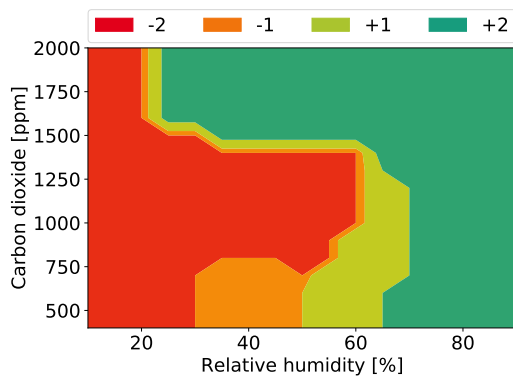


Figure A.33: Learned profile for the "less air" user after 50 votes.

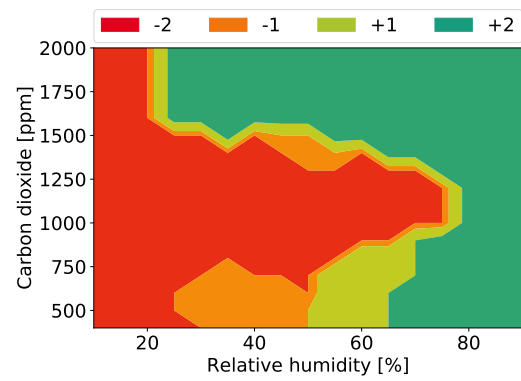


Figure A.34: Learned profile for the "less air" user after 100 votes.

More air user

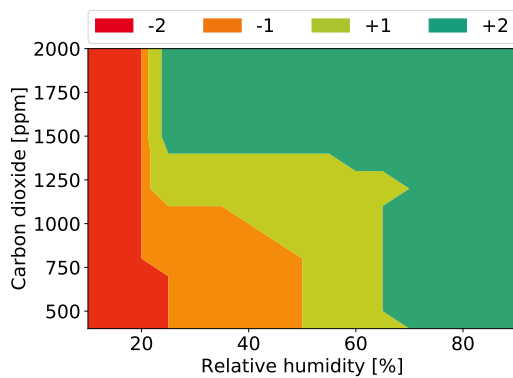


Figure A.35: Learned profile for the "more air" user after 10 votes.

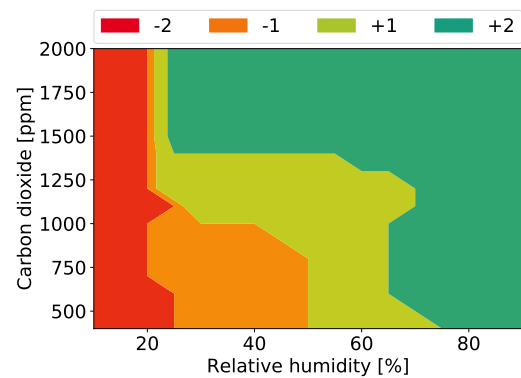


Figure A.36: Learned profile for the "more air" user after 30 votes.

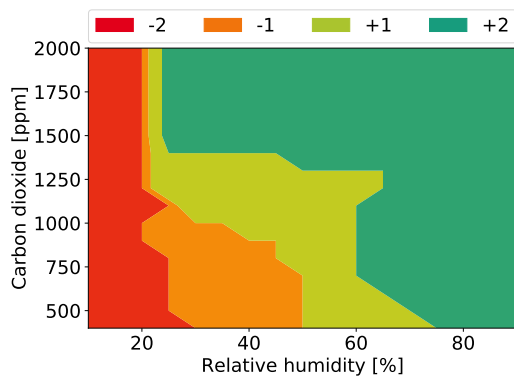


Figure A.37: Learned profile for the "more air" user after 50 votes.

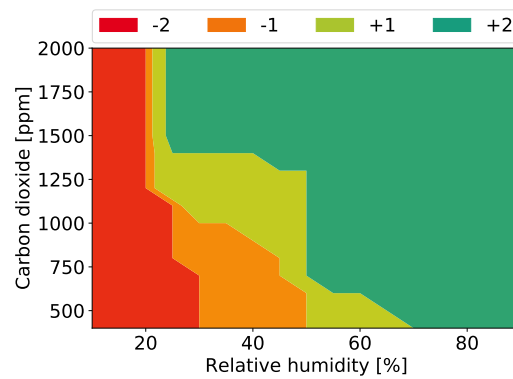


Figure A.38: Learned profile for the "more air" user after 100 votes.

Norm user

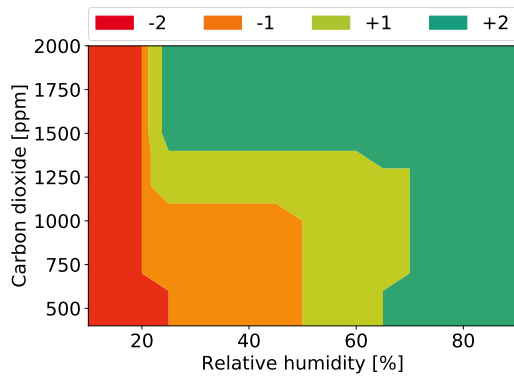


Figure A.39: Learned profile for the "norm user" after 10 votes.

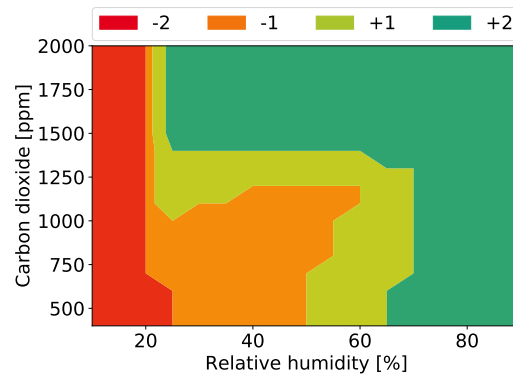


Figure A.40: Learned profile for the "norm user" after 30 votes.

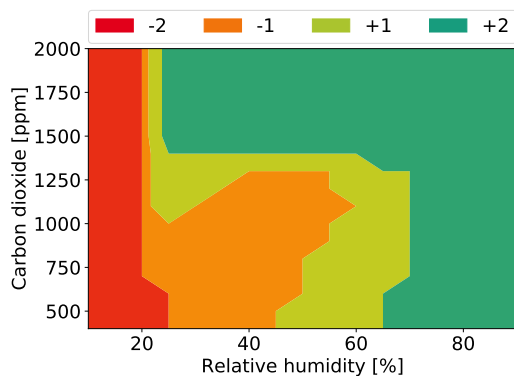


Figure A.41: Learned profile for the "norm user" after 50 votes.

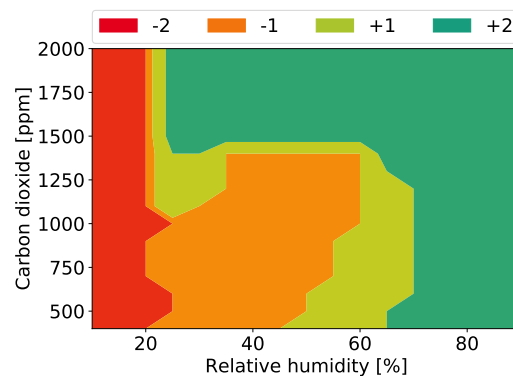


Figure A.42: Learned profile for the "norm user" after 100 votes.

Random user

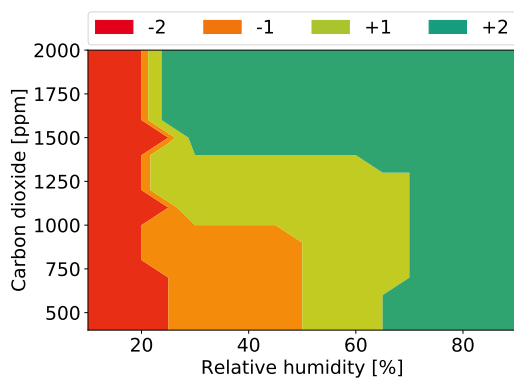


Figure A.43: Learned profile for the "random user" after 10 votes.

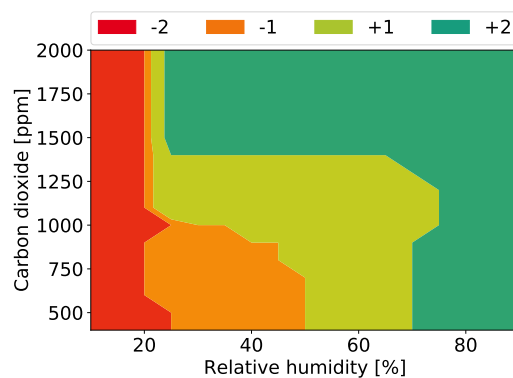


Figure A.44: Learned profile for the "random user" after 30 votes.

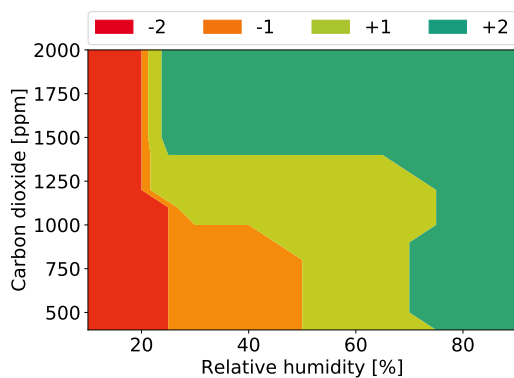


Figure A.45: Learned profile for the "random user" after 50 votes.

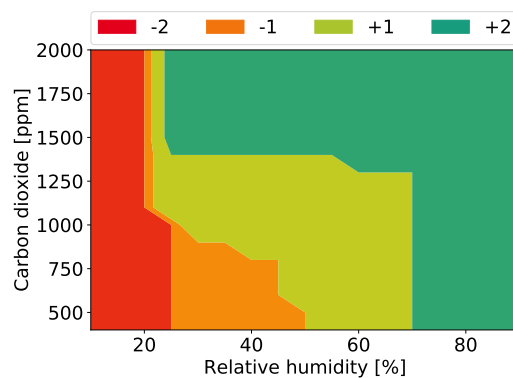


Figure A.46: Learned profile for the "random user" after 100 votes.

A.7 Room-individual results in the ESHL

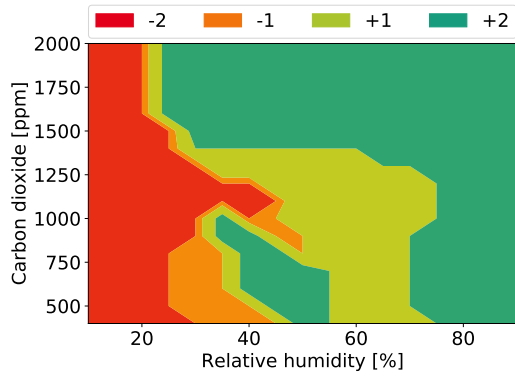


Figure A.47: Living room learned control field.

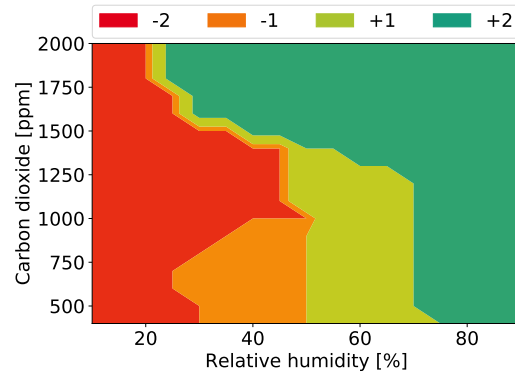


Figure A.48: Bedroom 2 learned control field.

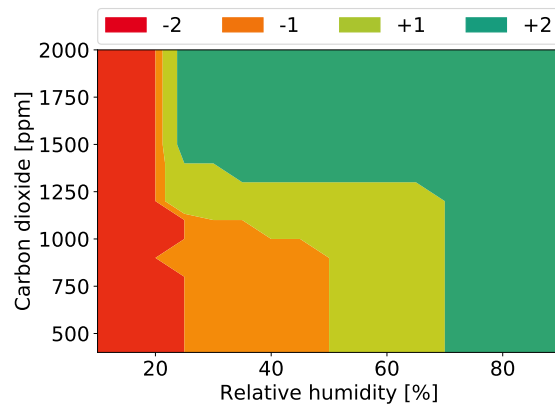


Figure A.49: Bathroom learned control field.

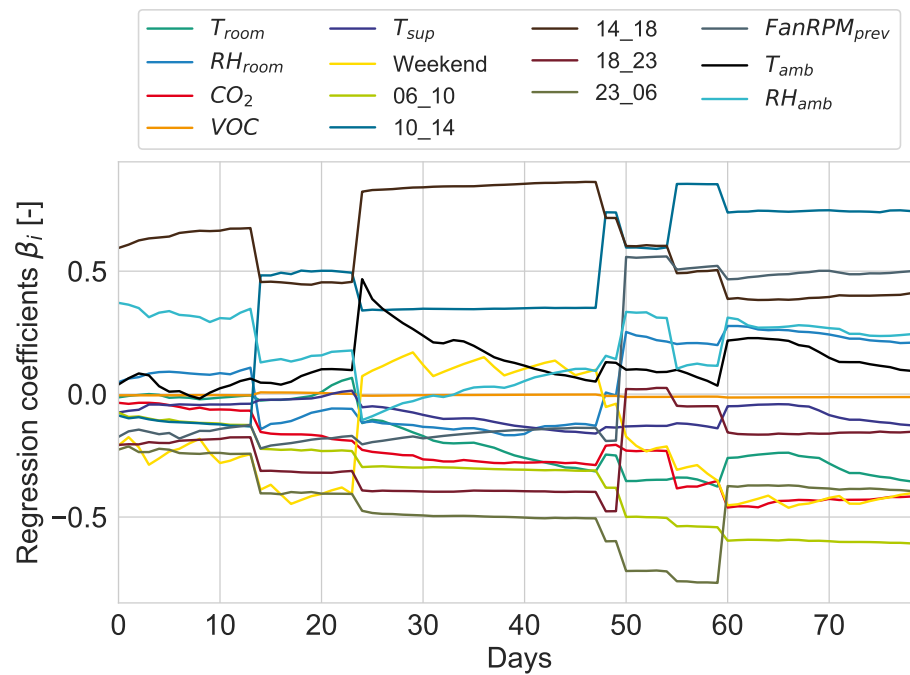


Figure A.50: Real-time evolution of the logistic regression coefficients for increasing fan level in bedroom 1.

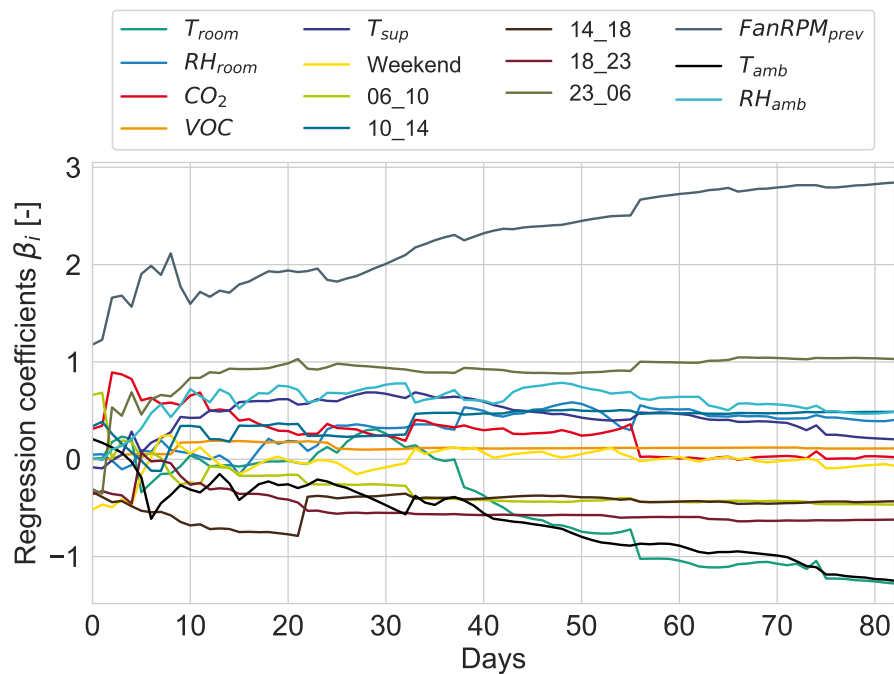


Figure A.51: Real-time evolution of the logistic regression coefficients for decreasing fan level in bedroom 1.

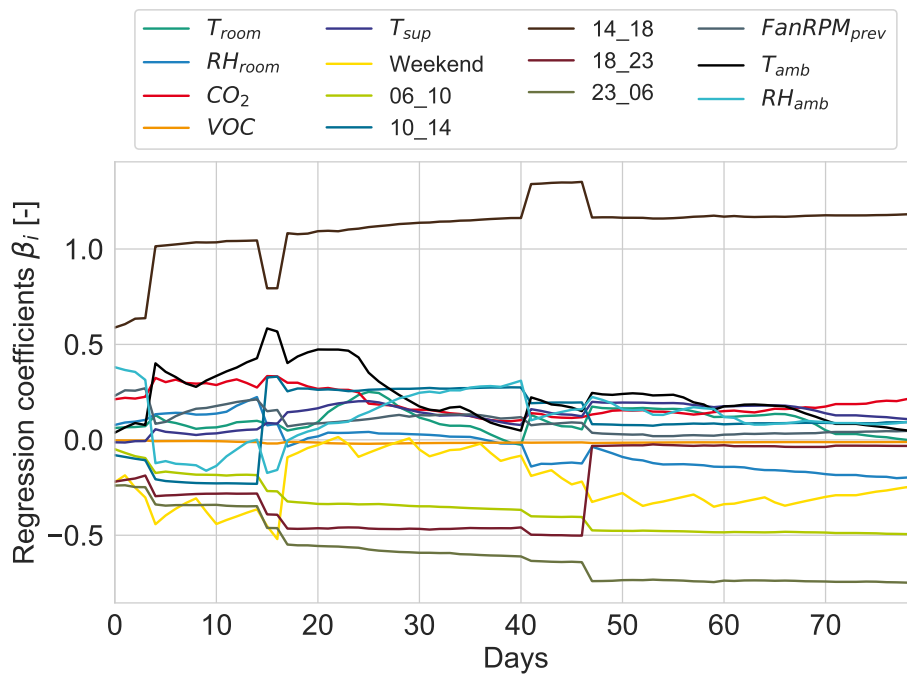


Figure A.52: Real-time evolution of the logistic regression coefficients for increasing fan level in bedroom 2.

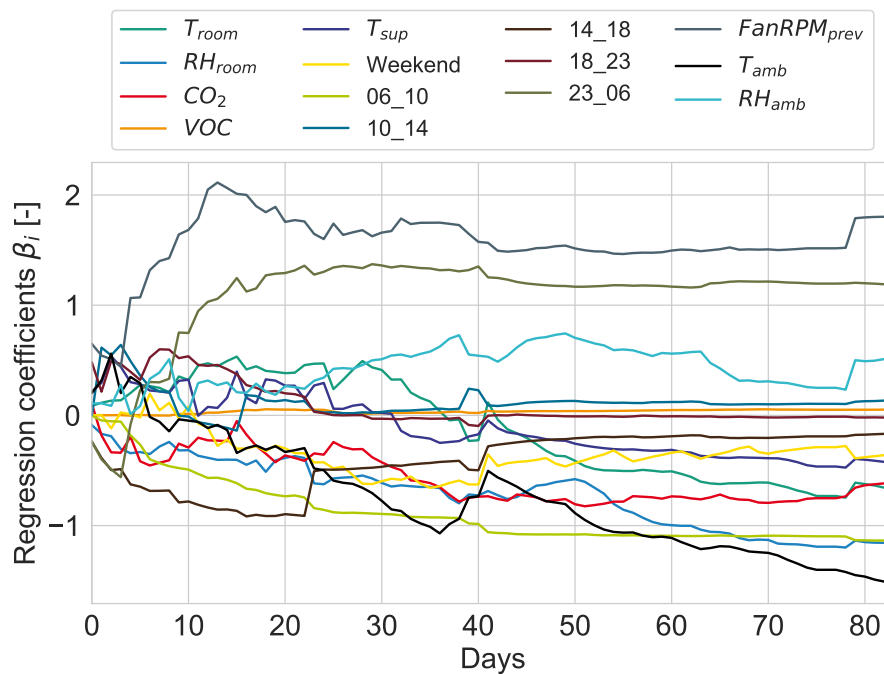


Figure A.53: Real-time evolution of the logistic regression coefficients for decreasing fan level in bedroom 2.

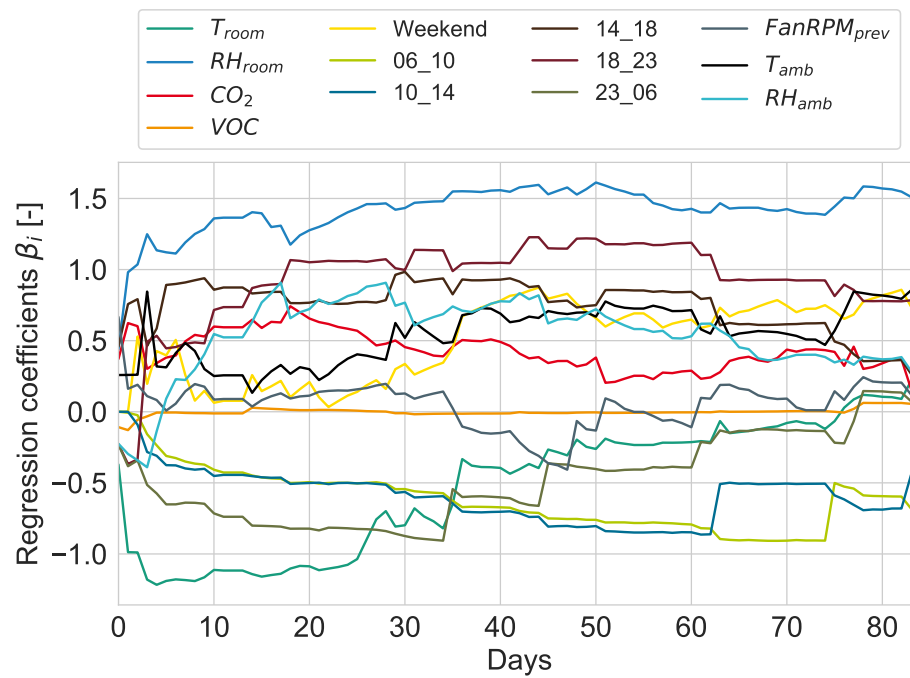


Figure A.54: Real-time evolution of the logistic regression coefficients for increasing fan level in the kitchen.

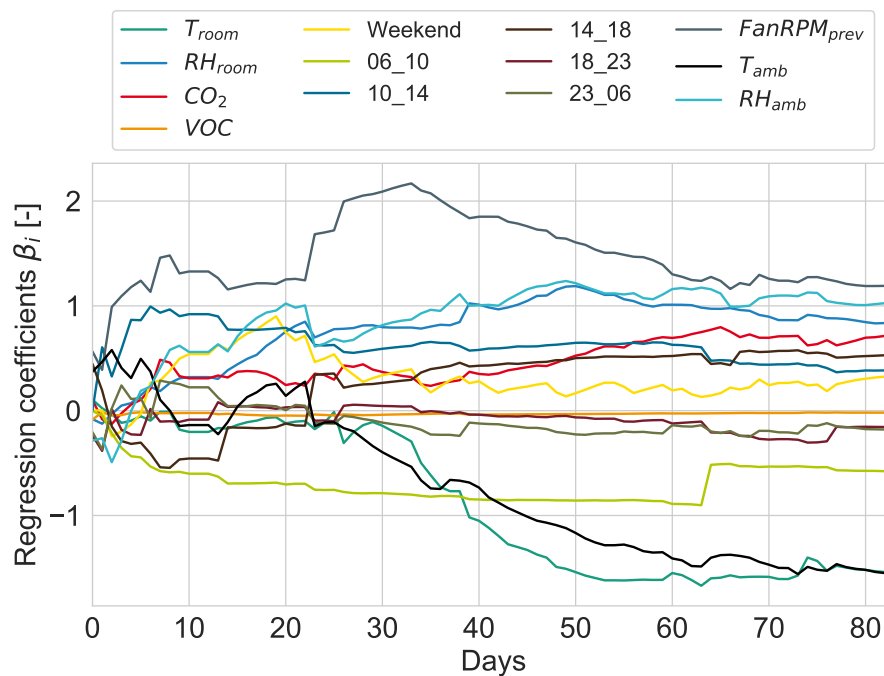


Figure A.55: Real-time evolution of the logistic regression coefficients for decreasing fan level in the kitchen.

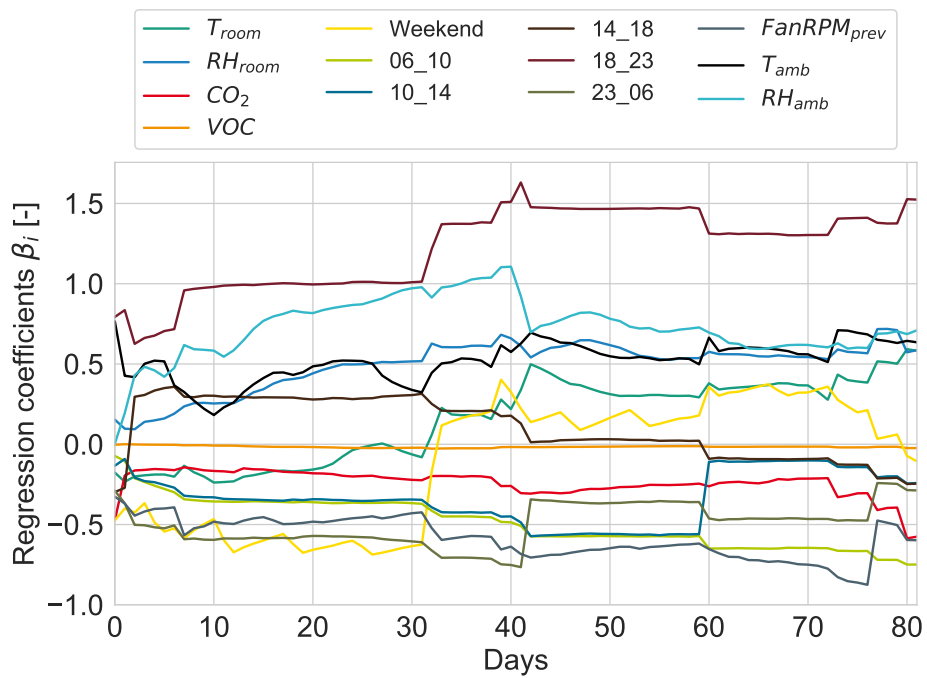


Figure A.56: Real-time evolution of the logistic regression coefficients for increasing fan level in the living room.

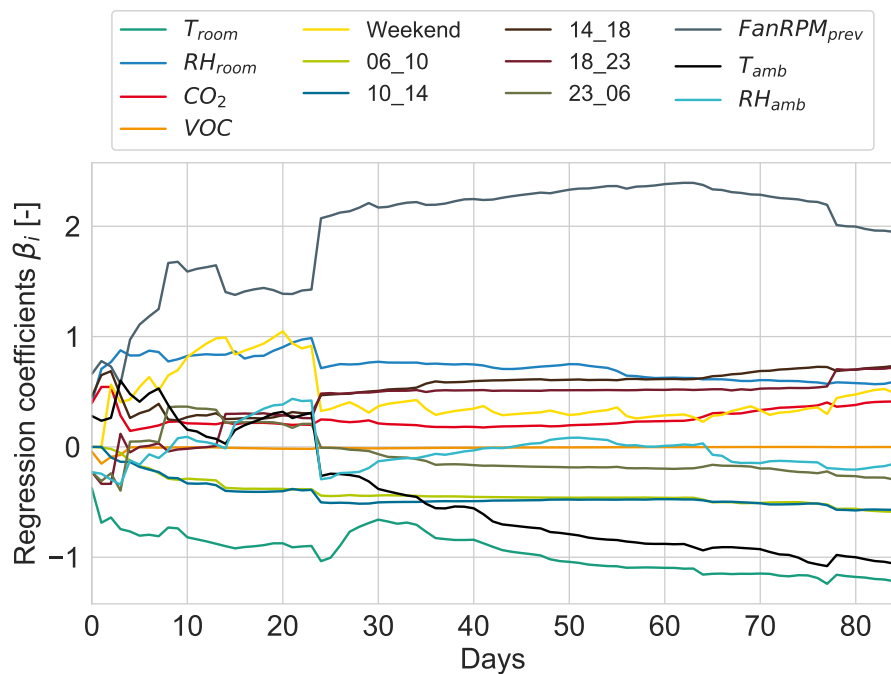


Figure A.57: Real-time evolution of the logistic regression coefficients for decreasing fan level in the living room.

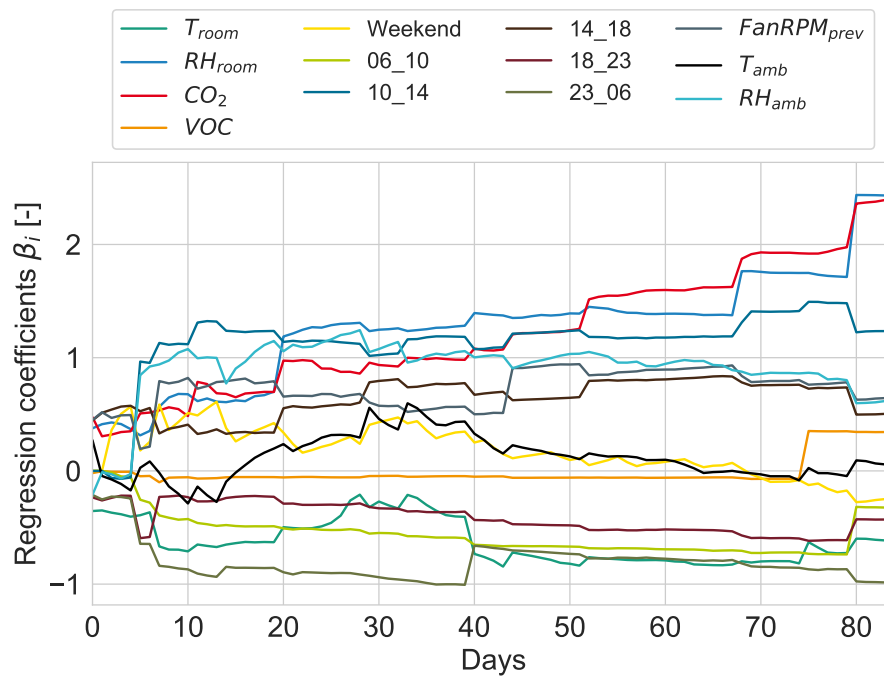


Figure A.58: Real-time evolution of the logistic regression coefficients for increasing fan level in the bathroom.

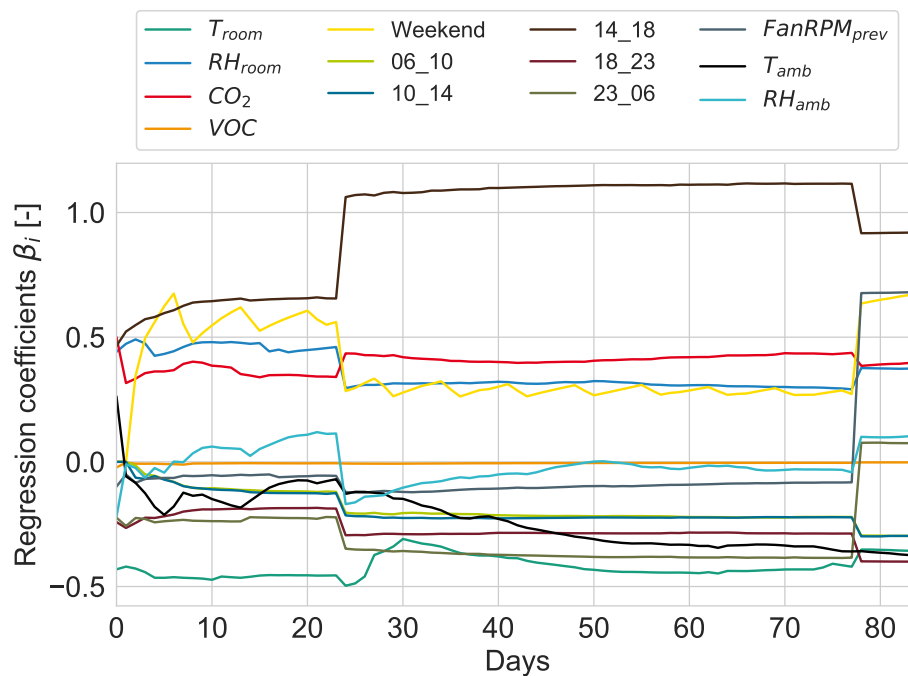


Figure A.59: Real-time evolution of the logistic regression coefficients for decreasing fan level in the bathroom.

Nomenclature

Latin letters

Variable	Unit	Definition
A_{dw}	m^2	Dwelling area
A_{ht}	m^2	Heat transfer area
AH_{amb}	g/kg	Ambient absolute humidity
b	-	Constant of vector $w_v x + b$ (SVM)
C	-	Cost coefficient (SVM)
C_{solid}	kJ/kg	Heat capacity of a solid
C_d	-	Discharge coefficient
C_p	-	Wind pressure coefficient
c_i	-	Cluster centroid
CO_2	ppm	Carbon dioxide concentration
$cost_{el}$	EUR/kWh	Electric costs
$cost_{heat}$	EUR/kWh	Heating costs
$cost_{op}$	EUR/kWh	Operative costs
d_{cyl}	m	Heat storage cylinder diameter
D_{CO_2}	-	Discomfort with CO_2
D_{RH}	-	Discomfort with relative humidity
$D(RH, CO_2)$	-	Discomfort cost function
$d(x, y)$	-	Euclidean distance between x and y
d_h	m	Hydraulic diameter
d_{eq}	m	Equivalent diameter
$E_{el, fan}$	kWh, el	Fan electrical energy consumption
e_z	-	Building placement coefficient
$f_{Hi/Hs}$	$\frac{kWh, gas, Hi}{kWh, gas, Hs}$	Inferior-superior energy factor
$f_{p, heat}$	$\frac{kWh, pe}{kWh, gas, Hi}$	Heating primary energy factor
$f_{p, elec}$	$\frac{kWh, pe}{kWh, el}$	Electricity primary energy factor
F_{LSt}	-	Ventilation level coefficient
G	-	Natural logarithm of the building width and length ratio
h_{air}	$W/K m^2$	Air specific convection coefficient

Ind_{opt}	-	Optimization indicator
k	$\frac{dm^3}{s \cdot m^2 \cdot Pa^n}$	Flow coefficient
k_{air}	$W/K \ m$	Air thermal conductivity
k_{solid}	$W/K \ m$	Heat storage thermal conductivity
k_{RBF}	-	Radial basis kernel function (SVM)
l_{chan}	m	Heat storage channel length
L_{ht}	m	Heat transfer length
m	-	Mass flow exponent
m_{cyl}	kg	Heat storage mass
Nu	-	Nusselt number
n_{50}	h^{-1}	air exchange rate at 50 Pa pressure difference
n_c	-	Number of clusters
n_{chan}	-	Honeycomb number of channels
OdR	-	Odds ratio
p	-	Associated probability
PD	%	Percentage dissatisfied
p_{comf}	-	Comfort probability
P_{heat}	W	Heating power
P_{fan}	W	Fan electric power
$P_{fan,nom}$	W	Nominal fan electric power
Pr	-	Prandtl number
$Q_{pe,vent}$	kWh, pe	Primary energy consumption due to ventilation
$Q_{heat,vent}$	$kWh, heat$	Heating energy losses due to ventilation
\dot{Q}_{heat}	W	Instantaneous heat flow rate of the heating system
\dot{Q}_{HRC}	W	Heat flux recovered
\dot{Q}_{sup}	W	Heat transfer rate in the supply phase of the DVS
\dot{Q}_{vent}	W	Heat transfer rate due to ventilation
Q_{HRC}	$kWh, heat$	Heat energy recovered
Q_{sup}	$kWh, heat$	Heat recovered in the supply phase of the DVS
Re	-	Reynolds number
RH / RH_{room}	%	Room relative humidity
RH_{amb}	%	Ambient relative humidity

NOMENCLATURE

t	s	Time
T_{amb}	$^{\circ}C$	Ambient temperature
T_{room}	$^{\circ}C$	Room temperature
T_{solid}	$^{\circ}C$	Solid temperature
T_{sup}	$^{\circ}C$	Supply temperature
t_{wall}	m	Regenerator wall thickness
\dot{V}_{air}	m^3/h	Volume flow in the DVS
\dot{V}_{fan}	m^3/h	Fan volume flow
$\dot{V}_{fan,nom}$	m^3/h	Nominal fan volume flow
$\dot{V}_{in,f}$	m^3/h	Volume flow due to infiltration
\dot{V}_{MV}	m^3/h	Volume flow due to mechanical ventilation
\dot{V}_{ref}	m^3/h	Reference volume flow
\dot{V}_{tot}	m^3/h	Volume flow total
\dot{V}_{WO}	m^3/h	Volume flow due to window opening
V_{room}	m^3	Room volume
V_{Dw}	m^3	Dwelling volume
v_{air}	m/s	Channel air velocity
w_{chan}	m	Heat storage channel width
w_v	-	Direction of vector $w_v x + b$ (SVM)

Greek letters

Variable	Unit	Definition
$\alpha_{i,j}$	-	Membership degree (Fuzzy logic)
β_i	-	Logistic regression coefficients
ΔCO_2	ppm	Carbon dioxide indicator
ΔP_{ref}	Pa	Reference pressure difference
ΔRH_{lower}	%	Lower relative humidity indicator
ΔRH_{up}	%	Upper relative humidity indicator
$\eta_{heat,boil}$	$\frac{kWh, heat}{kWh, gas, Hs}$	Boiler combustion efficiency
η_{HRC}	-	Heat recovery efficiency
η_{vent}	-	Ventilation effectiveness
γ	-	Kernel coefficient (SVM)
μ	-	Mean
μ_R	-	Rule degree levels (Fuzzy logic)
$\mu_{o,R}$	-	Fuzzy output for each rule (Fuzzy logic)
μ_o	-	Aggregated fuzzy output (Fuzzy logic)

ρ_{air}	kg/m^3	Air density
ρ_{solid}	kg/m^3	Solid density
σ	-	Standard deviation
θ	rad	Wind angle
ξ_i	-	Slack variables (SVM)

Acronyms

Acc	Accuracy
ACH	Air changes per hour
ACS	Average state changes
AIVC	Air, Infiltration and Ventilation Centre
AFN	Airflow network
ARBA	Automatic room balancing algorithm
ASHRAE	American Society of Heating, Refrigerating and Air-conditioning Engineers
CCV	Constant controlled ventilation
CFD	Computational fluid dynamics
CO_2	Carbon dioxide concentration
DCV	Demand controlled ventilation
DI	Dunn index
DIN	Deutsches Institut für Normung (German Institute for Standards)
DNS	Day-night score
DT	Decision tree classifie
DVS	Decentralized ventilation systems
ELA	Effective leakage area
EPBD	Energy performance of buildings directive
ESHL	Energy smart home lab
FMI	Functional mock-up interface
FMU	Functional mock-up unit
FN	False negatives
FP	False positives
GPC	Gaussian process classifier
HCS	Hour change score
HMI	Human-machine-interface
HMM	Hidden Markov model

HRC	Heat recovery systems
HVAC	Heat, ventilation and air conditioning
IAQ	Indoor air quality
IEQ	Indoor environmental quality
IoT	Internet of Things
LogR	Logistic regression classifier
LR	Learning rate
MAPE	Mean absolute percentage error
MFB	Multifamily building
MV	Mechanical ventilation
NB	Gaussian naïve bayes classifier
OB	Occupant behavior
Occ	Occupancy
PD	Percentage dissatisfied
PHI	Passive House Institute
PPV	Positive predictive value
RBF	Radial basis function
RF	Random forests classifier
RMSE	Root mean squared error
RH	Relative humidity
SBS	Sick building syndrome
SEC	Specific energy consumption
SFP	Specific fan power
SS	Seasonal score
SVM	Support vector machines classifier
TN	True negatives
TP	True positives
TPR	True positive rate
VOC	Volatile organic compounds
WkS	Weekend Score
WO	Window opening

List of Figures

1.1	Evolution of energy losses in residential buildings [102].	1
1.2	Evolution of residential ventilation market (2012-2018) in Germany [110].	3
1.3	Exploded axonometric of a DVS [216]. 1 - Indoor panel. 2 - Reversible fan. 3 - Heat storage system. 4 - Outdoor panel.	3
1.4	Flowchart of the thesis structure.	8
2.1	Overview of requirements for ventilation control systems.	9
2.2	Relative humidity and health effects - adapted from [19, F. 1].	16
2.3	Comparison of available dissatisfaction models due to CO_2 concentration.	21
2.4	Upper limit relative humidity and discomfort - adapted from [204].	23
3.1	Schematic flow diagram of research method in this chapter.	31
3.2	Dependence of the different window opening models on the ambient temperature at three different indoor room temperature levels.	35
3.3	Dependence of the different window opening models on the CO_2 concentration at three different indoor room temperature levels.	36
3.4	Schematic floor plan in apartment 1. Blue rooms are provided with supply air, and red rooms with exhaust air.	39
3.5	Schematic floor plan in apartment 2. Blue rooms are provided with supply air, and red rooms with exhaust air.	39
3.6	Window contact placement.	39
3.7	IAQ sensor placement.	39
3.8	Daily mean observed window opening (proportion of windows open) profiles for the 27 apartments.	41
3.9	Features point representation of the 27 apartments.	41
3.10	Dunn index - Intercluster (two different cluster points x and y) and intracluster (two points in the same group x_1 and x_2) comparison.	43
3.11	Percentage of variance explained with increasing number of clusters. Comparison between features (Mean and Hour-change score) and whole time series clustering procedure.	45
3.12	Cluster structure for training data set of observed proportion of windows open with features extraction. Dashed lines represent the daily mean profile of every cluster.	45

3.13	Cluster structure for test data set of observed proportion of windows open with features extraction and classification. Dashed lines represent the daily mean profile of every cluster.	47
3.14	Cluster structure for training data set of observed proportion of windows open with whole time series. Dashed lines represent the daily mean profile of every cluster.	48
3.15	Cluster structure for the daily average observed proportion of windows open in the living rooms in the second measurement campaign. The selected apartments are highlighted.	49
3.16	Measured daily mean indoor conditions in the living room for the two selected apartments.	50
3.17	Window opening model and measurements comparison for the selected apartments. The opening probability $P_{opening}$ is used for the black lines, and the proportion of windows open (in %) for the colored lines.	50
3.18	Schematic flow diagram of research method in this section.	52
3.19	Daily average window opening and opening action profile for the Apartments 1, 2, and 3, respectively.	54
3.20	Real-time evolution of the logistic regression coefficients in Apartment 1. Complete figure in Appendix A.1.	54
3.21	Real-time evolution of the logistic regression coefficients in Apartment 3. Complete figure in Appendix A.1	55
3.22	Sample day for real-time window opening detection algorithm, using the first order differences (FOD) of the CO_2 concentration as an input variable to detect the opening.	58
3.23	Real-time window opening detection results in the selected apartments and comparison with the measured window opening and opening action profile.	60
3.24	Real-time evolution of the logistic regression coefficients with measured window opening in Apartment 1. Complete figure in Appendix A.1.	61
3.25	Real-time evolution of the logistic regression coefficients with estimated window opening in Apartment 1. Complete figure in Appendix A.1.	61
3.26	Real-time evolution of the logistic regression coefficients with measured window opening in Apartment 3. Complete figure in Appendix A.1	61

3.27	Real-time evolution of the logistic regression coefficients with estimated window opening in Apartment 3. Complete figure in Appendix A.1	61
4.1	Working principle of a typical hysteresis cycle of a DCV in decentralized ventilation systems.	66
4.2	Proportion of publications that consider each input variable for different ventilation systems. The variable "Ambient" summarizes different outdoor environmental variables.	67
4.3	Number of publications reviewed for each controller type and ventilation system. Two publications review more than one system.	68
4.4	Baseline ventilation control strategy - "Steps".	69
4.5	Co-simulation scheme developed for control algorithm testing.	71
4.6	Floor plan of the simulated apartment.	72
4.7	Airflow network model of the dwelling. The circles represent the nodes (room volumes or outdoor nodes) and the resistances (airflow paths) represent the air exchange between nodes.	73
4.8	Decentralized ventilation system model in Modelica. The model includes pressure drop components, fan model and heat storage model. The details of this model are available in the Appendix A.3.	75
4.9	Supply and exhaust volume flow given the fan speed and pressure difference between room and façade.	75
4.10	Interpolation of the fan power as a function of the fan speed. Measurements are indicated with crosses.	76
4.11	Occupancy daily profile.	77
4.12	Heat loads daily profile.	77
4.13	Moisture loads daily profile.	78
4.14	CO_2 loads daily profile.	78
4.15	RH and CO_2 artificial comfort profiles given the probability distributions in Table 4.4.	81
4.16	Flow chart of the proposed model to simulate the interaction between user and mechanical ventilation system, given the comfort profile.	83
4.17	RH and CO_2 profile to test the proposed user interaction model.	84
4.18	Simulated user votes given the interaction frequency (left) and RH and CO_2 comfort profile (right).	84
4.19	Percentage dissatisfied (PD) functions for relative humidity (left) and carbon dioxide concentration (right). Comparison of the proposed cost function and the reviewed models in Chapter 2.	86

4.20	Cost function DCV strategies for RH (left) and CO_2 (right).	87
4.21	Fuzzy controller workflow.	88
4.22	Membership functions for the fuzzy controller. RH and CO_2 are the input variables x_i and the fan speed is the output variable y_o .	90
4.23	Fan speed control field resulting of the fuzzy control strategy.	91
4.24	RH ventilation preference votes for the default comfort profile.	93
4.25	CO_2 ventilation preference votes for the default comfort profile.	93
4.26	Resulting 3D field for the default comfort profile.	93
4.27	Evolution of the combined learning rate using SVM.	96
4.28	Workflow of the self-learning controller.	97
4.29	Default control field of the self-learning controller. The colored areas represent the prediction of the user vote.	99
4.30	Ambient conditions (left: ambient temperature, right: wind speed) in the selected weeks of the winter season for the sensitivity analysis.	101
4.31	Total air exchange rate in a single day for the four controllers.	102
4.32	RH and CO_2 cumulative distribution plots in selected rooms.	103
4.33	Primary energy savings of the proposed ventilation controllers. Constant airflow strategy is taken as baseline case.	105
4.34	Discomfort values due to RH and CO_2 in every room in a single day of the average week.	107
4.35	Sensitivity of the primary energy savings of the fuzzy controller against the steps controller for different simulated conditions.	108
4.36	Ambient conditions in the selected months for the simulation of the self-learning control strategy.	112
4.37	Total air exchange rate in a single day, after 75 days of learning.	113
4.38	RH and CO_2 cumulative distribution plots in relevant rooms for the different simulated control strategies.	114
4.39	Primary energy savings of the proposed controllers. Constant airflow strategy is taken as baseline case.	115
4.40	Total air exchange rate in a single day with whole-dwelling learning algorithm, after 75 days of learning.	116
4.41	CO_2 cumulative distribution plots in selected rooms with centralized learning scheme for the different user comfort profiles.	117
4.42	Primary energy consumption due to ventilation for the selected user profiles. "Norm" user is taken as baseline case.	118
4.43	Learned profile for the "distracted" user with whole-dwelling learning approach.	119

4.44	Learned profile for the "less air" user with whole-dwelling learning approach.	119
4.45	Learned profile for the "more air" user with whole-dwelling learning approach.	119
4.46	Learned profile for the "norm" user with whole-dwelling learning approach.	119
4.47	Percentage of time outside the RH comfort range.	120
4.48	Percentage of time outside the CO_2 comfort range.	120
4.49	Total air exchange rate in a single day with whole-dwelling learning, after 75 days of learning.	122
4.50	Learned control field for the active user with whole-dwelling learning.	123
4.51	Learned control field for the medium user with whole-dwelling learning.	123
4.52	Learned control field for the passive user with whole-dwelling learning.	123
4.53	Learned control field for the single-room scheme in the bedroom. . . .	125
4.54	Learned control field for the single-room scheme in the bathroom. . .	125
4.55	Learned control field for the whole-dwelling scheme.	126
4.56	Learned 3D comfort profile for the whole-dwelling scheme.	126
5.1	Living room area.	130
5.2	Bedroom 1.	130
5.3	Kitchen area.	131
5.4	Outdoor view.	131
5.5	Floor plan of the Energy Smart Home Lab. The placement of the DVS, user interfaces and central controller is indicated.	133
5.6	Flow diagram of the implemented controller.	134
5.7	IoT Scheme for the learning controller implementation.	136
5.8	Developed board for the learning controller implementation.	136
5.9	Operable user interface - decreasing level color (blue).	138
5.10	Operable user interface - increasing level color (red).	138
5.11	Daily mean ambient conditions during the measurement period. . . .	139
5.12	Indoor room temperature boxplot.	140
5.13	Indoor relative humidity boxplot.	140
5.14	Indoor CO_2 concentration boxplot.	140
5.15	Indoor VOC concentration boxplot.	140
5.16	Cumulative distribution of RH and CO_2 concentration in every room.	141
5.17	Total daily mean theoretical air exchange rate profile in the measurement period.	142
5.18	Fan level frequency in every room in the measurement period. . . .	143

5.19	User votes dispersion as a function of RH and CO_2 in the bedroom 1.	145
5.20	User votes dispersion as a function of RH and CO_2 in the kitchen area.	145
5.21	Starting control profile.	145
5.22	Bedroom 1 control field after learning.	146
5.23	Kitchen control field after learning.	146
5.24	Whole dwelling potential control field after learning.	146
5.25	Fan level frequencies in the first month.	147
5.26	Fan level frequencies in the last month.	147
5.27	RH , CO_2 and fan speed daily profile for the bedroom 1.	147
5.28	RH , CO_2 and fan speed daily profile for the kitchen.	148
5.29	Evolution of logistic regression coefficients for decreasing fan level in bedroom 1.	152
5.30	Evolution of logistic regression coefficients for increasing fan level in bedroom 1.	152
5.31	Evolution of logistic regression coefficients for decreasing fan level in the kitchen.	152
5.32	Evolution of logistic regression coefficients for increasing fan level in the kitchen.	152

List of Tables

2.1	Assumed primary energy factors and heating system efficiency values.	14
2.2	Air quality categories from DIN EN 16798-1 [60, p. 51, T. B.2.1.4-2].	19
2.3	Categories for air humidification and dehumidification, according to DIN EN 16798-1 [60, p. 52, T. B.2.2-1].	25
2.4	Class limits for residential HVAC systems' noise [181].	26
3.1	Logistic regression coefficients of window opening for each explanatory variable in three available models from the literature in winter (Solar rad. = solar radiation, n.a. = not available). *Room CO_2 concentration (Andersen et al. [13] in $[\log(ppm)]$ and Cali et al. [32] in $[ppm^{-1}]$).	34
3.2	Advantages and drawbacks of the evaluated window opening models (MV = mechanical ventilation. BPS = building performance simulation).	37
3.3	Sensors' properties for the second measurement campaign.	38
3.4	Definition of potential occupant-related features [96].	41
3.5	Feature combinations with the highest Dunn index.	44
3.6	Explanatory variables (input parameters) for the real-time logistic regression.	53
3.7	Window opening (WO) real-time detection results in the three selected apartments.	59
4.1	Simulated thermal properties of the dwelling.	72
4.2	Summary of the simulated internal loads.	77
4.3	Selected room temperature setpoints, in $^{\circ}C$ [58].	79
4.4	Definition of the artificial user comfort profiles. Mean (μ) and standard deviation (σ) characterize the probability distribution for each user type.	80
4.5	Measured interaction frequencies with mechanical ventilation [183].	82
4.6	Fuzzy rules for every fan output (FS = Fan speed).	89
4.7	Selection of DCV algorithm: comparison of performance indicators for every classification algorithm.	94
4.8	Selection of DCV algorithm: Combined learning rate results for every tested classification algorithm for the learning DCV controller.	95
4.9	Mean values of the weather conditions (ambient temperature, relative humidity, absolute humidity and wind speed - WS) in the selected weeks for the sensitivity analysis.	101
4.10	Summary of performance indicators for the simulated control strategies.	104

4.11	Summary of performance indicators in the different simulated weeks for the weather sensitivity. In addition, average fan speed ($FanRPM_{av}$) and total mechanical air exchange rate (ACH_{mech}) are considered. . .	106
4.12	Summary of performance indicators in the different simulated weeks for the internal loads sensitivity. In addition, average fan speed ($FanRPM_{av}$) and total mechanical air exchange rate (ACH_{mech}) are considered.	108
4.13	Summary of performance indicators for every simulated controller. . .	113
4.14	Number of votes per room and user comfort profile, with medium interaction frequency.	116
4.15	Performance indicators for the learning DCV strategy with all user comfort profiles and a whole-dwelling learning process.	117
4.16	30% PD threshold values for the artificial user comfort profiles. . . .	120
4.17	Number of votes per room and user interaction frequency for the "more air" comfort profile.	121
4.18	Summary of performance indicators for the learning DCV strategy with every user interaction frequency profile.	124
4.19	Number of votes per room and type for a mixed comfort profile. . . .	124
4.20	Performance indicators for the mixed comfort profile using single-room and whole-dwelling learning schemes.	125
5.1	Ventilation levels (in $\frac{m^3}{h}$) defined according to the system dimensioning procedure in DIN 1946-6 [58].*The bedrooms had additional 5% speed in level 2 and 3 to compensate the pressure losses of the extra sensors installed.	132
5.2	Sensor properties for the monitoring concept.*Additional sensors for the bedrooms.**Accuracy not reported.	137
5.3	Performance indicators in every room for the measurement period in the ESHL.	141
5.4	Number of votes per room and month in the measurement period. . .	144
5.5	Number of votes per room and type in the measurement period. . . .	144
5.6	Advantages and disadvantages of decentralized ventilation, as a result of the field implementation.	148
5.7	Average system failure time during the experiment.	149
5.8	Logistic regression coefficients for increasing mechanical ventilation volume flow in every room (n.a. = not available, * = p-value<0.05). .	150
5.9	Logistic regression coefficients for decreasing mechanical ventilation volume flow in every room (n.a. = not available, * = p-value<0.05). .	151

References

- [1] ABADIE, M., AND WARGOCKI, P. Indoor air quality design and control in low-energy residential buildings-Annex 68: Subtask 1: Defining the metrics: AIVC contributed report 17, 2017.
- [2] AGHABOZORGI, S., YING WAH, T., HERAWAN, T., JALAB, H. A., SHAYGAN, M. A., AND JALALI, A. A hybrid algorithm for clustering of time series data based on affinity search technique. *The Scientific World Journal* (2014), 562194.
- [3] AHLAWAT, A., WIEDENSOHLER, A., AND MISHRA, S. K. An overview on the role of relative humidity in airborne transmission of sars-cov-2 in indoor environments. *Aerosol and air quality research* 20, 9 (2020), 1856–1861.
- [4] AHMED, K., KURNITSKI, J., AND OLESEN, B. Data for occupancy internal heat gain calculation in main building categories. *Data in Brief* 15 (2017), 1030–1034.
- [5] AIR INFILTRATION AND VENTILATION CENTER. IEA EBC annex 86 on 'Energy efficient smart IAQ management for residential buildings' approved, 02.07.2020.
- [6] AIR, INFILTRATION AND VENTILATION CENTRE. Technical note AIVC 68: Residential ventilation and health, 2016.
- [7] ALSÉN, N. *Energetische und wirtschaftliche Bewertung von dezentralen Ventilatoren in zentralen Lüftungsanlagen*. PhD Thesis, Universität Kassel, Kassel, Germany, 2017.
- [8] ALZADE, A. *Balancing and Controlling Methods for Decentralized Ventilation Systems in Residential Buildings*. Master thesis, Universität Freiburg, Freiburg im Breisgau, Germany, 2020.
- [9] AMERICAN SOCIETY OF HEATING AND AIR-CONDITIONING ENGINEERS. ASHRAE Standard 62.1-2013: Ventilation for acceptable indoor air quality, 2013.
- [10] AMERICAN SOCIETY OF HEATING AND AIR-CONDITIONING ENGINEERS, Ed. *ASHRAE Fundamentals: (SI Edition)*. 2017.

- [11] AMERICAN SOCIETY OF HEATING AND AIR-CONDITIONING ENGINEERS. ASHRAE Standard 55-2017: Thermal environmental conditions for human occupancy, 2017.
- [12] ANAND, P., SEKCHAR, C., CHEONG, D., SANTAMOURIS, M., AND KONDEPUDI, S. Occupancy-based zone-level VAV system control implications on thermal comfort, ventilation, indoor air quality and building energy efficiency. *Energy and Buildings* 204 (2019), 109473.
- [13] ANDERSEN, R., FABI, V., TOFTUM, J., CORGNATI, S. P., AND OLESEN, B. W. Window opening behaviour modelled from measurements in danish dwellings. *Building and Environment* 69 (2013), 101–113.
- [14] ANDERSON, M., BUEHNER, M., YOUNG, P., HITTLE, D., ANDERSON, C., TU, J., AND HODGSON, D. MIMO robust control for HVAC systems. *IEEE Transactions on Control Systems Technology* 16, 3 (2008), 475–483.
- [15] ANDERSSON, C., AKESSON, J., AND FÜHRER, C. *PyFMI: A Python Package for Simulation of Coupled Dynamic Models with the Functional Mock-up Interface*, vol. LUTFNA-5008-2016 of *Technical Report in Mathematical Sciences*. Centre for Mathematical Sciences, Lund University, 2016.
- [16] ANGSTEN, R., AND HARTMANN, T. Raumweise Lüftungsgeräte in der Wohnungslüftung - pro und contra. *GI Wissenschaft* 3, 17 (2017), 210–215.
- [17] ARMSTRONG, J. S., AND COLLOPY, F. Error measures for generalizing about forecasting methods: empirical comparisons. *International Journal of Forecasting* 08 (1992), 69–80.
- [18] ARNESANO, M., BUENO, B., PRACUCCI, A., MAGNAGNI, S., CASADEI, O., AND REVEL, G. M. Sensors and control solutions for smart-IoT façade modules. *2019 IEEE International Symposium on Measurements & Networking (M&N)* (2019), 1–6.
- [19] ARUNDEL, A. V., STERLING, E. M., BIGGIN, J. H., AND STERLING, T. D. Indirect health effects of relative humidity in indoor environments. *Environmental health perspectives* 65 (1986), 351–361.
- [20] ASADOV, N. *Simulation and Measurement of Different Geometries and Materials for Heat Exchangers in Decentralized Regenerative Ventilation Devices*.

-
- Master thesis, Fraunhofer ISE and Universität Freiburg, Freiburg im Breisgau, Germany, 2019.
- [21] AWBI, H. B. Air movement in naturally-ventilated buildings. *Renewable Energy* 8, 1-4 (1996), 241–247.
- [22] BALDINI, L., GOFFIN, P., AND LEIBUNDGUT, H. Control strategies for effective use of wind loading through a decentralized ventilation system. *Roomvent 2011* (2011).
- [23] BALDINI, L., MEGGERS, F., AND LEIBUNDGUT, H. Advanced decentralized ventilation: How wind pressure can be used to improve system performance and energy efficiency. *PLEA 2008* (2008).
- [24] BERGLUND, L. G. Comfort and humidity. *ASHRAE Transactions* 40, 8 (1998).
- [25] BOERSTRA, A., BALVERS, J., BOGERS, R., JONGENEEL, R., AND VAN DIJKEN, F. Residential ventilation system performance: outcomes of a field study in the netherlands. *33rd AIVC Conference* (2012).
- [26] BOSER, B., GUYON, I., AND VAPNIK, V. A training algorithm for optimal margin classifiers. *COLT '92: Proceedings of the 5th annual workshop on Computational learning theory*, 144–152 (1992).
- [27] BOYER, H., LAURET, A. P., ADELARD, L., AND MARA, T. A. Building ventilation: a pressure airflow model computer generation and elements of validation. *Energy and Buildings* 29 (1999), 283–292.
- [28] BRAKEL, J.-P. Smoothed z-score algorithm, 2016.
- [29] BUNDESRAT DEUTSCHLAND. Energieeinsparverordnung: EnEV, 2016.
- [30] BURGESS, C. J. A tutorial on support vector machines for pattern recognition. *Data Mining and Knowledge Discovery* 2 (1998), 121–167.
- [31] CALÌ, D. *Occupants' behavior and its impact upon the energy performance of buildings*. PhD thesis, RWTH Aachen University, Aachen, Germany, 2016.
- [32] CALÌ, D., ANDERSEN, R. K., MÜLLER, D., AND OLESEN, B. W. Analysis of occupants' behavior related to the use of windows in german households. *Building and Environment* 103 (2016), 54–69.

- [33] CALÌ, D., WESSELING, M. T., AND MÜLLER, D. WinProGen: A markov-chain-based stochastic window status profile generator for the simulation of realistic energy performance in buildings. *Building and Environment* 136 (2018), 240–258.
- [34] CARBONARE, N., COYDON, F., DINKEL, A., AND BONGS, C. The influence of occupancy behaviour on the performance of mechanical ventilation systems regarding energy consumption and IAQ. *Proceedings of 38th AIVC Conference* (2017).
- [35] CARBONARE, N., FUGMANN, H., ASADOV, N., PFLUG, T., BONGS, C., AND SCHNABEL, L. Simulation and measurement of energetic performance in decentralized regenerative ventilation systems. *Energies* 13, 22 (2020), 6010.
- [36] CARBONARE, N., PFLUG, T., BONGS, C., AND WAGNER, A. Comfort-oriented control strategies for decentralized ventilation using co-simulation. *IOP Conf. Series: Materials Science and Engineering* 609, 032018 (2019), 1–6.
- [37] CARBONARE, N., PFLUG, T., BONGS, C., AND WAGNER, A. Simulative study of a novel fuzzy demand controlled ventilation for façade-integrated decentralized systems. *Science and Technology for the Built Environment* 26 (2020), 1412–1426.
- [38] CARBONARE, N., PFLUG, T., AND WAGNER, A. Clustering the occupant behavior in residential buildings: A method comparison. *Bauphysik* 40, 6 (2018), 427–433.
- [39] CARREIRA, P., COSTA, A. A., MANSUR, V., AND ARSÉNIO, A. Can HVAC really learn from users? a simulation-based study on the effectiveness of voting for comfort and energy use optimization. *Sustainable Cities and Society* 41 (2018), 275–285.
- [40] CARRER, P., WARGOCKI, P., FANETTI, A., BISCHOF, W., DE OLIVEIRA FERNANDES, E., HARTMANN, T., KEPHALOPOULOS, S., PALKONEN, S., AND SEPPÄNEN, O. What does the scientific literature tell us about the ventilation–health relationship in public and residential buildings? *Building and Environment* 94 (2015), 273–286.
- [41] CHANG, C.-C., AND LIN, C.-J. LIBSVM: A library for support vector machines. *National Taiwan University, Taipei, Taiwan* (2001), 1–39.

-
- [42] CHAO, C. Y., AND HU, J. S. Development of an enthalpy and carbon dioxide based demand control ventilation for indoor air quality and energy saving with neural network control. *Indoor and Built Environment* 13, 6 (2004), 463–475.
- [43] CHENARI, B., DIAS CARRILHO, J., AND GAMEIRO DA SILVA, M. Towards sustainable, energy-efficient and healthy ventilation strategies in buildings: A review. *Renewable and Sustainable Energy Reviews* 59 (2016), 1426–1447.
- [44] CHENG, Z., ZHAO, Q., WANG, F., JIANG, Y., XIA, L., AND DING, J. Satisfaction based Q-learning for integrated lighting and blind control. *Energy and Buildings* 127 (2016), 43–55.
- [45] CHIANG, T., MEVLEVIOLU, G., NATARAJAN, S., PADGET, J., AND WALKER, I. Inducing [sub]conscious energy behaviour through visually displayed energy information: A case study in university accommodation. *Energy and Buildings* 70 (2014), 507–515.
- [46] CHIESA, G., CESARI, S., GARCIA, M., ISSA, M., AND LI, S. Multisensor IoT platform for optimising iaq levels in buildings through a smart ventilation system. *Sustainability* 11, 20 (2019), 5777.
- [47] CLARK, J. D., LESS, B. D., DUTTON, S. M., WALKER, I. S., AND SHERMAN, M. H. Efficacy of occupancy-based smart ventilation control strategies in energy-efficient homes in the united states. *Building and Environment* 156 (2019), 253–267.
- [48] COMMISSION OF THE EUROPEAN COMMUNITIES. Guidelines for ventilation requirements in buildings: Report no. 11, 1992.
- [49] COYDON, F. *Holistic evaluation of conventional and innovative ventilation systems for the energy retrofit of residential buildings*. Phd thesis, Karlsruhe Institute for Technology, Karlsruhe, Germany, 2015.
- [50] CRAWLEY, D. B., LAWRIE, L. K., WINKELMANN, F. C., BUHL, W. F., HUANG, Y., PEDERSEN, C. O., STRAND, R. K., LIESEN, R. J., FISHER, D. E., WITTE, M. J., AND GLAZER, J. EnergyPlus: Creating a new-generation building energy simulation program. *Energy and Buildings* 33, 4 (2001), 319–331.
- [51] DAI, X., LIU, J., AND ZHANG, X. A review of studies applying machine learning models to predict occupancy and window-opening behaviours in smart buildings. *Energy and Buildings* 223 (2020), 110159.

- [52] DAUM, D., HALDI, F., AND MOREL, N. A personalized measure of thermal comfort for building controls. *Building and Environment* 46, 1 (2011), 3–11.
- [53] DE GIDS, W. F., AND WOUTERS, P. CO₂ as indicator for the indoor air quality - general principles. *AIVC Information Paper 33* (2010), 1–4.
- [54] DE SUTTER, R., POLLET, I., VENS, A., LOSFELD, F., AND LAVERGE, J. TVOC concentrations measured in belgium dwellings and their potential for DCV control. *Proceedings of 38th AIVC Conference* (2017), 889–896.
- [55] DER SPIEGEL. Zuviel Zugluft in Passivhäusern rechtfertigt Mietminderung. *Spiegel Online* (23.04.2018).
- [56] DEUTSCHER WETTERDIENST. CDC Opendata, 2020.
- [57] DEUTSCHES INSTITUT FÜR BAUTECHNIK. Zulassungsbericht Z-51.3-415: Dezentrales Wohnungslueftungsgeraet mit Waermerueckgewinnung vom Typ Vitovent 100-D.
- [58] DEUTSCHES INSTITUT FÜR NORMUNG E.V. DIN 1946-6 - Raumluftechnik - Teil 6 - Lüftung von Wohnungen – Allgemeine Anforderungen, Anforderungen an die Auslegung, Ausführung, Inbetriebnahme und Übergabe sowie Instandhaltung, 2019.
- [59] DEUTSCHES INSTITUT FÜR NORMUNG E.V., AND EUROPEAN COMMITTEE FOR STANDARDIZATION. DIN EN 15251 - Eingangsparemeter für das Raumklima zur Auslegung und Bewertung der Energieeffizienz von Gebäuden – Raumlufqualität, Temperatur, Licht und Akustik, 2007.
- [60] DEUTSCHES INSTITUT FÜR NORMUNG E.V., AND EUROPEAN COMMITTEE FOR STANDARDIZATION. DIN EN 16798-1: Gesamtenergieeffizienz von Gebäuden – Teil 1: Eingangsparemeter für das Innenraumklima zur Auslegung und Bewertung der Energieeffizienz von Gebäuden bezüglich Raumlufqualität, Temperatur, Licht und Akustik, 2015.
- [61] DEUTSCHES INSTITUT FÜR NORMUNG E.V., EUROPEAN COMMITTEE FOR STANDARDIZATION, AND INTERNATIONAL ORGANIZATION FOR STANDARDIZATION. DIN EN ISO 7730 - Ergonomie der thermischen Umgebung – Analytische Bestimmung und Interpretation der thermischen Behaglichkeit durch Berechnung des PMV- und des PPD-Indexes und Kriterien der lokalen thermischen Behaglichkeit, 2006.

-
- [62] D'OCA, S., FABI, V., CORGNATI, S. P., AND ANDERSEN, R. K. Effect of thermostat and window opening occupant behavior models on energy use in homes. *Building Simulation* 7, 6 (2014), 683–694.
- [63] D'OCA, S., AND HONG, T. A data-mining approach to discover patterns of window opening and closing behavior in offices. *Building and Environment* 82 (2014), 726–739.
- [64] DOUNIS, A. I., SANTAMOURIS, M. J., LEFAS, C. C., AND ARGIRIOU, A. Design of a fuzzy set environment comfort system. *Energy and Buildings* 22 (1995), 81–87.
- [65] DUNKLIN, E. W., AND PUCK, T. T. The lethal effect of relative humidity on air-borne bacteria. *Journal of Experimental Medicine* 87, 2 (1948), 87–101.
- [66] DURIER, F., CARRIÉ, R., AND SHERMAN, M. What is smart ventilation? *AIVC VIP 38* (2018).
- [67] DUTTON, S. M., SHAO, L., AND RIFFAT, S. Validation and parametric analysis of EnergyPlus: Airflow network model using CONTAM. *Third National Conference of IBPSA-USA (SimBuild) 2008* (2008), 124–131.
- [68] EBERT, B. LowEx-Bestand Analyse Abschlussbericht zu AP 1.1: Systematische Analyse von Mehrfamilien-Bestandsgebäuden, 2018.
- [69] EFTEKHARI, M. M., AND MARJANOVIC, L. D. Application of fuzzy control in naturally ventilated buildings for summer conditions. *Energy and Buildings* 35, 7 (2003), 645–655.
- [70] ERDMANN, C. A., STEINER, K. C., AND APTE, M. G. Indoor carbon dioxide concentrations and sick building syndrome symptoms in the base study revisited: analyses of the 100 building dataset. *Proceedings of Indoor Air 2002* (2002).
- [71] EUROPEAN UNION COMMISSION. Commission delegated regulation (EU) 1254/2014; supplementing directive 2010/30/EU of the European Parliament and of the Council with regard to energy labelling of residential ventilation units, 2014.
- [72] EUROPEAN UNION COMMISSION. Comprehensive study of building energy renovation activities and the uptake of nearly zero-energy buildings in the EU, 2019.

- [73] EVOLA, G., GAGLIANO, A., MARLETTA, L., AND NOCERA, F. Controlled mechanical ventilation systems in residential buildings: Primary energy balances and financial issues. *Journal of Building Engineering* 11 (2017), 96–107.
- [74] EVOLA, G., MARLETTA, L., GAGLIANO, A., NOCERA, F., AND PECI, D. Energy balances and payback time for controlled mechanical ventilation in residential buildings. *International Journal of Heat and Technology* 34, S2 (2016), S315–S322.
- [75] FABI, V., ANDERSEN, R. V., CORGNATI, S. P., AND OLESEN, B. W. Occupants’ window opening behaviour: A literature review of factors influencing occupant behaviour and models. *Building and Environment* 58 (2012), 188–198.
- [76] FANGER, P. O. *Thermal comfort. Analysis and applications in environmental engineering*. Copenhagen: Danish Technical Press., 1970.
- [77] FANGER, P. O. Introduction of the olf and the decipol units to quantify air pollution perceived by humans indoors and outdoors. *Energy and Buildings* 12 (1988), 1–6.
- [78] FARHAN, A. A., PATTIPATI, K., WANG, B., AND LUH, P. Predicting individual thermal comfort using machine learning algorithms. *2015 IEEE International Conference on Automation Science and Engineering (CASE)* (2015), 708–713.
- [79] FIRLAG, S., AND ZAWADA, B. Impacts of airflows, internal heat and moisture gains on accuracy of modeling energy consumption and indoor parameters in passive building. *Energy and Buildings* 64 (2013), 372–383.
- [80] FISK, W. J., AND DE ALMEIDA, A. T. Sensor-based demand-controlled ventilation: a review. *Energy and Buildings* 29, 29 (1998), 35–45.
- [81] FISK, W. J., AND ROSENFELD, A. H. Estimates of improved productivity and health from better indoor environments. *Indoor Air* 7, 3 (1997), 158–172.
- [82] FÖLDVÁRY, V., BEKÖ, G., LANGER, S., ARRHENIUS, K., AND PETRÁŠ, D. Effect of energy renovation on indoor air quality in multifamily residential buildings in slovakia. *Building and Environment* 122 (2017), 363–372.

-
- [83] FRANCISCO, P. W., JACOBS, D. E., TARGOS, L., DIXON, S. L., BREYSSE, J., ROSE, W., AND CALI, S. Ventilation, indoor air quality, and health in homes undergoing weatherization. *Indoor Air* 27, 2 (2017), 463–477.
- [84] FRITSCH, R., KOHLER, A., NYGÅRD-FERGUSON, M., AND SCARTEZZINI, J.-L. A stochastic model of user behaviour regarding ventilation. *Building and Environment* 25, 2 (1990), 173–181.
- [85] FRITSCH, U. R., AND GRESS, H.-W. Der nichterneuerbare kumulierte Energieverbrauch und THG-Emissionen des deutschen Strommix im Jahr 2018 sowie Ausblicke auf 2020 bis 2050, 2019.
- [86] GAETANI, I., HOES, P.-J., AND HENSEN, J. L. Occupant behavior in building energy simulation: Towards a fit-for-purpose modeling strategy. *Energy and Buildings* 121 (2016), 188–204.
- [87] GATEAU, P., NAMY, P., AND HUC, N. Comparison between honeycomb and fin heat exchangers. *Comsol conference* (2011).
- [88] GHAFFARIANHOSEINI, A., ALWAER, H., OMRANY, H., GHAFFARIANHOSEINI, A., ALALOUC, C., CLEMENTS-CROOME, D., AND TOOKEY, J. Sick building syndrome: are we doing enough? *Architectural Science Review* 61, 3 (2018), 99–121.
- [89] GHAHRAMANI, A., PANTELIC, J., LINDBERG, C., MEHL, M., SRINIVASAN, K., GILLIGAN, B., AND ARENS, E. Learning occupants’ workplace interactions from wearable and stationary ambient sensing systems. *Applied Energy* 230 (2018), 42–51.
- [90] GOYAL, S., AND BAROOAH, P. Energy-efficient control of an air handling unit for a single-zone VAV system. *52nd IEEE Conference on Decision 2013* (2013), 4796–4801.
- [91] GRUNER, M. *The Potential of Façade-Integrated Ventilation Systems in Nordic Climate: Advanced decentralised ventilation systems as sustainable alternative to conventional systems*. Master thesis, Norwegian University of Science and Technology, 2012.
- [92] GRYGIEREK, K., AND FERDYN-GRYGIEREK, J. Multi-objectives optimization of ventilation controllers for passive cooling in residential buildings. *Sensors* 18, 4 (2018).

- [93] GUNAY, H. B., O'BRIEN, W., BEAUSOLEIL-MORRISON, I., AND BURSILL, J. Development and implementation of a thermostat learning algorithm. *Science and Technology for the Built Environment* 24, 1 (2018).
- [94] GUNNARSEN, L., AND FANGER, P. O. Adaptation to indoor air pollution. *Environment International* 18 (1992), 43–54.
- [95] GUYON, I., AND ELISSEEFF, A. An introduction to variable and feature selection. *Journal of Machine Learning Research* 3 (2003), 1157–1182.
- [96] HABEN, S., SINGLETON, C., AND GRINDROD, P. Analysis and clustering of residential customers energy behavioral demand using smart meter data. *IEEE Transactions on Smart Grid* 7, 1 (2015), 136–144.
- [97] HAGHIGHAT, F., DONNINI, G., AND D'ADDARIO, R. Relationship between occupant discomfort as perceived and as measured objectively. *Indoor Environment* 1 (1992), 112–118.
- [98] HALDEN, U. *Development and validation of a full occupancy model for residential buildings: Master Thesis for M.Sc. in Renewable Energy Engineering and Management*. Master thesis, Fraunhofer ISE and Universität Freiburg, Freiburg im Breisgau, Germany, 2019.
- [99] HALDI, F., CALÌ, D., ANDERSEN, R. K., WESSELING, M., AND MÜLLER, D. Modelling diversity in building occupant behaviour: a novel statistical approach. *Journal of Building Performance Simulation* 10, 5-6 (2016), 527–544.
- [100] HALDI, F., AND ROBINSON, D. Interactions with window openings by office occupants. *Building and Environment* 44, 12 (2009), 2378–2395.
- [101] HANBAY, D. An expert system based on least square support vector machines for diagnosis of the valvular heart disease. *Expert Systems with Applications* 36, 3, Part 1 (2009), 4232–4238.
- [102] HÄNDEL, C. Ventilation with heat recovery is a necessity in “nearly zero” energy buildings. *REHVA Journal 2011* (2011), 18–22.
- [103] HASSELAAR, E. Why this crisis in residential ventilation? *Indoor Air 2008: Proceedings of the 11th International Conference on Indoor Air Quality and Climate, 1-8* (2008).

-
- [104] HASTIE, T., TIBSHIRANI, R., AND FRIEDMAN, J. *The Elements of Statistical Learning: Data Mining, Inference, and Prediction*. Springer New York, USA, 2009.
- [105] HERKEL, S., KNAPP, U., AND PFAFFEROTT, J. Towards a model of user behaviour regarding the manual control of windows in office buildings. *Building and Environment* 43, 4 (2008), 588–600.
- [106] HONG, T., TAYLOR-LANGE, S. C., D’OCA, S., YAN, D., AND CORGNATI, S. P. Advances in research and applications of energy-related occupant behavior in buildings. *Energy and Buildings* 116 (2016), 694–702.
- [107] HÖRBERG, C. *Lüftungswirksamkeit und hygrothermische Behaglichkeit von alternierend arbeitenden fassadenintegrierten Lüftungsgeräten*. Master thesis, Hochschule Biberach and Fraunhofer ISE, Biberach, Germany, 2019.
- [108] HUBER, M., CONSTANTIN, A., AND MÜLLER, D. Optimierung der Regelungsstrategie für ein Fassadenlüftungsgerät mit Hilfe von Simulation. *DKV-Tagung 2011* (2011), 1–11.
- [109] IGLESIAS, F., AND KASTNER, W. Analysis of similarity measures in times series clustering for the discovery of building energy patterns. *Energies* 6, 2 (2013), 579–597.
- [110] INTERCONNECTION CONSULTING. IC market tracking: Kontrollierte Wohnraumlüftung in Europa 2018.
- [111] INTERNATIONAL ORGANIZATION FOR STANDARDIZATION. ISO 18523-2:2018 - energy performance of buildings - schedule and condition of building - zone and space usage for energy calculation. part 2: Residential buildings, 2018.
- [112] JANSSENS, A., WILLEMS, L., AND LAVERGE, J. Performance evaluation of residential ventilation systems based on multi-zone ventilation models. *Proceedings of 4th international building physics conference* (2009), 833–839.
- [113] JARADAT, M. A. K., AND AL-NIMR, M. A. Fuzzy logic controlled deployed for indoor air quality control in naturally ventilated environments. *Journal of Electrical Engineering* 60, 1 (2009), 12–17.
- [114] JAZIZADEH, F., GHAHRAMANI, A., BECERIK-GERBER, B., KICHKAYLO, T., AND OROSZ, M. Human-building interaction framework for personalized

- thermal comfort-driven systems in office buildings. *Journal of Computing in Civil Engineering* 28, 1 (2014), 2–16.
- [115] JEONG, B., JEONG, J.-W., AND PARK, J. S. Occupant behavior regarding the manual control of windows in residential buildings. *Energy and Buildings* 127 (2016), 206–216.
- [116] JOACHIMS, T. Text categorization with support vector machines: Learning with many relevant features. In *Machine Learning: ECML-98* (Berlin, Heidelberg, 1998), C. Nédellec and C. Rouveirol, Eds., Springer Berlin Heidelberg, pp. 137–142.
- [117] JOHANSSON, P., EKSTRAND-TOBIN, A., SVENSSON, T., AND BOK, G. Laboratory study to determine the critical moisture level for mould growth on building materials. *International Biodeterioration & Biodegradation* 73 (2012), 23–32.
- [118] JOKL, M. V. New units for indoor air quality: decicarbdiiox and decitvoc. *International Journal of Biometeorology* 42 (1998), 93–111.
- [119] JOKL, M. V. Thermal comfort and optimum humidity: Part i. *Acta Polytechnica* 1, 42 (2002), 12–24.
- [120] KAGERER, F., HERKEL, S., AND BRÄU, R. Sanierung eines Hochhauses auf Passivhausstandard – ein Jahr Betriebserfahrungen, 2013.
- [121] KASTNER, W., KOFLER, M. J., AND REINISCH, C. Using AI to realize energy efficient yet comfortable smart homes. *2010 IEEE International Workshop* (2010), 169–172.
- [122] KIM, S. H., AND MOON, H. J. Case study of an advanced integrated comfort control algorithm with cooling, ventilation, and humidification systems based on occupancy status. *Building and Environment* 133 (2018), 246–264.
- [123] KNERR, S., PERSONNAZ, L., AND DREYFUS, G. Single-layer learning revisited: A stepwise procedure for building and training neural network. *Neurocomputing: Algorithms, Architectures and Applications*, (1990).
- [124] KNISSEL, J., AND ALSÉN, N. Einsatz von dezentralen Ventilatoren zur Luftförderung in zentralen RLT-Anlagen. *HLH Lüftung - Klima - Kälte* 64, 4 (2013), 35–38.

-
- [125] KOLOKOTSA, D., TSIAVOS, T., STAVRAKAKIS, G. S., KALAITZAKIS, K., AND ANTONIDAKIS, E. Advanced fuzzy logic controllers design and evaluation for buildings' occupants thermal±visual comfort and indoor air quality satisfaction. *Energy and Buildings* 33 (2001), 531–543.
- [126] KOVÁCS, F., LEGÁNY, C., AND BABOS, A. Cluster validity measurement techniques. *Report* (2006).
- [127] KRAJČÍK, M., SIMONE, A., AND OLESEN, B. W. Air distribution and ventilation effectiveness in an occupied room heated by warm air. *Energy and Buildings* 55 (2012), 94–101.
- [128] LACHHAB, F., BAKHOUYA, M., OULADSINE, R., AND ESSAAIDI, M. Towards an intelligent approach for ventilation systems control using IoT and big data technologies. *Procedia Computer Science* 130 (2018), 926–931.
- [129] LACHHAB, F., ESSAAIDI, M., BAKHOUYA, M., AND OULADSINE, R. A state-feedback approach for controlling ventilation systems in energy efficient buildings. *2015 3rd International Renewable 2015* (2015), 1–6.
- [130] LAI, D., QI, Y., LIU, J., DAI, X., ZHAO, L., AND WEI, S. Ventilation behavior in residential buildings with mechanical ventilation systems across different climate zones in China. *Building and Environment* 143 (2018), 679–690.
- [131] LATIF, M., AND NASIR, A. Decentralized stochastic control for building energy and comfort management. *Journal of Building Engineering* 24 (2019).
- [132] LAVERGE, J., POLLET, I., AND VANDEKERCKHOVE, S. Big data and DCV: smart ventilation? *Proceedings of the ISIAQ Indoor Air 2018 conference*. (2018).
- [133] LAVERGE, J., VAN DEN BOSSCHE, N., HEIJMANS, N., AND JANSSENS, A. Energy saving potential and repercussions on indoor air quality of demand controlled residential ventilation strategies. *Building and Environment* 46, 7 (2011), 1497–1503.
- [134] LEEPHAKPREEDA, T., THITIPATANAPONG, R., GRITTIYACHOT, T., AND YUNGCHAREON, V. Occupancy-based control of indoor air ventilation: A theoretical and experimental study. *ScienceAsia* 2001, 27 (2001), 279–284.

- [135] LESS, B. D., DUTTON, S. M., WALKER, I. S., SHERMAN, M. H., AND CLARK, J. D. Energy savings with outdoor temperature-based smart ventilation control strategies in advanced california homes. *Energy and Buildings* 194 (2019), 317–327.
- [136] LI, Q., BAI, F., YANG, B., WANG, Z., EL HEFNI, B., LIU, S., KUBO, S., KIRIKI, H., AND HAN, M. Dynamic simulation and experimental validation of an open air receiver and a thermal energy storage system for solar thermal power plant. *Applied Energy* 178 (2016), 281–293.
- [137] LIANG, JING, DU, RUXU. Thermal comfort control based on neural network for HVAC application. *Proceedings of the IEEE International Conference on Control Applications* (2005), 819–824.
- [138] LIU, D., NIU, D., WANG, H., AND FAN, L. Short-term wind speed forecasting using wavelet transform and support vector machines optimized by genetic algorithm. *Renewable Energy* 62 (2014), 592–597.
- [139] LOKERE, L., JANSSENS, A., VANDEKERCKHOVE, S., POLLET, I., DELGHUST, M., DE JONGE, K., AND LAVERGE, J. Big humidity data from smart ventilation systems. *From energy crisis to sustainable indoor climate : 40 years of AIVC*. (2019), 150–151.
- [140] LOWEN, A. C., MUBAREKA, S., STEEL, J., AND PALESE, P. Influenza virus transmission is dependent on relative humidity and temperature. *PLoS Pathog* 3, 10 (2007), 1470–1476.
- [141] MAHLER, B., AND HIMMLER, R. Results of the evaluation study deal decentralized facade integrated ventilation systems. *8th International Conference for Enhanced Building Operations* (2008), 1–8.
- [142] MAIER, D. *Aufbau und Durchführung einer Mixed-Methods-Studie zu Lüftungsverhalten und Raumklima sowie der Einstellung bezüglich Lüftungssystemen*. Master thesis, Katholischen Universität Eichstätt-Ingolstadt, Ingolstadt, Germany, 2020.
- [143] MAIER, T., KRZACZEK, M., AND TEJCHMAN, J. Comparison of physical performances of the ventilation systems in low-energy residential houses. *Energy and Buildings* 41, 3 (2009), 337–353.

-
- [144] MAMDANI, E. H. Application of fuzzy logic to approximate reasoning using linguistic synthesis. *IEEE Transactions on Computers C-26*, 12 (1977), 1182–1191.
- [145] MANZ, H., HUBER, H., SCHÄLIN, A., WEBER, A., FERRAZZINI, M., AND STUDER, M. Performance of single room ventilation units with recuperative or regenerative heat recovery. *Energy and Buildings* 31, 1 (2000), 37–47.
- [146] MARKOVIC, R., GRINTAL, E., WÖLKI, D., FRISCH, J., AND VAN TREECK, C. Window opening model using deep learning methods. *Building and Environment* 145 (2018), 319–329.
- [147] MATTSSON, S. E., AND ELMQVIST, H. Modelica – an international effort to design the next generation modeling language. *7th IFAC Symposium on Computer Aided Control Systems Design, Gent, Belgium* (1997), 1–5.
- [148] MERCKX, M., BRUYNEEL, G., POLLET, I., AND LAVERGE, J. Temperature, draft and ventilation efficiency of room based decentralised heat recovery ventilation systems. *Proceedings of 39th AIVC Conference* (2018), 838–847.
- [149] MERZKIRCH, A. *Energieeffizienz, Nutzerkomfort und Kostenanalyse von Lüftungsanlagen in Wohngebäuden: Feldtests von neuen Anlagen und Vorstellung bedarfsgeführter Prototypen*. PhD Thesis, Université du Luxembourg, 2015.
- [150] MERZKIRCH, A., MAAS, S., SCHOLZEN, F., AND WALDMANN, D. A semi-centralized, valveless and demand controlled ventilation system in comparison to other concepts in field tests. *Building and Environment* 93 (2015), 21–26.
- [151] MERZKIRCH, A., MAAS, S., SCHOLZEN, F., AND WALDMANN, D. Field tests of centralized and decentralized ventilation units in residential buildings – specific fan power, heat recovery efficiency, shortcuts and volume flow unbalances. *Energy and Buildings* 116 (2016), 376–383.
- [152] MIKOLA, A., SIMSON, R., AND KURNITSKI, J. The impact of air pressure conditions on the performance of single room ventilation units in multi-story buildings. *Energies* 12, 13 (2019), 2633.
- [153] MITSU, T. *Temporal Data Mining*. Chapman & Hall/CRC, USA, 2010.

- [154] MO, H., SUN, H., LIU, J., AND WEI, S. Developing window behavior models for residential buildings using XGBoost algorithm. *Energy and Buildings* 205, 109564 (2019).
- [155] MOLINA-SOLANA, M., ROS, M., AND DELGADO, M. Unifying fuzzy controller for indoor environment quality. *2013 Joint IFSA World Congress and NAFIPS Annual Meeting (IFSA/NAFIPS)* (2013), 1080–1085.
- [156] MOON, H. J., AND AUGENBROE, G. L. Towards a practical mould growth risk indicator. *Building Services Engineering Research and Technology* 25, 4 (2004), 317–326.
- [157] MORTENSEN, D. K., WALKER, I. S., AND SHERMAN, M. H. Optimization of occupancy based demand controlled ventilation in residences. *International Journal of Ventilation* 10, 1 (2011), 49–60.
- [158] MOSSOLLY, M., GHALI, K., AND GHADDAR, N. Optimal control strategy for a multi-zone air conditioning system using a genetic algorithm. *Energy* 34, 1 (2009), 58–66.
- [159] NASSIF, N. A robust CO₂-based demand-controlled ventilation control strategy for multi-zone HVAC systems. *Energy and Buildings* 45 (2012), 72–81.
- [160] NAYLOR, S., GILLOTT, M., AND LAU, T. A review of occupant-centric building control strategies to reduce building energy use. *Renewable and Sustainable Energy Reviews* 96 (2018), 1–10.
- [161] NEST LABS. Meet the nest learning thermostat.
- [162] NICOL, J. F. Characterising occupant behaviour in building: towards a stochastic model of occupant use of windows, lights, blinds heaters and fans. *7th IBPSA Conference* (2001), 1073–1078.
- [163] ÖHRSTRÖM, E., AND SKÅNBERG, A. Sleep disturbances from noise - laboratory experiment on road traffic and ventilation noise. *Journal of Sound and Vibration* 271, 1-2 (2004), 279–296.
- [164] ORME, M., LIDDAMENT, M. W., AND WILSON, A. Numerical data for air infiltration & natural ventilation calculations: Technical note AIVC 44.
- [165] PANG, X., PIETTE, M. A., AND ZHOU, N. Characterizing variations in variable air volume system controls. *Energy and Buildings* 135 (2017), 166–175.

-
- [166] PARK, J. S., AND KIM, H. J. A field study of occupant behavior and energy consumption in apartments with mechanical ventilation. *Energy and Buildings* 50 (2012), 19–25.
- [167] PARK, J. Y., DOUGHERTY, T., FRITZ, H., AND NAGY, Z. LightLearn: An adaptive and occupant centered controller for lighting based on reinforcement learning. *Building and Environment* 147 (2019), 397–414.
- [168] PARK, J. Y., OUF, M. M., GUNAY, B., PENG, Y., O’BIEN, W., KJÆRGAARD, M. B., AND NAGY, Z. A critical review of field implementations of occupant-centric building controls. *Building and Environment* 165 (2019), 106351.
- [169] PASSIVHAUS INSTITUT. Requirements and testing procedures for energetic and acoustical assessment of passive house ventilation systems for certification as ‘passive house suitable component’.
- [170] PASSIVHAUS INSTITUT. Kriterien für den Passivhaus-, EnerPHit- und PHI-Energiesparhaus-Standard, 2016.
- [171] PAVLOVAS, V. Demand controlled ventilation: A case study for existing swedish multifamily buildings. *Energy and Buildings* 36, 10 (2004), 1029–1034.
- [172] PEDREGOSA, F., VAROQUAX, G., GRAMFORT, A., MICHEL, V., THIRION, B., GRISEL, O., BLONDEL, M., PRETTENHOFER, P., WEISS, R., DUBOURG, V., VANDERPLAS, J., PASSOS, A., COURNAPEAU, D., BRUCHER, M., PERROT, M., AND DUCHESNAY, É. Scikit-learn: Machine learning in python. *Journal of Machine Learning Research* 12 (2011), 2825–2830.
- [173] PEITZSCH, M., BLOOM, E., HAASE, R., MUST, A., AND LARSSON, L. Remediation of mould damaged building materials—efficiency of a broad spectrum of treatments. *Journal of environmental monitoring : JEM* 14, 3 (2012), 908–915.
- [174] PEREIRA, P. F., RAMOS, N. M., ALMEIDA, R. M., AND SIMÕES, M. L. Methodology for detection of occupant actions in residential buildings using indoor environment monitoring systems. *Building and Environment* 146 (2018), 107–118.

- [175] PERNIGOTTO, G., AND GASPARELLA, A. Classification of european climates for building energy simulation analyses. *5th International High Performance Buildings Conference* (2018), 3516, 1–11.
- [176] PERSILY, A., AND DE JONGE, L. Carbon dioxide generation rates for building occupants. *Indoor Air* 27, 5 (2017), 868–879.
- [177] PITALÚA-DÍAZ, N., HERRERA-LÓPEZ, E. J., VELÁZQUEZ CONTRERAS, L. E., ÁLVAREZ CHÁVEZ, C. R., AND VEGA, N. M. Controlling indoor benzene concentrations using a fuzzy system. *IFAC Proceedings Volumes* 46, 16 (2013), 449–454.
- [178] PLATT, J. C. Probabilistic outputs for support vector machines and comparisons to regularized likelihood methods. In *Advances in Large Margin Classifiers*, A. J. Smola, P. Bartlett, B. Schölkopf, and D. Schuurmans, Eds. MIT Press, Cambridge, Massachusetts, 2000.
- [179] RAFTERY, P., LEE, E., WEBSTER, T., HOYT, T., AND BAUMAN, F. Effects of furniture and contents on peak cooling load. *Energy and Buildings* 85 (2014), 445–457.
- [180] RASCHKA, S. *Python Machine Learning: Unlock deeper insights into machine learning with this vital guide to cutting-edge predictive analytics*. Packt Publishing, Birmingham B3 2PB, UK, 2015.
- [181] RASMUSSEN, B., AND MACHIMBARRENA, M. Integrating and harmonizing sound insulation aspects in sustainable urban housing constructions. *COST Action TU0901* (2014).
- [182] REINER, U., KAHL, M., LEIBFRIED, T., ALLERDING, F., AND SCHMECK, H. MeRegioMobil-Lab – a development environment for future smarthomes. *Proceedings of the VDE Kongress* (2010).
- [183] REN, X., ZHANG, C., ZHAO, Y., BOXEM, G., ZEILER, W., AND LI, T. A data mining-based method for revealing occupant behavior patterns in using mechanical ventilation systems of dutch dwellings. *Energy and Buildings* 193 (2019), 99–110.
- [184] RICHTER, W., HARTMANN, T., GRITZKI, R., BOLSIOUS, J., KREMONKE, A., AND PERSCHK, A. *Bedarfslüftung im Wohnungsbau*. Fraunhofer IRB, Stuttgart, 2001.

-
- [185] RIJAL, H. B., TUOHY, P., NICOL, F., HUMPHREYS, M. A., SAMUEL, A., AND CLARKE, J. Development of an adaptive window-opening algorithm to predict the thermal comfort, energy use and overheating in buildings. *Journal of Building Performance Simulation* 1, 1 (2008), 17–30.
- [186] ROHRER, S. *Entwicklung und Simulation von fassadenintegrierten haustechnischen Systemen: im Hinblick auf die energetische Optimierung von Luftkanälen und Heizungsleitungen*. Bachelor thesis, Fraunhofer ISE and Hochschule Offenburg, Freiburg im Breisgau, Germany, 2018.
- [187] ROWAN, N., JOHNSTONE, C., MCLEAN, R., ANDERSON, J., AND CLARKE, J. Prediction of toxigenic fungal growth in buildings by using a novel modelling system. *Applied and environmental microbiology* 11, 65 (1999), 4814–4821.
- [188] ROYAPOOR, M., ANTONY, A., AND ROSKILLY, T. A review of building climate and plant controls, and a survey of industry perspectives. *Energy and Buildings* 158 (2018), 453–465.
- [189] SCHIBUOLA, L., SCARPA, M., AND TAMBANI, C. Performance optimization of a demand controlled ventilation system by long term monitoring. *Energy and Buildings* 169 (2018), 48–57.
- [190] SCHIEWECK, A., UHDE, E., SALTHAMMER, T., SALTHAMMER, L. C., MORAWSKA, L., MAZAHARI, M., AND KUMAR, P. Smart homes and the control of indoor air quality. *Renewable and Sustainable Energy Reviews* 94 (2018), 705–718.
- [191] SCHWEIKER, M., HALDI, F., SHUKUYA, M., AND ROBINSON, D. Verification of stochastic models of window opening behaviour for residential buildings. *Journal of Building Performance Simulation* 5, 1 (2012), 55–74.
- [192] SEDLBAUER, K. Prediction of mould growth by hygrothermal calculation. *Journal of Thermal Envelope and Building Science* 25, 4 (2002), 321–336.
- [193] SEPPÄNEN, O. A., AND FISK, W. J. Summary of human responses to ventilation.
- [194] SHAH, R. K., AND SEKULIĆ, D. P. *Fundamentals of heat exchanger design*. John Wiley & Sons, Hoboken NJ, 2003.

- [195] SHAIKH, P. H., NOR, N. B. M., NALLAGOWNDEN, P., ELAMVAZUTHI, I., AND IBRAHIM, T. A review on optimized control systems for building energy and comfort management of smart sustainable buildings. *Renewable and Sustainable Energy Reviews* 34 (2014), 409–429.
- [196] SHERMAN, M. H., AND WALKER, I. S. Meeting residential ventilation standards through dynamic control of ventilation systems. *Energy and Buildings* 43 (2011), 1904–1911.
- [197] SMITH, K., AND SVENDSEN, S. Control of single-room ventilation with regenerative heat recovery for indoor climate and energy performance. *CLIMA 2016 - 12th REHVA World Congress* (2016).
- [198] SMITH, K. M. *Development and operation of Decentralized Ventilation for Indoor Climate and Energy Performance*. PhD thesis, Technical University of Denmark,, 2015.
- [199] SONG, Y., WU, S., AND YAN, Y. Y. Control strategies for indoor environment quality and energy efficiency—a review. *International Journal of Low-Carbon Technologies* 10, 3 (2015), 305–312.
- [200] SUNWOO, Y., CHOU, C., TAKESHITA, J., MURAKAMI, M., AND TOCHIHARA, Y. Physiological and subjective responses to low relative humidity in young and elderly men. *Journal of Physiological Anthropology* 25 (2006), 229–238.
- [201] SWAMI, M. V., AND CHANDRA, S. Procedures for calculating natural ventilation airflow rates in buildings.
- [202] TENWOLDE, A., AND PILON, C. L. The effect of indoor humidity on water vapor release in homes. *Proceedings Thermal Performance of the Exterior Envelopes of Buildings X* (2007).
- [203] TIAN, W., HAN, X., ZUO, W., AND SOHN, M. D. Building energy simulation coupled with CFD for indoor environment: A critical review and recent applications. *Energy and Buildings* 165 (2018), 184–199.
- [204] TOFTUM, J., JORGENSEN, A. S., AND FANGER, P. O. Upper limits of air humidity for preventing warm respiratory discomfort. *Energy and Buildings* 28 (1998), 15–23.

-
- [205] TUFEKCI, Z. We need to talk about ventilation: How is it that six months into a respiratory pandemic, we are still doing so little to mitigate airborne transmission? *The Atlantic* (30.07.2020).
- [206] TURNER, W. J., LOGUE, J. M., AND WRAY, C. P. A combined energy and IAQ assessment of the potential value of commissioning residential mechanical ventilation systems. *Building and Environment* 60 (2013), 194–201.
- [207] UMWELTBUNDESAMT. Gesundheitliche Bewertung von Kohlendioxid in der Innenraumluft. Mitteilungen der Ad-hoc-Arbeitsgruppe Innenraumrichtwerte der Innenraumluftthygiene-Kommission des Umweltbundesamtes und der Obersten Landesgesundheitsbehörden. *Gesundheitsschutz* 51, 11 (2008), 1358–1369.
- [208] VAN DONGEN, J. Occupant behaviour and attitudes with respect to ventilation of dwellings, 2007.
- [209] VAN ROSSUM, G. Python tutorial, CWI Report CS-R9526, 1995.
- [210] VANDERPLAS, J. *Python Data Science Handbook: Essential Tools for Working with Data*, 1st ed. O’Reilly Media, 2016.
- [211] VAPNIK, V., AND LERNER, A. Pattern recognition using generalized portrait method. *Automat. Remote Control* 24 (1963), 774–780.
- [212] VASILE, V., PETRAN, H., DIMA, A., AND PETCU, C. Indoor air quality – a key element of the energy performance of the buildings. *Energy Procedia* 96 (2016), 277–284.
- [213] VÁZQUEZ-CANTELI, J., ULYANIN, S., KAMPF, J., AND NAGY, Z. Adaptive multi-agent control of HVAC systems for residential demand response using batch reinforcement learning. *2018 Building Performance Analysis Conference* (2018), 683–690.
- [214] VELLEI, M., HERRERA, M., FOSAS, D., AND NATARAJAN, S. The influence of relative humidity on adaptive thermal comfort. *Building and Environment* 124 (2017), 171–185.
- [215] VEREIN DER DEUTSCHEN INGENIEUREN. VDI 2081-1 - noise generation and noise reduction in air-conditioning systems, 2001.

- [216] VIESSMANN GBMH. Dezentrales Wohnungslüftungsgerät Vitovent 100-D mit Wärmerückgewinnung, 01.08.19.
- [217] VIITANEN, H., AND RITSCHKOFF, A.-C. Mould growth in pine and spruce sapwood in relation to air humidity and temperature. *Swedish University of Agricultural Sciences, Report of Forest Products N. 221* (1991).
- [218] WALKER, I. S., SHERMAN, M. H., CLARK, J. D., AND GUYOT, G. Residential smart ventilation: A review, 2017.
- [219] WALLNER, P., TAPPLER, P., MUNOZ, U., DAMBERGER, B., WANKA, A., KUNDI, M., AND HUTTER, H.-P. Health and wellbeing of occupants in highly energy efficient buildings: A field study. *International journal of environmental research and public health* 14, 3 (2017).
- [220] WANG, X., SMITH, K. A., AND HYNDMAN, R. J. Dimension reduction for clustering time series using global characteristics. *ICCS 2005 3516* (2005), 792–795.
- [221] WARGOCKI, P., SHERMAN, M., DE GIDS, W., WOUTERS, P., ALLARD, F., CARRIE, R., CARRER, P., AND KEPHALOPOULOS, S. Proposed research agenda for achieving indoor air quality supporting health and comfort in highly energy efficient buildings. *35th AIVC Conference, Air Infiltration and Ventilation Centre 2013* (2013).
- [222] WETTER, M. Multizone airflow model in modelica. *Modelica Association Conference 2006* (2006), 1–4.
- [223] WETTER, M. Fan and pump model that has a unique solution for any pressure boundary condition and control signal. *Proceedings of Building Simulation 2013* (2013), 3505–3512.
- [224] WIRTH, S. Ist mit der kontrollierten Wohnungslüftung eine Primärenergieeinsparung möglich? *Bauphysik* 24 (2002), 236–239.
- [225] WOLFF, D., TEUBER, P., BUDDE, J., AND JAGNOW, K. Felduntersuchung: Betriebsverhalten von Heizungsanlagen mit Gas-Brennwertkessel, 2004.
- [226] WOLKOFF, P. The mystery of dry indoor air - An overview. *Environment International* 121 (2018), 1058–1065.

-
- [227] WORLD HEALTH ORGANIZATION. “World Health Organization. Indoor air pollutants: Exposure and health effects. *EURO Reports and Studies 78* (1983).
- [228] WORLD HEALTH ORGANIZATION. *WHO guidelines for indoor air quality: dampness and mould*. Druckpartner Moser, 2009.
- [229] WU, X., LIU, Y., LIU, G., WANG, F., AND WANG, Z. Effect of supply air temperature on indoor thermal comfort in a room with radiant heating and mechanical ventilation. *Energy Procedia 121* (2017), 206–213.
- [230] XU, Y., CHEN, S., JAVED, M., LI, N., AND GAN, Z. A multi-occupants’ comfort-driven and energy-efficient control strategy of VAV system based on learned thermal comfort profiles. *Science and Technology for the Built Environment 24*, 10 (2018), 1141–1149.
- [231] YERUSHALMY, J. Statistical problems in assessing methods of medical diagnosis, with special reference to x-ray techniques. *Public Health Reports 62*, 40 (1947), 1432–1449.
- [232] YU, C. W. F., AND KIM, J. T. Building pathology, investigation of sick buildings — VOC emissions. *Indoor and Built Environment 19*, 1 (2010), 30–39.
- [233] YUN, G. Y., AND STEEMERS, K. Time-dependent occupant behaviour models of window control in summer. *Building and Environment 43*, 9 (2008), 1471–1482.
- [234] ZHAO, H. X., AND MAGOULÈS, F. Parallel support vector machines applied to the prediction of multiple buildings energy consumption. *Journal of Algorithms & Computational Technology 4*, 2 (2010), 231–249.
- [235] ZHAO, L., AND LIU, J. Operating behavior and corresponding performance of mechanical ventilation systems in chinese residential buildings. *Building and Environment 170* (2020), 106600.
- [236] ZHOU, B., CHEN, F., DONG, Z., AND NIELSEN, P. V. Study on pollution control in residential kitchen based on the push-pull ventilation system. *Building and Environment 107* (2016), 99–112.